

PDF hosted at the Radboud Repository of the Radboud University Nijmegen

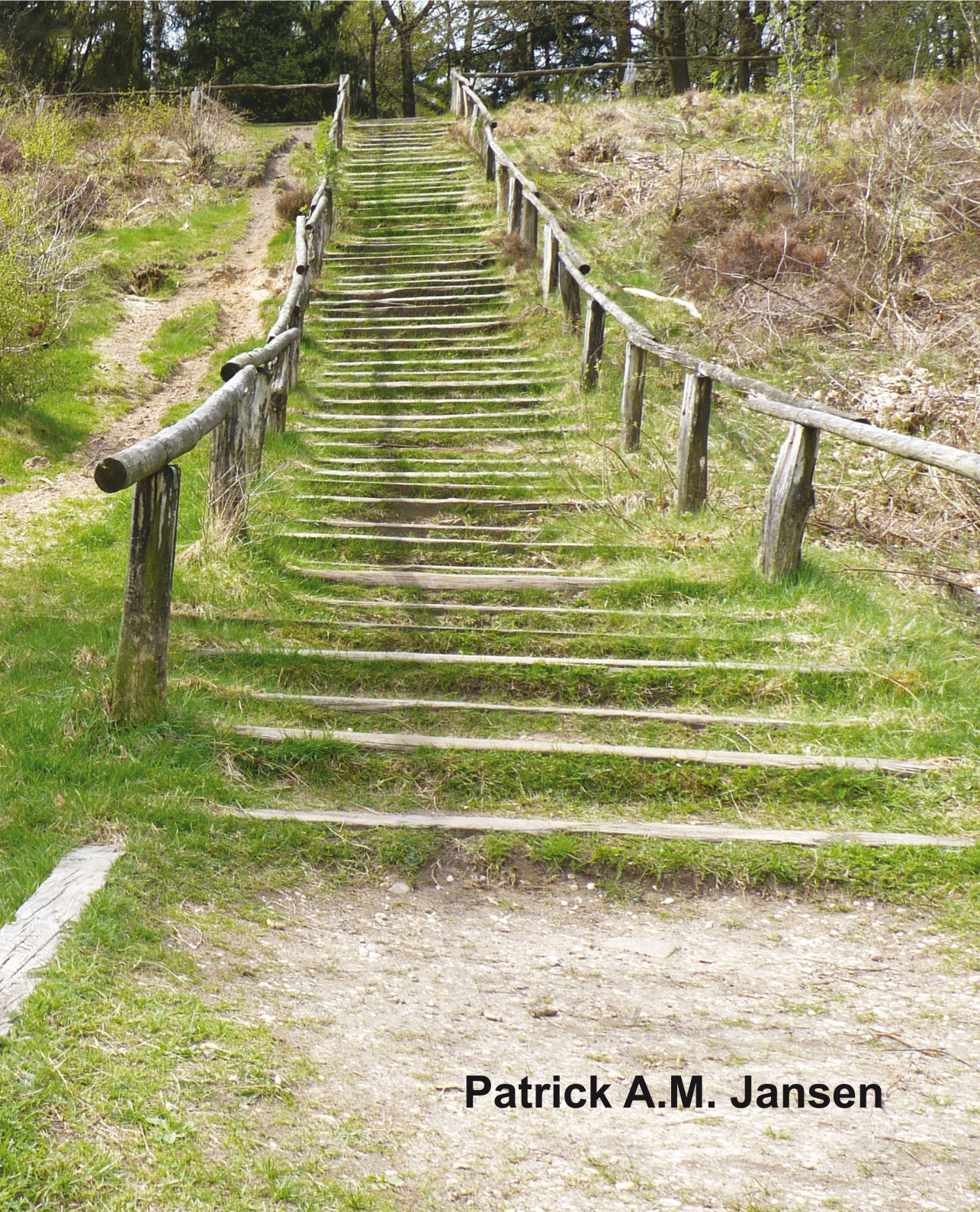
The following full text is a publisher's version.

For additional information about this publication click this link.

<http://hdl.handle.net/2066/111572>

Please be advised that this information was generated on 2017-12-06 and may be subject to change.

Analysis of keratinocyte gene expression: a tale of molecules, markers, models and medicines



Patrick A.M. Jansen

Analysis of keratinocyte gene expression:
a tale of molecules, markers, models and medicines

Patrick A.M. Jansen

Thesis Radboud University Nijmegen Medical Centre, Nijmegen, The Netherlands, with summary in Dutch; 221 pp. © 2013.

ISBN: 978-94-6191-759-1
Print: Ipskamp Drukkers B.V., Enschede
Design and layout: Patrick Jansen

Analysis of keratinocyte gene expression: a tale of molecules, markers, models and medicines

Proefschrift

ter verkrijging van de graad van doctor
aan de Radboud Universiteit Nijmegen
op gezag van de rector magnificus prof. mr. S.C.J.J. Kortmann,
volgens besluit van het college van decanen
in het openbaar te verdedigen op woensdag 26 juni 2013
om 13.30 uur precies

door

Patrick Antonius Martinus Jansen
geboren op 28 augustus 1979
te Cuijk

Promotor:

Prof. dr. J. Schalkwijk

Copromotor:

Dr. P.L.J.M. Zeeuwen

Manuscriptcommissie:

Prof. dr. R.E. Brock

Dr. A.A.J. van de Loo

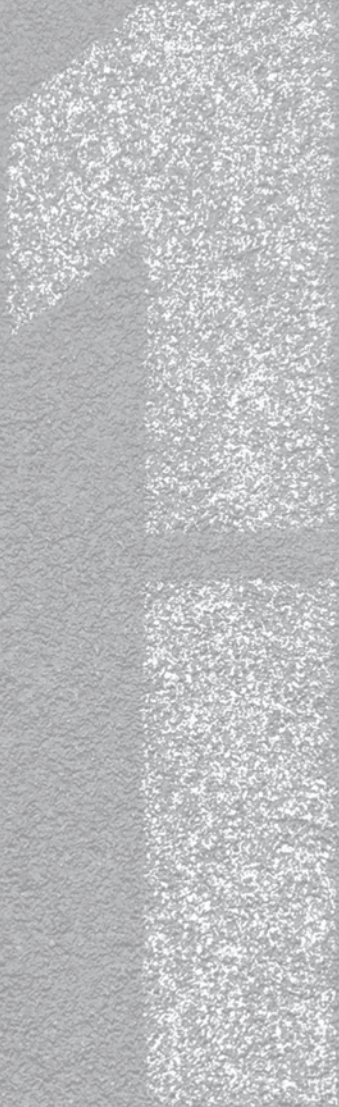
Prof. dr. P.S. Hiemstra (Leids Universitair Medisch Centrum)

Table of contents

Chapter 1	7
General introduction	
Chapter 2	41
β -defensin-2 protein is a serum biomarker for disease activity in psoriasis and reaches biologically relevant concentrations in lesional skin	
Chapter 3	59
Molecular diagnostics of psoriasis, atopic dermatitis, allergic contact dermatitis and irritant contact dermatitis	
Chapter 4	83
Rho Kinase Inhibitor Y-27632 Prolongs the Life Span of Adult Human Keratinocytes, Enhances Skin Equivalent Development, and Facilitates Lentiviral Transduction	
Chapter 5	113
Cystatin M/E knockdown by lentiviral delivery of shRNA impairs epidermal morphogenesis of human skin equivalents	
Chapter 6	137
Expression of the vanin gene family in normal and inflamed human skin: Induction by pro-inflammatory cytokines	
Chapter 7	155
Discovery of small molecule vanin inhibitors: new tools to study metabolism and disease	
Chapter 8	177
Combination of pantothenamides with vanin inhibitors: a novel antibiotic strategy against gram-positive bacteria	
Chapter 9	197
Summary and concluding remarks	
Appendix	207
Nederlandse samenvatting	208
Dankwoord	216
List of publications	219
Curriculum Vitae	221

General introduction

1 CHAPTER



Patrick AM Jansen¹
Patrick LJM Zeeuwen¹
Joost Schalkwijk¹

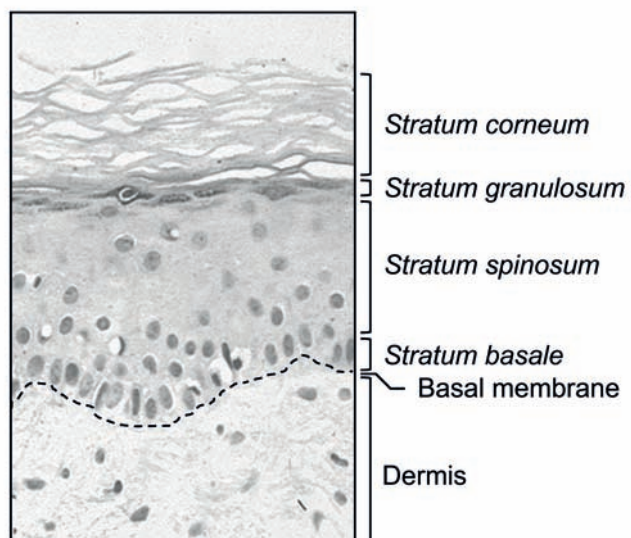
¹Department of Dermatology and Nijmegen Centre for Molecular Life Sciences, Radboud University Nijmegen Medical Centre, The Netherlands



Part 1: Skin Introduction

The skin is the largest organ of the body, and accounts for 15% of the total body weight of adults¹. Besides giving the body strength, the skin has a dual protective function. From the outside it protects the body against extracellular stimuli like UV and other radiation, but also against pathogens. From the inside the skin protects against dehydration and regulates body-temperature. The skin consists of a stratified, cellular epidermis, separated by a basement membrane to the underlying dermis of connective tissue and the subcutaneous fat². The different characteristic features of the skin are schematically represented in figure 1.1. The dermis gives the skin its tightness and is host for hair follicles, sweat glands and sebaceous glands, nerves and blood vessels. The epidermis consist of various cell types, but the majority, up to 90-95%, are keratinocytes. Other cells that are represented in the epidermis are melanocytes, Langerhans cells, Merkel cells and circulating lymphocytes. The epidermal keratinocytes are arranged in continuous layers with, from the inside to the outside, the basal layer or *stratum basale* (single layer), the prickle-cell layer or *stratum spinosum* (5-15 layers), the granular layer or *stratum granulosum* (1-3 layers) and the horny layer or *stratum corneum* (5-10 layers). Keratinocytes arise from mitotic division of stem cells in the basal layer. Daughter keratinocytes, also known as transit amplifying cells, migrate towards the skin surface while undergoing morphological and biochemical differentiation (a process called keratinisation). In the *stratum corneum* the cells lose their nucleus and fuse to squamous sheets, which are eventually shed from the surface (a process called desquamation). In normal skin, the complete journey from the basal layer to the shedding takes about 30 days and the rate of desquamation equals the rate of production^{3,4}.

Figure 1.1 Structure of the human skin. The dermis contains the hair follicles, sweat glands and sebaceous glands. The basal membrane separates the dermis from the epidermis. In the epidermis four well-defined morphologically different layers (*Stratum basale*, *stratum spinosum*, *stratum granulosum* and *stratum corneum*) can be distinguished.



Keratinocytes that start dividing will soon accumulate cell-cell junctions on their surface, mainly desmosomes. Desmosomes anchor keratin intermediate filaments to the cell membrane, which is essential for withstanding trauma⁵. There are two types of keratins: type I (acidic) keratins and type II (basic to neutral) keratins. The process in which a type I keratin forms a heterodimer with a type II keratin is called pairing⁶. Through the epidermis different combinations of heterodimers can be distinguished, depending on the state of differentiation. The keratinocytes just above the basal layers are characterized by the presence of K5/K14 keratin pairs, while the uppermost layers of differentiated keratinocytes consist of K1/K10 and K2/K10 keratin pairs^{7,8}. The last layer of viable cells in the epidermis is the *stratum granulosum*, which name is derived from the presence of keratohyalin granules in the cytoplasm of cells in this layer⁹. Cells in the *stratum granulosum* will ultimately undergo programmed cell death and the rupture of cellular integrity results in the release of lysosomal proteases and other lytic enzymes. This leads to the loss of their nuclei and cytoplasmic organelles, resulting in the formation of corneocytes. Corneocytes form a stable and insoluble cornified envelope (CE), consisting of several specific proteins that are cross-linked together via Ca²⁺-dependent transglutaminases in an orchestrated way¹⁰. The *stratum corneum* is the layer of the epidermis that contain most of the defensive functions that the skin harbours¹¹.

Skin barrier function

The physical barrier of the skin is formed by lipid-depleted corneocytes embedded in a lipid-enriched, extracellular matrix, which is often compared with a wall composed of bricks and mortar¹²⁻¹⁴. The proteins and lipids involved in this process are secreted by lamellar granules, which are present in the cytoplasm of keratinocytes in the upper *stratum spinosum* layer and *stratum granulosum*¹¹. The CE consists of at least 20 proteins of which loricrin accounts for more than 70% of total cross-linked proteins¹⁵. Involucrin, the first identified CE protein, is expressed at the onset of terminal differentiation and is eventually incorporated into CEs in a cross-linking reaction catalyzed by transglutaminase-1^{16,17}. It has been shown that involucrin could be cross-linked to almost all CE-associated proteins¹⁸. Loricrin is expressed at the end of the differentiation process, but represents the majority of the CE proteins¹⁹. Another important protein of the CE is filaggrin, which is formed after dephosphorylation and proteolysis of profilaggrin during epidermal terminal differentiation. Filaggrin rapidly aggregates the cytoskeleton of granular keratinocytes, which contributes to the collapse of these cells resulting in the formation of corneocytes²⁰. The importance of filaggrin for a correct epidermal barrier was shown by mutations in the filaggrin gene of ichthyosis vulgaris patients²¹, and also in patients with atopic dermatitis, which are both diseases characterized by a disturbed barrier function²².

Various classes of lipids are found in the *stratum corneum*, like ceramides, free fatty acids and cholesterol²³. Keratinocytes in the *stratum granulosum* produce ceramides and deliver them to the *stratum corneum* via lamellar granules.

Insufficient production of ceramides, but also cholesterol, results in a delayed barrier repair after damage^{24,25}. Free fatty acids and cholesterol sulphate are the only lipids in the *stratum corneum* with a charged/ionisable headgroup and therefore necessary for the formation of the *stratum corneum* lipid bilayer²³. They also are expected to play a role in causing the acidic pH in the upper layers of the *stratum corneum*²³. The importance of fatty acid for epidermal barrier function is illustrated by the defective barrier after fatty acid deficiency²³.

Another protective function of the epidermis is the ability to absorb harmful UV light. Trans-urocanic acid is the major UV-absorbing pigment that is formed by the deimination of histidine. Histidine is released after hydrolysis of filaggrin¹¹. Another mechanism to protect the skin against UV light is performed by melanocytes, who deposit melanin containing melanosomes via dendrites into adjacent keratinocytes. Melanosomes form complexes that are located close to the nucleus, preferentially at the apical site to form “caps” that protect the keratinocytes nuclei against UV light²⁶.

The epidermis has its own innate immune host defense system, as it is able to express peptides that possess antimicrobial activity. These antimicrobial peptides include human β -defensin (hBD)-1, 2, 3 and 4, secretory leukocyte proteinase inhibitor (SLPI), elafin, cathelicidin (LL-37), S100 proteins, RNase 7, dermcidin and cystatin A. Some of them (elafin, psoriasin, LL-37 and β -defensins with the exception of hBD-1) are only expressed upon barrier disruption or chronic inflammation²⁷, although psoriasin might also be expressed on normal skin, depending on the location of the body surface²⁸. Each peptide is active against his own spectrum of antimicrobial targets. For example, hBD-3 is mainly directed against *S. aureus*²⁹, while hBD-2 is mainly active against gram-negative bacteria like *P. aeruginosa* and *E. coli*²⁸. It has been shown that hBD-2 expression is induced by *P. aeruginosa*^{30,31} or by stimulation with interleukin (IL)-1 α , IL-1 β or IL-22³⁰. SLPI and elafin are protease inhibitors that are produced early during inflammation as response to IL-1 and TNF- α . They are primarily expressed to prevent injurious effects of excessive release of proteolytic enzymes from inflammatory cells. Aside, SLPI and elafin have been shown to have a broad antibacterial spectrum as well as anti-HIV and anti-fungal properties³²⁻³⁵. LL-37 can be induced in human skin upon inflammatory conditions. It is secreted by keratinocytes and neutrophils and serves as a chemo-attractant for neutrophils, monocytes and T-cells³⁶. LL-37 has also been shown to possess broad-antimicrobial activity, including antiviral activity³⁷. The S100 protein psoriasin (S100A7) is constitutively expressed in normal skin and can be upregulated by exposing keratinocytes to calcitriol (1,25 (OH)₂D3)³⁸. Low concentration of psoriasin preferentially kills *E. coli*³⁹, but at higher doses it could also possess antimicrobial activity against *P. aeruginosa* and *S. aureus*⁴⁰. Calgranulins also belong to the S100 proteins and contain 3 proteins: calgranulin A (S100A8), B (S100A9) and C (S100A12). Calgranulin A and B can form a complex, which is called calprotectin⁴¹. Calgranulins exert proinflammatory functions, but they have also antimicrobial properties against bacteria (including *E. coli*, *S. aureus* and *S.*

epidermidis) and yeast (including *C. Albicans*)⁴². RNase 7 is constitutively present at high levels in normal skin, although it can be induced in diseases like atopic dermatitis and psoriasis⁴³. RNase 7 exhibits a broad spectrum of antimicrobial activity against both gram-positive and gram-negative bacteria, but also against *C. albicans*^{28,44}. Dermcidin is the principal sweat antimicrobial peptide that is constitutively expressed exclusively by eccrine gland cells²⁸ and has antibacterial activity (*S. aureus*, *E. faecalis* and *E. coli*) and antifungal activity (*C. Albicans*)⁴⁵. Cystatin A is a cysteine protease inhibitor present in keratohyalin granules and is, after phosphorylation, a minor cross-linked constituent of the CE. Cystatin A is proposed to possess both antibacterial and antiviral properties⁴⁶.

Skin diseases

Atopic dermatitis

Atopic dermatitis, or eczema, is a common inflammatory, chronically relapsing skin disorder. The skin of patients become red, flaky and is often very itchy (see figure 1.2). Affected regions are mainly found on the flexural surfaces of the joints. Disease onset might occur at any age, but in 85% it starts before the age of 5⁴⁷. The prevalence of atopic dermatitis in children is 5-20% worldwide, but is increased in industrialized countries⁴⁸. In most of the cases (up to 70%), the disease disappears spontaneously before they reach adolescence⁴⁷.

Patients with an extrinsic or allergic form atopic dermatitis are characterized with a cutaneous infiltration containing highly reactive cells of dendritic lineage, including Langerhans cells and epidermal dendritic cells both of which express the high-affinity receptor for the Fc region of IgE (FcεRI) on their membrane⁴⁹. Although most patients with atopic dermatitis (70-85%) contain elevated levels of IgE⁵⁰, a minority of patients is characterized with normal IgE levels⁵¹. This type of atopic dermatitis as referred to as intrinsic or nonallergic atopic dermatitis.

Atopic dermatitis is a multifactorial disease in which both genetic and environmental factors are thought to be involved in its etiology. Several studies on twins have shown that the occurrence of atopic dermatitis among monozygotic twins is higher than among dizygotic twins^{52,53}. Factors like stress and infections may influence the severity and amount of exacerbations in atopic dermatitis patients^{54,55}. In general, two hypothesis have been proposed concerning the mechanism of atopic dermatitis⁴⁷. In the first hypothesis the primary defect is ascribed to an immunologic disturbance that causes IgE-mediated sensitization, with epithelial-barrier dysfunction as a consequence of the local inflammation. This hypothesis is supported by the identification of several candidate genes on chromosome 5q31-33 that are associated with atopic dermatitis. All of them encode cytokines involved in the regulation of IgE synthesis: IL-4, IL-5, IL-12, IL-13 and granulocyte-macrophage colony-stimulating factor (GM-CSF). The second hypothesis points to an inherent defect in epithelial cells, with subsequently could lead to immunological abnormalities. Single nucleotide polymorphisms (SNPs) associated with atopic dermatitis in genes located on chromosome 1q21, which harbours a family of epithelial-related genes known as the epidermal

differentiation complex (EDC), support the second hypothesis. Besides these two loci, also other atopic dermatitis-associated loci are found on chromosome 3q21, 17q25, 20p and 3p26⁴⁷. The most striking support for the second hypothesis was found when researchers identified mutations in filaggrin, a gene on chromosome 1q21.3, in 30% of European patients⁵⁶. These results were replicated in other cohorts⁵⁷⁻⁵⁹. Mutations in filaggrin result in reduced epidermal barrier function, fully supporting the second hypothesis.



Figure 1.2 Atopic dermatitis. Typical atopic dermatitis lesions on the back and in the face of a child and on the flexural sites of the knees with erythema, oozing and excoriations.

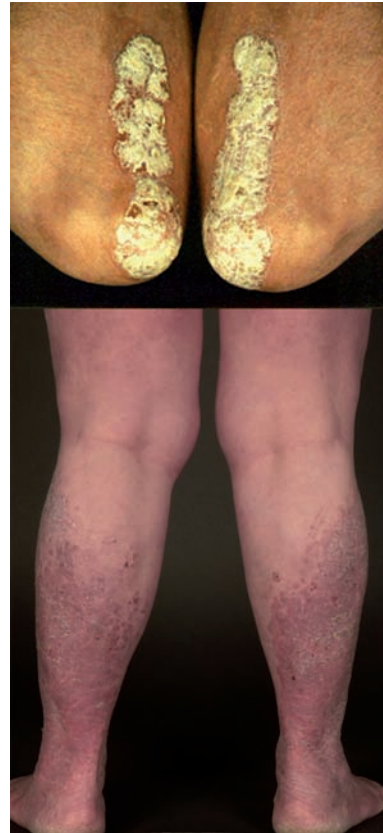


Figure 1.3 Psoriasis. Typical plaques of psoriatic skin. Thick, sharply demarcated plaques on the extensor site of elbows and legs with erythema and squamae.

Psoriasis

Psoriasis is a common, incurable chronic skin disease affecting 2-3% of the Western population⁶⁰. This inflammatory disease is characterized by an increased epidermal growth and altered differentiation leading to the typical clinical features. There are several different types of psoriasis described, of which chronic plaque psoriasis (psoriasis vulgaris) is the most common one (approximately 90% of all cases). This form of psoriasis is characterized by sharply demarcated and erythematous papulosquamous plaques (see figure 1.3). Less common types of psoriasis include nail psoriasis, inverse psoriasis, guttate psoriasis, pustular psoriasis and scalp psoriasis. Although psoriasis can occur in children, its initial

outbreak typically affects people in late adolescence or early adulthood⁶¹. Once initiated psoriasis usually persists for life, with a history of eruptions followed by temporary remissions⁶². In contrast to atopic dermatitis, there is a predilection for extensor sites of extremities. Also the scalp is often affected, as are hands, feet and presacrum. Based on linkage studies in twins and pedigrees, psoriasis has been characterized as a multifactorial disease in which both genomic^{63,64} and environmental factors as stress⁶⁵, trauma⁶⁶ and infection⁶⁷ might influence disease onset and activity. When patients develop lesions in response to physical trauma this is termed the Koebner effect⁶⁶, which has been observed in up to 25% of patients⁶⁸.

Histological examination of a stable psoriatic plaque show elongated and tortuous capillaries in the dermis, expanding upward into elongated club-shaped dermal papillae. Only a small suprapapillary plate of epidermal cells covers the tip of these dermal papillae. A modest perivascular infiltrate consists primarily of lymphocytes and macrophages. There are elongated rete ridges, foci with parakeratosis and a diminished presence or absence of the granular layer. Other defining histological features of psoriasis include the presence of neutrophils within small foci in the horny layer and significant mononuclear infiltrate in the epidermis⁶⁹.

Initially, it was thought that the cause of psoriasis was the hyperproliferative state of keratinocytes. Keratinocytes in psoriatic epidermis are indeed hyperproliferative, their journey from basal layer to desquamation is accelerated to 6-8 days, which results in an altered differentiation as well⁷⁰. Later the hypothesis was favoured that psoriasis is rather an immunological disease in which T lymphocytes are indirectly responsible for the phenotype of psoriasis⁷¹. According to the current point of view leukocytes and keratinocytes itself cause the characteristic changes in psoriasis⁷². Keratinocytes are no longer seen as bystander cells, but are actively involved in recruitment and activation of leukocytes in psoriatic lesions⁷³. Clinical observations suggest an important role of the innate cytokine IFN- α that induces the production of IL-12 and IL-23 by myeloid dendritic cells. This leads to the differentiation of naïve T cells in Th1 type (by IL-12) and Th17 type (by IL-23) cells. As a result, cytokines are produced that lead to the production of several antimicrobial peptides, proinflammatory cytokines, chemokines and S100 proteins involved in attracting activated dendritic cells and T cells. So, both the effector cells of the innate and adaptive immune system as well as the intrinsic character of keratinocytes are involved in inducing an inflammatory process leading to a psoriatic lesion⁷⁴.

As described above, psoriasis is a multifactorial disease in which genetic components could influence its onset. Classic genome wide linkage analysis have identified at least nine chromosomal loci with statistically significant linkage to psoriasis, referred as psoriasis susceptibility 1 till 9 (PSORS1 till PSORS9). PSORS1 accounts probably for 35-50% of the heritability of the disease⁷⁵ and this loci is the strongest and invariably reproduced psoriasis susceptibility locus, which is located within the major histocompatibility complex (MHC) on

chromosome 6p. More detailed characterization of PSORS1 identified HLA-Cw6 on 6p21.3 as very likely to be the disease allele at PSORS1⁷⁶. In addition to linkage studies genome wide association studies (GWAS) have subsequently resulted in numerous genetic variants linked to psoriasis. Most notably are the sequence variants in the genes coding for interleukin-23 receptor (IL23R) and its ligand (IL12B) that confer protection against psoriasis⁷⁷. In contrast to these immunological oriented associations, also genomic associations that address an important role for keratinocytes in the onset of psoriasis are described. First, an increased risk for psoriasis was associated with an increased beta-defensin copy number on chromosome 8p23.1⁷⁸. One of the genes on this cluster, beta-defensin 2 (hBD-2) is extremely upregulated in psoriatic skin⁷⁹. Furthermore, a deletion of late cornified envelope genes LCE3B and LCE3C was associated with increased risk for psoriasis^{80,81}.

Keratinocytes: key players in psoriasis and atopic dermatitis

Psoriasis and atopic dermatitis are the two most common chronic inflammatory skin diseases. In both disorders an important role in the pathogenesis is fulfilled by T cells, although the type of T cell lineage and the chemokine/cytokine profiles are different. Despite the role that the immune system plays in the pathogenesis of both diseases, there is growing evidence that also the keratinocytes themselves have an important role^{22,80,82}. Several studies have compared lesional skin of patients with psoriasis and atopic dermatitis^{27,83,84}. Initially, these studies were restricted to one or only a few genes or proteins^{43,85}. The first large-scale study was performed by microarray analysis on RNA obtained from full-thickness skin biopsies from lesional psoriatic and atopic dermatitis skin⁸³. In this study the differential expression of thousands of genes was compared resulting in a list of 80 genes that were significantly increased (>2-fold) in either psoriasis or atopic dermatitis. The maximal difference in gene expression level was found for the gene coding for Nel-like 2 (Nell2) protein, a neural tissue-specific epidermal growth factor (EGF)-like repeat domain-containing protein, which was upregulated in atopic dermatitis. Also several CC chemokines, known to attract Th2 cells, showed increased expression in atopic dermatitis when compared with psoriasis. The most highly upregulated gene in psoriasis as compared with atopic dermatitis was small proline-rich protein 2C (SPRR2C). Other genes with high expression levels in psoriasis code for several antimicrobial peptides and chemokines and cytokines that are known to attract Th1 cells and neutrophils. Although this microarray analysis showed differences in gene expression between psoriasis and atopic dermatitis, it is not clear which cells are responsible for the expression, because full-thickness biopsies were used. Keratinocytes are the main population of the epidermis, but resident dermal cells and immune cells were not removed in this study.

To gain more insight on keratinocytes expression profiles in lesional psoriasis and atopic dermatitis skin, our group performed microarray studies on epidermal sheets²⁷. Overall, we found more genes to be overexpressed in psoriasis, with

Table 1.1 Top 20 proteins upregulated in psoriasis detected by microarray analysis

Classification	Symbol	PS/AD ^a	RnRel ^b
Vanin 3	VNN3	18.90	17.56
Absent in melanoma 2 (PYHIN4)	AIM2	17.88	3.60
Hyaluronoglucosaminidase	HYAL4	9.71	4.68
Kynureninase (L-kynurenine hydrolase)	KYNU	8.40	3.63
Human β -defensin-2 (hBD-2)	DEFB4	7.94	7.79
Polycystic kidney disease 2-like2	PKD2L2	7.52	5.03
Calgranulin A (MRP8)	S100A8	7.36	4.65
Calgranulin C (MRP6)	S100A12	6.92	7.92
Solute carrier family 6, member 14	SLC6A14	6.87	7.70
Viperin (cig5)	RSAD2	6.50	4.29
Interleukin receptor 2 gamma (CD132)	IL2RG	5.66	4.49
Interleukin 1 family, member 8	IL1F8	5.66	6.51
Interferon inducible protein 44	IFI44	5.31	5.77
Nasopharyngeal epithelium specific protein 1	CCDC19	5.24	7.33
Interferon stimulated ubiquitin-like modifier	ISG15	4.69	4.38
Inducible T-cell co-stimulator ligand (B7H2)	ICOSLG	4.66	6.71
Guanine deaminase	GDA	4.63	4.39
Nitric oxide synthase 2 (iNOS)	NOS2	4.56	9.76
C-type lectin domain 7A (Dectin-1)	CLEC7A	4.35	5.85
Interleukin 1 family, member 9	IL1F9	4.20	6.28

^aFold difference of gene expression level in psoriasis compared with atopic dermatitis

^bt-statistics; significant as RnRel>3.5

vanin-3 (VNN3) as the highest differentially expressed one (19-fold). Vanin family members had not been demonstrated in the epidermis before, and their possible role in psoriasis is unclear, but a role in inflammatory bowel disease has been suggested⁸⁶. In line with previous studies, genes encoding antimicrobial peptides (hBD-1, hBD-2, elafin, calgranulin C and iNOS) were confirmed to be higher expressed in psoriasis compared with atopic dermatitis. In addition, also other antimicrobial peptides such as psoriasin, calgranulin A and B, chitinase and cystatin A, showed higher expression in psoriasis skin²⁷. From these antimicrobial peptides, hBD-2, calgranulin A and C showed up in the top twenty of proteins being overexpressed in psoriasis compared with atopic dermatitis. Furthermore, several genes encoding cytokines known to be overexpressed in psoriasis are present in Table 1.1. One of the genes with the highest differential expression in atopic dermatitis compared with psoriasis is carbonic anhydrase II (CAII), which

was also confirmed at the protein level⁸⁷. CAII participates in several processes that involve pH regulation and water- and electrolyte homeostasis⁸⁸. Other genes that are more abundant in atopic dermatitis skin compared with psoriasis are listed in Table 1.2 and include genes that code for chemokines and cytokines known to be involved in atopic dermatitis.

The challenge for researchers is to estimate whether these up- or downregulated genes are involved in the pathogenesis of psoriasis or atopic dermatitis and whether there are druggable genes among them that might be suitable for specific therapy. Besides involved in pathogenesis or being druggable genes, highly expressed genes might also be good candidates for biomarkers.

Table 1.2 Top 20 proteins downregulated in psoriasis detected by microarray analysis

Classification	Symbol	PS/AD ^a	RnRel ^b
Neurogenin 1	NEUROG1	7.89	5.03
Carbonic anhydrase II	CA2	7.68	21.19
Claudin 8	CLDN8	5.15	6.20
ADAM metalloproteinase domain 8	ADAM8	4.88	6.47
Chemokine (C-C motif) ligand 17	CCL17	4.57	3.71
Calpain 2, (m/II) large subunit	CAPN2	4.28	9.62
Amphiregulin	AREG	3.97	6.25
Janus kinase 1	JAK1	3.81	5.42
TNF receptor superfamily, member 6	FAS	3.61	5.63
Inhibin, beta A	INHBA	3.44	5.84
Pleckstrin homology-like domain A2	PHLDA2	3.37	7.50
Kruppel-like factor 4	KLF4	3.37	4.58
SLIT-ROBO Rho GTPase activating protein 1	SRGAP1	3.33	5.96
Integrin, alpha 6	ITGA6	3.32	3.99
Solute carrier family 43, member 1	SLC43A1	3.20	5.53
Platelet derived growth factor C	PDGFC	3.13	7.60
Adrenergic, beta-2-, receptor, surface	ADRB2	3.09	4.01
TSC22 domain family, member 1	TSC22D1	3.05	8.82
Actin, gamma 1	ACTG1	3.05	12.22
Peripheral myelin protein 22	PMP22	3.03	13.74

^aFold difference of gene expression level in psoriasis compared with atopic dermatitis

^bt-statistics; significant as RnRel>3.5

Part 2: Techniques

Reconstructed skin models: suitable for screening and *in vitro* skin research

Skin research has a history of different culture systems and models. In 1975, Rheinwald and Green⁸⁹ were the first describing a method for cultivation of keratinocytes in *in vitro* systems. They showed that keratinocytes need fibroblasts to initiate colony formation. To overcome that fibroblasts could overgrow keratinocytes, they irradiated the fibroblasts prior to keratinocyte seeding. Once these colonies are formed they are able to maintain themselves in subsequent subcultures, although primary keratinocytes have a limited lifespan and proliferation rate decreases in time. Morphologically, these colonies contain features of differentiation with dividing keratinocytes and differentiated keratinocytes on top. Studies based on this system have gained much information about these cells in both a biological and pharmacological point of view. Although the utilization of culturing keratinocytes in monolayers on the bottom of a culture plates was historically important as this was an initial step in maintaining keratinocytes in *in vitro* models, scientifically these keratinocytes fail to reproduce the complex and dynamic processes of *in vivo* skin. Furthermore, 2D culture systems do not completely resemble the *in vivo* situation, as cultured keratinocytes are forced to adapt to an artificial, flat surface, which might result in altered gene expression profiles⁹⁰. In order to study cell-cell interactions and effects on the regulation of melanogenesis, proliferation and differentiation of keratinocytes, but also the re-epithelialisation process after (burn)wounding, a model is required that resembles the basic architecture of the human skin. Therefore, a fully stratified epidermis containing all different layers beginning with basal cells on the bottom and a *stratum corneum* on top, is required. Over the past decades several systems have been published, describing 3D reconstructed skin equivalents. Basically all of these systems are based on the method described by Pruniéras⁹¹ in which keratinocytes are grown submerged on a dermal substitute to form a basal layer followed by an air-lifted phase in which the keratinocytes are forced to differentiate upwards, resulting in a stratified reconstructed skin. The dermal substitute can be composed of cell-free dermal matrices like de-epidermized dermis (DED), but also inert filters, fibroblast-populated collagen matrices and lyophilized collagen-GAG membranes might act as dermal substitute. Initially, the cellular components of the epidermis consist of solely primary keratinocytes which represents about 90% of the epidermal cells in human skin *in vivo*. More recently, also small proportions of melanocytes are introduced in reconstructed skin models, resulting in even more lifelike constructs⁹². Main drawback of these increasing sophisticated reconstructed skin models is that they became more labour intensive, thus more expensive. As a consequence, the number of commercially available skin models has increased over the past years. These skin equivalents are mostly derived from foreskin keratinocytes and used in a wide variety of biological studies, skin corrosion testing and irradiation studies⁹³.

Although reconstructed skin models were primarily developed for treatment of skin defects like burn wounds and ulcers, they have had great impact on both basic and applied research⁹⁴. Reconstructed skin models might also be a suitable alternative for animal testing. This would lead to a significant reduction of animal use and discomfort, and furthermore, testing for skin irritation in animals is not always predictive for human responses.

Reconstructed diseased skin models: psoriasis and atopic dermatitis

A specific and challenging use of reconstructed skin models is to mimic a disease-specific pheno- and genotype. These models may be useful to investigate the epidermal aspects of pathology and to study therapeutics that act at the level of keratinocytes biology. The first *in vitro* reconstructed model for diseased skin was described by Barker *et al.*⁹⁵. They used keratinocytes and fibroblasts from psoriatic patients and compared the reconstructed skin with constructs obtained with keratinocytes and fibroblasts from healthy controls. Besides an increase in proliferation, as measured with Ki67-positive cell counting, in their patient derived constructs, they were also able to detect increased psoriasis associated gene expression of CXCR2 and induced expression of pro-inflammatory genes TNF- α , IFN- γ and IL-8. Another approach to achieve a psoriasis-like reconstructed skin construct was described by Harrison *et al.*⁹⁶. They used keratinocytes derived from healthy individuals in combination with transglutaminase inhibitors. The inhibitors resulted in hyperproliferation and parakeratosis in their constructs, both hallmarks of a psoriatic phenotype. To obtain a psoriasis-like phenotype in a more controllable way using normal human keratinocytes, psoriasis-associated cytokines (TNF- α , IL-1 α , IL-6, IL-22) can be added during the last 4 days of the air-exposed phase. These cytokines are able to induce psoriasis-associated protein expression of hBD-2, elafin and K16⁹⁷. Furthermore, it was shown that the anti-psoriatic drug retinoic acid was able to inhibit the cytokine-induced keratinocyte gene expression at both the mRNA and protein level⁹⁷.

In an attempt to obtain a reconstructed skin model with properties resembling atopic dermatitis, lymphocytes were integrated⁹⁸. Infiltration of activated CD45RO+ T cells into the construct induces apoptosis in keratinocytes, which leads to reduced expression of the adhesion molecule E-cadherin and disruption of the epidermal barrier. Pro-inflammatory cytokines (IL-1 α and IL-6 and chemokines (i.e. IL-8 and RANTES) are induced and production could be inhibited with therapeutics (dexamethasone and FK506). Also other atopic dermatitis associated properties like upregulation of neurotrophin-4 (NT-4), involved in mediating pruritus in lesions, and intercellular adhesion molecule-1 (ICAM-1), responsible for the attachment of leukocytes to epidermal cells, are found in these constructs⁹⁸. Another atopic dermatitis model is principally similar to the psoriasis model described by Tjabringa *et al.*⁹⁷. Normal human keratinocytes in a reconstructed skin model are stimulated with Th2 cytokines IL-4 and IL-13. Morphologically, these Th2 cytokines induced intercellular oedema similar to spongiotic changes found in lesional atopic dermatitis. Furthermore, induced

apoptosis and atopic dermatitis associated gene expression of CAII and Nell2 was observed⁹⁹.

Transgenic expression systems: transfection and infection

In order to study specific gene function *in vitro*, two different approaches can be distinguished: overexpression and knockdown experiments. Both approaches could gain useful information about protein function. This section will give an overview on overexpression systems and their suitability for primary keratinocytes. The next section will focus on gene functionality studies after knockdown experiments.

Overexpression is achieved after introducing foreign DNA into host cells that ultimately lead to transcription and translation of the introduced gene. Main problem is that cells, including mammalian cells, are impenetrable to large molecules that, like DNA, are electrically charged. Therefore, systems were created to overcome this problem (see figure 1.4). In general, two types of gene delivery systems can be distinguished, non-viral and viral systems. The non-viral system dates from the early 70s when researchers used carrier molecules that form, together with DNA, a non-charged molecule. DNA was coated with DEAE-dextran that help DNA to pass the membrane, a process they termed 'transfection'¹⁰⁰. Another carrier molecule, calcium phosphate appeared less toxic than DEAE-dextran¹⁰¹. To date, these systems are still used, although many labs prefer the subsequently described lipid-based transfection reagents. These reagents are, though more expensive than the previously described carrier molecules, easier to use and obtain higher efficiencies with lower toxicity. The first lipid-based reagents contain cationic and other lipids that envelope DNA, forming artificial liposomes that can fuse with the cellular membrane leading to the release of the DNA into cells¹⁰². The next generation of lipid-based reagents consists of lipids combined with polymers and are thought to form a complex with DNA in a non-liposomal way that will interact with the cell membrane. After endocytosis, the DNA is released in the cytoplasm. In contrast to liposomes, non-liposomal reagents form micelles of a uniform size resulting in more reproducible results¹⁰³. Commercially available reagents like Lipofectamine 2000 and FuGENE 6 are based on this system, although their exact composition remain commercial secrecy¹⁰⁴. Lipid- or polymer-based gene delivery systems are sometimes referred to as chemical transfection reagents, which is rather a strange name as no chemical reactions are involved.

Another non-viral method to introduce DNA into cells is by using physical power. A common method to physically transfect cells is by using high-voltage pulses of electricity, called electroporation¹⁰⁵. The electric pulse produces holes in the cell membrane, through which DNA can enter. This method can be used for many cell types, including primary cells. Cells must be in solution and high amount of cells are needed as many cells die after the electric shock. Another physical system available for transfection is the gene gun. Using the gene gun particles of gold coated with DNA are shot via an adjustable low pressure helium pulse into cells or tissue. Although gene guns are mostly applied in plant biology, they also have been successfully used in animal and human research, including

skin research¹⁰⁶.

Although non-viral gene delivery systems are suitable for a wide variety of cell types, their transfection efficiencies might be disappointing, especially when working with primary cells. To achieve high efficiencies in hard-to-transfect cell-types, one could consider using a viral gene delivery system¹⁰⁷. Although working with viruses is more time-consuming and often requires special biosafety facilities, viruses became a very popular alternative to the traditional gene delivery methods. Viruses are able to infect near 100% of almost any cell-type, a process referred as transduction: introducing nucleic acid into cells via virus particles. The mechanism by which viruses are able to enter the host cell are virus-specific¹⁰⁸. In general viruses attach to specific receptors on the host cell surface via viral capsid proteins followed by endocytosis or membrane fusion, a process called penetration. Depending on the nature of the virus, mRNA transcription or the genomic integration mechanism will start. There are several viral vectors suitable for transduction of mammalian cells¹⁰⁹, of which lentiviruses are the most promising. The modification of viruses in order to induce exogenous gene expression was

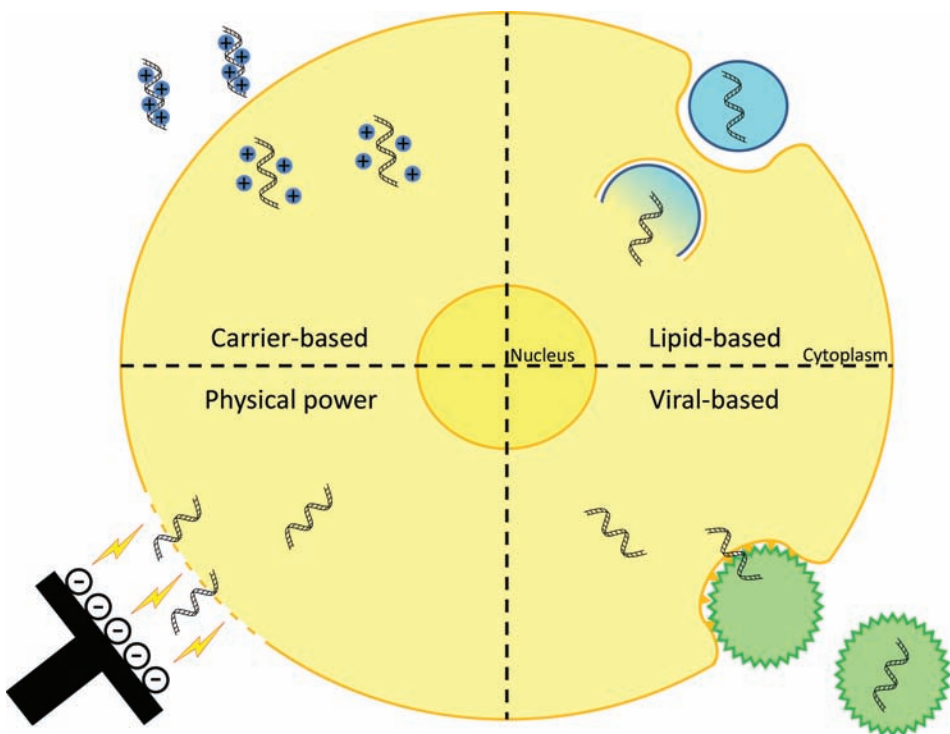


Figure 1.4 Transfection methods. Schematic representation of four general transfection methods. DNA can be transferred into cells using a carrier to neutralize the DNA molecule like calcium phosphate. Lipid-based transfection reagents were developed that envelope the DNA. After endocytosis, the DNA is released in the cell. The third method uses physical power, e.g. high-voltage pulses of electricity, to create holes in the cell membrane through which DNA can enter the cell. Also viruses can be used for transfecting cells. Viruses attach to the membrane via specific receptors on the cell membrane. Via penetration the DNA enters the host cell.

first described in tobacco plants that were successfully infected with modified tobacco mosaic virus¹¹⁰. For transgenic expression in mammalian cells several virus-derived systems have been developed. The most common used viruses are derived from retrovirus, lentivirus, adenovirus and adeno-associated virus¹⁰⁹. But also vectors derived from herpes simplex virus, poxvirus and Epstein-Barr virus have been successfully used to transduce mammalian cells¹¹¹⁻¹¹³. Focusing on the most used viral vector systems, retroviruses are highly infectious viruses, but only dividing cells are susceptible for infection¹¹⁴. Once a cell is transduced with retrovirus, its DNA will be stable integrated into the host cells genome, resulting in sustained transgenic expression. In contrast, adenovirus and adeno-associated viruses are able to induce both dividing and non-dividing cells, but do not integrate into the genome of their host¹¹⁵. Thereby the transgenic effect will fade away upon cell division. The last common-used viral gene delivery system, the lentiviruses, are able to infect both dividing and non-dividing cells and are able to integrate into the genome of infected cells¹¹⁵. For safety issues it took a while before lentiviruses were suitable for routine laboratory use. After the introduction of so-called self-inactivating (SIN) lentiviral vectors, the use of lentiviral particles for transgenic expression grew extensively¹¹⁶.

For a long time it has been a challenge to induce stable transgenic protein expression in primary human keratinocytes. Non-viral gene delivery systems like calcium phosphate precipitation or commercially available reagents result in low transfection efficiencies of maximal 30% positive cells¹¹⁷. Another problem using primary cells versus cell-lines, is that primary cells have a limited lifespan, which makes it almost impossible to obtain clones using antibiotic selection. Therefore, viral gene delivery systems are ideal for human keratinocytes, as they are able to achieve high transduction efficiencies¹⁰⁷. For *in vitro* studies retroviral systems are not favoured for primary human keratinocytes as they are unable to transduce non-dividing cells, however *in vivo* retrovirus based gene therapy has been successfully implemented¹¹⁸. Adenovirus and adeno-associated viruses are able to transduce both dividing and non-dividing cells, but these viruses are unable to integrate into the host cells genome, thereby causing a transient transgenic expression. These viruses are suitable for research on keratinocytes, but because of the transient expression properties lentiviral particles are preferred, as these result in a sustained transgenic expression^{119,120}. It has been shown that primary human keratinocytes transduced with lentivirus containing a green fluorescent protein, result in nearly 100% fluorescent positive cells¹⁰⁷. Furthermore, it was shown that these keratinocytes continue expressing the fluorescent protein in time¹⁰⁷.

RNA interference

In the previous section systems were described to study gene function after overexpression. Another method to study gene function is by decreasing its expression, termed RNA interference (RNAi). RNAi is a mechanism that induces posttranscriptional gene silencing via sequence specific mRNA degradation^{121,122}.

It was first described in 1984 when scientists observed transcriptional inhibition by antisense RNA^{123,124}. In the early 90s it became clear that it was a conserved process functioning as an antiviral system via the silencing of viral genes^{125,126}. RNAi occurs naturally in fungi, plants and animals, where long double stranded RNA (dsRNA) triggers RNAi¹²⁷. RNAi involves a multistep process. First double-stranded RNA (dsRNA) is recognized by Dicer, an RNase III family member, and cleaved into small interfering RNA (siRNA) molecules of about 20-25 nucleotides long^{127,128}. Dicer also initiates the formation of the RNA-Induced Silencing Complex (RISC), which contains argonaute as catalytic component with endonuclease activity capable of degrading messenger RNA (mRNA) whose sequence is complementary to that of the siRNA guiding strand¹²⁹. Subsequently, the guiding strand binds to the target mRNA, which is also cleaved by argonaute resulting in translational repression¹²⁷ (see figure 1.5).

RNAi has become an important research tool as an alternative for knock-out animals to investigate gene function by repressing its expression. Since the discovery of RNAi several approaches were designed and described to perform RNAi in an easy and safe environment. In general there are three main types of RNAi that can be used to study gene function: synthetic RNAi delivery systems, plasmid transfection systems and viral infection systems.

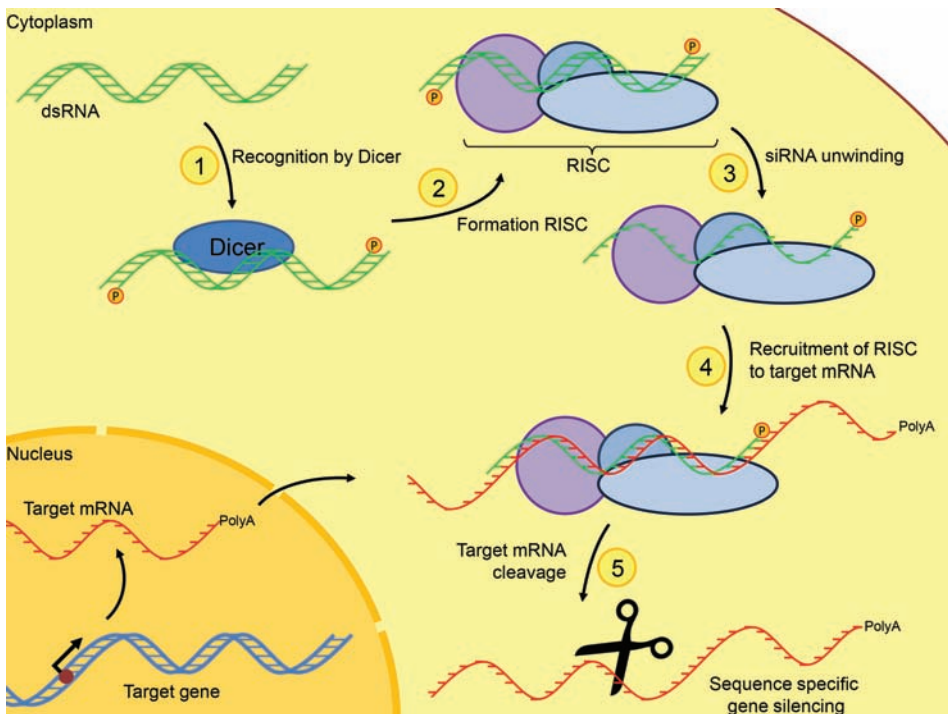


Figure 1.5 RNAi mechanism. Double-stranded RNA (dsRNA) is recognized by Dicer and cleaved into small interfering RNA (siRNA). Subsequently, Dicer initiates the formation of the RNA-induced silencing complex (RISC). RISC unwinds the siRNA molecule and degrades the complementary strand, resulting in a single stranded RNA molecule. The guiding strand is guided to the target mRNA molecule, which will be degraded by RISC, resulting in sequence specific gene silencing.

The less labour-intensive way to achieve RNAi is by using synthetic RNA oligos¹³⁰. Two complementary primers are designed that target a specific part of the gene of interest. Prior to transfection the primers are annealed, resulting in a double-stranded siRNA molecule. After transfection these molecules are recognized and processed by Dicer and enter the RNAi pathway¹³⁰. Because this is an easy and quick method, it is feasible for testing different target sequences for testing which part of the mRNA is most sensitive for RNAi. A disadvantage is the relative short effect of these oligos. Each siRNA molecule is only active for one time and after cell division the oligo duplexes left are divided over two daughter cells. This can be overcome by transfecting cells multiple times, which increases the costs extensively.

The second method uses plasmids containing a small hairpin under control of a polymerase III promoter (e.g. U6 or H1)¹³¹. After transformation into mammalian cells these plasmids start to produce small hairpin RNAs (shRNA) which are recognized by Dicer and are subsequently transformed into siRNA molecules resulting in sequence specific gene silencing. The disadvantage of this method is that it is a cloning-based approach which requires more intensive laboratory work. First, plasmids containing your specific hairpins should be cloned. The advantage above synthetic oligos is that there is, once transformed into a cell, a continuous production of siRNAs, resulting in an almost infinite stock.

The last method to achieve RNAi is by using viral constructs to infect cells. This method has a lot of similarities with the second one, but instead of using plasmids as shRNA delivery system a virus is used. The hairpin is cloned into a viral transfer plasmid, which is used to produce recombinant virus. These viruses can infect cells and the shRNAs are expressed under control of a H9 or U1 polymerase III promoter. As described in the previous section various viral vectors are available to date. For knock-down experiments mainly the same advantages and disadvantages account as for overexpression experiments using viral vectors. For primary human keratinocytes the lentiviral system is most suitable, as they will integrate into the target cells genome resulting in sustained shRNA expression.

Part 3: background on specific molecules studied in this thesis

β -defensins

Defensins are secreted cationic peptides with a small molecular mass of 3-5 kDa and are divided on alpha and beta subfamilies based on the intramolecular disulfide bonds¹³². Defensins are microbicidal peptides active against both gram-negative and gram-positive bacteria, fungi and enveloped viruses¹³³. Alpha-defensins are almost exclusively expressed in neutrophils, while beta-defensins expression is more found on epithelial cells¹³⁴.

The genes coding for human β -defensins (DEFB genes) are grouped in three main gene clusters. Two clusters are located on chromosome 20 (20p13 and 20q11.21) and one cluster is located on chromosome 8 (8p23.1)¹³⁴. β -defensins are characterized by three pairs of intramolecular disulphide bonds and possess broad antimicrobial activity¹³³. The spectrum of antimicrobial activity varies for each of the β -defensins. DEFB1 (hBD-1) and DEFB4 (hBD-2) have been shown to be particularly active against gram-negative bacteria and some fungi, but are relatively less potent against gram-positive bacteria¹³⁵. In contrast, DEFB103 (hBD-3) has a broad range of antimicrobial activity against yeast, gram-negative and gram-positive bacteria²⁹. Besides antimicrobial activity β -defensins are also described to exhibit proinflammatory properties as chemoattractants for memory T-cells, immature dendritic cells, mast cells and neutrophils¹³⁶.

The cluster on chromosome 8 contains eight beta-defensin genes. All but DEFB1 are on a large repeat that is variable in copy number¹³⁷. It was found that the human genome could contain up to 12 copies of this repeat per diploid genome, with a mode of four. Because expression of DEFB103 and DEFB4, both positioned on the repeat, is induced in psoriatic skin, it was tempting to search for a correlation between beta-defensin copy number and psoriasis. Indeed, an association was found between a higher genomic copy number and risk for psoriasis⁷⁸. Subsequently beta-defensin copy number is associated with other, mainly epithelial, diseases: Crohn's disease (initially a lower copy number was associated¹³⁸, but Bentley *et al.*¹³⁹ found an association with higher copy numbers of the beta-defensin cluster), celiac disease (lower copy numbers are associated with patient¹⁴⁰), severe acute pancreatitis (association between lower copy number and disease¹⁴¹), chronic obstructive pulmonary disease (copy number greater or equal to 5 was associated with increased risk¹⁴²) and sporadic prostate cancer (high copy numbers above 9 are underrepresented in patients¹⁴³).

The vanin gene family

The first reference to vanins was in 1996. Mouse vanin-1 was found as a molecule involved in the regulation of thymus homing in hematopoietic precursor cells¹⁴⁴. Its exact function remains unclear; no homology with other adhesion molecules was found, but sequence analysis showed some homology with human biotinidase¹⁴⁵.

The name vanin was derived from vascular non-inflammatory molecule, pointing to the state and cell-type the protein was found¹⁴⁴. Independently, Suzuki *et al.*¹⁴⁶ found a GPI-anchored protein (referred as GPI-80) on human leukocytes that was involved in the regulation of neutrophil adherence and migration. They found that GPI-80 was highly homologous with vanin-1 and subsequently GPI-80 was identified as VNN2. Finally the human vanin gene family appeared to consist of three genes (VNN1, VNN2 and VNN3), which are located on the long arm of chromosome 6 (6q23.2). Mice lack an orthologue of VNN2, so they only contain vanin-1 and vanin-3, which are located on mouse chromosome 10A2B1¹⁴⁷. Via a glycosylphosphatidylinositol (GPI) anchor VNN1 and VNN2 are membrane-bound ectoenzymes, while VNN3 is expected to be secreted as it lacks a GPI anchor. Free VNN2 has also been described¹⁴⁸, possibly as a results of alternative splicing¹⁴⁹.

Already in 1968, an enzymatic conversion of pantetheine to pantothenic acid (vitamin B5, a coenzyme A precursor) and the antioxidant cysteamine via hydrolysis of the carboamide linkage between them was found in horse kidneys^{150,151}. The protein responsible for this conversion was called pantetheinase and its enzymatic conversion was termed pantetheinase activity (see figure 1.6a). The human enzyme had never been isolated, but pantetheinase activity has been observed in various human cells (fibroblasts, leukocytes and intestinal cells) and plasma¹⁵²⁻¹⁵⁴. In 1999, vanins were identified to be responsible for this activity after sequencing and aligning tryptic and chemotryptic peptides of this protein isolated from pig kidney¹⁵⁵. This was confirmed for membrane-bound vanin-1 in vanin-1 deficient mice, since these mice lack free cysteamine in tissues that express vanin-1 in wild-type mice¹⁵⁶.

As described above, vanins are enzymes that posses pantetheinase activity by hydrolyzing pantetheine into pantothenic acid and cysteamine and thus are likely to be involved in coenzyme A synthesis^{151,157}. Wilson *et al.*¹⁵⁸ described a theory in which vanin-1 has a central role in the recycling of coenzyme A after degradation, which releases free pantetheine (see figure 1.6b). They found transcription factor sites in the proximal promoter region that are involved in vanin-1 transcription. Steroidogenic factor-1 (SF-1) initiates the expression, which is further augmented by SOX8/9. Vanin-1 is suggested to be required to provide an appropriate environment for male cell development and thereby being a regulator during mouse testis development^{158,159}.

The development of a vanin-1 knockout mouse resulted in many new insights in the function of vanins. Vanins have been proposed to exert a role in inflammatory bowel disease, as mice lacking vanin-1 showed a decreased non-steroidal anti-inflammatory drug (NSAID)- and *Schistosoma*-induced intestinal inflammation, which can be completely reversed by oral administration of cystamine, the oxidized form of cysteamine⁸⁶. Vanin-1 licenses the production of inflammatory mediators by intestinal epithelial cells by antagonizing peroxisome proliferator-activated receptor (PPAR) γ ¹⁶⁰. In a colitis-associated colon cancer model vanin-1 knockout mice display a drastically reduced incidence of colorectal

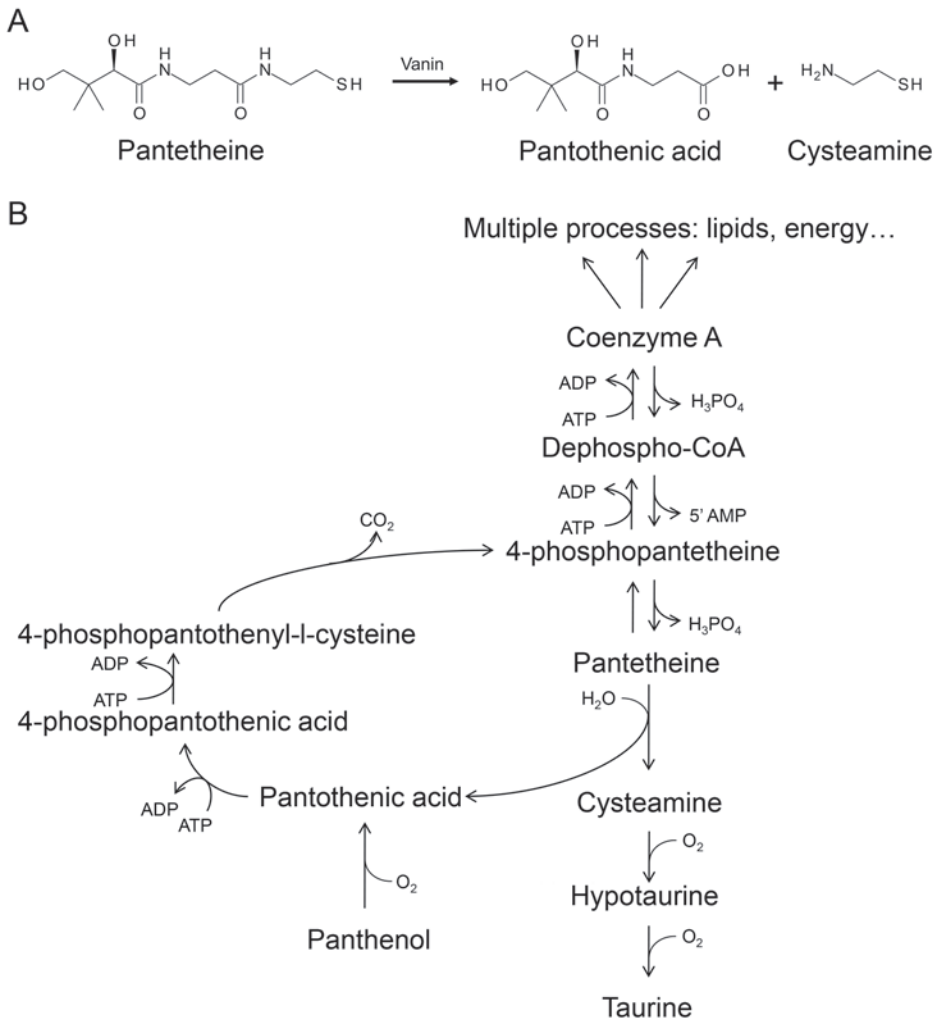


Figure 1.6 Biological processes of vanins. (A) Vanins are enzymes that possess pantetheinase activity by the hydrolysis of pantetheine into pantothenic acid (vitamin B5) and cysteamine. (B) Vanins are thought to play a role in CoA metabolism by recycling pantothenic acid.

cancer¹⁶¹. Furthermore, infecting vanin-1 deficient mice with *Coxiella burnetii*, a bacterium that causes Q fever, the formation of granuloma is reduced as compared with wild-type mice while mortality and morbidity of the mice were not affected¹⁶². These findings were correlated to a decreased expression of inducible nitric oxide synthase (iNOS) and MCP-1, while IL-10 and arginase expression were increased. On the other hand, the absence of vanin-1 in mice aggravates the development of type 1 diabetes. Apparently, cysteamine has a major cytoprotective role for islet cells, which cell death is a key initiating and perpetuating event in type 1 diabetes development¹⁶³.

Studies on VNN2 showed expression mainly on neutrophils in various organs. VNN2 expression is sublocated in secretory vesicles and linked to play a role in

neutrophil extravasation as a regulator of β_2 integrin in neutrophils^{164,165}. In resting neutrophils VNN2 expression is associated with β_2 integrin, but during neutrophil migration VNN2 is located on the pseudopodia while β_2 integrin remains located on the cell body¹⁶⁶. Using another antibody against VNN2, contradictory results were found where VNN2 expression appears associated with β_2 integrin during migration¹⁶⁷, suggesting two different populations of VNN2. Indeed Nitto *et al.*¹⁴⁹ found four splice variants of VNN2 expressed in neutrophils, resulting in different proteins. These findings suggest multiple functions for VNN2. TNF- α induces the release of VNN2 from human neutrophils, but did not affect surface VNN2 levels¹⁶⁸. Besides on neutrophils VNN2 expression was also found on the subpopulation of monocytes that is more involved in phagocytosis and reactive oxygen production than antigen presentation (CD14-positive monocytes)¹⁶⁹. Exogenous expression of VNN2 in Chinese hamster ovary (CHO) cells influences cell spreading via extracellular matrix molecules¹⁷⁰.

Occasionally, members of the vanin gene family are described in genomic studies in which the expression is altered, or an association with disease is found. In most cases the link between vanin expression and disease activity remains unclear. The absence of vanin-1 and vanin-3 mRNA in A/J mice is associated with susceptibility to malaria¹⁷¹. In this study the relation between malaria susceptibility and vanin activity appears clear as administration of cystamine to A/J mice partially restores their susceptibility as measured by reduced blood parasitemia and decreased mortality. Subsequently this group showed that cystamine acts specifically against plasmodium parasites, as cystamine does not protect against the parasite *Trypanosoma cruzi* or the fungal pathogen *Candida albicans*¹⁷², suggesting that cystamine does act directly on Plasmodium and does not modulate a host inflammatory response. Finally, they describe that cystamine potentiates the antimalarial agent artemisinin¹⁷³. In an approach to discover cis-regulated transcripts that influence complex traits in human, sequence variations in the VNN1 gene appear to influence high-density lipoprotein cholesterol concentration¹⁷⁴. The VNN1 promoter contains methylation-sensitive SNPs, which makes the gene sensitive for allele-specific DNA methylation¹⁷⁵. Another association was found in synovial fluids of rheumatoid arthritis patients, where high levels of soluble VNN2 were detected as compared with their serum concentration suggesting an active role of VNN2 in inflammation¹⁴⁸. More recently, VNN1 has been ascribed as a blood biomarker in a 7-gene panel for colorectal cancer¹⁷⁶. These results were independently confirmed in another group of patients¹⁷⁷. The expression van VNN1 combined with expression of metalloproteinase 9 (MMP9) could be used to discriminate pancreatic cancer-associated diabetes from type 2 diabetes¹⁷⁸. A study for differentially expressed genes between invasive and noninvasive human thymoma revealed VNN2 to be highly upregulated¹⁷⁹. As described in the previous section, VNN3 appears highly upregulated in lesional psoriatic epidermis as compared with affected epidermis derived from atopic dermatitis patients²⁷. At this point, nothing was known of the expression of vanins in skin.

1.10. Aims of this thesis

Over the last 6 years, the role of keratinocytes in the most common skin diseases has been extensively investigated. A microarray study by our group formed the basis of a PhD project granted by the Radboud University Nijmegen Medical Centre to our department. The broad aim was to investigate disease-specific epidermal gene expression, and to examine the relevance of genes (DEFB4 and VNN3) in the aetiology, diagnostics and therapy of psoriasis and eczematous diseases (chapters 2, 3 and 4) . We improved and designed skin models to investigate gene function with new sophisticated methods (chapters 5 and 6). Finally, we designed small molecules that target the vanins (chapter 7), which might be useful in applications (antibiotics) that fall beyond the dermatological scope (chapter 8).

References

1. Kanitakis J. Anatomy, histology and immunohistochemistry of normal human skin. *Eur J Dermatol* 12, 390-9 (2002)
2. Fuchs E, Raghavan S. Getting under the skin of epidermal morphogenesis. *Nat Rev Genet* 3, 199-209 (2002)
3. Candi E, Schmidt R, Melino G. The cornified envelope: a model of cell death in the skin. *Nat rev Mol Cell Bio* 6, 328-40 (2005)
4. Segre JA. Epidermal barrier formation and recovery in skin disorders. *J Clin Invest* 116, 1150-8 (2006)
5. Green KJ, Gaudry CA. Are desmosomes more than tethers for intermediate filaments? *Nat Rev Mol Cell Bio* 1, 208-16 (2000)
6. Moll R, Divo M, Langbein L. The human keratins: biology and pathology. *Histochem Cell Biol* 129, 705-33 (2008)
7. Fuchs E. Epidermal differentiation: the bare essentials. *J Cell Biol* 111, 2807-14 (1990)
8. Eckert RL, Crish JF, Robinson NA. The epidermal keratinocyte as a model for the study of gene regulation and cell differentiation. *Physiol Rev* 77, 397-424 (1997)
9. Madison KC. Barrier function of the skin: "la raison d'être" of the epidermis. *J Invest Dermatol* 121, 231-41 (2003)
10. Lorand L, Graham RM. Transglutaminases: crosslinking enzymes with pleiotropic functions. *Nat rev Mol Cell Bio* 4, 140-56 (2003)
11. Elias PM. Stratum corneum defensive functions: an integrated view. *J Invest Dermatol* 125, 183-200 (2005)
12. Nemes Z, Marekov LN, Fesus L, Steinert PM. A novel function for transglutaminase 1: attachment of long-chain omega-hydroxyceramides to involucrin by ester bond formation. *Proc Natl Acad Sci USA* 96, 8402-7 (1999)
13. Steinert PM, Marekov LN. Initiation of assembly of the cell envelope barrier structure of stratified squamous epithelia. *Mol Biol Cell* 10, 4247-61 (1999)
14. Kalinin AE, Kajava AV, Steinert PM. Epithelial barrier function: assembly and structural features of the cornified cell envelope. *Bioessays* 24, 789-800 (2002)
15. Steinert PM, Marekov LN. The proteins elafin, filaggrin, keratin intermediate filaments, loricrin, and small proline-rich proteins 1 and 2 are isodipeptide cross-linked components of the human epidermal cornified cell envelope. *J Biol Chem* 270, 17702-11 (1995)
16. Eckert RL, Yaffe MB, Crish JF, Murthy S, Rorke EA, Welter JF. Involucrin--structure and role in envelope assembly. *J Invest Dermatol* 100, 613-7 (1993)
17. Nemes Z, Marekov LN, Steinert PM. Involucrin cross-linking by transglutaminase 1. Binding to membranes directs residue specificity. *J Biol Chem* 274, 11013-21 (1999)
18. Steinert PM, Marekov LN. Direct evidence that involucrin is a major early isopeptide cross-linked component of the keratinocyte cornified cell envelope. *J Biol Chem* 272, 2021-30 (1997)
19. Mehrel T, Hohl D, Rothnagel JA, Longley MA, Bundman D, Cheng C *et al.* Identification of a major keratinocyte cell envelope protein, loricrin. *Cell* 61, 1103-12 (1990)
20. Dale BA, Holbrook KA, Steinert PM. Assembly of stratum corneum basic protein and keratin filaments in microfibrils. *Nature* 276, 729-31 (1978)

21. Smith FJ, Irvine AD, Terron-Kwiatkowski A, Sandilands A, Campbell LE, Zhao Y *et al.* Loss-of-function mutations in the gene encoding filaggrin cause ichthyosis vulgaris. *Nat Genet* 38, 337-42 (2006)
22. Irvine AD, McLean WH. Breaking the (un)sound barrier: filaggrin is a major gene for atopic dermatitis. *J Invest Dermatol* 126, 1200-2 (2006)
23. Proksch E, Brandner JM, Jensen JM. The skin: an indispensable barrier. *Exp Dermatol* 17, 1063-72 (2008)
24. Proksch E, Feingold KR, Man MQ, Elias PM. Barrier function regulates epidermal DNA synthesis. *J Clin Invest* 87, 1668-73 (1991)
25. Mao-Qiang M, Feingold KR, Elias PM. Inhibition of cholesterol and sphingolipid synthesis causes paradoxical effects on permeability barrier homeostasis. *J Invest Dermatol* 101, 185-90 (1993)
26. Lavker RM, Kaidbey KH. Redistribution of melanosomal complexes within keratinocytes following UV-A irradiation: a possible mechanism for cutaneous darkening in man. *Arch Dermatol Res* 272, 215-28 (1982)
27. de Jongh GJ, Zeeuwen PL, Kucharekova M, Pfundt R, van der Valk PG, Blokx W *et al.* High expression levels of keratinocyte antimicrobial proteins in psoriasis compared with atopic dermatitis. *J Invest Dermatol* 125, 1163-73 (2005)
28. Schroder JM, Harder J. Antimicrobial skin peptides and proteins. *Cell Mol Life Sci* 63, 469-86 (2006)
29. Harder J, Bartels J, Christophers E, Schroder JM. Isolation and characterization of human beta -defensin-3, a novel human inducible peptide antibiotic. *J Biol Chem* 276, 5707-13 (2001)
30. Liu AY, Destoumieux D, Wong AV, Park CH, Valore EV, Liu L *et al.* Human beta-defensin-2 production in keratinocytes is regulated by interleukin-1, bacteria, and the state of differentiation. *J Invest Dermatol* 118, 275-81 (2002)
31. Harder J, Bartels J, Christophers E, Schroder JM. A peptide antibiotic from human skin. *Nature* 387, 861 (1997)
32. Sallenave JM. Antimicrobial activity of antiproteases. *Biochem Soc Trans* 30, 111-5 (2002)
33. Hiemstra PS, Maassen RJ, Stolk J, Heinzel-Wieland R, Steffens G, Dijkman JH. Antibacterial activity of antileukoprotease. *Infect Immun* 64, 4520-24 (1996)
34. Dumas S, Kolokotronis A, Stefanopoulos P. Anti-inflammatory and antimicrobial roles of secretory leukocyte protease inhibitor. *Infect Immun* 73, 1271-4 (2005)
35. Simpson AJ, Maxwell AI, Govan JR, Haslett C, Sallenave JM. Elafin (elastase-specific inhibitor) has anti-microbial activity against gram-positive and gram-negative respiratory pathogens. *FEBS Lett* 452, 309-13 (1999)
36. Gilliet M, Lande R. Antimicrobial peptides and self-DNA in autoimmune skin inflammation. *Curr Opin Immunol* 20, 401-7 (2008)
37. Howell MD, Jones JF, Kisich KO, Streib JE, Gallo RL, Leung DY. Selective killing of vaccinia virus by LL-37: implications for eczema vaccinatum. *J Immunol* 172, 1763-7 (2004)
38. Wang TT, Nestel FP, Bourdeau V, Nagai Y, Wang Q, Liao J *et al.* Cutting edge: 1,25-dihydroxyvitamin D3 is a direct inducer of antimicrobial peptide gene expression. *J Immunol* 173, 2909-12 (2004)
39. Glaser R, Harder J, Lange H, Bartels J, Christophers E, Schroder JM. Antimicrobial psoriasin (S100A7) protects human skin from *Escherichia coli* infection. *Nat Immunol*

- 6, 57-64 (2004)
40. Glaser R, Meyer-Hoffert U, Harder J, Cordes J, Wittersheim M, Kobliakova J *et al.* The antimicrobial protein psoriasin (S100A7) is upregulated in atopic dermatitis and after experimental skin barrier disruption. *J Invest Dermatol* 129, 641-9 (2009)
 41. Perera C, McNeil HP, Geczy CL. S100 Calgranulins in inflammatory arthritis. *Immunol Cell Biol* 88, 41-9 (2010)
 42. Steinbakk M, Naess Andresen CF, Lingaas E, Dale I, Brandtzaeg P, Fagerhol MK. Antimicrobial actions of calcium binding leucocyte L1 protein, calprotectin. *Lancet* 336, 763-5 (1990)
 43. Gambichler T, Skrygan M, Tomi NS, Othlinghaus N, Brockmeyer NH, Altmeyer P *et al.* Differential mRNA expression of antimicrobial peptides and proteins in atopic dermatitis as compared to psoriasis vulgaris and healthy skin. *Int Arch Allergy Immunol* 147, 17-24 (2008)
 44. Harder J, Schroder JM. RNase 7, a novel innate immune defense antimicrobial protein of healthy human skin. *J Biol Chem* 277, 46779-84 (2002)
 45. Schittek B, Hipfel R, Sauer B, Bauer J, Kalbacher H, Stevanovic S *et al.* Dermcidin: a novel human antibiotic peptide secreted by sweat glands. *Nat Immunol* 2, 1133-7 (2001)
 46. Takahashi M, Tezuka T, Katunuma N. Inhibition of growth and cysteine proteinase activity of *Staphylococcus aureus* V8 by phosphorylated cystatin alpha in skin cornified envelope. *FEBS Lett* 355, 275-8 (1994)
 47. Bieber T. Atopic dermatitis. *N Engl J Med* 358, 1483-94 (2008)
 48. Williams H, Robertson C, Stewart A, Ait-Khaled N, Anabwani G, Anderson R *et al.* Worldwide variations in the prevalence of symptoms of atopic eczema in the International Study of Asthma and Allergies in Childhood. *J Allergy Clin Immunol* 103, 125-38 (1999)
 49. Novak N, Allam JP, Bieber T. Allergic hyperreactivity to microbial components: a trigger factor of "intrinsic" atopic dermatitis? *J Allergy Clin Immunol* 112, 215-6 (2003)
 50. Bardana EJ, Jr. Immunoglobulin E- (IgE) and non-IgE-mediated reactions in the pathogenesis of atopic eczema/dermatitis syndrome (AEDS). *Allergy* 59 Suppl 78, 25-9 (2004)
 51. Schmid-Grendelmeier P, Simon D, Simon HU, Akdis CA, Wuthrich B. Epidemiology, clinical features, and immunology of the "intrinsic" (non-IgE-mediated) type of atopic dermatitis (constitutional dermatitis). *Allergy* 56, 841-9 (2001)
 52. Larsen FS, Holm NV, Henningsen K. Atopic dermatitis. A genetic-epidemiologic study in a population-based twin sample. *J Am Acad Dermatol* 15, 487-94 (1986)
 53. Schultz Larsen F. Atopic dermatitis: a genetic-epidemiologic study in a population-based twin sample. *J Am Acad Dermatol* 28, 719-23 (1993)
 54. Wright RJ, Cohen RT, Cohen S. The impact of stress on the development and expression of atopy. *Curr Opin Allergy Clin Immunol* 5, 23-9 (2005)
 55. Baker BS. The role of microorganisms in atopic dermatitis. *Clin Exp Immunol* 144, 1-9 (2006)
 56. Palmer CN, Irvine AD, Terron-Kwiatkowski A, Zhao Y, Liao H, Lee SP *et al.* Common loss-of-function variants of the epidermal barrier protein filaggrin are a major predisposing factor for atopic dermatitis. *Nat Genet* 38, 441-6 (2006)
 57. Nomura T, Akiyama M, Sandilands A, Nemoto-Hasebe I, Sakai K, Nagasaki A *et al.* Specific filaggrin mutations cause ichthyosis vulgaris and are significantly associated

- with atopic dermatitis in Japan. *J Invest Dermatol* 128, 1436-41 (2008)
58. Ma L, Zhang L, Di ZH, Zhao LP, Lu YN, Xu J *et al.* Association analysis of filaggrin gene mutations and atopic dermatitis in Northern China. *Br J Dermatol* 162, 225-7 (2010)
 59. Chen H, Common JE, Haines RL, Balakrishnan A, Brown SJ, Goh CS *et al.* Wide spectrum of filaggrin-null mutations in atopic dermatitis highlights differences between Singaporean Chinese and European populations. *Brit J Dermatol* 165, 106-14 (2011)
 60. Christophers E. Psoriasis--epidemiology and clinical spectrum. *Clin Exp Dermatol* 26, 314-20 (2001)
 61. Gudjonsson JE, Elder JT. Psoriasis: epidemiology. *Clin Dermatol* 25, 535-46 (2007)
 62. Koo J, Lebwohl M. Duration of remission of psoriasis therapies. *J Am Acad Dermatol* 41, 51-9 (1999)
 63. Farber EM, Nall ML, Watson W. Natural history of psoriasis in 61 twin pairs. *Arch Dermatol* 109, 207-11 (1974)
 64. Brandrup F, Holm N, Grunnet N, Henningsen K, Hansen HE. Psoriasis in monozygotic twins: variations in expression in individuals with identical genetic constitution. *Acta Derm Venereol Stockh* 62, 229-36 (1982)
 65. Seville RH. Stress and psoriasis: the importance of insight and empathy in prognosis. *J Am Acad Dermatol* 20, 97-100 (1989)
 66. Eyre RW, Krueger GG. Response to injury of skin involved and uninvolved with psoriasis, and its relation to disease activity: Koebner and 'reverse' Koebner reactions. *Brit J Dermatol* 106, 153-9 (1982)
 67. Gudjonsson JE, Thorarinsson AM, Sigurgeirsson B, Kristinsson KG, Valdimarsson H. Streptococcal throat infections and exacerbation of chronic plaque psoriasis: a prospective study. *Brit J Dermatol* 149, 530-4 (2003)
 68. Ghadially R, Reed JT, Elias PM. Stratum corneum structure and function correlates with phenotype in psoriasis. *J Invest Dermatol* 107, 558-64 (1996)
 69. Griffiths CE, Barker JN. Pathogenesis and clinical features of psoriasis. *Lancet* 370, 263-71 (2007)
 70. Halprin KM. Epidermal "turnover time"--a re-examination. *Brit J Dermatol* 86, 14-9 (1972)
 71. Strange P, Cooper KD, Hansen ER, Fisher G, Larsen JK, Fox D *et al.* T-lymphocyte clones initiated from lesional psoriatic skin release growth factors that induce keratinocyte proliferation. *J Invest Dermatol* 101, 695-700 (1993)
 72. Bergboer JG, Zeeuwen PL, Schalkwijk J. Genetics of Psoriasis: Evidence for Epistatic Interaction between Skin Barrier Abnormalities and Immune Deviation. *J Invest Dermatol* 132, 2320-31 (2012)
 73. Lowes MA, Bowcock AM, Krueger JG. Pathogenesis and therapy of psoriasis. *Nature* 445, 866-73 (2007)
 74. Nestle FO, Kaplan DH, Barker J. Psoriasis. *N Engl J Med* 361, 496-509 (2009)
 75. Bowcock AM, Krueger JG. Getting under the skin: the immunogenetics of psoriasis. *Nat Rev Immunol* 5, 699-711 (2005)
 76. Nair RP, Stuart PE, Nistor I, Hiremagalore R, Chia NV, Jenisch S *et al.* Sequence and haplotype analysis supports HLA-C as the psoriasis susceptibility 1 gene. *Am J Hum Genet* 78, 827-51 (2006)
 77. Capon F, Di MP, Szaub J, Prescott NJ, Dunster C, Baumber L *et al.* Sequence

- variants in the genes for the interleukin-23 receptor (IL23R) and its ligand (IL12B) confer protection against psoriasis. *Hum Genet* 122, 201-206 (2007)
78. Hollox EJ, Huffmeier U, Zeeuwen PL, Palla R, Lascorz J, Rodijk-Olthuis D *et al.* Psoriasis is associated with increased beta-defensin genomic copy number. *Nat Genet* 40, 23-5 (2008)
 79. Schroder JM, Harder J. Human beta-defensin-2. *Int J Biochem Cell Biol* 31, 645-51 (1999)
 80. de Cid R, Riveira-Munoz E, Zeeuwen PL, Robarge J, Liao W, Dannhauser EN *et al.* Deletion of the late cornified envelope LCE3B and LCE3C genes as a susceptibility factor for psoriasis. *Nat Genet* 41, 211-5 (2009)
 81. Zhang XJ, Huang W, Yang S, Sun LD, Zhang FY, Zhu QX *et al.* Psoriasis genome-wide association study identifies susceptibility variants within LCE gene cluster at 1q21. *Nat Genet* 41, 205-10 (2009)
 82. Smith FJ, Irvine AD, Terron-Kwiatkowski A, Sandilands A, Campbell LE, Zhao Y *et al.* Loss-of-function mutations in the gene encoding filaggrin cause ichthyosis vulgaris. *Nat Genet* 38, 337-42 (2006)
 83. Nomura I, Gao B, Boguniewicz M, Darst MA, Travers JB, Leung DY. Distinct patterns of gene expression in the skin lesions of atopic dermatitis and psoriasis: a gene microarray analysis. *J Allergy Clin Immunol* 112, 1195-202 (2003)
 84. Choy DF, Hsu DK, Seshasayee D, Fung MA, Modrusan Z, Martin F *et al.* Comparative transcriptomic analyses of atopic dermatitis and psoriasis reveal shared neutrophilic inflammation. *J Allergy Clin Immunol* 130, 1335-43 e5 (2012)
 85. Kakinuma T, Nakamura K, Wakugawa M, Mitsui H, Tada Y, Saeki H *et al.* Thymus and activation-regulated chemokine in atopic dermatitis: Serum thymus and activation-regulated chemokine level is closely related with disease activity. *J Allergy Clin Immunol* 107, 535-41 (2001)
 86. Martin F, Penet MF, Malergue F, Lepidi H, Dessein A, Galland F *et al.* Vanin-1(-/-) mice show decreased NSAID- and Schistosoma-induced intestinal inflammation associated with higher glutathione stores. *J Clin Invest* 113, 591-7 (2004)
 87. kamsteeg M, Zeeuwen PL, de Jongh GJ, Rodijk-Olthuis D, Zeeuwen-Franssen ME, van Erp PE *et al.* Increased expression of carbonic anhydrase II (CA II) in lesional skin of atopic dermatitis: regulation by Th2 cytokines. *J Invest Dermatol* 127, 1786-9 (2007)
 88. Sly WS, Hu PY. Human carbonic anhydrases and carbonic anhydrase deficiencies. *Annu Rev Biochem* 64, 375-401 (1995)
 89. Rheinwald JG, Green H. Serial cultivation of strains of human epidermal keratinocytes: the formation of keratinizing colonies from single cells. *Cell* 6, 331-44 (1975)
 90. Mazzoleni G, Di Lorenzo D, Steimberg N. Modelling tissues in 3D: the next future of pharmaco-toxicology and food research? *Genes Nutr* 4, 13-22 (2009)
 91. Prunieras M, Regnier M, Woodley D. Methods for cultivation of keratinocytes with an air-liquid interface. *J Invest Dermatol* 81, 28s-33s (1983)
 92. Duval C, Chagnoleau C, Pouradier F, Sextius P, Condom E, Bernerd F. Human Skin Model Containing Melanocytes: Essential Role of Keratinocyte Growth Factor for Constitutive Pigmentation-Functional Response to alpha-Melanocyte Stimulating Hormone and Forskolin. *Tissue Eng Part C Methods* 18, 947-57 (2012)
 93. Netzlaff F, Lehr CM, Wertz PW, Schaefer UF. The human epidermis models EpiSkin, SkinEthic and EpiDerm: an evaluation of morphology and their suitability for testing

- phototoxicity, irritancy, corrosivity, and substance transport. *Eur J Pharm Biopharm* 60, 167-78 (2005)
94. MacNeil S. Progress and opportunities for tissue-engineered skin. *Nature* 445, 874-80 (2007)
 95. Barker CL, McHale MT, Gillies AK, Waller J, Pearce DM, Osborne J *et al.* The development and characterization of an in vitro model of psoriasis. *J Invest Dermatol* 123, 892-901 (2004)
 96. Harrison CA, Layton CM, Hau Z, Bullock AJ, Johnson TS, MacNeil S. Transglutaminase inhibitors induce hyperproliferation and parakeratosis in tissue-engineered skin. *Br J Dermatol* 156, 247-57 (2007)
 97. Tjabringa G, Bergers M, van Rens D, de Boer R, Lamme E, Schalkwijk J. Development and validation of human psoriatic skin equivalents. *Am J Pathol* 173, 815-23 (2008)
 98. Engelhart K, El Hindi T, Biesalski HK, Pfitzner I. In vitro reproduction of clinical hallmarks of eczematous dermatitis in organotypic skin models. *Arch Dermatol Res* 297, 1-9 (2005)
 99. Kamsteeg M, Bergers M, de Boer R, Zeeuwen PL, Hato SV, Schalkwijk J *et al.* Type 2 helper T-cell cytokines induce morphologic and molecular characteristics of atopic dermatitis in human skin equivalent. *Am J Pathol* 178, 2091-99 (2011)
 100. Graham FL, van der Eb AJ. Transformation of rat cells by DNA of human adenovirus 5. *Virology* 54, 536-9 (1973)
 101. McCutchan JH, Pagano JS. Enhancement of the infectivity of simian virus 40 deoxyribonucleic acid with diethylaminoethyl-dextran. *J Natl Cancer Inst* 41, 351-7 (1968)
 102. Felgner PL, Gadek TR, Holm M, Roman R, Chan HW, Wenz M *et al.* Lipofection: a highly efficient, lipid-mediated DNA-transfection procedure. *Proc Natl Acad Sci USA* 84, 7413-7 (1987)
 103. Hofland HE, Shephard L, Sullivan SM. Formation of stable cationic lipid/DNA complexes for gene transfer. *Proc Natl Acad Sci USA* 93, 7305-9 (1996)
 104. Madry H, Trippel SB. Efficient lipid-mediated gene transfer to articular chondrocytes. *Gene therapy* 7, 286-91 (2000)
 105. Neumann E, Schaefer-Ridder M, Wang Y, Hofschneider PH. Gene transfer into mouse lyoma cells by electroporation in high electric fields. *EMBO J* 1, 841-5 (1982)
 106. Distler JH, Jungel A, Kurowska-Stolarska M, Michel BA, Gay RE, Gay S *et al.* Nucleofection: a new, highly efficient transfection method for primary human keratinocytes*. *Exp Dermatol* 14, 315-20 (2005)
 107. Chen M, Li W, Fan J, Kasahara N, Woodley D. An efficient gene transduction system for studying gene function in primary human dermal fibroblasts and epidermal keratinocytes. *Clin Exp Dermatol* 28, 193-9 (2003)
 108. Horvath CA, Boulet GA, Renoux VM, Delvenne PO, Bogers JP. Mechanisms of cell entry by human papillomaviruses: an overview. *Virology* 411, 11 (2010)
 109. Kay MA, Glorioso JC, Naldini L. Viral vectors for gene therapy: the art of turning infectious agents into vehicles of therapeutics. *Nat Med* 7, 33-40 (2001)
 110. Ishikawa M, Meshi T, Motoyoshi F, Takamatsu N, Okada Y. In vitro mutagenesis of the putative replicase genes of tobacco mosaic virus. *Nucleic Acids Res* 14, 8291-305 (1986)
 111. Goins WF, Wolfe D, Krisky DM, Bai Q, Burton EA, Fink DJ *et al.* Delivery using herpes simplex virus: an overview. *Methods Mol Biol* 246, 257-99 (2004)

112. Jenne L, Hauser C, Arrighi JF, Saurat JH, Hugin AW. Poxvirus as a vector to transduce human dendritic cells for immunotherapy: abortive infection but reduced APC function. *Gene Ther* 7, 1575-83 (2000)
113. Mucke S, Polack A, Pawlita M, Zehnpfennig D, Massoudi N, Bohlen H *et al.* Suitability of Epstein-Barr virus-based episomal vectors for expression of cytokine genes in human lymphoma cells. *Gene Ther* 4, 82-92 (1997)
114. Yamashita M, Emerman M. Retroviral infection of non-dividing cells: old and new perspectives. *Virology* 344, 88-93 (2006)
115. Sliva K, Schnierle BS. Selective gene silencing by viral delivery of short hairpin RNA. *Virol J* 7, 248 (2010)
116. Zufferey R, Dull T, Mandel RJ, Bukovsky A, Quiroz D, Naldini L *et al.* Self-inactivating lentivirus vector for safe and efficient in vivo gene delivery. *J Virol* 72, 9873-80 (1998)
117. Staedel C, Remy JS, Hua Z, Broker TR, Chow LT, Behr JP. High-efficiency transfection of primary human keratinocytes with positively charged lipopolyamine:DNA complexes. *J Invest Dermatol* 102, 768-72 (1994)
118. Choate KA, Khavari PA. Sustainability of keratinocyte gene transfer and cell survival in vivo. *Hum Gene Ther* 8, 895-901 (1997)
119. Doebis C, Ritter T, Brandt C, Schonberger B, Volk HD, Seifert M. Efficient in vitro transduction of epithelial cells and keratinocytes with improved adenoviral gene transfer for the application in skin tissue engineering. *Transpl Immunol* 9, 323-9 (2002)
120. Braun-Falco M, Doenecke A, Smola H, Hallek M. Efficient gene transfer into human keratinocytes with recombinant adeno-associated virus vectors. *Gene Ther* 6, 432-41 (1999)
121. Morris KV, Rossi JJ. Antiviral applications of RNAi. *Curr Opin Mol Ther* 8, 115-21 (2006)
122. Sharp PA. RNA interference--2001. *Genes & development* 15, 485-90 (2001)
123. Ecker JR, Davis RW. Inhibition of gene expression in plant cells by expression of antisense RNA. *Proc Natl Acad Sci USA* 83, 5372-6 (1986)
124. Izant JG, Weintraub H. Inhibition of thymidine kinase gene expression by anti-sense RNA: a molecular approach to genetic analysis. *Cell* 36, 1007-15 (1984)
125. Dougherty WG, Lindbo JA, Smith HA, Parks TD, Swaney S, Proebsting WM. RNA-mediated virus resistance in transgenic plants: exploitation of a cellular pathway possibly involved in RNA degradation. *Mol Plant Microbe Interact* 7, 544-52 (1994)
126. Ratcliff F, Harrison BD, Baulcombe DC. A similarity between viral defense and gene silencing in plants. *Science* 276, 1558-60 (1997)
127. Rana TM. Illuminating the silence: understanding the structure and function of small RNAs. *Nat Reviews Mol Cell Biol* 8, 23-36 (2007)
128. Bernstein E, Caudy AA, Hammond SM, Hannon GJ. Role for a bidentate ribonuclease in the initiation step of RNA interference. *Nature* 409, 363-6 (2001)
129. Ender C, Meister G. Argonaute proteins at a glance. *J Cell Science* 123, 1819-23 (2010)
130. Elbashir SM, Harborth J, Lendeckel W, Yalcin A, Weber K, Tuschl T. Duplexes of 21-nucleotide RNAs mediate RNA interference in cultured mammalian cells. *Nature* 411, 494-8 (2001)
131. Brummelkamp TR, Bernards R, Agami R. A system for stable expression of short interfering RNAs in mammalian cells. *Science* 296, 550-3 (2002)

132. Fellermann K, Stange EF. Defensins -- innate immunity at the epithelial frontier. *Eur J Gastroen Hepat* 13, 771-6 (2001)
133. White SH, Wimley WC, Selsted ME. Structure, function, and membrane integration of defensins. *Curr Opin Struct Biol* 5, 521-7 (1995)
134. Ganz T. Defensins: antimicrobial peptides of innate immunity. *Nat Rev Immunol* 3, 710-20 (2003)
135. Pazgier M, Hoover DM, Yang D, Lu W, Lubkowski J. Human beta-defensins. *Cell Mol Life Sci* 63, 1294-313 (2006)
136. Niyonsaba F, Ogawa H, Nagaoka I. Human beta-defensin-2 functions as a chemotactic agent for tumour necrosis factor-alpha-treated human neutrophils. *Immunology* 111, 273-81 (2004)
137. Hollox EJ, Armour JA, Barber JC. Extensive normal copy number variation of a beta-defensin antimicrobial-gene cluster. *Am J Hum Genet* 73, 591-600 (2003)
138. Fellermann K, Stange DE, Schaeffeler E, Schmalzl H, Wehkamp J, Bevins CL *et al.* A chromosome 8 gene-cluster polymorphism with low human Beta-defensin 2 gene copy number predisposes to crohn disease of the colon. *Am J Hum Genet* 79, 439-448 (2006)
139. Bentley RW, Pearson J, Gearry RB, Barclay ML, McKinney C, Merriman TR *et al.* Association of higher DEFB4 genomic copy number with Crohn's disease. *Am J Gastroenterol* 105, 354-9 (2010)
140. Fernandez-Jimenez N, Castellanos-Rubio A, Plaza-Izurieta L, Gutierrez G, Castano L, Vitoria JC *et al.* Analysis of beta-defensin and Toll-like receptor gene copy number variation in celiac disease. *Hum Immunol* 71, 833-6 (2010)
141. Tiszlavicz Z, Szabolcs A, Takacs T, Farkas G, Kovacs-Nagy R, Szantai E *et al.* Polymorphisms of beta defensins are associated with the risk of severe acute pancreatitis. *Pancreatology* 10, 483-90 (2010)
142. Janssens W, Nuytten H, Dupont LJ, Van Eldere J, Vermeire S, Lambrechts D *et al.* Genomic copy number determines functional expression of {beta}-defensin 2 in airway epithelial cells and associates with chronic obstructive pulmonary disease. *Am J Respir Crit Care Med* 182, 163-9 (2010)
143. Huse K, Taudien S, Groth M, Rosenstiel P, Szafranski K, Hiller M *et al.* Genetic variants of the copy number polymorphic beta-defensin locus are associated with sporadic prostate cancer. *Tumour Biol* 29, 83-92 (2008)
144. Aurrand-Lions M, Galland F, Bazin H, Zakharyev VM, Imhof BA, Naquet P. Vanin-1, a novel GPI-linked perivascular molecule involved in thymus homing. *Immunity* 5, 391-405 (1996)
145. Granjeaud S, Naquet P, Galland F. An ESTs description of the new Vanin gene family conserved from fly to human. *Immunogenetics* 49, 964-72 (1999)
146. Suzuki K, Watanabe T, Sakurai S, Ohtake K, Kinoshita T, Araki A *et al.* A novel glycosylphosphatidyl inositol-anchored protein on human leukocytes: a possible role for regulation of neutrophil adherence and migration. *J Immunol* 162, 4277-84 (1999)
147. Martin F, Malergue F, Pitari G, Philippe JM, Philips S, Chabret C *et al.* Vanin genes are clustered (human 6q22-24 and mouse 10A2B1) and encode isoforms of pantetheinase ectoenzymes. *Immunogenetics* 53, 296-306 (2001)
148. Huang J, Takeda Y, Watanabe T, Sendo F. A sandwich ELISA for detection of soluble GPI-80, a glycosylphosphatidyl-inositol (GPI)-anchored protein on human

- leukocytes involved in regulation of neutrophil adherence and migration--its release from activated neutrophils and presence in synovial fluid of rheumatoid arthritis patients. *Microbiol Immunol* 45, 467-71 (2001)
149. Nitto T, Inoue T, Node K. Alternative spliced variants in the pantetheinase family of genes expressed in human neutrophils. *Gene* 426, 57-64 (2008)
150. Cavallini D, Dupre S, Graziani MT, Tinti MG. Identification of pantethinase in horse kidney extract. *FEBS letters* 1, 119-21 (1968)
151. Dupre S, Rosei MA, Bellussi L, Del Grosso E, Cavallini D. The substrate specificity of pantethinase. *Eur J Biochem* 40, 103-7 (1973)
152. Wittwer CT, Schweitzer C, Pearson J, Song WO, Windham CT, Wyse BW *et al.* Enzymes for liberation of pantothenic acid in blood: use of plasma pantetheinase. *Am J Clin Nutr* 50, 1072-8 (1989)
153. Orloff S, Butler JD, Towne D, Mukherjee AB, Schulman JD. Pantetheinase activity and cysteamine content in cystinotic and normal fibroblasts and leukocytes. *Pediatr Res* 15, 1063-7 (1981)
154. Wittwer CT, Gahl WA, Butler JD, Zatz M, Thoene JG. Metabolism of pantethine in cystinosis. *J Clin Invest* 76, 1665-72 (1985)
155. Maras B, Barra D, Dupre S, Pitari G. Is pantetheinase the actual identity of mouse and human vanin-1 proteins? *FEBS Lett* 461, 149-52 (1999)
156. Pitari G, Malergue F, Martin F, Philippe JM, Massucci MT, Chabret C *et al.* Pantetheinase activity of membrane-bound Vanin-1: lack of free cysteamine in tissues of Vanin-1 deficient mice. *FEBS Lett* 483, 149-54 (2000)
157. Dupre S, Graziani MT, Rosei MA, Fabi A, Del Grosso E. The enzymatic breakdown of pantethine to pantothenic acid and cystamine. *Eur J Biochem* 16, 571-8 (1970)
158. Wilson MJ, Jeyasuria P, Parker KL, Koopman P. The transcription factors steroidogenic factor-1 and SOX9 regulate expression of Vanin-1 during mouse testis development. *J Biol Chem* 280, 5917-23 (2005)
159. Grimmond S, Van Hateren N, Siggers P, Arkell R, Larder R, Soares MB *et al.* Sexually dimorphic expression of protease nexin-1 and vanin-1 in the developing mouse gonad prior to overt differentiation suggests a role in mammalian sexual development. *Hum Mol Genet* 9, 1553-60 (2000)
160. Berruyer C, Pouyet L, Millet V, Martin FM, LeGoffic A, Canonici A *et al.* Vanin-1 licenses inflammatory mediator production by gut epithelial cells and controls colitis by antagonizing peroxisome proliferator-activated receptor gamma activity. *J Exp Med* 203, 2817-27 (2006)
161. Pouyet L, Roisin-Bouffay C, Clement A, Millet V, Garcia S, Chasson L *et al.* Epithelial vanin-1 controls inflammation-driven carcinogenesis in the colitis-associated colon cancer model. *Inflamm Bowel Dis* 16, 96-104 (2010)
162. Meghari S, Berruyer C, Lepidi H, Galland F, Naquet P, Mege JL. Vanin-1 controls granuloma formation and macrophage polarization in *Coxiella burnetii* infection. *Eur J Immunol* 37, 24-32 (2007)
163. Roisin-Bouffay C, Castellano R, Valero R, Chasson L, Galland F, Naquet P. Mouse vanin-1 is cytoprotective for islet beta cells and regulates the development of type 1 diabetes. *Diabetologia* 51, 1192-201 (2008)
164. Yoshitake H, Takeda Y, Nitto T, Sendo F. Cross-linking of GPIIb/IIIa, a possible regulatory molecule of cell adhesion, induces up-regulation of CD11b/CD18 expression on neutrophil surfaces and shedding of L-selectin. *J Leukoc Biol* 71, 205-11 (2002)

165. Koike S, Takeda Y, Hozumi Y, Okazaki S, Aoyagi M, Sendo F. Immunohistochemical localization in human tissues of GPI-80, a novel glycosylphosphatidyl inositol-anchored protein that may regulate neutrophil extravasation. *Cell Tissue Res* 307, 91-9 (2002)
166. Yoshitake H, Takeda Y, Nitto T, Sendo F, Araki Y. GPI-80, a beta2 integrin associated glycosylphosphatidylinositol-anchored protein, concentrates on pseudopodia without association with beta2 integrin during neutrophil migration. *Immunobiology* 208, 391-9 (2003)
167. Nitto T, Takeda Y, Yoshitake H, Sendo F, Araki Y. Structural divergence of GPI-80 in activated human neutrophils. *Biochem Biophys Res Commun* 359, 227-33 (2007)
168. Nitto T, Araki Y, Takeda Y, Sendo F. Pharmacological analysis for mechanisms of GPI-80 release from tumour necrosis factor-alpha-stimulated human neutrophils. *Br J Pharmacol* 137, 353-60 (2002)
169. Sendo D, Takeda Y, Ishikawa H, Sendo F, Araki Y. Localization of GPI-80, a beta2-integrin-associated glycosylphosphatidyl-inositol anchored protein, on strongly CD14-positive human monocytes. *Immunobiology* 207, 217-21 (2003)
170. Anzai-Takeda Y, Takeda Y, Sendo F, Araki Y. Inhibition of cell spreading in CHO cells transfected with cDNA of a glycosylphosphatidyl inositol-anchored protein, GPI-80. *Immunobiology* 210, 1-10 (2005)
171. Min-Oo G, Fortin A, Pitari G, Tam M, Stevenson MM, Gros P. Complex genetic control of susceptibility to malaria: positional cloning of the Char9 locus. *J Exp Med* 204, 511-24 (2007)
172. Min-Oo G, Ayi K, Bongfen SE, Tam M, Radovanovic I, Gauthier S *et al.* Cysteamine, the natural metabolite of pantetheinase, shows specific activity against Plasmodium. *Exp Parasitol* 125, 315-24 (2010)
173. Min-Oo G, Fortin A, Poulin JF, Gros P. Cysteamine, the molecule used to treat cystinosis, potentiates the antimalarial efficacy of artemisinin. *Antimicrob Agents Chemother* 54, 3262-70 (2010)
174. Goring HH, Curran JE, Johnson MP, Dyer TD, Charlesworth J, Cole SA *et al.* Discovery of expression QTLs using large-scale transcriptional profiling in human lymphocytes. *Nat Genet* 39, 1208-16 (2007)
175. Kerker K, Spadola A, Yuan E, Kosek J, Jiang L, Hod E *et al.* Genomic surveys by methylation-sensitive SNP analysis identify sequence-dependent allele-specific DNA methylation. *Nat Genet* 40, 904-8 (2008)
176. Marshall KW, Mohr S, Khettabi FE, Nossova N, Chao S, Bao W *et al.* A blood-based biomarker panel for stratifying current risk for colorectal cancer. *Int J Cancer* 126, 1177-86 (2010)
177. Yip KT, Das PK, Suria D, Lim CR, Ng GH, Liew CC. A case-controlled validation study of a blood-based seven-gene biomarker panel for colorectal cancer in Malaysia. *J Exp Clin Canc Res* 29, 128 (2010)
178. Huang H, Dong X, Kang MX, Xu B, Chen Y, Zhang B *et al.* Novel blood biomarkers of pancreatic cancer-associated diabetes mellitus identified by peripheral blood-based gene expression profiles. *Am J Gastroenterol* 105, 1661-9 (2010)
179. Sasaki H, Ide N, Sendo F, Takeda Y, Adachi M, Fukai I *et al.* Glycosylphosphatidyl inositol-anchored protein (GPI-80) gene expression is correlated with human thymoma stage. *Cancer Sci* 94, 809-13 (2003)

Expression of the vanin gene family in normal and inflamed human skin: Induction by pro-inflammatory cytokines

2 CHAPTER

Patrick AM Jansen¹
Marijke Kamsteeg¹
Diana Rodijk-Olthuis¹
Ivonne MJJ van Vlijmen-Willems¹
Gys J de Jongh¹
Mieke Bergers¹
Geuranne S Tjabringa¹
Patrick LJM Zeeuwen¹
Joost Schalkwijk¹

¹Department of Dermatology and Nijmegen Centre for Molecular Life Sciences, Radboud University Nijmegen Medical Centre, The Netherlands

Published in: *J Invest Dermatol* 129, 2167-74 (2009)

Abstract

The vanin gene family encodes secreted and membrane-bound ectoenzymes that convert pantetheine to pantothenic acid and cysteamine. Recent studies in a mouse colitis model indicated that vanin-1 has proinflammatory activity and suggest that pantetheinases are potential therapeutic targets in inflammatory diseases. In a microarray analysis of epidermal gene expression of psoriasis and atopic dermatitis lesions we identified vanin-3 as the gene showing the highest differential expression of all annotated genes that we studied (19-fold upregulation in psoriasis). Quantitative real-time PCR analysis confirmed the microarray data on vanin-3 and showed similar induction of vanin-1, but not of vanin-2, in psoriatic epidermis. Immunohistochemistry showed that vanin-3 is expressed in the differentiated epidermal layers. Using submerged and organotypic keratinocyte cultures we found that vanin-1 and vanin-3 are induced at the mRNA and protein level by psoriasis-associated proinflammatory cytokines (Th17/Th1) but not by Th2 cytokines. We hypothesize that increased levels of pantetheinase activity are part of the inflammatory-regenerative epidermal differentiation program, and may contribute to the phenotype observed in psoriasis.

Introduction

The human vanin gene family consists of three genes, vanin-1 (VNN1), vanin-2 (VNN2) and vanin-3 (VNN3) that are located on chromosome 6q22-24^{1,2}. These genes show a similar structure consisting of seven exons, and encode proteins with a high degree of homology (~65% sequence identity)³. Human vanin-1 and vanin-2 being membrane-associated ectoenzymes and vanin-3 a secreted enzyme. Vanins are conserved among species and two mice orthologues (vanin-1 and vanin-3, but not vanin-2) have been identified³. Vanin-1 was first described as a regulator of the late adhesion steps in thymus homing in mice⁴. Human vanin-2 was characterized as a molecule involved in the regulation of adherence and migration of neutrophils⁵. Subsequent studies identified vanins as enzymes that are involved in Coenzyme A (CoA) synthesis. Their enzymatic activity catalyzes the conversion of pantetheine to pantothenic acid (vitamin B5, a CoA precursor) and the anti-oxidant cysteamine^{2,6}. In mice deficient for vanin-1 no free cysteamine was found in tissues, suggesting that at least in mice vanin-1 is a major pantetheinase⁷. These mice show decreased NSAID- and Schistosoma-induced intestinal inflammation, which can be completely reversed by oral administration of cystamine, the oxidized form of cysteamine⁸. Vanin-1 deficiency is also able to control colitis in the 2,4,6-trinitrobenzene sulfonic acid (TNBS)-colitis model⁹. Another biological activity of cysteamine is its presumed antagonism of the peroxisome proliferator-activated receptor gamma (PPAR- γ). Based on these findings it was proposed that vanin-1 is an epithelial sensor of stress that exerts a dominant control over innate immune responses in mouse tissue⁹. Therefore, the pantetheinase activity of vanin family members could be a novel therapeutic target in inflammatory diseases.

Psoriasis vulgaris and atopic dermatitis are two common chronic inflammatory skin diseases, characterized by various different clinical and histological features depending on the stage of the disease. Both diseases are generally regarded as immune-mediated conditions involving activated T-cells and cytokines of the Th1/Th17 type (psoriasis) or the Th2 type (atopic dermatitis)¹⁰⁻¹². In lesional psoriatic skin, increased levels of pro-inflammatory cytokines like IL-1, TNF α , IFN γ , IL-6, IL-8, IL-17 and IL-22 are found. These cytokines, which are produced by T-cells, dendritic cells and/or keratinocytes, can act both on immunocytes and keratinocytes. Activation of keratinocytes by these cytokines induces specific gene expression profiles, that include secretion of antimicrobial proteins and chemokines¹³. In addition to the role of the adaptive immune system, recent genetic studies have indicated the importance of abnormalities in epithelium-expressed genes as a primary cause. Loss of function alleles of the skin barrier protein filaggrin were found to be a major predisposing factor for atopic dermatitis¹⁴, and we have recently demonstrated that copy number variation of a beta defensin gene cluster was associated with increased risk for psoriasis¹⁵. The differences in gene expression between lesional psoriatic epidermis and lesional atopic dermatitis epidermis have been investigated by various methods^{13,16,17}.

Using a microarray approach on purified epidermis we identified 183 genes to be differentially expressed between psoriasis and atopic dermatitis¹⁶. These data are accessible through GEO Series accession number GSE6601, <http://www.ncbi.nlm.nih.gov/geo>. Remarkably, we identified vanin-3 as the gene showing the highest differential expression of all annotated genes that we studied (unpublished data). As there was no information on expression of vanin family members in human epidermis, and vanin-1 has recently been described as a potential drug target in inflammatory bowel disease, we decided to investigate the expression and induction of vanin-3 and other vanin family members in human epidermal keratinocytes *in vivo* and *in vitro*. Our results suggest that vanin-1 and vanin-3 could be relevant mediators in Th17/Th1-driven inflammatory skin conditions.

Results

High expression levels of vanin-1 and vanin-3 in lesional psoriatic skin

The transcriptome of epidermal sheets of lesional epidermis from psoriasis and atopic dermatitis was analyzed using high-density oligonucleotide arrays as previously described (GEO Series accession number GSE6601). All known human vanin genes were present on the microarray. Vanin-1 and vanin-3 were detectable in all 12 samples, whereas vanin-2 was detected in none of them. Vanin-3 showed the highest upregulation (19-fold) of the annotated genes on the array in psoriasis compared to atopic dermatitis. Also vanin-1 was found to be relatively overexpressed in psoriasis (2.3-fold). Microarray data were confirmed by qPCR analysis on mRNA from lesional skin of psoriatic patients and atopic dermatitis patients, and normal skin of healthy volunteers. Figure 2.1 shows that vanin-3 expression is high in psoriatic epidermis, but low in normal

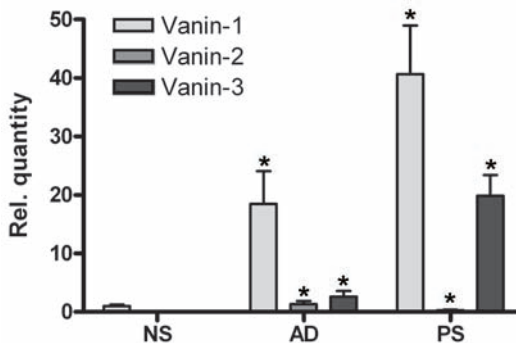


Figure 2.1 Analysis of vanin mRNA in healthy, psoriasis and atopic dermatitis skin. Quantitative real-time PCR for vanin-1, vanin-2 and vanin-3 was performed on RNA of epidermal sheets from skin biopsies of healthy controls (n=7), psoriatic patients (n=9) and atopic dermatitis patients (n=6). Expression of target genes was normalized to that of RPLP0. For graphical representation all values were expressed relative to vanin-1 in normal skin, which was set at unity¹⁸. Primer sequences and efficiency of amplification are given in table 2.1. Vanin-1, vanin-2 and vanin-3 expression is induced in both psoriasis and atopic dermatitis as compared to normal skin. Values are presented as mean and SD. One-way ANOVA; *P < 0.001.

skin and atopic dermatitis. Vanin-1 expression was strongly induced in psoriasis patients and moderately in atopic dermatitis patients as compared to normal skin. Although Vanin-2 expression was significantly induced in both psoriasis and atopic dermatitis, its expression is very low compared with vanin-1 and vanin-3

As there is little quantitative information on relative expression levels of human vanin family members in most organs, we performed qPCR on a large panel of tissues including many epithelia, to allow comparison with epidermis. Figure 2.2 shows the expression of the vanin genes in different tissues. The highest expression levels of vanin-3 were found in liver and blood, being of similar magnitude as found in psoriatic epidermis. Other tissues where vanin-3 expression was found are the urethra, the lymph nodes, parts of the respiratory tract and most parts of the gastrointestinal tract. Vanin-2 expression was found in almost all tissues, but by far the highest expression was found in spleen and blood. In lesional psoriatic epidermis vanin-2 expression was near the average expression. Vanin-1 was mainly expressed in the same tissues as vanin-3, but relatively high expression was found in spleen, kidney and blood. In lesional psoriatic epidermis vanin-1 expression was of the same magnitude as kidney and liver.

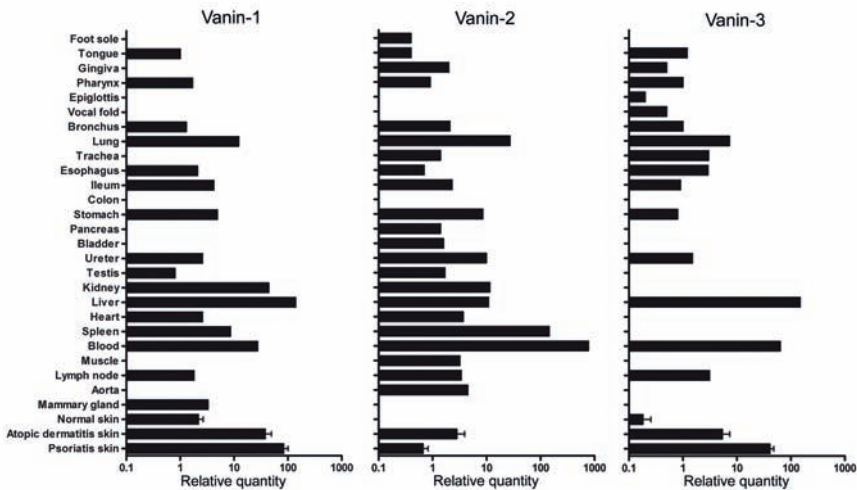


Figure 2.2 mRNA expression of vanin family members in normal human tissues. Quantitative real-time PCR was performed on RNA of normal human tissues. Expression of target genes was normalized to that of RPLP0. For graphical representation all values were expressed relative to vanin-1 in tongue, which was set at unity, to allow comparison of the expression levels between tissues and genes¹⁸. Normal human tissues are from one individual. Values from epidermis (at least 6 biopsies) are given for comparison.

Vanin-3 protein is expressed by differentiated keratinocytes

To investigate which cellular compartment of the epidermis express vanins, we performed immunohistochemical staining on normal skin, atopic dermatitis skin and psoriatic skin. As there were no commercial antisera available that were suitable for immunohistochemistry, we expressed recombinant vanin-3 as a

TrXA-fusion protein which was used to raise a polyclonal antiserum in rabbits. Figure 2.3 shows that epidermal vanin-3 protein expression is largely confined to differentiated keratinocytes, both in normal and psoriatic epidermis. Vanin-3 expression in normal and atopic dermatitis epidermis is restricted to the *stratum granulosum*, while in psoriatic epidermis strong vanin-3 expression is also found in the *stratum spinosum*. Dermal vanin-3 expression was limited to endothelial cells and a small proportion of the cellular infiltrate.

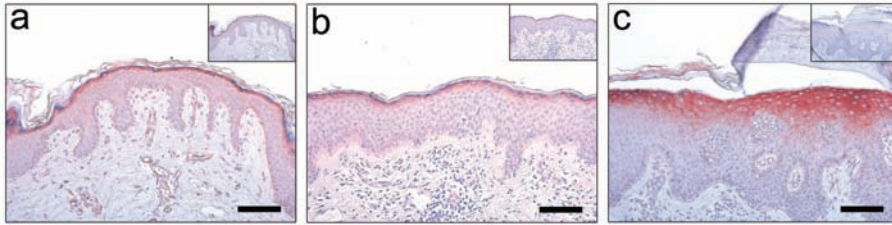


Figure 2.3 Immunolocalization of vanin-3 in normal, atopic dermatitis and psoriasis skin. Immunohistochemical staining of normal skin (a) and lesional skin of an atopic dermatitis patient (b) and a psoriasis patient (c) with a polyclonal rabbit antiserum against recombinant vanin-3. Expression of vanin-3 in normal skin and atopic dermatitis skin was limited to the *stratum granulosum*, whereas in psoriasis skin strong vanin-3 expression is found in multiple layers of the *stratum spinosum*. Bar = 100 µm. Control sections stained with pre-immune serum were virtually negative (see inserts).

Induction of vanin expression by cytokines

The psoriasis-specific induction of vanin-1 and vanin-3 suggested to us that psoriasis-associated cytokines could be involved in vanin gene regulation. We have previously shown that *in vitro* stimulation of cultured normal keratinocytes by mixtures of psoriasis-associated cytokines (IFN- γ , TNF- α and IL-1 herein further referred to as Th1 cytokines) or atopic dermatitis associated cytokines (IL-4 and IL-13, herein further referred to as Th2 cytokines) results in disease-specific gene expression in these cells. Figure 2.4 shows expression of vanin-1 and vanin-3 by submerged cultures of human keratinocytes stimulated with

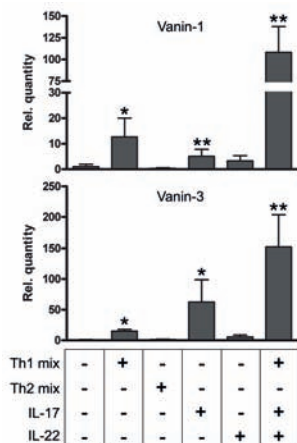


Figure 2.4 Induction of vanin expression in submerged culture by proinflammatory cytokines. Quantitative real-time PCR of vanin-1 and vanin-3 was performed on RNA obtained from submerged cultured keratinocytes after stimulation with various combinations of proinflammatory cytokines and compared with non-stimulated keratinocytes (n=6). Concentrations of cytokines were previously optimized for induction of psoriasis-like phenotypes *in vitro*. Vanin-1 and vanin-3 expression was strongly induced by the Th1-cytokine mixture (IFN- γ , TNF- α and IL-1 α ; n=6) and IL-17 (n=5). IL-22 (n=5) induces vanin-1 expression, but not vanin-3 expression. A Th2-cytokine mixture (IL-4 and IL-13; n=5) has no effects on vanin expression. A mixture of all cytokines showed a strong, synergistic induction of vanin expression (n=5). Repeated measures ANOVA; *P < 0.05, **P < 0.005.

cytokines. The cytokine mixtures and concentrations were chosen based on previous experiments to establish optimal concentrations for induction of a psoriatic phenotype (expression of beta-defensin-2 (hBD-2) and elafin) or atopic dermatitis phenotype (expression of carbonic anhydrase II)^{13,19}. We found that both vanin-1 and vanin-3 expression is induced after Th1-cytokine stimulation. Vanin-2 is not upregulated following cytokine stimulation (data not shown). Th2-cytokines did not have a significant effect on expression of any of the vanin genes. In addition, we also tested the Th17 cytokines IL-17 and IL-22. Both vanin-1 and vanin-3 expression was increased upon stimulation with IL-17, but not after IL-22 stimulation which only has a small stimulatory effect on vanin-1 expression. A combination of Th1 cytokines and Th17 cytokines resulted in a strong synergistic induction of both vanin-1 and vanin-3 expression, of similar magnitude as found *in vivo* in psoriatic epidermis (not shown).

Induction of vanin-1 and vanin-3 in reconstructed human epidermis by cytokines

We have recently described a reconstructed skin model in which we could induce a psoriatic phenotype (as witnessed by expression of the surrogate markers hBD-2 and elafin) by the addition of psoriasis-associated cytokines. We found that in these reconstructed skin models the addition of interferon- γ was dispensable, whereas IL-6 strongly potentiated the effect of IL-1 α and TNF- α ²⁰. For this reason we used cytokine mixtures of TNF- α , IL-1 α and IL-6 or individual Th17 cytokines such as IL-17 and IL-22 to examine the effect on vanin gene induction. Here these constructs were stimulated with various cytokines to investigate the induction of vanins. Using qPCR analysis we found similar effects of psoriasis and atopic dermatitis associated cytokines on vanin expression as found in submerged cultures (figure 2.5). Both IL-17 and the mix of TNF- α , IL-1 α and IL-6 induced strong vanin-1 and vanin-3 expression. IL-22 induced a weak, non-significant expression of vanin-1 and vanin-3. Th2 cytokine mix did not induce vanin-1 but showed a small but non-significant increase in vanin-3 expression. Immunohistochemical staining of these skin constructs confirmed the qPCR results, showing a strong induction of vanin-3 staining in the upper epidermal layers of cultures stimulated with IL-17 or with the mix of TNF- α , IL-1 α and IL-6 (figure 2.6).

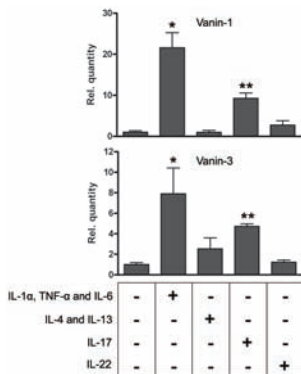


Figure 2.5 Induction of vanin expression in reconstructed skin by proinflammatory cytokines. Quantitative real-time PCR of vanin-1 and vanin-3 was performed on RNA obtained from reconstructed skin after stimulation with various combinations of proinflammatory cytokines and compared with non-stimulated reconstructed skin (n=5). Here we used a cytokine mixture containing TNF- α , IL-1 α and IL-6 based on previous experiments for optimal induction of a psoriatic phenotype *in vitro* in reconstructed skin. Both this cytokine mixture (n=2) and IL-17 alone (n=3) strongly induced vanin-1 and vanin-3 expression. The Th2-cytokine mixture (n=2) and the Th17 cytokine IL-22 (n=3) had no effects on vanin expression. One-way ANOVA; *P < 0.05, **P < 0.005.

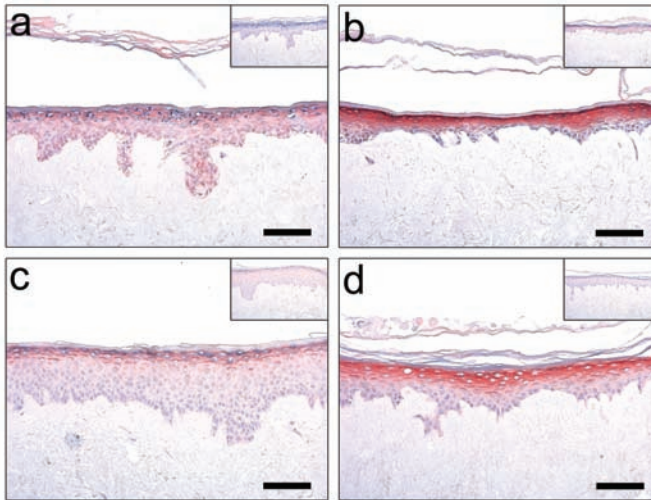


Figure 2.6 Immunohistochemical staining of vanin-3 in reconstructed skin. Reconstructed skin, with or without cytokine stimulation, was stained for vanin-3 using a polyclonal rabbit antiserum against recombinant vanin-3. Control cultures (a) or Th2-cytokine stimulated cultures (c) showed a weak expression of vanin-3, predominantly in the upper differentiated layers. Stimulation with a cytokine mixture of TNF- α , IL-1 α and IL-6 (b) or with IL-17 (c) results in strong expression of vanin-3 in the upper differentiated layers. Bar = 100 μ m. Control sections stained with pre-immune serum were virtually negative (see inserts).

Discussion

Using microarray analysis, qPCR and immunohistochemistry we have analyzed expression of the vanin gene family, which has not been previously reported in skin. Expression of vanin-1 and vanin-3 was shown to be part of the inflammatory-regenerative differentiation program that is characteristic for psoriasis. High expression levels of vanin-1 and vanin-3 could be induced by psoriasis-associated pro-inflammatory cytokines in submerged and air-exposed keratinocyte cultures. *In vitro* reconstructed skin can be used as a model for further study of the role of vanins in epidermal biology.

Apart from studies on gene structure, very little is known on human vanin gene expression at the mRNA and protein level. A putative function of vanin-2 in cell adherence has been reported for human neutrophils, and recently the expression of vanin splice forms has been reported in these cells²¹. The existence of splice variants in the pantetheinase gene family suggested the possibility of alternative roles in addition to their enzymatic activity. Most functional data on vanin family members (predominantly vanin-1) come from studies in knockout mice (see introduction section). From these mouse studies vanins emerge as a class of enzymes that can have both proinflammatory effects and protective effects. Although there is no information at this moment whether increased vanin-1 and vanin-3 expression leads to increased levels of metabolites (cysteamine, pantothenic acid) in psoriatic epidermis, we would argue that this could possibly

contribute to the skin abnormalities observed in psoriasis, as will be discussed in the next paragraphs.

In this study we have found that vanin-3 is expressed in differentiated keratinocytes. Although the exact function of vanins in skin remains to be elucidated it is attractive to speculate about a role of vanins in terminal differentiation. The products of the vanin-mediated enzymatic conversion of pantetheine are pantothenic acid and cysteamine. Pantothenic acid, a precursor of CoA, is involved in epidermal lipid synthesis. In normal human epidermis, high levels of lipid synthesis are found in both the basal layer and the *stratum granulosum*²². Lipids are important for skin barrier function as they are part of the lamellar bodies formed by keratinocytes in the *stratum spinosum*²³. The contents of lamellar bodies are secreted into the extracellular spaces and transformed into lamellar bilayers to form an impermeable, lipid-containing sheet that serves as a water barrier. The increased expression of vanins in psoriatic epidermis could reflect the increased requirement of precursors to keep up with the lipid synthesis that is necessary to compensate the increased keratinocyte turnover (i.e. shortened half-life) in psoriasis. Notwithstanding this potentially increased supply of lipid precursors, the skin barrier function in psoriasis is abnormal with respect to water loss²⁴. This could be due to the biochemical activity of cysteamine, the other metabolite of the vanin-mediated enzymatic conversion of pantetheine. Cysteamine is a strong transglutaminase (TGase) inhibitor by its binding to an important cysteine residue in the active site of the enzyme^{25,26}. In skin TGase-1, TGase-3 and TGase-5 are the major TGases that catalyze the formation of ϵ -(γ -glutamyl)lysine bonds between cornified envelope precursor proteins²⁷⁻²⁹. TGases play an important role in normal skin development and they are expressed at different stages of epidermal differentiation and at different levels within the epidermis. In psoriatic skin TGase-5 expression is unaffected, while it has been demonstrated that TGase-3 expression is slightly downregulated²⁷. The expression of TGase-1 is shifted from the granular layer in normal skin to the suprabasal spinous layer in psoriatic skin³⁰. As most studies only determine the presence of TGase enzymes and not their activity within the tissue this does not provide information on a possible effect of epidermal cysteamine. Some authors argue that TGase activity in psoriasis is increased^{31,32}, but these findings are mainly based on *ex vivo* experiments where endogenous epidermal cysteamine could easily be washed away resulting in active TGase proteins in their assays. A recent study by Harrisson *et al.* has investigated the effect of TGase inhibitors in a reconstructed skin model. Interestingly, they found that TGase inhibition caused a psoriatic phenotype *in vitro*, including hyperproliferation, parakeratosis and cytokeratin 16 expression which are hallmarks of the disease³³. These findings support a role for vanin-dependent cysteamine production in the pathogenesis of the disease.

Another enzyme whose activity is inhibited by cysteamine is caspase-3³⁴. This enzyme is activated during terminal differentiation of keratinocytes. In normal skin caspase-3 is involved in both nuclear loss and correct filaggrin processing³⁵.

Addition of caspase-3 inhibitors to reconstructed skin models prevents nuclei to be degraded which may lead to parakeratosis³⁵. Also the alteration of filaggrin processing as a result of caspase-3 inhibition could contribute to a disturbed skin barrier as found in psoriasis and atopic dermatitis. Speculatively, increased cysteamine levels caused by vanin-1 and vanin-3 overexpression could inhibit caspase-3 activity thereby contributing to the phenotypic changes such as parakeratosis and compromised skin barrier seen in psoriasis.

Finally, cysteamine is reported to be an antagonist for PPAR γ ⁹. In human epidermis PPARs (PPAR α , PPAR β/δ and PPAR γ) are important ligand-activated transcription factors that are involved in the maintenance of skin homeostasis by inhibiting epidermal cell growth, promoting epidermal terminal differentiation and regulating skin inflammatory responses³⁶. These properties make PPARs interesting molecules with respect to psoriasis and other inflammatory skin disorders. In psoriasis the epidermal expression of PPAR α and PPAR γ is decreased, suggesting a role for these proteins³⁷. In the last few years PPAR γ activators have been used as an antipsoriatic drug; PPAR agonists thiazolidinedione (TZD) and its derivatives rosiglitazone and pioglitazone have shown to be beneficial for psoriasis patients³⁸⁻⁴⁰. In a murine model, also the TZD derivatives ciglitazone and troglitazone improve skin homeostasis⁴¹. The exact role of PPAR γ in psoriasis is still not completely clear, but increased levels of an endogenous antagonist like cysteamine could explain the positive effects of these PPAR γ activators.

Since cysteamine is a potent antioxidant and skin is exposed to oxidative stress, vanin could very well have a role in these processes. Surprisingly, vanin-1 knockout mice, which lack cysteamine in tissues where vanin-1 is predominantly expressed, display resistance to systemic oxidative stress caused by paraquat administration or a lethal dose of γ -irradiation. This effect was ascribed to increased levels of glutathione, an even more potent antioxidant, in liver of these knockout mice and was reversible after administration of cysteamine. Some papers argue that oxidative stress plays a role in the pathogenesis of psoriasis^{42,43} and it has also been reported that there is insufficient antioxidant activity in psoriatic lesions⁴⁴. In plasma of psoriatic patients the total plasma antioxidant capacity was increased compared with healthy individuals⁴⁵, which could be the result of increased vanin expression in lesional skin leading to increased levels of cysteamine. One of the functions of the *stratum corneum* implies antioxidant defense, but most oxidative stress was found in the dermis and basal layers of psoriatic skin⁴⁶. Vanin expression was predominantly found in the *stratum granulosum* and *stratum spinosum* indicating a possible role in the antioxidant defense against reactive oxygen species (ROS) generated by exogenous mechanisms (e.g. UV-light) rather than endogenous ROS.

In conclusion, this is the first report describing the strongly increased expression of vanin-1 and vanin-3 in psoriatic skin. However, many questions remain to be answered regarding the function of vanins in normal and psoriatic skin. Induction of vanin expression as part of the inflammatory-regenerative differentiation program of human epidermis could be a beneficial response to

supply the skin with anti-oxidant activity and sufficient pantothenic acid to restore skin barrier function. Alternatively, cysteamine could, via its inhibitory activity towards TGases and caspase-3, and its agonistic activity towards PPAR γ , contribute to the pathology observed in lesional skin, which is clearly an area for future research.

Material and methods

Human tissues

Biopsies of normal human skin, psoriatic lesions and atopic dermatitis lesions were taken under local anesthesia with 4 mm punches. Psoriasis biopsies were taken from the centre of a chronique plaque. All samples were collected with written informed consent using protocols that comply with the Declaration of Helsinki Principles. Permission for these studies was obtained from the medical ethics committee (Commissie Mensgebonden Onderzoek Arnhem-Nijmegen). Archival autopsy material was obtained from the Department of Pathology, University of Nijmegen, The Netherlands.

Submerged keratinocyte cultures

Primary human keratinocytes obtained from biopsies of healthy volunteers, psoriasis patients and atopic dermatitis patients were cultured following the Rheinwald-Green system⁴⁷ and stored in liquid nitrogen until use. First-passage cells were cultured to confluency in keratinocyte growth medium (KGM), and induced to differentiate by growth factor depletion as described before^{48,49}. Differentiating cell cultures were stimulated with a mix of 10 U/ml interferon- γ , 30 ng/ml TNF- α and 30 ng/ml IL-1 α (referred to as Th1 cytokine mix), a mix of 50 ng/ml IL-4 and 50 ng/ml IL-13 (referred to as Th2 mix), 30 ng/ml IL-17, 30 ng/ml IL-22, a combination of IL-17, IL-22 and the Th1 mix, or left untreated (control)¹³. IL-1 α , TNF- α , IL-4, IL-13, IL-17 and IL-22 were obtained from Peprotech (London, UK) and interferon- γ from HyCult Biotechnology (HBT, Uden, The Netherlands). The cells were harvested after 48 hours for mRNA isolation.

Three-dimensional reconstructed skin

Reconstructed skin was generated as described before²⁰. Briefly, de-epidermized human dermis (DED) of 0.8 mm thickness and 8 mm diameter was used as a scaffold for keratinocytes in tissue culture inserts in a 24-well plate. These were cultured submerged for three days, and subsequently the medium level was lowered to allow air-exposure to induce terminal differentiation. After seven days of air exposure a fully stratified epidermis has developed that expresses all normal differentiation markers, but is negative for psoriasis-associated genes like cytokeratin 16 (CK16), elafin and hBD-2. At this point a mixture of proinflammatory cytokines (10 ng/ml IL-1 α , 5 ng/ml TNF- α and 5 ng/ml IL6), Th2-cytokines (50 ng/ml IL-4 and 50 ng/ml IL-13) or Th17-cytokines (100 ng/ml IL-17 or 100 ng/ml IL-22) is added for 72 hours, which induces cytokine-specific gene expression. IL-6

was obtained from Gentaur (Brussels, Belgium). Two different donors of human keratinocytes were used.

Real-time quantitative polymerase chain reaction

Epidermal sheets from skin biopsies or skin constructs were separated from the underlying dermis according to previously described protocols^{20,50}. RNA extracted from twenty-six different normal human tissues, punch biopsies and cultured human keratinocytes was used for first strand cDNA synthesis with the iScript cDNA synthesis kit (Bio-Rad, Hercules, CA, USA) according to the manufacturer's recommendation with an input of 1 µg of RNA. The reverse transcriptase product was used as a template for real-time quantitative PCR amplification of genes of interest with the MyiQ Single-Color Real-Time Detection System for quantification with Sybr Green and melting curve analysis (Bio-Rad, Richmond, CA, USA). Expression of target genes vanin1, vanin-2 and vanin-3 was normalized to that of the housekeeping gene human ribosomal phosphoprotein P0 (RPLP0). Primer sequences (Biolegio, Nijmegen, the Netherlands) and efficiency of amplification are given in table 2.1.

Table 2.1 Primers for qPCR

Gene	Forward primer (5' → 3')	Reverse primer (5' → 3')	E'
Vanin-1	gaaccagatgtgtcttct	catacaacctcccaaacaga	2.06
Vanin-2	gtgctacttaccgaaattcatc	tttaccaaacgcccattctt	2.00
Vanin-3	gatcattctaagtgggagtca	cgtcctctcttgaaatctca	2.20
RPLP0	caccattgaaatcctgagtgatgt	tgaccagcccaaggagaag	2.00

E is efficiency as fold increase in fluorescence per PCR cycle

Vanin-3 antibody production

A vanin-3 PCR product from cDNA derived from cultured keratinocytes was cloned into pET-32a vector (Novagen, Madison, WI, USA), expressed as a TrxA-Vanin-3 fusion protein in *Escherichia coli*. The fusion protein was emulsified with complete Freund's adjuvant to immunize rabbits to generate polyclonal serum. Animals were boosted with TrxA-Vanin-3, and blood was obtained for serum preparation. Pre-immune serum was drawn for control staining in immunohistochemistry.

Immunohistochemistry

Human skin biopsies and human reconstructed skin were fixed in buffered 4% formalin for 4 hours and processed for routine histology. Subsequently, the reconstructed skin was embedded in paraffin and 6 µm sections were cut. Sections were processed for staining using an indirect immunoperoxidase technique with avidin-biotin complex enhancement. All procedures have been described previously in detail⁵¹. Vanin-3 staining was performed using our vanin-3 antibody raised in rabbit as primary antibody and a goat-anti-rabbit antibody as

secondary antibody (Vector Laboratories, Burlingame, CA, USA). As a control, also the pre-immune serum was used in the same dilution (1:500) as the vanin-3 antibody.

Statistics

Data are expressed as mean \pm standard deviation. Statistical analysis of qPCR data was done on deltaCt values using the SPSS software (release 16.0 Chicago, IL, USA). One-way analysis of variance (ANOVA) and repeated measures ANOVA were performed followed by post-hoc testing corrected for multiple testing (Bonferroni). P-values of <0.05 were considered statistically significant.

References

1. Galland F, Malergue F, Bazin H, Mattei MG, Aurrand-Lions M, Theillet C *et al.* Two human genes related to murine vanin-1 are located on the long arm of human chromosome 6. *Genomics* 53, 203-13 (1998)
2. Martin F, Malergue F, Pitari G, Philippe JM, Philips S, Chabret C *et al.* Vanin genes are clustered (human 6q22-24 and mouse 10A2B1) and encode isoforms of pantetheinase ectoenzymes. *Immunogenetics* 53, 296-306 (2001)
3. Granjeaud S, Naquet P, Galland F. An ESTs description of the new Vanin gene family conserved from fly to human. *Immunogenetics* 49, 964-972 (1999)
4. Aurrand-Lions M, Galland F, Bazin H, Zakharyev VM, Imhof BA, Naquet P. Vanin-1, a novel GPI-linked perivascular molecule involved in thymus homing. *Immunity* 5, 391-405 (1996)
5. Suzuki K, Watanabe T, Sakurai S, Ohtake K, Kinoshita T, Araki A *et al.* A novel glycosylphosphatidyl inositol-anchored protein on human leukocytes: a possible role for regulation of neutrophil adherence and migration. *J Immunol* 162, 4277-84 (1999)
6. Maras B, Barra D, Dupre S, Pitari G. Is pantetheinase the actual identity of mouse and human vanin-1 proteins? *FEBS Lett* 461, 149-152 (1999)
7. Pitari G, Malergue F, Martin F, Philippe JM, Massucci MT, Chabret C *et al.* Pantetheinase activity of membrane-bound Vanin-1: lack of free cysteamine in tissues of Vanin-1 deficient mice. *FEBS Lett* 483, 149-154 (2000)
8. Martin F, Penet MF, Malergue F, Lepidi H, Dessein A, Galland F *et al.* Vanin-1(-/-) mice show decreased NSAID- and Schistosoma-induced intestinal inflammation associated with higher glutathione stores. *J Clin Invest* 113, 591-7 (2004)
9. Berruyer C, Pouyet L, Millet V, Martin FM, LeGoffic A, Canonici A *et al.* Vanin-1 licenses inflammatory mediator production by gut epithelial cells and controls colitis by antagonizing peroxisome proliferator-activated receptor gamma activity. *J Exp Med* 203, 2817-2827 (2006)
10. Nickoloff BJ, Qin JZ, Nestle FO. Immunopathogenesis of psoriasis. *Clin Rev Allergy Immunol* 33, 45-56 (2007)
11. Nograles KE, Zaba LC, Guttman-Yassky E, Fuentes-Duculan J, Suarez-Farinas M, Cardinale I *et al.* Th17 cytokines interleukin (IL)-17 and IL-22 modulate distinct inflammatory and keratinocyte-response pathways. *Br J Dermatol* 159, 1092-102 (2008)
12. Leung DY, Bieber T. Atopic dermatitis. *Lancet* 361, 151-160 (2003)
13. Zeeuwen PL, de Jongh GJ, Olthuis D, Kamsteeg M, Verhoosel R, Hiemstra PS *et al.* Genetically programmed differences in epidermal host defense between psoriasis and atopic dermatitis patients. *PLoS One* (2008)
14. Palmer CN, Irvine AD, Terron-Kwiatkowski A, Zhao Y, Liao H, Lee SP *et al.* Common loss-of-function variants of the epidermal barrier protein filaggrin are a major predisposing factor for atopic dermatitis. *Nat Genet* 38, 441-446 (2006)
15. Hollox EJ, Huffmeier U, Zeeuwen PL, Palla R, Lascorz J, Rodijk-Olthuis D *et al.* Psoriasis is associated with increased beta-defensin genomic copy number. *Nat Genet* 40, 23-25 (2008)
16. de Jongh GJ, Zeeuwen PL, Kucharekova M, Pfundt R, van de Valk PG, Blokx W *et al.* High expression levels of keratinocyte antimicrobial proteins in psoriasis compared

- with atopic dermatitis. *J Invest Dermatol* 125, 1163-1173 (2005)
17. Nomura I, Goleva E, Howell MD, Hamid QA, Ong PY, Hall CF *et al.* Cytokine milieu of atopic dermatitis, as compared to psoriasis, skin prevents induction of innate immune response genes. *J Immunol* 171, 3262-3269 (2003)
 18. Livak KJ, Schmittgen TD. Analysis of relative gene expression data using real-time quantitative PCR and the 2(-Delta Delta C(T)) Method. *Methods* 25, 402-408 (2001)
 19. kamsteeg M, Zeeuwen PL, de Jongh GJ, Rodijk-Olthuis D, Zeeuwen-Franssen ME, van Erp PE *et al.* Increased expression of carbonic anhydrase II (CA II) in lesional skin of atopic dermatitis: regulation by Th2 cytokines. *J Invest Dermatol* 127, 1786-1789 (2007)
 20. Tjabringa G, Bergers M, van RD, de BR, Lamme E, Schalkwijk J. Development and validation of human psoriatic skin equivalents. *Am J Pathol* 173, 815-823 (2008)
 21. Nitto T, Inoue T, Node K. Alternative spliced variants in the pantetheinase family of genes expressed in human neutrophils. *Gene* 426, 57-64 (2008)
 22. Monger DJ, Williams ML, Feingold KR, Brown BE, Elias PM. Localization of sites of lipid biosynthesis in mammalian epidermis. *J Lipid Res* 29, 603-12 (1988)
 23. Elias PM. Stratum corneum defensive functions: an integrated view. *J Invest Dermatol* 125, 183-200 (2005)
 24. Grice KA, Bettley FR. Skin water loss and accidental hypothermia in psoriasis, ichthyosis, and erythroderma. *Br Med J* 4, 195-8 (1967)
 25. Jeon JH, Lee HJ, Jang GY, Kim CW, Shim DM, Cho SY *et al.* Different inhibition characteristics of intracellular transglutaminase activity by cystamine and cysteamine. *Exp Mol Med* 36, 576-81 (2004)
 26. Candi E, Schmidt R, Melino G. The cornified envelope: a model of cell death in the skin. *Nat Rev Mol Cell Biol* 6, 328-40 (2005)
 27. Candi E, Oddi S, Paradisi A, Terrinoni A, Ranalli M, Teofoli P *et al.* Expression of transglutaminase 5 in normal and pathologic human epidermis. *J Invest Dermatol* 119, 670-677 (2002)
 28. Kim IG, Gorman JJ, Park SC, Chung SI, Steinert PM. The deduced sequence of the novel protransglutaminase E (TGase3) of human and mouse. *J Biol Chem* 268, 12682-90 (1993)
 29. Polakowska R, Herting E, Goldsmith LA. Isolation of cDNA for human epidermal type I transglutaminase. *J Invest Dermatol* 96, 285-8 (1991)
 30. Nonomura K, Yamanishi K, Hosokawa Y, Doi H, Hirano J, Fukushima S *et al.* Localization of transglutaminase 1 mRNA in normal and psoriatic epidermis by non-radioactive in situ hybridization. *Br J Dermatol* 128, 23-28 (1993)
 31. Bernard BA, Reano A, Darmon YM, Thivolet J. Precocious appearance of involucrin and epidermal transglutaminase during differentiation of psoriatic skin. *Br J Dermatol* 114, 279-283 (1986)
 32. Esmann J, Voorhees JJ, Fisher GJ. Increased membrane-associated transglutaminase activity in psoriasis. *Biochem Biophys Res Commun* 164, 219-24 (1989)
 33. Harrison CA, Layton CM, Hau Z, Bullock AJ, Johnson TS, MacNeil S. Transglutaminase inhibitors induce hyperproliferation and parakeratosis in tissue-engineered skin. *Br J Dermatol* 156, 247-257 (2007)
 34. Lesort M, Lee M, Tucholski J, Johnson GV. Cystamine inhibits caspase activity. Implications for the treatment of polyglutamine disorders. *J Biol Chem* 278, 3825-

- 3830 (2003)
35. Weil M, Raff MC, Braga VM. Caspase activation in the terminal differentiation of human epidermal keratinocytes. *Curr Biol* 9, 361-4 (1999)
 36. Michalik L, Wahli W. Peroxisome proliferator-activated receptors (PPARs) in skin health, repair and disease. *Biochim Biophys Acta* 1771, 991-8 (2007)
 37. Rivier M, Safonova I, Lebrun P, Griffiths CE, Ailhaud G, Michel S. Differential expression of peroxisome proliferator-activated receptor subtypes during the differentiation of human keratinocytes. *J Invest Dermatol* 111, 1116-21 (1998)
 38. Bongartz T, Coras B, Vogt T, Scholmerich J, Muller-Ladner U. Treatment of active psoriatic arthritis with the PPARgamma ligand pioglitazone: an open-label pilot study. *Rheumatology (Oxford)* 44, 126-9 (2005)
 39. Ellis CN, Varani J, Fisher GJ, Zeigler ME, Pershadsingh HA, Benson SC *et al.* Troglitazone improves psoriasis and normalizes models of proliferative skin disease: ligands for peroxisome proliferator-activated receptor-gamma inhibit keratinocyte proliferation. *Arch Dermatol* 136, 609-16 (2000)
 40. Robertshaw H, Friedmann PS. Pioglitazone: a promising therapy for psoriasis. *Br J Dermatol* 152, 189-91 (2005)
 41. Demerjian M, Man MQ, Choi EH, Brown BE, Crumrine D, Chang S *et al.* Topical treatment with thiazolidinediones, activators of peroxisome proliferator-activated receptor-gamma, normalizes epidermal homeostasis in a murine hyperproliferative disease model. *Exp Dermatol* 15, 154-60 (2006)
 42. Shilov VN, Sergienko VI. Oxidative stress in keratinocytes as an etiopathogenetic factor of psoriasis. *Bull Exp Biol Med* 129, 309-13 (2000)
 43. Wojas-Pelc A, Marcinkiewicz J. What is a role of haeme oxygenase-1 in psoriasis? Current concepts of pathogenesis. *Int J Exp Pathol* 88, 95-102 (2007)
 44. Yildirim M, Inaloz HS, Baysal V, Delibas N. The role of oxidants and antioxidants in psoriasis. *J Eur Acad Dermatol Venereol* 17, 34-6 (2003)
 45. Rocha-Pereira P, Santos-Silva A, Rebelo I, Figueiredo A, Quintanilha A, Teixeira F. The inflammatory response in mild and in severe psoriasis. *Br J Dermatol* 150, 917-28 (2004)
 46. Dimon-Gadal S, Gerbaud P, Therond P, Guibourdenche J, Anderson WB, Evain-Brion D *et al.* Increased oxidative damage to fibroblasts in skin with and without lesions in psoriasis. *J Invest Dermatol* 114, 984-9 (2000)
 47. Rheinwald JG, Green H. Serial cultivation of strains of human epidermal keratinocytes: the formation of keratinizing colonies from single cells. *Cell* 6, 331-344 (1975)
 48. van Ruissen F, de Jongh GJ, Zeeuwen PL, van Erp PE, Madsen P, Schalkwijk J. Induction of normal and psoriatic phenotypes in submerged keratinocyte cultures. *J Cell Physiol* 168, 442-452 (1996)
 49. Pfundt R, van Ruissen F, van Vlijmen IM, Alkemade JA, Zeeuwen PL, Jap PK *et al.* Constitutive and inducible expression of SKALP/elafin provides anti-elastase defense in human epithelia. *J Clin Invest* 98, 1389-1399 (1996)
 50. van Ruissen F, Jansen BJ, de Jongh GJ, Vlijmen-Willems IM, Schalkwijk J. Differential gene expression in premalignant human epidermis revealed by cluster analysis of serial analysis of gene expression (SAGE) libraries. *FASEB J* 16, 246-248 (2002)
 51. Le M, Schalkwijk J, Siegenthaler G, van de Kerkhof PC, Veerkamp JH, van der Valk PG. Changes in keratinocyte differentiation following mild irritation by sodium dodecyl sulphate. *Arch Dermatol Res* 288, 684-690 (1996)



β -defensin-2 protein is a serum biomarker for disease activity in psoriasis and reaches biologically relevant concentrations in lesional skin

3 CHAPTER

Patrick AM Jansen¹
Diana Rodijk-Olthuis¹
Edward J Hollox²
Marijke Kamsteeg¹
Geuranne S Tjabringa¹
Gys J de Jongh¹
Ivonne MJJ van Vlijmen-Willems¹
Judith GM Bergboer¹
Michelle M van Rossum¹
Elke MGJ de Jong¹
Martin den Heijer³
Andrea WM Evers⁴
Mieke Bergers¹
John AL Armour⁵
Patrick LJM Zeeuwen¹
Joost Schalkwijk¹

¹Department of Dermatology and Nijmegen Centre for Molecular Life Sciences, Radboud University Nijmegen Medical Centre, The Netherlands

²Department of Genetics, University of Leicester, UK

³Department of Endocrinology and Department of Epidemiology and Biostatistics, Radboud University Nijmegen Medical Centre, The Netherlands

⁴Department of Medical Psychology, Radboud University Nijmegen Medical Centre, The Netherlands

⁵Institute of Genetics, University of Nottingham, UK

Abstract

Background

Previous studies have extensively documented antimicrobial and chemotactic activities of beta-defensins. Human beta-defensin-2 (hBD-2) is strongly expressed in lesional psoriatic epidermis, and recently we have shown that high beta-defensin genomic copy number is associated with psoriasis susceptibility. It is not known, however, if biologically and pathophysiologically relevant concentrations of hBD-2 protein are present *in vivo*, which could support an antimicrobial and proinflammatory role of beta-defensins in lesional psoriatic epidermis.

Methodology/Principal Findings

We found that systemic levels of hBD-2 showed a weak but significant correlation with beta defensin copy number in healthy controls but not in psoriasis patients with active disease. In psoriasis patients but not in atopic dermatitis patients, we found high systemic hBD-2 levels that strongly correlated with disease activity as assessed by the PASI score. Our findings suggest that systemic levels in psoriasis are largely determined by secretion from involved skin and not by genomic copy number. Modelling of the *in vivo* epidermal hBD-2 concentration based on the secretion rate in a reconstructed skin model for psoriatic epidermis provides evidence that epidermal hBD-2 levels *in vivo* are probably well above the concentrations required for *in vitro* antimicrobial and chemokine-like effects.

Conclusions/Significance

Serum hBD-2 appears to be a useful surrogate marker for disease activity in psoriasis. The discrepancy between hBD-2 levels in psoriasis and atopic dermatitis could explain the well known differences in infection rate between these two diseases.

Introduction

Psoriasis is a highly prevalent inflammatory skin disease that has both environmental and genetic components to its etiology^{1,2}. Genetic evidence for an (auto)immune basis of psoriasis is provided by the well-known association of the disease with the HLA-Cw6 gene³ and the recently discovered associations with IL12B and IL23R^{4,5}. Lesional psoriatic skin is characterized by various morphological abnormalities of the epidermis, and a cellular infiltrate of activated T-cells. There are several arguments to invoke an important role of activated T-cells such as the oligoclonal T-cell expansion in psoriatic skin⁶ and the therapeutic efficacy of T-cell directed drugs such as cyclosporin A and some of the biologics that are currently available. Recent evidence also points to a role of other cell types such as plasmacytoid dendritic cells⁷, and cytokine networks associated with cells from the adaptive and innate immune system^{1,8}. Based on clinical studies in humans and experimental studies in mice, several of these cytokines have been identified including IL-1, TNF α , interferon- γ and IL-6. In the epidermis a regenerative epidermal differentiation program is induced that includes hyperproliferation and expression of genes such as cytokeratin 16 (CK16), SKALP/elafin, psoriasin and hBD-2^{9,10}. Expression of these genes is to some extent specific for psoriasis, as they are expressed at low levels, if at all, in lesional atopic dermatitis skin¹¹⁻¹³.

Recent findings from various labs including our own have indicated that polymorphisms of genes that are expressed in the epithelium, but not necessarily in immunocytes, could also be risk factors for inflammatory skin diseases such as atopic dermatitis and psoriasis¹⁴⁻¹⁷. This finding was further supported at the cellular level when we found cell-autonomous differences between keratinocytes from psoriasis and atopic dermatitis patients¹⁸. From these studies we concluded that psoriatic keratinocytes are programmed to secrete large amounts of host defense proteins such as beta-defensins, in response to Th1 or Th17 cytokines.

Beta-defensins are secreted peptides of low molecular weight ranging from 3 to 5 kDa. These peptides, which are expressed by epithelia, possess a broad spectrum of antimicrobial activity against both gram-positive and gram-negative bacteria, fungi and viruses¹⁹. Besides antimicrobial activity, they also exhibit pro-inflammatory properties as chemoattractants for memory T-cells, immature dendritic cells, mast cells and neutrophils²⁰⁻²². These peptides, encoded by the *DEFB* genes, are present in three main gene clusters, two on chromosome 20 and one on 8p23.1. The cluster on 8p23.1 contains eight beta-defensin genes of which seven (all but *DEFB1*) are on a large repeat that is variable in copy number. In humans up to 12 copies of this repeat have been found, with a mode of four copies per diploid genome²³. Of the eight beta-defensin genes located on 8p23.1, human beta-defensin-1 (hBD-1) protein, (encoded by *DEFB1*) and hBD-3 (encoded by *DEFB103*) are constitutively expressed at low levels in skin²⁴. hBD-2 (encoded by *DEFB4*) is not expressed in normal skin but is highly expressed in psoriatic skin. hBD-4 (encoded by *DEFB104*) is less well characterized at

the protein level but is found in skin by RT-PCR. hBD-2, hBD-3 and hBD-4 can be induced by cytokines and bacterial lipopolysaccharides in various epithelial cell types²⁵. It has also been shown that antimicrobial peptides in general, and above all hBD-2, are induced in lesional epidermal cells of patients with psoriasis, compared with lesional epidermal cells of patients with atopic dermatitis and normal skin^{10,11}. These findings have been interpreted to explain the observed high infection rate in atopic dermatitis and the relatively low prevalence of bacterial and viral infections among psoriasis patients²⁶.

In addition to their direct antimicrobial activity, the chemotactic properties of antimicrobial proteins like LL-37 and beta-defensins are thought to amplify leukocyte recruitment²⁷, thereby contributing to an effective antimicrobial response. In non-infectious inflammatory diseases like psoriasis, beta-defensins could augment the influx of T-cells and dendritic cells, and thereby contribute to chronicity and sustained disease. Although the antimicrobial and chemotactic activities *in vitro* have been well documented, there are no quantitative data on *in vivo* concentrations of beta-defensins to substantiate a role of these molecules in host defense or inflammation. In this study we have made a detailed analysis of systemic and epidermal defensin concentrations. We show that both genetic factors and disease activity determine defensin protein expression. Evidence is provided that the *in vivo* concentration of hBD-2 is well above the minimal concentrations that are required for biological activity *in vitro*.

Results

Expression of beta-defensin mRNA and protein in normal tissues and inflamed skin

Although expression of beta-defensins in some human tissues has been documented before, we wanted to obtain a comprehensive picture of beta-defensin tissue distribution in order to estimate which specific tissues would contribute to systemic protein levels. We performed a qPCR analysis of two beta-defensin genes that are contained in the repeat on chromosome 8 (*DEFB4* and *DEFB103*) and one beta-defensin outside the repeat (*DEFB1*). Figure 3.1 shows that hBD-1 mRNA is widely expressed whereas significant levels of hBD-2 are predominantly found in oral epithelia. hBD-3 is expressed more broadly than hBD-2 as it is also found at low levels in normal epidermis and a few other tissues. As indicated in figure 3.1 (log scale) hBD-2 expression levels in lesional psoriatic epidermis are extremely high compared to any other tissue. hBD-2 mRNA expression in atopic dermatitis is also increased, compared to normal skin where it is undetectable. We analyzed the expression of hBD-2 at the protein level by immunohistochemistry. Figure 3.2 confirm the moderate expression levels in tongue and plantar epidermis, and the absence of expression in normal skin. The extremely high mRNA expression level in psoriatic epidermis was indeed reflected by high levels of protein as we have described before¹⁰.

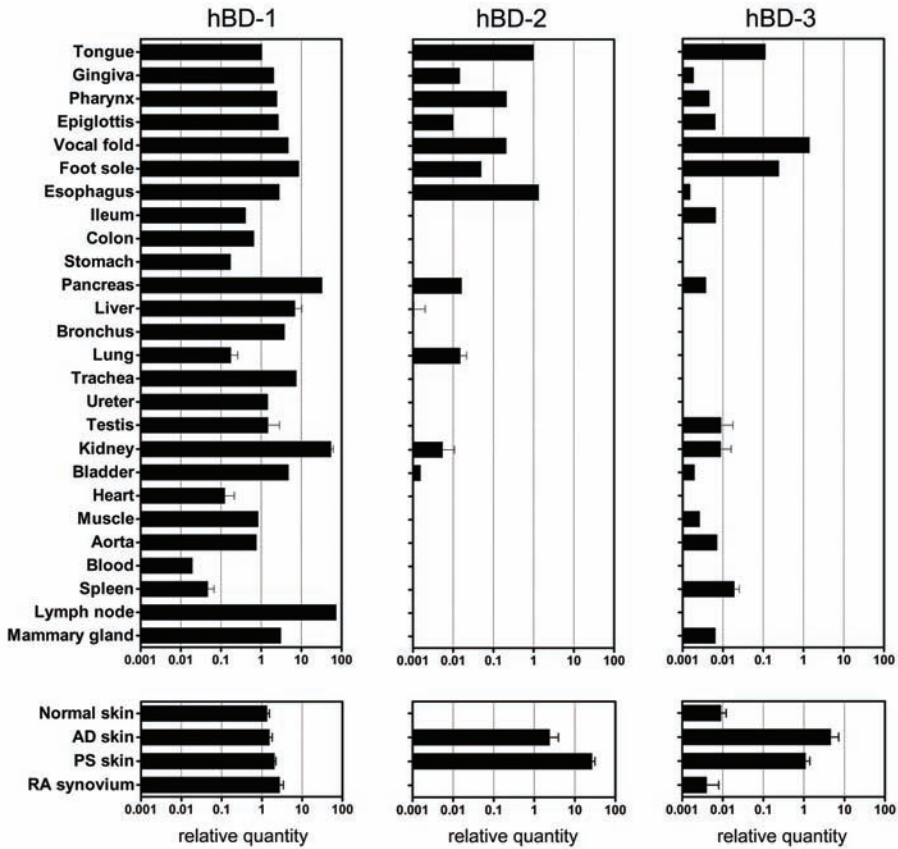


Figure 3.1 Analysis of beta-defensin mRNA expression in normal and inflamed human tissues. Quantitative real-time PCR was performed on RNA of normal human tissues (mostly obtained from one individual), purified epidermis from skin biopsies of healthy controls, psoriasis patients and atopic dermatitis patients, and inflamed synovium from rheumatoid arthritis patients. Expression of target genes was normalized to that of RPLP0. For graphical representation all values were expressed relative to hBD-2 in tongue, which was set at unity [34]. Primer sequences and efficiency of amplification are given in table 3.2. For details on normal human tissues see materials and methods. Bars represent mean and SD.

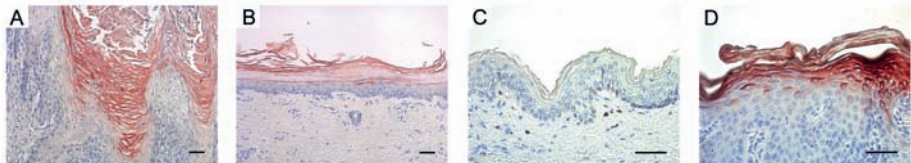


Figure 3.2 Immunolocalization of hBD-2 in human epithelia. Immunohistochemical staining of normal human tissues (tongue, plantar skin and trunk skin, A-C) and psoriatic skin (D) with a polyclonal rabbit antiserum against recombinant hBD-2. Note that protein data largely follow the mRNA data demonstrating the absence in normal skin, low expression in tongue and plantar skin. Bar = 100 μ m. Control sections stained with pre-immune serum were negative (not shown).

Serum hBD-2 levels in healthy volunteers correlate with genomic copy number

As a next step we wanted to make a quantitative determination of systemic defensin protein levels. Defensins are secreted proteins that will easily pass basal membranes, and we expected that epithelium-expressed defensins would reach the circulation and could be measured in serum by ELISA. On the basis of the limited expression of hBD-2 in normal human tissues, as demonstrated in figure 3.1, we expected low levels of protein in normal human serum. We developed and validated an ELISA that was sensitive and specific for hBD-2 to allow measurement of low serum hBD-2 levels. In addition, commercially available ELISA kits were used to measure hBD-2 and hBD-3 protein in serum. We have previously shown that most beta-defensin genes on 8p23.1 (including those that encode hBD-2 and hBD-3) are subject to copy number variation. So far no studies have been published that investigated the relation between copy number and protein expression. Here we selected 70 healthy individuals without inflammatory skin disease, that were typed for beta-defensin copy number using multiplex amplifiable probe hybridization (MAPH), restriction enzyme digest variant ratio (REDVR) and paralogue ratio test (PRT). In the normal population, copy number classes of 3 to 5 defensin repeats per diploid genome are the most prevalent. We selected individuals to include sufficient numbers of the more rare copy classes of

Table 3.1 Disease severity and serum hBD-2 of patients and controls

Diagnosis	Disease severity	Disease score	N	Serum hBD-2 (ng/ml)
Controls	n.a.	n.a.	70	0.21 ± 0.17
Psoriasis	remission, PASI 0-1	0.4 + 0.4	3	0.64 ± 0.36
	low, PASI 1-10	6.0 + 2.7	18	4.5 ± 4.6
	moderate, PASI 10-20	15.1 + 2.8	12	11.5 ± 9.1
	high, PASI > 20	30.2 + 3.6	5	84.2 ± 80.0
Atopic dermatitis	remission, SCORAD 0-5	0 + 0	2	0.10 ± 0.01
	low, SCORAD 5-15	12.0 + 2.8	2	0.12 ± 0.03
	moderate, SCORAD 15-40	27.9 + 9.4	6	1.05 ± 0.95
	high, SCORAD > 40	47.6 + 5.0	2	1.39 ± 0.74
Rheumatoid arthritis	remission, DAS28 0-2.6	2.1 + 0.5	10	0.33 ± 0.16
	low DAS28, 2.6-3.2	2.9 + 0.1	5	0.34 ± 0.19
	moderate, DAS28 3.2-5.1	4.2 + 0.6	16	0.51 ± 0.41
	high, DAS28 > 5.1	6.0 + 0.4	9	0.83 ± 0.59

Serum hBD-2 levels were determined by ELISA. Analysis of variance on log transformed data showed that there was a significant correlation between disease severity and serum hBD-2 levels in psoriasis patients ($p < 2 \times 10^{-5}$). Disease scores and serum hBD-2 concentration are given as mean and SD. n.a. not applicable.

2 and 6 to allow analysis of correlation between genomic copy number and serum hBD-2 protein. Figure 3.3 shows that there is a modest but highly significant correlation between copy number and hBD-2 protein concentration in serum. No correlation between serum hBD-2 and age or gender was found. Low hBD-2 levels were found up to 0.80 ng/ml in these human sera (mean and SD: 0.21 ± 0.17 ng/ml, see table 3.1), but clearly the variance is only partially explained by copy number. A similarly weak correlation (Pearson's $R=0.4$, $p=0.001$) between copy number and serum protein was found using a commercially available hBD-2 ELISA, although absolute levels of hBD-2 appeared to be higher for the commercial kit, which was probably due to the difference in standards used (not shown). hBD-3 serum levels of individuals without inflammatory skin disease were all below the detection limit (0.1 ng/ml). These data show that hBD-2 (but not hBD-3) can be measured in normal human serum, and that these uninduced levels are at least in part determined by genomic copy number.

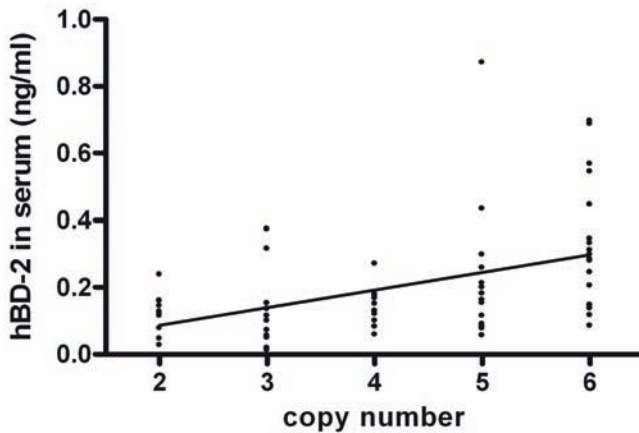


Figure 3.3 Correlation between serum hBD-2 protein levels and genomic copy number. Serum hBD-2 protein levels of 70 healthy controls (determined by ELISA) were plotted against the genomic copy number of the beta-defensin repeat on chromosome 8p23, as determined by MAPH, REDVR and PRT. A significant linear correlation was found. Pearson's $R = 0.46$ and $p < 7 \times 10^{-5}$.

hBD-2 serum levels of psoriasis patients correlate with clinical severity

Because of the modest expression of hBD-2 mRNA in most normal tissues we expected relatively low levels of hBD-2 protein in the circulation, as was indeed found by ELISA in control individuals (figure 3.3). In view of the huge increase of hBD-2 mRNA in lesional psoriatic epidermis, the inflamed skin of psoriasis patients was likely to cause increased systemic levels of hBD-2 protein. We measured hBD-2 in sera of 38 psoriasis patients in a range of clinical severity as determined by the Psoriasis Area and Severity Index (PASI) score (see table 3.1). We could indeed demonstrate high levels of serum hBD-2 in psoriasis patients, which were found to be about 400-fold increased in severely affected patients compared to healthy individuals (see table 3.1). A significant effect of disease severity on serum hBD-2 was found by analysis of variance ($p < 2 \times 10^{-6}$). Figure

3.4 shows that there is a strong linear correlation between PASI score and the log-transformed serum hBD-2 concentration. Strongly increased levels were also found in the urine of psoriasis patients whereas hBD-2 could not be detected in urine of healthy controls. Urinary hBD-2 levels were showed strong interindividual variation ($2.2 + 3.2$ ng/ml). These findings suggest that increased systemic levels are derived from high cutaneous production. It is obvious from figure 3.4 that the clinical severity in psoriasis patients is a far stronger determinant of hBD-2 serum concentration than copy number for uninduced levels in healthy controls (figure 3.3). There were insufficient numbers of informative psoriasis patients from whom defensin copy numbers and PASI scores were available, to make a reliable estimate of the effect of copy number and disease severity on hBD-2 levels. Remarkably, only in a minority of psoriasis patients we could demonstrate hBD-3 levels that exceeded the detection limit of the assay (not shown).

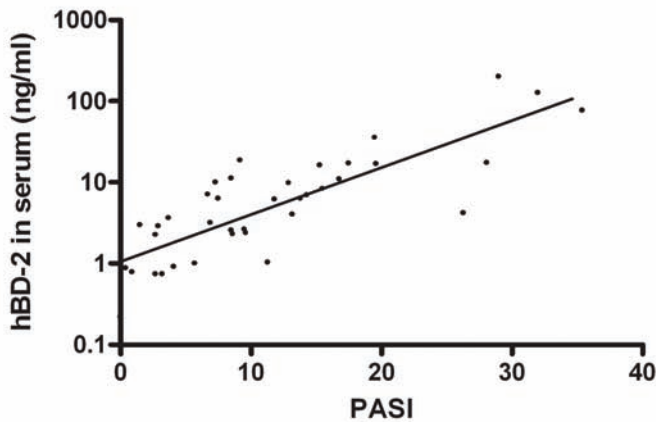


Figure 3.4 Correlation between serum hBD-2 protein and PASI score. Serum hBD-2 protein levels of 38 psoriasis patients of varying disease severity were plotted against their PASI score. A significant linear correlation was found. Pearson's $R = 0.82$, $p < 4 \times 10^{-10}$.

To investigate if high systemic hBD-2 levels could be caused by inflammation per se, irrespective of the tissue localization, we compared serum hBD-2 levels in psoriasis patients with that of 40 patients with rheumatoid arthritis (RA). Low hBD-2 serum levels were found in RA patients with low to high disease activity and in RA patients that were in remission (see table 3.1). In the combined RA patients with moderate to high disease activity, a small but significant increase of serum hBD-2 was found compared to the control group (t-test, $p < 10^{-5}$). qPCR analysis of synovial tissue from RA patients with active disease showed that the synovium is unlikely to be the source of this small increase in hBD-2 protein, as no mRNA for hBD-2 could be detected (see figure 3.1). No significant correlation was found between serum hBD-2 and clinical severity as determined by Disease Activity Score (DAS28).

As previously reported¹⁰, hBD-2 protein is expressed at low to undetectable levels (immunohistochemistry) in lesional atopic dermatitis, despite strong

induction at the mRNA level. In sera from 8 patients with moderate to severe atopic dermatitis we found that, although serum hBD-2 levels were significantly higher than in control sera (t-test, $p < 10^{-5}$), they were far lower than in sera of psoriasis patients of similar disease severity (see table 3.1). A significant linear correlation between log-transformed serum hBD-2 and atopic dermatitis disease severity, as determined by SCORing Atopic Dermatitis (SCORAD), was found (Pearson $r = 0.7$, $p < 0.01$), suggesting that also in atopic dermatitis increased systemic levels are derived from increased cutaneous production.

Serum hBD-2 is a disease marker in individual psoriasis patients

As serum hBD-2 showed a correlation with disease activity over a group of psoriasis patients, we next investigated if hBD-2 levels correlate with clinical status of individual patients. Serum hBD-2 was measured in 15 patients that participated in clinical studies for which PASI scores and serum was available on two different occasions over a 6-18 week interval. Figure 3.5 shows that there is a strong correlation between the change in hBD-2 (Δ hBD-2) and change in PASI score (Δ PASI) in eleven patients that showed clinical improvement and four patients that showed exacerbation of disease.

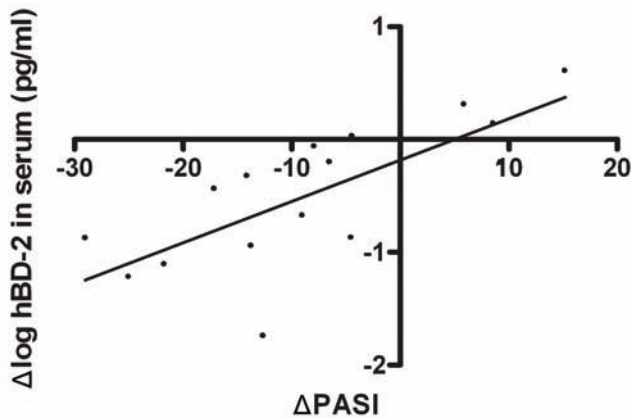


Figure 3.5 Correlation between the change in serum hBD-2 concentration and change in clinical score. Serum hBD-2 protein levels of 15 patients for which PASI scores and serum was available on two different occasions over a 6-18 week interval, were plotted against the change in PASI score (Δ PASI). A significant linear correlation was found. Pearson $R = 0.74$, $p < 0.002$. Note that there was a decrease in serum hBD-2 in most patients that showed clinical improvement (negative Δ PASI) and an increase in serum hBD-2 in a few patients that showed exacerbation (positive Δ PASI).

Estimation of in vivo hBD-2 concentration in psoriatic epidermis using in vitro reconstructed skin

The high serum levels of hBD-2 in psoriasis patients (up to 190 ng/ml), which we interpret to be derived from local production by the keratinocytes, suggest that the concentrations to which keratinocytes and infiltrated cells in the epidermis and papillary dermis are exposed must be several orders of magnitude higher.

Based on *in vitro* studies, the concentrations required to have a relevant biological effect would vary between 0.1 and 100 $\mu\text{g/ml}$. Because these local tissue concentrations are difficult to estimate directly from *in vivo* data, we measured the production of hBD-2 in reconstructed skin as a model for human epidermis. Human reconstructed skin equivalents were obtained as described previously²⁹, and stimulated with IL-1 α , TNF- α and IL-6. This cytokine mixture was recently found to be optimal for induction of a psoriatic phenotype *in vitro*, as witnessed by high expression levels of CK16, SKALP/elafin and hBD-2³⁰. qPCR analysis of isolated epidermal sheets indicated that hBD-2 mRNA levels (determined as deltaCt values) in these cultures were much higher than in keratinocytes from submerged cultures (not shown), and reached similar high values as found in epidermal sheets from lesional psoriatic skin (see figure 3.1). Figure 3.6 shows hBD-2 protein expression by differentiated keratinocytes in the reconstructed skin model stimulated with pro-inflammatory cytokines. We collected culture medium from cytokine-stimulated reconstructed skin of two donors during 24 hours starting two days after addition of the cytokine mix. Using ELISA we found that these cultures, consisting of 8 mm diameter skin constructs, secreted approximately 66 ± 19 ng hBD-2 per 24 hours into the tissue culture medium (mean and SD of four cultures). We derived the local epidermal concentration using an approximation based on the known diffusion coefficient of a small cationic protein in aqueous solution (see supplementary information for assumptions and dimensions of the system, used for modelling). Alternatively, a theoretical value for the diffusion coefficient was obtained based on Graham's law (see supplementary information). The most conservative estimation of the hBD-2 local concentration in the compartment of the epidermis was 1.2 mg/ml (0.3 mM), which is far higher than concentrations required for *in vitro* antimicrobial activity, or those reported for chemotactic activity towards T-cells and dendritic cells.

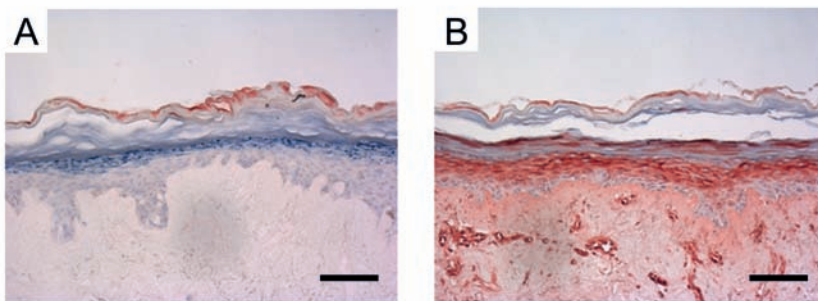


Figure 3.6 Induction of hBD-2 protein expression in reconstructed skin by proinflammatory cytokines. Expression of hBD-2 in 3-D reconstructed skin following stimulation with psoriasis-associated cytokines (10 ng/ml IL-1 α , 5 ng/ml TNF α and 5 ng/ml IL-6) for 72 hours. Note that without stimulation there is no hBD-2 expression (A), whereas the cytokine mixture induces high expression levels that are secreted into the underlying culture medium (147 ng/ml in 24 h). Part of the hBD-2 protein remains adsorbed to the dermal matrix as witnessed by the staining of structures in the dermis (B). Bar = 100 μm .

Discussion

Psoriasis is associated with increased beta-defensin genomic copy number but no quantitative information on defensin protein expression *in vivo*, as a function of copy number or disease status was available. We now present evidence that both genomic copy number and epidermal activation by psoriasis-associated cytokines determine expression levels of hBD-2. We conclude that these increased circulating hBD-2 levels in patients are derived from cutaneous production, indicating that local hBD-2 concentrations in psoriatic epidermis are likely to be extremely high. Extrapolation from an *in vitro* model system suggests that the concentration in the epidermis or papillary dermis (0.3 mM) by far exceeds the concentrations required to be antimicrobial (2.5 to 25 μ M) and chemotactic *in vitro* (250 nM) as described previously by others^{9,31}.

A number of studies have reported expression of human beta-defensins in various tissues, including normal skin, inflamed skin and non-cutaneous epithelia, using semi-quantitative RT-PCR or immunohistochemistry. Here we have quantified circulating levels of hBD-2 and hBD-3 by ELISA in healthy volunteers and patients with inflammatory diseases. To assess which of the normal human epithelia would contribute to steady state systemic protein levels, we first performed a comprehensive qPCR analysis of the three major epidermal defensins, hBD-1, -2 and -3 in a large panel of human tissues. As shown in figure 3.1, hBD-1 mRNA is widely expressed, and is not subject to regulation by inflammation, as it is not highly induced in psoriatic skin. Measurement of hBD-1 protein in serum would have provided a reference value for a beta-defensin that is expected to be rather constant as it is not present on the psoriasis-associated repeat. We were however unsuccessful in measuring hBD-1 protein by ELISA (not shown). hBD-2 mRNA appears to be expressed constitutively by a few tissues (e.g. oral epithelia), and was indeed found at the protein level albeit weakly (figure 3.2). hBD-2 is absent from normal trunk skin, but it is expressed at low levels in plantar skin. Consequently, serum hBD-2 levels in healthy individuals are very low (less than 1 ng per ml). In addition to our own ELISA (recombinant hBD-2 for calibration), we also used a commercial hBD-2 ELISA kit that uses synthetic hBD-2 for calibration. Although there was a good correlation between the data of both assays (Pearson $r = 0.9$), the commercial ELISA yielded apparent hBD-2 serum concentrations 10-fold higher than our ELISA. We found that this was caused by a difference in immunoreactivity of the calibration standards used. We used the values obtained with recombinant hBD-2 throughout this paper, as a conservative estimate of hBD-2 concentration.

As shown in figure 3.3, genomic copy number only explains part of the variance in serum hBD-2 levels. This is unlikely to be caused by experimental error. We considered sampling error as a potential cause, but we did not find variation in serum hBD-2 level depending on the time of blood sample collection (early morning versus late afternoon). Longitudinal data showed only minor fluctuation of serum hBD-2 levels in blood taken with two-year intervals (not

shown). We speculate that the large variation of protein levels in each copy class could be caused by variation in expression regulation, or alternatively, by genetic variation in the defensin copies themselves. Although there is currently no information on the existence of non-functional gene copies within the repeat, this would obviously affect the gene-protein correlation, and it could also affect the observed association with psoriasis, which clearly requires further investigation.

Although our findings indicate that uninduced hBD-2 production is subject to gene dosage effects, the high systemic serum levels in psoriasis patients are caused by disease activity itself. We think this indicates that hBD-2 can be used as an objective, quantitative marker for disease activity in psoriasis. There are very few reliable serum markers for disease activity in psoriasis. Candidate proteins that are overexpressed in lesional epidermis include SKALP/elafin and psoriasin/S100A7, but only SKALP/elafin was found to correlate with disease activity^{32,33}. Previous studies have suggested that conventional surrogate markers for disease activity in rheumatoid arthritis and psoriatic arthritis, such as erythrocyte sedimentation rate and levels of C-reactive protein (CRP) are not useful for chronic plaque psoriasis³⁴. For this reason we looked at the correlation between PASI scores and CRP in a cohort of our own patients that were monitored over time. We did not find a significant correlation between CRP and PASI for 1305 patient visits (data not shown), again suggesting that serum hBD-2 could be a convenient way to monitor disease activity or therapeutic effects.

At the tissue level, hBD-2 secretion will be determined both by copy number and by stimulation with proinflammatory cytokines. Our data also suggest that disease activity in atopic dermatitis is correlated with serum hBD-2. However, the epidermal expression in atopic dermatitis is far lower than in psoriasis^{10,11}, presumably resulting from the distinct cytokine environments of these diseases^{8,35}. We could indeed show that Th2 cytokines do not induce hBD-2 expression in cultured keratinocytes¹⁸ and that Th2 cytokines repress the Th1 induced expression (not shown here), as was previously shown for hBD-3³⁶. An additional level of regulation of hBD-2 expression is the responsiveness of cells to pro-inflammatory cytokines. We have recently shown that cell-autonomous differences exist between keratinocytes of psoriasis patients, atopic dermatitis patients and controls with respect to innate immune responses following Th1 cytokine stimulation¹⁸. We would speculate that there are apparently three mechanisms that contribute to high levels of hBD-2 in psoriatic epidermis: a dominant Th1 or Th17 cytokine profile, increased cell-autonomous responsiveness to cytokine stimulation, and high defensin genomic copy number. Although defensins are endowed with cytokine-like properties themselves, there is no information on a possible autocrine effect of hBD-2 on keratinocytes whereby it would induce or sustain its own production. This is clearly an area worth investigating.

Several studies have demonstrated the biological activities of human and mouse beta-defensins, such as antimicrobial activity⁹, chemotaxis of T-cells and dendritic cells³⁷, and activation of TLR4³⁸. In general, many antimicrobial proteins appear to be endowed with other immune-modulatory activities³⁹⁻⁴¹.

These findings have raised the intriguing possibility that beta-defensins are part of the innate immune system that provides a link between the epithelium and the adaptive immune system. This would fit the emerging concept of inflammatory epithelial diseases¹⁴ that is supported by findings on the genetics of atopic dermatitis¹⁵, Crohn's disease⁴² and celiac disease⁴³. This would also explain the clinical observation that both T-cell directed drugs (cyclosporine A, UVB, some biologicals) and keratinocyte-directed drugs (retinoids, vitamin D3 derivatives) are effective in the treatment of psoriasis.

The defensin concentrations used in *in vitro* studies to demonstrate their biological activity and their relevance for the *in vivo* situation, should be interpreted with some caution. For example, the antimicrobial activity of hBD-2 can only be demonstrated at low salt conditions⁴⁴, at least in low micromolar concentrations. Notwithstanding these considerations, we attempted to make an estimate of the actual hBD-2 concentration in an active psoriatic lesion. Although there are some caveats associated with modelling of the *in vivo* tissue concentrations based on an *in vitro* reconstructed skin model, it is clear that the hBD-2 levels in epidermis and papillary dermis are well above the minimal concentrations that would cause a biological effect in an experimental setting, even allowing for an error of one order of magnitude. Remarkably, we found very little hBD-3 protein in the circulation. Only in a few psoriasis patients we observed detectable levels up to 0.5 ng/ml, which is 160-fold lower than the hBD-2 concentration in patients with severe psoriasis. Whether this also reflects low hBD-3 protein production in the epidermis requires further investigation.

Our previous finding on the genetic association of psoriasis with the defensin cluster did not allow discrimination between the seven defensins or defensin-like genes contained in the repeated segment. On the basis of available expression data we predicted that hBD-2 and hBD-3 would be the best candidates. Here we provide further evidence that, based on copy number dependent and disease-specific gene expression, high cutaneous protein levels and its known proinflammatory properties, hBD-2 is one of the strongest psoriasis candidate genes contained in the beta defensin cluster on chromosome 8.

Materials and methods

Patients and healthy subjects

All psoriasis patients had plaque-type psoriasis diagnosed by a dermatologist. Atopic dermatitis was diagnosed by a dermatologist, according to the Hanifin criteria, and were of the extrinsic type³⁵. Rheumatoid arthritis patients were diagnosed by a rheumatologist, according to the ACR criteria. Patients were recruited via the in-patient or out-patient departments of the Radboud University Nijmegen Medical Centre. Control sera and DNA samples were from the Nijmegen Biomedical Study (NBS)⁴⁵. All controls and patients were of native European Dutch origin. Demographic data were as follows (age: mean and SD, and % female); Controls: 50 ± 16, 59% female; Psoriasis patients: 47 ± 13 year,

42% female; Rheumatoid arthritis patients: 59 ± 8 years, 66% female. Available information of medication used during sample collection: 59% of the psoriasis patients were on biologicals (all TNF-blockers) and 36% were on other types of systemic medication (retinoids, MTX). Nearly all rheumatoid arthritis patients used NSAIDs, 45% was on MTX and 25% was on biologicals (various kinds, mostly TNF blockers). Blood was stored at -80°C and genomic DNA was isolated by standard procedures. Permission for these studies was obtained from the local medical ethics committee (Commissie Mensgebonden Onderzoek Arnhem-Nijmegen), and volunteers gave written informed consent. The study was conducted according to the Declaration of Helsinki principles.

Clinical scores

As a measure of disease severity the clinical score was determined by medical specialists. For psoriatic patients the PASI (0 to 72 scale)⁴⁶, for atopic dermatitis patients the SCORAD (0 to 103 scale)⁴⁷ and for rheumatic arthritic patients the DAS28 (0 to 10 scale)⁴⁸ was used to measure disease severity. Patients were classified as being in remission, or having low disease activity, moderate disease activity or high disease activity (see table 3.1).

Immunohistochemistry

Autopsy material and skin biopsies were fixed in 4% phosphate-buffered formalin and embedded in paraffin as described before⁴⁹. Sections of seven micrometer were stained according to the avidin biotinylated-enzyme-complex method (Vector Laboratories, Burlingame, CA) using a goat anti-hBD-2 serum (Abcam, Cambridge, UK).

RNA extraction and real-time quantitative polymerase chain reaction

RNA from a variety of organs that included many epithelial tissues, was available from autopsy material of one individual. For this reason the qPCR data in figure 3.1 have only $n=1$ for most organs. Additional RNA samples from lung (8), kidney (2), heart (1), testis (1), spleen (1) and liver (1), normal (5) and inflamed epidermis (7) and inflamed synovium (5) were obtained from different individuals and analyzed for beta defensin expression. Variability between the different samples from one type of organ was low, and similar profiles of differential expression of beta defensins 1, 2 and 3 were found. When multiple samples per organ were available, expression values are given as mean and SD in figure 3.1.

RNA was extracted from twenty-four different normal human tissues, punch biopsies and cultured human keratinocytes, and first strand cDNA was synthesized using an input of 1 μg of RNA with the iScript cDNA synthesis kit (Bio-Rad, Hercules, CA) according to the manufacturer's recommendation. The reverse transcriptase product was used as a template for quantitative real-time PCR amplification of genes of interest hBD-1, hBD-2 and hBD-3 and the housekeeping gene human ribosomal phosphoprotein P0 (RPLP0) with the MyiQ Single-Color Real-Time Detection System for quantification with Sybr Green and

melting curve analysis (Biorad, Richmond, CA). Expression of target genes was normalized to that of RPLP0. This housekeeping gene was not found to be subject to regulation in keratinocyte cultures, irrespective of stimulation or diagnosis, and is more reliable than other reference genes such as ACTB (actin) or GAPDH (data not shown). RPLP0 levels of the various tissues did not show large differences (mean and SD of Ct values of normal human tissues was 21.7 ± 1.6). The deltaCt values were used for statistical analysis. For graphical representation (figure 3.1) all values were expressed relative to hBD-2 in tongue, which was set at unity²⁸. This allows comparison of all genes and all tissues for relative expression levels. Primer sequences (Biolegio, Nijmegen, The Netherlands) and efficiency of amplification are given in table 3.2.

Table 3.2 Primers for qPCR

Gene	Forward primer (5' → 3')	Reverse primer (5' → 3')	E'
hBD-1	atggcctcaggtgtaactttc	cacttggccttccctctgtaac	2.00
hBD-2	gatgcctcttccaggtgtttt	ggatgacatatggctccactctt	1.97
hBD-3	gtgaagcctagcagctatgaggat	tgattcctccatgacctggaa	2.06
RPLP0	caccattgaaatcctgagtgatgt	tgaccagcccaaaggagaag	2.00

E' is efficiency as fold increase in fluorescence per PCR cycle

Production of recombinant hBD-2 and rabbit antiserum

A hBD-2 PCR product from cDNA derived from cultured keratinocytes was cloned into pGEX-2T vector (Amersham Pharmacia Biotech, Uppsala, Sweden), expressed as a GST-hBD-2 fusion protein in *Escherichia coli* and affinity-purified. Commercial recombinant hBD-2 (Peprotech, Rocky Hill, NJ) was cross-linked to ovalbumin, using glutaraldehyde, to increase immunogenicity. This preparation was dialysed against phosphate-buffered saline and emulsified with complete Freund's adjuvant to immunize rabbits to generate polyclonal serum. Animals were boosted with GST-hBD-2, and blood was obtained for serum preparation.

ELISA

Affinity-purified goat anti-hBD-2 (Abcam) was used to coat 96-well microtiter plates. After blocking in 1% (v/v) bovine serum albumin, serum samples were applied in a serial 2-fold dilution range, followed by our rabbit anti-hBD-2 as a second antibody, and detection by the ABC kit (Vector). All steps were followed by appropriate washing in phosphate-buffered saline with 0.05% (v/v) Tween-20. The serum hBD-2 concentrations were read from a calibration curve of recombinant hBD-2 (Peprotech). The detection limit of this ELISA was 0.03 ng/ml, using recombinant hBD-2 (Peprotech) for calibration. Anti-hBD-2 antibodies were checked for specificity against hBD-2, and we found that recombinant hBD-1 (Abcam) and hBD-3 (Abcam) were not recognized. We found no evidence for circadian differences in serum hBD-2 in healthy individuals (data

not shown). Serum hBD-2 was found to be stable upon storage at -20°C. No large differences were found for individuals from whom we had serum samples taken with a two-year interval. Commercially available ELISA kits for hBD-2 and hBD-3 were purchased from Phoenix (Belmont, CA) and performed according to manufacturer's recommendations. The detection limits for these assays were 0.05 and 0.1 ng/ml respectively, using synthetic hBD-2 and hBD-3 for calibration.

Genotyping of defensin copy number

Genomic DNA from seventy control individuals without inflammatory skin disease was analyzed for genomic copy number. Most of these individuals were analyzed by three methods: MAPH, REDVR and PRT as described previously in great detail^{16,23,50}. These analyses were used to obtain the best estimate of integral copy number.

Three-dimensional reconstructed skin

Reconstructed skin was generated as described before³⁰. Briefly, de-epidermized human dermis (DED) of 0.8 mm thickness and 8 mm diameter was used as a scaffold for keratinocytes in tissue culture inserts in a 24-well plate. These were cultured submerged for three days, and subsequently the medium level was lowered to allow air-exposure to induce terminal differentiation. After seven days of air exposure a fully stratified epidermis has developed that expresses all normal differentiation markers, but is negative for psoriasis-associated genes like CK16, SKALP/elafin and hBD-2. At this point a mixture of 10 ng/ml IL-1 α , 5 ng/ml TNF α and 5 ng/ml IL-6 is added for 72 hours, which induces high expression levels of psoriasis-associated genes. The culture medium, 450 μ l per culture, was harvested and changed at 24, 48 and 72 hours and used for hBD-2 ELISA. Two different donors for human keratinocytes were used.

Statistics

All statistical analyses were performed using the Statistica software package version 7, Statsoft Inc. Analysis of variance was performed on log transformed data of serum hBD-2. Analysis of qPCR data was done on deltaCt values.

Modelling of epidermal hBD-2 concentrations

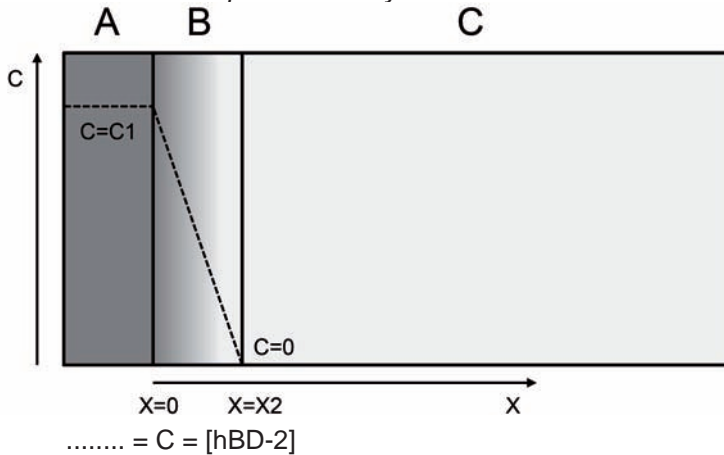
Fick's law for mass transport was applied. For the diffusion coefficient (D) of hBD-2 we used 1.44×10^{-10} m²/sec as experimentally determined for bovine pancreatic trypsin inhibitor (BPTI)⁵¹, a protein of similar mass and isoelectric point as hBD-2, or we used an approximation based on Graham's law using the known value for BSA (10^{-10} m²/sec). The hBD-2 production in a reconstructed skin model stimulated with proinflammatory cytokines was used estimate the concentration in the epidermal compartment *in vitro*, as an approximation of the concentration in psoriatic epidermis. See supplementary information for details.

Acknowledgements

We acknowledge prof P.C.M. van de Kerkhof, dr P.G.M. van der Valk and dr R. Driessen (department of Dermatology, Radboud University Nijmegen Medical Centre), prof P. van Riel, dr C. Popa (department of Rheumatology Radboud University Nijmegen Medical Centre), and dr L.A.B. Joosten (department of Internal Medicine, Radboud University Nijmegen Medical Centre) for providing clinical samples, and helpful discussions. We acknowledge dr A. de Brouwer (department of Human Genetics, Radboud University Nijmegen Medical Centre), dr J. Hoenderop (department of Physiology, Radboud University Nijmegen Medical Centre) and dr A. van Kuppevelt (department of Biochemistry, Radboud University Nijmegen Medical Centre) for providing mRNA samples. We gratefully acknowledge all patients and healthy volunteers who donated blood and skin biopsies for these investigations.

Supplementary information

Diffusion model of the air-liquid keratinocyte culture



Compartment A:
Multiple layers of keratinocytes
Unstirred compartment, [hBD-2]=constant, 50 μm thick

Compartment B:
De-epidermised dermis
Unstirred compartment, gradient of [hBD-2], 800 μm thick

Compartment C:
Unstirred compartment, [hBD-2] = low and homogenous, volume is large

All compartments have a cylindrical shape with a diameter of 4 mm

	In 3 dimensions	In 1 dimension
Fick's first law is used in steady-state diffusion, i.e., when the concentration within the diffusion volume does not change with respect to time	$J = -D\nabla\Phi$	$J = D \frac{\delta\Phi}{\delta x}$
Fick's second law is used when the concentration within the diffusion volume changes with respect to time	$\frac{\delta\Phi}{\delta t} = D\nabla^2\Phi$	$\frac{\delta\Phi}{\delta t} = D \frac{\delta^2\Phi}{\delta x^2}$
J = The diffusion flux; (amount of substance) * length ⁻² * time ⁻¹		
D = The diffusion coefficient of diffusivity; length ⁻² * time ⁻¹		
Φ = The concentration; (amount of substance) * length ⁻³		
x = The position; length		

D is inversely proportional to the square root of the (molecular) mass of the particle (Graham's law). D can also be described by the Stokes-Einstein relation:

$$D = \frac{kT}{6\pi\eta r}$$

k = The Boltzman constant
 T = The absolute temperature
 η = The viscosity of the medium
 r = The radius of the particle

For the biological molecules the differentiation coefficients normally range from 10^{-10} to 10^{-11} .

Calculation of hBD-2 mass transport in reconstructed skin model

We apply Fick's First law, because [hBD-2] is not a function of time. We use the condition only in 1 dimension, because [hBD-2] changes only in the X-direction. So:

$$\text{Mass transport hBD-2} = J = \frac{dm}{dt} = -D * \frac{dc}{dx} = a_0 = \text{constant} \quad (1)$$

$$\begin{aligned} \text{or } \frac{dc}{dx} &= -\frac{a_0}{D} \\ \text{or } dc &= -\frac{a_0}{D} * dx \\ \text{or } c &= \int -\frac{a_0}{D} * dx \\ \text{or } c &= -\frac{a_0}{D} * x + a_1 \end{aligned} \quad (2)$$

$$\text{First boundary condition for } x = 0; c = c_1 \quad (3)$$

$$\text{Second boundary condition for } x = x_2; c = 0 \quad (4)$$

$$(2) + (3) \quad \rightarrow c_1 = -\frac{a_0}{D} * 0 + a_1 \quad \rightarrow a_1 = c_1 \quad (5)$$

$$(2) + (4) + (5) \quad \rightarrow 0 = -\frac{a_0}{D} * x_2 + c_1 \quad \rightarrow a_0 = c_1 * \frac{D}{x_2} \quad (6)$$

$$(2) + (5) + (6) \quad \rightarrow c = -\frac{c_1}{x_2} * x + c_1 \quad (7)$$

The graph of this function is plotted in compartment B:

$$(1) + (7) \quad \rightarrow J = \frac{dm}{dt} = -D * \frac{dc}{dx} = -D * \frac{d(-\frac{c_1}{x_2} * x + c_1)}{dx}$$

or $J = \frac{D}{x_2 * c_1}$ per surface unit.

When we ignore the boundary conditions and the DED has a surface O, than:

Mass transport of hBD-2 = $D * \frac{O}{x_2} * c_1$ in Mol/sec.

- D = the Diffusion constant of the DED
- O = the Surface of the DED
- x_2 = the thickness of the DED
- c_1 = the [hBD-2] we wanted to know

References

1. Bowcock AM, Krueger JG. Getting under the skin: the immunogenetics of psoriasis. *Nat Rev Immunol* 5, 699-711 (2005)
2. Nickoloff BJ, Qin JZ, Nestle FO. Immunopathogenesis of psoriasis. *Clin Rev Allergy Immunol* 33, 45-56 (2007)
3. Nair RP, Stuart PE, Nistor I, Hiremagalore R, Chia NV, Jenisch S *et al.* Sequence and haplotype analysis supports HLA-C as the psoriasis susceptibility 1 gene. *Am J Hum Genet* 78, 827-51 (2006)
4. Cargill M, Schrodi SJ, Chang M, Garcia VE, Brandon R, Callis KP *et al.* A large-scale genetic association study confirms IL12B and leads to the identification of IL23R as psoriasis-risk genes. *Am J Hum Genet* 80, 273-90 (2007)
5. Capon F, Di MP, Szaub J, Prescott NJ, Dunster C, Baumber L *et al.* Sequence variants in the genes for the interleukin-23 receptor (IL23R) and its ligand (IL12B) confer protection against psoriasis. *Hum Genet* 122, 201-6 (2007)
6. Menssen A, Trommler P, Vollmer S, Schendel D, Albert E, Gurtler L *et al.* Evidence for an antigen-specific cellular immune response in skin lesions of patients with psoriasis vulgaris. *J Immunol* 155, 4078-83 (1995)
7. Nestle FO, Conrad C, Tun-Kyi A, Homey B, Gombert M, Boyman O *et al.* Plasmacytoid predendritic cells initiate psoriasis through interferon- α production. *J Exp Med* 202, 135-43 (2005)
8. Nickoloff BJ, Xin H, Nestle FO, Qin JZ. The cytokine and chemokine network in psoriasis. *Clin Dermatol* 25, 568-73 (2007)
9. Harder J, Bartels J, Christophers E, Schroder JM. A peptide antibiotic from human skin. *Nature* 387, 861 (1997)
10. de Jongh GJ, Zeeuwen PL, Kucharekova M, Pfundt R, van der Valk PG, Blokk W *et al.* High expression levels of keratinocyte antimicrobial proteins in psoriasis compared with atopic dermatitis. *J Invest Dermatol* 125, 1163-73 (2005)
11. Ong PY, Ohtake T, Brandt C, Strickland I, Boguniewicz M, Ganz T *et al.* Endogenous antimicrobial peptides and skin infections in atopic dermatitis. *N Engl J Med* 347, 1151-60 (2002)
12. Nomura I, Gao B, Boguniewicz M, Darst MA, Travers JB, Leung DY. Distinct patterns of gene expression in the skin lesions of atopic dermatitis and psoriasis: a gene microarray analysis. *J Allergy Clin Immunol* 112, 1195-202 (2003)
13. Nomura I, Goleva E, Howell MD, Hamid QA, Ong PY, Hall CF *et al.* Cytokine milieu of atopic dermatitis, as compared to psoriasis, skin prevents induction of innate immune response genes. *J Immunol* 171, 3262-9 (2003)
14. Cookson W. The immunogenetics of asthma and eczema: a new focus on the epithelium. *Nat Rev Immunol* 4, 978-88 (2004)
15. Palmer CN, Irvine AD, Terron-Kwiatkowski A, Zhao Y, Liao H, Lee SP *et al.* Common loss-of-function variants of the epidermal barrier protein filaggrin are a major predisposing factor for atopic dermatitis. *Nat Genet* 38, 441-6 (2006)
16. Hollox EJ, Huffmeier U, Zeeuwen PL, Palla R, Lascorz J, Rodijk-Olthuis D *et al.* Psoriasis is associated with increased beta-defensin genomic copy number. *Nat Genet* 40, 23-5 (2008)
17. de Cid R, Riveira-Munoz E, Zeeuwen PL, Robarge J, Liao W, Dannhauser EN *et al.* Deletion of the late cornified envelope LCE3B and LCE3C genes as a susceptibility

- factor for psoriasis. *Nat Genet* 41, 211-5 (2009)
18. Zeeuwen PL, de Jongh GJ, Rodijk-Olthuis D, kamsteeg M, Verhoosel RM, van Rossum MM *et al.* Genetically programmed differences in epidermal host defense between psoriasis and atopic dermatitis patients. *PLoS ONE* 3, e2301 (2008)
 19. Ganz T. Defensins: antimicrobial peptides of innate immunity. *Nat Rev Immunol* 3, 710-20 (2003)
 20. Yang D, Chertov O, Bykovskaia SN, Chen Q, Buffo MJ, Shogan J *et al.* Beta-defensins: linking innate and adaptive immunity through dendritic and T cell CCR6. *Science* 286, 525-8 (1999)
 21. Niyonsaba F, Ogawa H, Nagaoka I. Human beta-defensin-2 functions as a chemoattractant agent for tumour necrosis factor-alpha-treated human neutrophils. *Immunology* 111, 273-81 (2004)
 22. Niyonsaba F, Iwabuchi K, Matsuda H, Ogawa H, Nagaoka I. Epithelial cell-derived human beta-defensin-2 acts as a chemotaxin for mast cells through a pertussis toxin-sensitive and phospholipase C-dependent pathway. *Int Immunol* 14, 421-6 (2002)
 23. Hollox EJ, Armour JA, Barber JC. Extensive normal copy number variation of a beta-defensin antimicrobial-gene cluster. *Am J Hum Genet* 73, 591-600 (2003)
 24. Harder J, Schroder JM. Antimicrobial peptides in human skin. *Chem Immunol Allergy* 86, 22-41 (2005)
 25. Liu AY, Destoumieux D, Wong AV, Park CH, Valore EV, Liu L *et al.* Human beta-defensin-2 production in keratinocytes is regulated by interleukin-1, bacteria, and the state of differentiation. *J Invest Dermatol* 118, 275-81 (2002)
 26. Henseler T, Christophers E. Disease concomitance in psoriasis. *J Am Acad Dermatol* 32, 982-6 (1995)
 27. Gallo RL, Murakami M, Ohtake T, Zaiou M. Biology and clinical relevance of naturally occurring antimicrobial peptides. *J Allergy Clin Immunol* 110, 823-31 (2002)
 28. Livak KJ, Schmittgen TD. Analysis of relative gene expression data using real-time quantitative PCR and the 2(-Delta Delta C(T)) Method. *Methods* 25, 402-8 (2001)
 29. Schalkwijk J, Lamme E, de Jongh G, Zeeuwen P, Bergers M. Psoriatic Skin Equivalents. Patent application WO2007073151 (2006)
 30. Tjabringa G, Bergers M, van RD, de BR, Lamme E, Schalkwijk J. Development and validation of human psoriatic skin equivalents. *Am J Pathol* 173, 815-23 (2008)
 31. Yang D, Chen Q, Chertov O, Oppenheim JJ. Human neutrophil defensins selectively chemoattract naive T and immature dendritic cells. *J Leukoc Biol* 68, 9-14 (2000)
 32. Alkemade HA, de Jongh GJ, Arnold WP, van de Kerkhof PC, Schalkwijk J. Levels of skin-derived antileukoproteinase (SKALP)/elafin in serum correlate with disease activity during treatment of severe psoriasis with cyclosporin A. *J Invest Dermatol* 104, 189-93 (1995)
 33. Anderson KS, Wong J, Polyak K, Aronzon D, Enerback C. Detection of psoriasin/S100A7 in the sera of patients with psoriasis. *Br J Dermatol* 160, 325-32 (200)
 34. Laurent MR, Panayi GS, Shepherd P. Circulating immune complexes, serum immunoglobulins, and acute phase proteins in psoriasis and psoriatic arthritis. *Ann Rheum Dis* 40, 66-9 (1981)
 35. Leung DY, Bieber T. Atopic dermatitis. *Lancet* 361, 151-60 (2003)
 36. Howell MD, Boguniewicz M, Pastore S, Novak N, Bieber T, Girolomoni G *et al.* Mechanism of HBD-3 deficiency in atopic dermatitis. *Clin Immunol* 121, 332-8 (2006)
 37. Yang D, Biragyn A, Kwak LW, Oppenheim JJ. Mammalian defensins in immunity:

- more than just microbicidal. *Trends Immunol* 23, 291-6 (2002)
38. Biragyn A, Ruffini PA, Leifer CA, Klyushnenkova E, Shakhov A, Chertov O *et al.* Toll-like receptor 4-dependent activation of dendritic cells by beta-defensin 2. *Science* 298, 1025-9 (2002)
 39. Di Nardo A, Braff MH, Taylor KR, Na C, Granstein RD, McInturf JE *et al.* Cathelicidin antimicrobial peptides block dendritic cell TLR4 activation and allergic contact sensitization. *J Immunol* 178, 1829-34 (2007)
 40. Lande R, Gregorio J, Facchinetti V, Chatterjee B, Wang YH, Homey B *et al.* Plasmacytoid dendritic cells sense self-DNA coupled with antimicrobial peptide. *Nature* 449, 564-9 (2007)
 41. Braff MH, Hawkins MA, Di Nardo A, Lopez-Garcia B, Howell MD, Wong C *et al.* Structure-function relationships among human cathelicidin peptides: dissociation of antimicrobial properties from host immunostimulatory activities. *J Immunol* 174, 4271-8 (2005)
 42. Fellermann K, Stange DE, Schaeffeler E, Schmalzl H, Wehkamp J, Bevins CL *et al.* A chromosome 8 gene-cluster polymorphism with low human Beta-defensin 2 gene copy number predisposes to crohn disease of the colon. *Am J Hum Genet* 79, 439-48 (2006)
 43. Monsuur AJ, de Bakker PI, Alizadeh BZ, Zhernakova A, Bevova MR, Strengman E *et al.* Myosin IXB variant increases the risk of celiac disease and points toward a primary intestinal barrier defect. *Nat Genet* 37, 1341-4 (2005)
 44. Bals R, Wang X, Wu Z, Freeman T, Bafna V, Zasloff M *et al.* Human beta-defensin 2 is a salt-sensitive peptide antibiotic expressed in human lung. *J Clin Invest* 102, 874-80 (1998)
 45. Hoogendoorn EH, Hermus AR, de VF, Ross HA, Verbeek AL, Kiemeney LA *et al.* Thyroid function and prevalence of anti-thyroperoxidase antibodies in a population with borderline sufficient iodine intake: influences of age and sex. *Clin Chem* 52, 104-11 (2006)
 46. Schmitt J, Wozel G. The psoriasis area and severity index is the adequate criterion to define severity in chronic plaque-type psoriasis. *Dermatology* 210, 194-9 (2005)
 47. Kunz B, Oranje AP, Labreze L, Stalder JF, Ring J, Taieb A. Clinical validation and guidelines for the SCORAD index: consensus report of the European Task Force on Atopic Dermatitis. *Dermatology* 195, 10-9 (1997)
 48. van Riel PL, Schumacher HR Jr. How does one assess early rheumatoid arthritis in daily clinical practice? *Best Pract Res Clin Rheumatol* 15, 67-76 (2001)
 49. Alkemade HA, Molhuizen HO, van Vlijmen-Willems IM, van Haelst UJ, Schalkwijk J. Differential expression of SKALP/Elafin in human epidermal tumors. *Am J Pathol* 143, 1679-87 (1993)
 50. Armour JA, Palla R, Zeeuwen PL, den Heijer M, Schalkwijk J, Hollox EJ. Accurate, high-throughput typing of copy number variation using paralogue ratios from dispersed repeats. *Nucleic Acids Res* 35, e19 (2007)
 51. Gallagher WH, Woodward CK. The concentration dependence of the diffusion coefficient for bovine pancreatic trypsin inhibitor: a dynamic light scattering study of a small protein. *Biopolymers* 28, 2001-24 (1989)



Molecular diagnostics of psoriasis, atopic dermatitis, allergic contact dermatitis and irritant contact dermatitis

4 CHAPTER

Marijke Kamsteeg¹
Patrick AM Jansen¹
Ivonne MJJ van Vlijmen-Willems¹
Piet E van Erp¹
Diana Rodijk-Olthuis¹
Pieter G van der Valk¹
Ton Feuth²
Patrick LJM Zeeuwen¹
Joost Schalkwijk¹

¹Department of Dermatology and Nijmegen Centre for Molecular Life Sciences, Radboud University Nijmegen Medical Centre

²Department of Epidemiology, Biostatistics and Health Technology Assessment, Radboud University Nijmegen Medical Centre, Nijmegen, The Netherlands

Abstract

Background

Microarray studies on the epidermal transcriptome in psoriasis and atopic dermatitis have revealed genes with disease-specific expression in keratinocytes of lesional epidermis. These genes are possible candidates for disease-specific pathogenetic changes, but could also provide a tool for molecular diagnostics of inflammatory skin conditions in general.

Objectives

To analyze if gene expression signatures as found in purified epidermal cells from atopic dermatitis are also present in other eczematous conditions such as allergic and irritant contact dermatitis.

Methods

We used real-time quantitative PCR, immunohistochemistry and bioinformatics to investigate gene expression in different forms of eczema. Normal epidermis and psoriatic epidermis were analysed for comparison.

Results

Carbonic anhydrase II was highly induced in epidermis from all forms of eczema but not in psoriasis. Remarkably, the presumed neuron-specific Nel-like protein 2 showed a strong induction only in atopic dermatitis epidermis. Interleukin-1F9, elafin, beta-defensin-2 and vanin-3 were strongly induced in psoriasis, but not in any type of eczema. High levels of the chemokines CCL17 and CXCL10 were predominantly found in epidermis of allergic contact dermatitis. The chemokine CXCL8 was highly expressed in psoriasis, atopic dermatitis, and allergic contact dermatitis, but not in irritant contact dermatitis. Cluster analysis or multinomial logistic regression indicated that expression levels of a set of seven genes are a strong predictor of the type of inflammatory response.

Conclusions

These observations contribute to molecular diagnostic criteria for inflammatory skin conditions.

Introduction

Atopic dermatitis and psoriasis are two major chronic inflammatory skin diseases that show distinct differences with respect to clinical appearance of the lesions, itch, trans-epidermal water loss, surface pH and bacterial colonization/infection¹. Several non-overlapping genetic associations have recently been established for both diseases, including genes involved in adaptive immunity, innate immunity and skin barrier function²⁻⁵. Although there are some histopathological similarities such as epidermal hyperproliferation, acanthosis and a pronounced T cell infiltrate, a number of differences at the cellular and molecular level can be noted. The immune responses are markedly polarized towards Th1 and Th17 cytokine profiles in psoriasis^{6,7}, and a Th2 profile in atopic dermatitis, particularly in the (sub)acute phase⁸. Using expression profiling by microarrays or large scale real-time quantitative PCR (qPCR), several studies have found striking differences between expressed genes in the epidermis of lesional skin from patients with psoriasis and with atopic dermatitis, which appear to be determined both by the cytokine environment and cell-autonomous processes⁹⁻¹¹. The transcriptome of lesional psoriasis skin is very similar to that of cultured keratinocytes stimulated with pro-inflammatory cytokines (interleukin (IL)-1 or IL-1/tumour necrosis factor (TNF)- α /Interferon (IFN)- γ) as demonstrated by several groups^{11,12}. In contrast, it was shown that the transcriptome of atopic dermatitis skin is quite distinct and is similar to that of Th2 cytokine-stimulated cultured keratinocytes. Large differences between epidermal gene expression in psoriasis and atopic dermatitis were found for antimicrobial proteins such as human β -defensin (hBD)-2, hBD-3, S100 proteins and elafin, for chemokines such as CCL18, CCL27, CCL13, CXCL8, and for genes that do not have obvious functions in inflammation such as vanin-3 (VNN3), Nel-like 2 (NELL2) and carbonic anhydrase II (CAII)^{9-11,13-16}. It was demonstrated that induction of these genes is likely to be under control of the specific psoriasis and atopic dermatitis cytokine environments^{11,17,18}. Antimicrobial proteins, many chemokines and VNN3 were found to be induced in cultured keratinocytes by psoriasis-associated cytokines (e.g. TNF- α , IL-1, IL-6, IL-17 and IL-22), whereas the atopic dermatitis specific genes CAII and NELL2 were induced by Th2 cytokines (IL-4 and IL-13). Low expression levels of antimicrobial proteins in atopic dermatitis have been interpreted to contribute to the high prevalence of skin infections in atopic dermatitis compared with psoriasis^{10,11,13}. It remains to be investigated to what extent other highly differential genes, notably the psoriasis-associated vanin genes (VNN1 and VNN3), and the atopic dermatitis-associated genes NELL2 and CAII, contribute to the pathogenesis of these skin conditions. Based on the disease-specific patterns and the biological properties, there is sufficient reason to suspect that differentially expressed genes detected in the aforementioned studies are not merely innocent bystanders, but could have a causal relationship with the disease process. For this reason we wanted to investigate if atopic dermatitis-associated epidermal gene expression was specific for atopic dermatitis or could also be

demonstrated in other eczematous conditions such as allergic and irritant contact dermatitis. Allergic contact dermatitis and irritant contact dermatitis represent two common skin conditions that are mechanistically different but share clinical and histopathological similarities with atopic dermatitis such as itch, spongiosis and increased transepidermal water loss due to skin barrier disruption^{19,20}. Here we have compared gene expression patterns in lesional skin of patients with psoriasis and atopic dermatitis with experimentally induced eczematous lesions of allergic contact dermatitis and irritant contact dermatitis. Our results indicate that psoriasis is molecularly quite distinct from atopic dermatitis, allergic contact dermatitis and irritant contact dermatitis. The eczematous conditions, however, show similar expression patterns for some but not for all genes. Our results indicate that, using a set of only seven genes, a molecular distinction can be made between epidermis from normal skin, psoriasis, atopic dermatitis, allergic contact dermatitis and irritant contact dermatitis.

Results

mRNA expression profiles in psoriasis, atopic dermatitis, allergic contact dermatitis and irritant contact dermatitis

Previous studies have identified a number of genes that are associated with psoriasis and atopic dermatitis. Some of these studies used microarrays without confirmation by qPCR or protein expression. We therefore first tested a number of these proposed candidate genes by qPCR to confirm microarray data as published previously. We focused on genes that were reported to be differentially expressed in two different studies⁹⁻¹¹, and gave robust signals in qPCR assays (see supplementary information and Table S4.1). The following inflammation-associated genes were selected for further study by qPCR: the antimicrobial proteins elafin and hBD-2; the cytokines IL-1F9, IL-1 β and IL-18; the chemokines CCL17, CXCL8 and CXCL10; the hyperproliferation-associated keratin KRT6. Based on two microarray studies and subsequent qPCR confirmation we selected four additional genes not known to have a function in inflammatory processes. These genes NELL2, CAII, VNN3 and VNN1 were among the most highly differential genes in studies that compared psoriasis and atopic dermatitis gene expression. The skin conditions studied here can be quite diverse in their clinical manifestations, but care was taken to include lesions of similar clinical severity with respect to erythema. Lesions of all skin conditions were from strongly inflamed skin. Irritant contact dermatitis and allergic contact dermatitis were by definition in an acute phase as they were induced for that purpose, the atopic dermatitis skin was from erythematous skin of individuals with chronic eczema during a relapse, and psoriasis biopsies were taken from chronic plaques that were nevertheless clearly inflamed. As the skin conditions studied here are likely to have varying amounts of cellular infiltrate in the epidermal compartment, we measured CD45 mRNA expression as a semiquantitative marker for cells from hematopoietic origin. Figure 4.1 shows the results of these analyses for mRNA expression

of the most informative genes in epidermal sheets from normal skin and from individuals with psoriasis, atopic dermatitis, allergic contact dermatitis and irritant contact dermatitis. Our results confirmed findings from previous studies on atopic dermatitis and psoriasis, showing a strong increase of antimicrobial genes (hBD-2, elafin), IL-1F9 and vanins in psoriasis, whereas C11 and NELL2 were strongly increased in atopic dermatitis. Remarkably, hBD-2, elafin, IL-1F9 and VNN3 were

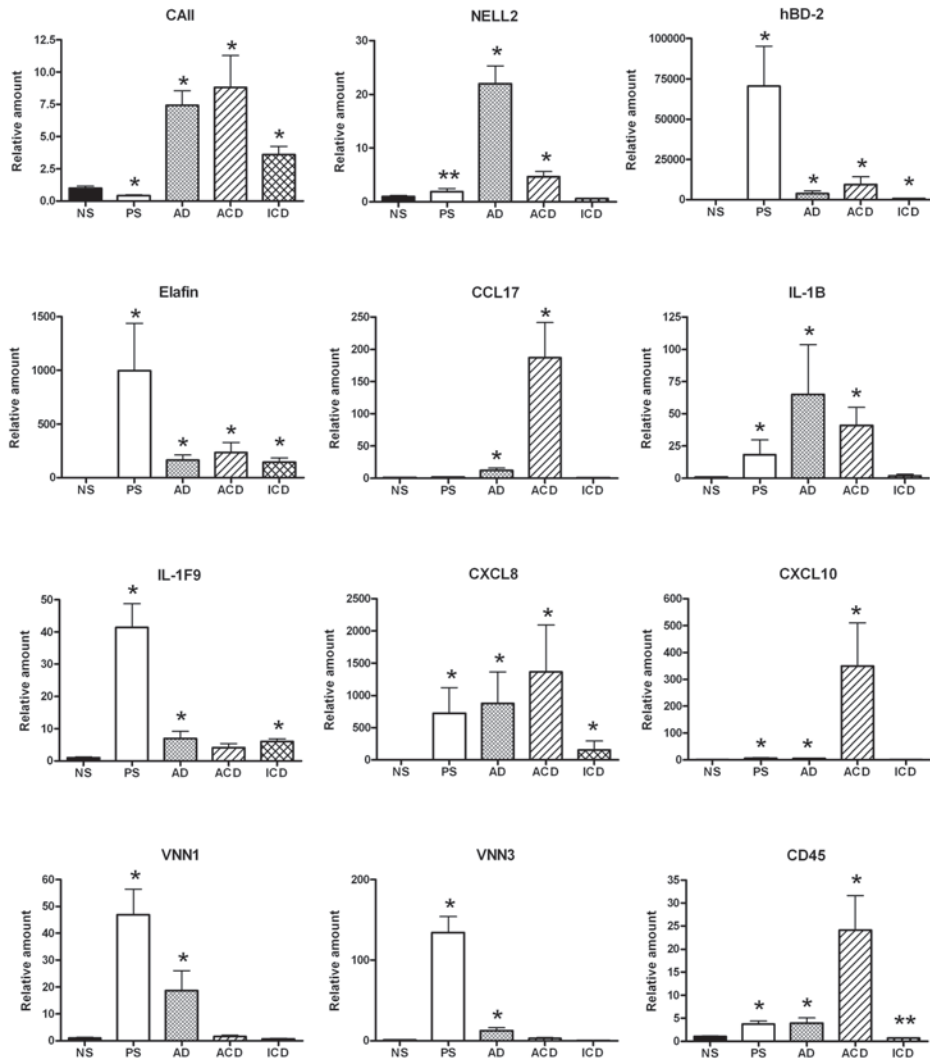


Figure 4.1 qPCR data on informative genes. qPCR data on 12 informative genes, i.e. genes that showed differential expression between the 5 diagnoses normal skin (NS), psoriasis (PS), atopic dermatitis (AD), allergic contact dermatitis (ACD) and irritant contact dermatitis (ICD). Fold induction was expressed relative to normal skin (set at 1). Statistical analysis was performed on ΔC_t values. ANOVA showed that for each gene there was a significant effect of the factor diagnosis on the gene expression level. Post-hoc analysis (Bonferroni test) was used to analyze significant differences between diagnoses. * and ** indicate significant p-values of < 0.01 and < 0.05 respectively, compared with normal skin.

quite specific for psoriasis. Although some induction was found in eczematous conditions compared with normal skin, the expression levels in psoriasis were significantly higher. The induction of CAll, first observed for atopic dermatitis and not for psoriasis, was also found for allergic and irritant contact dermatitis. High expression of NELL2 was only found for atopic dermatitis, and a small but significant increase compared with normal skin was found in allergic contact dermatitis. The functional significance of this highly specific atopic dermatitis-associated molecule for the disease process remains to be investigated. Two chemokine genes, CCL17 and CXCL10, showed high expression levels only in allergic contact dermatitis epidermis. Although the number of infiltrating T lymphocytes is also higher in allergic contact dermatitis than in any other of the conditions studied (see qPCR data in Figure 4.1 and immunohistochemistry in Figure 4.2) we assume that high levels of CCL17 and CXCL10 are derived from keratinocytes as T lymphocytes are not known to be strong producers of these chemokines. None of the studied molecular markers was specifically upregulated in irritant contact dermatitis as shown in Figure 4.1. IL-1 β and CXCL8 were found to discriminate between irritant contact dermatitis and the other inflammatory conditions, as irritant contact dermatitis was the only condition that did not show strong induction of these genes compared with normal skin. IL-18 and KRT6 expression did not significantly discriminate between the four inflammatory conditions (not shown).

Protein expression of selected genes in normal skin, psoriasis, atopic dermatitis, allergic contact dermatitis and irritant contact dermatitis

Although qPCR is by far the most sensitive and accurate method for gene expression quantitation, these findings do not necessarily reflect protein expression levels. We used immunohistochemistry and flow cytometry to analyse a number of markers for which reliable staining protocols were available. Staining of hBD-2 and elafin confirmed the known high levels of expression in lesional skin of patients with psoriasis (Figure 4.2). Sixteen of seventeen allergic contact dermatitis patients showed no or hardly any hBD-2 staining. In all patients with atopic dermatitis and irritant contact dermatitis hBD-2 staining was minimal to absent. Elafin, however, was strongly expressed in the *stratum granulosum* of all patients with irritant contact dermatitis. Staining for elafin in patients with allergic contact dermatitis and atopic dermatitis was variable and less intense. Normal skin was, as expected, always negative for hBD-2 as well as for elafin. In general there was a good correlation between mRNA and protein expression levels of elafin and hBD-2.

In earlier studies we showed that CAll mRNA and protein is upregulated in lesional skin of atopic dermatitis, whereas in psoriasis a downregulation of CAll mRNA is found¹⁴. In Figure 4.1 of this study we show that CAll induction is found in all three eczematous conditions as it is also elevated in allergic and irritant contact dermatitis. Immunohistochemistry, however, was not suitable to reliably detect quantitative differences in CAll staining between atopic dermatitis, allergic

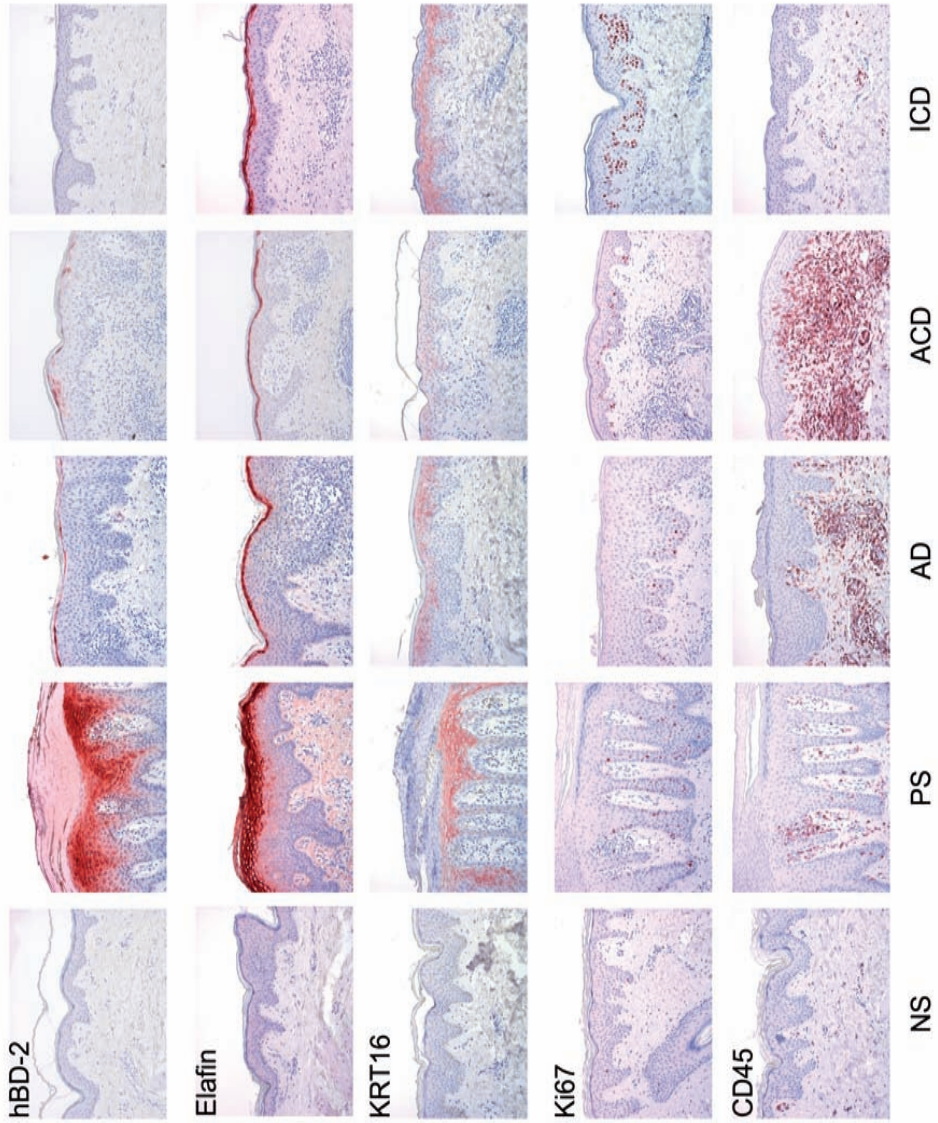


Figure 4.2 Immunohistochemical staining for marker proteins. Immunohistochemical staining for 5 marker proteins associated with epidermal activation (hBD-2, elafin and KRT16), cellular proliferation (Ki67) and infiltration by cells of hematopoietic origin (CD45). Staining patterns were largely similar to the quantitative data obtained by qPCR for hBD-2, elafin, KRT16 and CD45. A representative picture is shown here, without further quantification.

contact dermatitis, irritant contact dermatitis and normal skin (not shown). To investigate whether upregulation of CAII protein could be demonstrated in allergic contact dermatitis, a flow cytometric analysis was performed on epidermal cells obtained from nonlesional and lesional allergic contact dermatitis skin. Staining of epidermal cell populations for CAII was found to be heterogeneous. All six patients showed an elevated CAII signal and/or a higher percentage of epidermal cells positive for CAII (Figure 4.3). These results indicate that similar to atopic dermatitis, CAII protein is also upregulated in allergic contact dermatitis, albeit less strongly than at the mRNA level.

Keratin 16 (KRT16) is generally regarded as a keratin that is induced in the context of epidermal hyperproliferation, as found in psoriasis. KRT16 forms a heterodimer with KRT6, which was not found to be informative at the mRNA level to distinguish between the four inflammatory conditions. Recent studies in our laboratory have shown that KRT16 expression and epidermal hyperproliferation are also present in atopic dermatitis. Here we also investigated

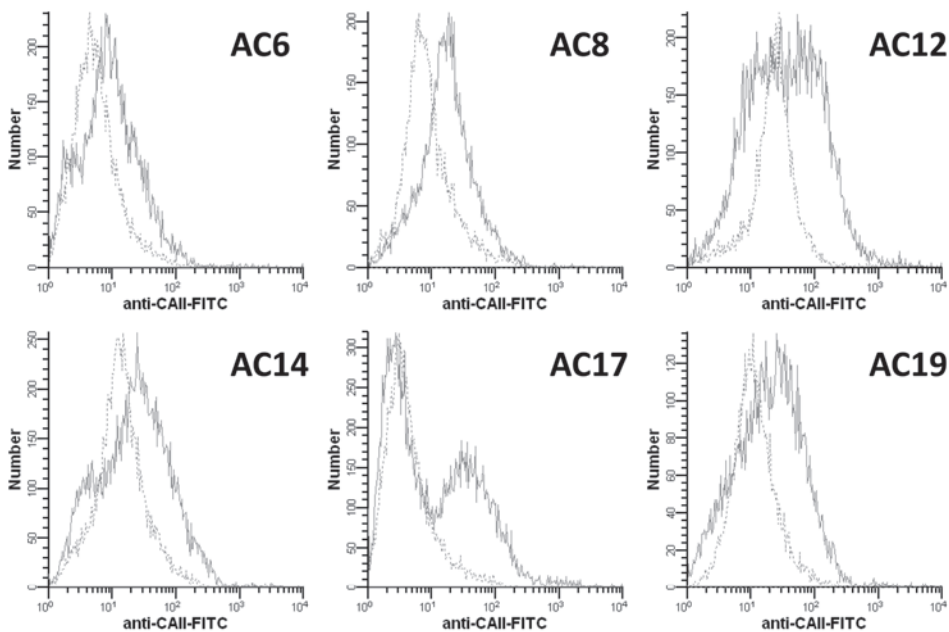


Figure 4.3 Flow cytometric analysis of CAII protein expression in epidermal cell suspensions derived from six individuals with allergic contact dermatitis. Cell suspensions were labeled indirectly using a polyclonal anti-CAII antibody and a Alexa fluor 488-conjugated secondary antibody. CAII expression of six patients (AC6, AC8, AC12, AC14, AC17 and AC19) is shown in frequency histograms. Lesional skin (solid line) and normal skin (dotted line) are overlaid after normalization. Expression of CAII in epidermal cells was heterogeneous and in all cases it was higher in cell suspensions derived from lesional skin compared with normal skin. In three out of six patients (AC12, AC14 and AC19) part of the cells in the lesional skin showed a lower CAII expression compared to control skin, suggesting that these cells were newly formed in the basal layer and had lowest CAII protein content. Overall CAII expression in allergic contact dermatitis involved skin was on average two times higher than the uninvolved skin from the same patient.

allergic and irritant contact dermatitis for KRT16 and Ki67 staining. Increased numbers of Ki67 positive nuclei correlated with suprabasal KRT16 expression, but both were found to be quite variable among all inflammatory conditions. KRT16 expression and increases of Ki67 positive nuclei were least prominent in allergic contact dermatitis. Collectively, Ki67 and KRT16 staining appeared to be poor discriminators for these inflammatory conditions as was already suggested by qPCR experiments (not shown).

Although most of the aforementioned marker genes investigated here are predominantly expressed by keratinocytes, there could be a small contribution of infiltrating cells to the mRNA levels described in Figure 4.1. To investigate the presence of cells of hematopoietic origin in the epidermis, immunohistochemical staining for CD45 was performed, which showed a massive amount of immune cells in the dermis of patients with allergic contact dermatitis, and to a lesser extent in atopic dermatitis and psoriasis. In irritant contact dermatitis, only a mild perivascular infiltrate was observed compared with normal skin. Epidermal presence of immune cells, as determined by CD45 expression, was highest in allergic contact dermatitis, less so in psoriasis and atopic dermatitis, and nearly absent in irritant contact dermatitis skin. These immunohistochemical data confirm the observed qPCR data on CD45, which indicated that allergic contact dermatitis epidermis showed the highest number of infiltrating cells.

Classification of inflammatory skin conditions based on seven selected genes

In the previous paragraphs we showed that several genes were selectively expressed in one or more specific inflammatory conditions. It remains to be investigated whether these genes are involved in the pathogenesis, as will be discussed hereafter. We next wondered whether a limited set of informative genes could be used to distinguish the four inflammatory dermatoses that we studied based on their expression levels. We used a one-way clustering approach to analyze the similarity between the inflammatory conditions based on the ΔC_t -values obtained from our qPCR data of CAlI, NELL2, hBD-2, IL-1F9, CXCL8, CXCL10 and CCL17. Figure 4.4 shows that clustering of the 63 individuals based on expression of these 7 genes provides a good separation of sample groups. Normal skin samples are distinct from all biopsies of inflamed skin. Secondly, psoriasis could be discriminated from the different forms of eczema (atopic dermatitis, allergic contact dermatitis and irritant contact dermatitis), which are all clustered together. Within the eczematous skin conditions, three distinct clusters emerge for atopic dermatitis, allergic contact dermatitis and irritant contact dermatitis. Only two samples (one atopic dermatitis and one allergic contact dermatitis) were classified in other clusters. The separation of psoriasis and atopic dermatitis is not surprising because the genes were selected on the basis of known differential expression in these conditions. It is, however, striking that allergic contact dermatitis and irritant contact dermatitis could also be discriminated on the basis of the same gene set.

Polytomous logistic regression analysis, in combination with a forward

selection procedure, using the expression levels of the 7 selected genes as continuous predictors and the diagnosis group (five levels: normal skin, psoriasis, atopic dermatitis, allergic contact dermatitis, irritant contact dermatitis) as the nominal outcome variable, resulted in 'perfect' prediction with error rate $0/63 = 0\%$. Only the genes CCL17, hBD-2 and NELL2 were selected by the forward selection procedure, that is to say that the 'perfect' prediction rule used only these 3 genes. To account for possible overfitting, leave-out-one cross-validation was performed, including the same forward selection procedure. This resulted in an internally validated error rate of $8/63 = 12.7\%$. In 55 of the 63 models (87.3%) of the leave-out-one analyses the same genes CCL17, hBD-2 and NELL2 were selected as predictors.

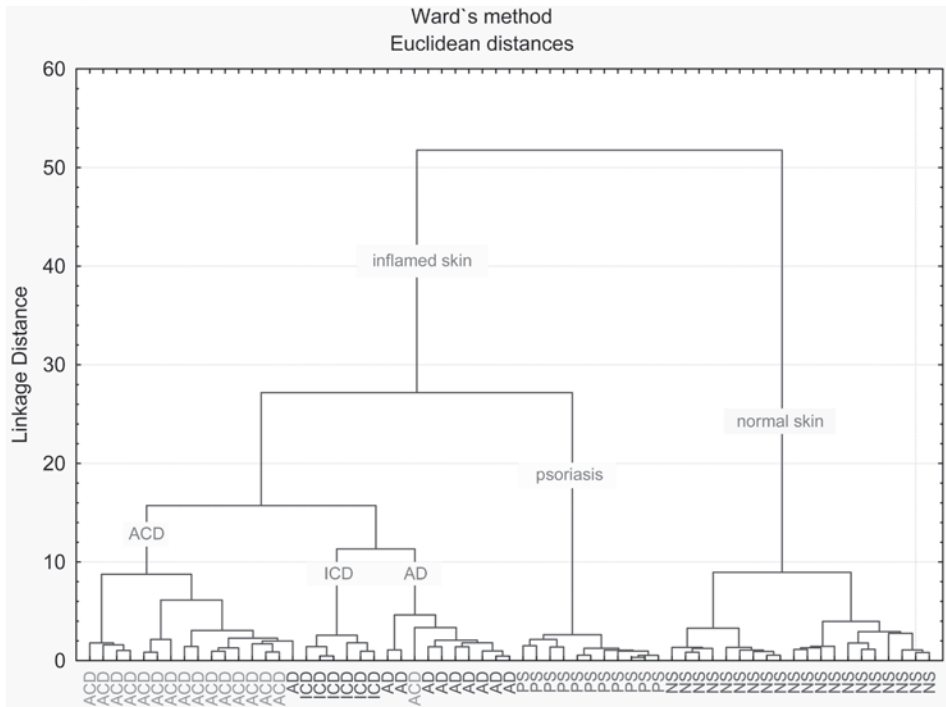


Figure 4.4 One-way clustering approach to assess the similarity between the inflammatory conditions. qPCR data from skin biopsy samples were analyzed using a one-way clustering approach to assess the similarity between the inflammatory conditions based on the ΔCt -values from CAIL, NELL2, hBD-2, IL-1F9, CXCL8, CXCL10 and CCL17. A good separation of diagnosis groups is obtained. Normal skin (NS) samples are distinct from all biopsies of inflamed skin. Secondly, psoriasis (PS) could be discriminated from the different forms of eczema, atopic dermatitis (AD), allergic contact dermatitis (ACD) and irritant contact dermatitis (ICD) which are clustered under a separate node. Within the eczematous skin conditions, three distinct clusters emerge for atopic dermatitis, allergic contact dermatitis and irritant contact dermatitis. Only two samples (one AD and one ACD) were classified in other clusters.

Discussion

Recent genetic and cell biological investigations from various labs including our own have indicated that epidermal keratinocytes are not passive bystanders in cutaneous inflammation, but play an active role in diseases such as psoriasis and various forms of eczema. For this reason we have studied gene expression in isolated epidermal sheets rather than full thickness skin biopsies. Our data specify the contribution of the epidermis and as such they convey a different message than other studies that use full thickness biopsies, with varying contributions of inflammatory cells and resident dermal cells. In this study we analysed if gene expression signatures as found in atopic dermatitis are also present in lesional epidermis of other eczematous skin conditions such as allergic and irritant contact dermatitis. Normal epidermis and psoriatic epidermis were analysed for comparison. While CAll was found in all investigated forms of eczema, NELL2 showed a strong induction only in atopic dermatitis epidermis. CXCL10 and CCL17, in contrast, were highly upregulated predominantly in epidermis from patients with allergic contact dermatitis. IL-1F9, elafin and hBD-2 were strongly induced in psoriasis, but not in any type of eczema. The chemokine CXCL8 was highly expressed in psoriasis, atopic dermatitis and allergic contact dermatitis but not in irritant contact dermatitis. Cluster analysis on a limited set of genes allowed a molecular discrimination between these four inflammatory conditions.

To date, no specific keratinocyte-derived biomarkers have been identified to distinguish atopic dermatitis from other forms of eczema at the molecular level. Several genes including CAll and NELL2 were, however, found to be overexpressed in atopic dermatitis lesions compared to psoriatic epidermis^{9,10,14}. Although our data do not allow conclusions on the involvement of these genes in the disease-specific pathogenetic processes, we observed a remarkable, strong expression of CAll in all eczematous conditions (Figure 4.1). Previous *in vitro* studies showed that CAll is induced by atopic dermatitis-associated Th2 cytokines but not by Th1 cytokines that are predominantly associated with psoriasis, and to a lesser extent with chronic atopic dermatitis¹⁴. Although the cytokine environment of atopic dermatitis, allergic contact dermatitis and irritant contact dermatitis is generally thought to be different, there are several publications that report the involvement of overlapping cytokine/chemokine profiles, including both Th1 and Th2 cytokines, in these conditions²¹⁻²⁵. We speculate that the presence of Th2 cytokines in all three eczematous conditions could drive the CAll expression. Another characteristic that is present in all forms of eczema is a decreased barrier function that results in increased trans-epidermal water loss. As carbonic anhydrases are involved in water transport²⁶, CAll upregulation could be a response to restore fluid balance following impaired barrier function. Obviously this assumption requires further investigation. Analysis of CAll at the protein level showed a discrepancy between mRNA and protein data. Similar to earlier findings in atopic dermatitis, we now observed a strong increase in allergic contact dermatitis at the mRNA level but only a minor increase at the protein level,

as determined by flow cytometric analysis. From this analysis it can be concluded that CAII induction is only useful as a disease marker at the mRNA level, in view of the low and heterogeneous expression of the protein. In contrast, NELL2 was predominantly upregulated in atopic dermatitis, to a much lesser extent in allergic contact dermatitis, and not at all in irritant contact dermatitis. NELL2 is a thrombospondin-like molecule that shows a significant homology with NEL, which is strongly expressed in neuronal tissues of chicken²⁷. NELL2 contains six EGF-like repeats and is strongly expressed in adult and fetal brain, weakly in the kidney²⁸. It promotes the survival of hippocampal and cortical neurons¹⁵ and increases the differentiation of spinal cord progenitors, while at the same time exerting paracrine proliferative activity²⁹. In a previous study we showed that cultured keratinocytes do express NELL2¹¹, and in the present study we show that NELL2 is expressed in keratinocytes of atopic dermatitis skin *in vivo*. Bearing in mind its function in brain, NELL2 expression could be associated with the increased amount of nerve fibers in the epidermis that are found in lesional skin of atopic dermatitis³⁰.

Earlier studies have shown CXCL10 upregulation in several diseases that are associated with a Th1-response, like allergic contact dermatitis³¹ and psoriasis³², while in atopic dermatitis only a weak staining was shown by immunohistochemistry³³. We, however, found a high expression of CXCL10 mRNA in allergic contact dermatitis, but only a comparatively minor upregulation in psoriasis. Another chemokine we found highly upregulated in allergic contact dermatitis and only mildly in atopic dermatitis is CCL17. This chemokine can bind to the CC chemokine receptor (CCR)8³⁴ and CCR4³⁵, which is expressed by Th2-type lymphocytes, and is a chemoattractant for these cells³⁶. Injection of CCL17 in the skin of mice results in a Th2-dominated inflammation³⁷. CCL17 expression is found in lesional skin of patients with atopic dermatitis and high serum levels of CCL17 correspond to disease severity^{38,39}. The high CCL17 expression we found in allergic contact dermatitis suggests that besides a Th1-type of inflammation also Th2-type lymphocytes are involved. This is in agreement with several studies that have reported an overlap of cytokine/chemokine profiles in eczematous diseases (see above).

Irritant contact dermatitis is mainly caused by epidermal reactivity to skin penetrating agents, resulting in inflammation largely mediated by innate immunity²⁰. The types of cytokines released after exposure to an irritant are not the same for all irritants. TNF- α , for example, is induced after exposure to tributyltin⁴⁰ and sodium dodecyl sulphate (SDS)⁴¹ in mice, but not after benzalkonium chloride exposure⁴². Despite a vigorous inflammatory response, most of the cytokines and chemokines we investigated were only weakly upregulated in experimental irritant contact dermatitis compared to other eczematous conditions. Another difference we observed was the absence of a strong inflammatory infiltrate in irritant contact dermatitis, both in the dermis (Figure 4.2) and in the epidermis (Figures 4.1 and 4.2). In previous studies IL-1 β and CXCL10 were only upregulated after allergen painting and not after irritant exposure in BALB/c mice⁴¹ and also in human

studies CXCL10 and CCL17 were upregulated in allergic contact dermatitis but not in irritant contact dermatitis⁴³. This is in contrast with data on elevated levels of CXCL10 in (epi)dermal fluid samples after exposure of forearm skin to 10% SLS²³. This could be due to the time point measured: samples were collected 16 hours after exposure to SLS, while the biopsies in our study were taken after 48 hours. Alternatively, the CXCL10 could be entirely derived from the dermal compartment and not from the keratinocytes. The acute irritant contact dermatitis reaction that we observed here has features of both psoriasis (elafin induction, hyperproliferation and KRT16 expression) and atopic dermatitis (absence of hBD-2, induction of CAII).

Cluster analysis clearly shows that psoriasis is distinct from all forms of eczema, and the high expression levels of genes such as hBD-2, IL-1F9 and VNN3 were unique to psoriasis. Recent studies have indicated that the transcriptome of psoriasis resembles that of keratinocytes stimulated by IL-1¹² or a combination of IL-1, TNF- α and IFN-g¹¹. Indeed, all psoriasis-associated genes reported here are strongly induced by these cytokines^{11,12,16}. We would speculate that the similarities between the eczematous conditions are caused by their similar, albeit not identical, cytokine environments, which could include IL-4 and/or IL-13 produced by Th2 lymphocytes. The question whether the induced genes also contribute to the disease process remains to be addressed.

A number of caveats should be considered for our study. For practical reasons the number of samples is limited and internal validation of the predictive power indicated a 12.7% error rate. We have not considered the effect of disease severity on expression of genes and disease classification, as we included only strongly inflamed skin lesions. Another limitation is the fact that atopic dermatitis and psoriasis biopsies were taken from existing lesions in patients, whereas in allergic and irritant contact dermatitis induced lesions were biopsied at 48 hours after elicitation by allergen or irritant. Recent studies have shown that cytokine profiles of acute and chronic irritant reactions are largely similar, but some cytokines like CCL5 are different²³.

Finally, the question arises whether a classification based on molecular diagnostic criteria has any practical significance for a group of inflammatory conditions. Although these conditions can usually be discriminated quite well by clinical criteria, it is not uncommon to encounter diagnostic difficulties in discriminating irritant contact dermatitis from allergic contact dermatitis, e.g. in hand eczema⁴⁴. Likewise, nonpustular palmoplantar psoriasis is often difficult to delineate from hyperkeratotic eczema of the palms or soles⁴⁵. It would be interesting to analyse expressed genes in these conditions, and to see if clear-cut molecular patterns emerge. Alternatively, molecular diagnostics could also result in mixed, inconclusive results thereby confirming the assertion that these conditions represent intermediate phenotypes both clinically and molecularly.

Materials and methods

Patients and healthy volunteers

Patients and healthy volunteers were recruited by the Dermatology clinic of the Radboud University Nijmegen Medical Centre. All diagnoses were made by a dermatologist. The study was approved by the local medical ethical committee (Commissie Mensgebonden Onderzoek Arnhem-Nijmegen) and conducted according to the Declaration of Helsinki principles. Written informed consent was obtained from each volunteer. Patients who suffered from chronic atopic dermatitis, diagnosed according to the Hanifin criteria⁴⁶, were in an active phase of disease for which they were hospitalized and biopsies were taken from subacute lesions. Care was taken to exclude vesicles or scratched skin. All patients with psoriasis had moderate to severe plaque type psoriasis. To induce allergic contact dermatitis, patients with a known allergy were exposed for 48 hours to nickel or perfume I (European standards series) on the lower back. 72 hours after exposure 3-mm biopsies were taken from these allergic contact dermatitis patients, and healthy skin was used as a control. To induce irritant contact dermatitis, 400 μ l 5% SDS solution was applied on a 2x2 cm patch of absorbent non-woven fabric (Medicomp, Hartmann, Heidenheim, Germany), which was subsequently placed on the lower back of healthy volunteers and covered with Tegaderm (3M Health care, Neuss, Germany) and Soft Cloth Surgical Tape (3M Health care) as described previously. After 4 or 8 hours the patch with SDS was removed. 48 hours after exposure, 3-mm biopsies were taken from these patients with irritant contact dermatitis, and healthy skin was used as a control. Skin reactions to SDS application were found to be variable. Biopsies were only taken from individuals that showed a clear response as witnessed by strong erythema. Some individuals showed severe epidermal damage and a subsequent wound-healing response as assessed by histological analysis. These samples were excluded from the analysis.

Isolation of epidermal sheets and preparation of cells for flow cytometry

Isolation of epidermal sheets for mRNA isolation was performed as previously described⁴⁷. In short, a 3-mm punch biopsy was incubated for four hours at 4°C in phosphate-buffered saline (PBS) with $\text{Ca}^{2+}/\text{Mg}^{2+}$, containing 12 mg/ml Dispase (Roche diagnostics, Basel, Switzerland) and 5 $\mu\text{g}/\text{ml}$ Actinomycin-D (Sigma-Aldrich, St. Louis, MO, USA). After incubation, the epidermis was removed with tweezers and stored in Trizol (Invitrogen, Groningen, the Netherlands) at -80°C until use. Cell suspensions for flow cytometry were prepared as described before⁴⁸. Biopsies were incubated overnight in PBS containing 2.5 mg/ml trypsin (trypsin 250, Difco Laboratories, Detroit, MI, USA) at 4°C. Ten percent fetal calf serum (Harlan Sera-Lab, Loughborough, UK) was added and the epidermis and dermis were separated with tweezers. The epidermal side of the dermis was gently scraped to ensure detachment of basal cells. Both the epidermis and dermis were mixed on a vortex to allow detachment of all keratinocytes.

Table 4.1 Primer sequences of all genes examined by qPCR

HUGO Gene Symbol	Description gene/protein in parentheses: name used in text	Forward primer (5' → 3')	Reverse primer (5' → 3')
CA2	Carbonic anhydrase II (CAII)	aacaatggcatgctttccaag	tgfccaatcaaggaacccccag
CCL17	chemokine (C-C motif) 17, TARC, ABCD-2 (CCL17)	cagggatgccatgctttttg	actgcattctcactctctgtgtt
PTPRC	CD45 (CD45)	gggaaacaagcatcacaagagtaca	tgttccgcactttcttaagagattt
IL8	interleukin 8, IL-8, CXCL8 (CXCL8)	ctfggagccttctgattt	ttcttagcactccttggcaaaa
IL18	interleukin 8 (IL-18)	atcgcttctctcgaaca	cattgccacaaagttgatga
CXCL10	IP-10, chemokine (C-X-C motif) ligand 10 (CXCL10)	ttctgcaagccaattttgct	ttcttcaccctctttttcattgt
KRT6	Keratin 6A (KRT6)	agagaatgaatttgactctgaaagaag	tacaaggctctcaggaagttgatct
DEFB4	hBD-2, β -defensin-2 (hBD-2)	gatgccttctccagggttttt	ggatgacataatggctccactct
IL1B	interleukin 1 β , IL-1 β (IL-1 β)	aatctgtaccctgctctcgtgtt	tgggtaatttttggatctacactct
IL1F9	IL1 family member 9, IL-1F9 (IL-1F9)	aggaaagggccgtctatcaatc	gaactgccacaaggctctgac
NELL2	Nel-like2 (NELL2)	taagggtataatgcaagatgtccaatt	agatctgggcactgagcaataaa
RPLP0	Ribosomal phosphoprotein P0 (RPLP0)	caccatgaaatctgagtgatgt	tgaccagcccaagaggagaag
PI3	SKALP, elafin (elafin)	catgagggccacagcctt	tftaacaggaaactcccgtgaca
VNN1	Vanin-1 (VNN1)	gaaccagatgtcttctct	catacaaccctcccaaacaga
VNN3	Vanin-3 (VNN3)	gatcattctaagtgaggatca	cgccaatcttgaatctca

Subsequently, the *stratum corneum* and dermis were removed and the remaining cells were pelleted and fixed by slowly adding 1 ml cold ethanol while vortexing at low speed. Cell suspensions were stored at 4°C for at least two hours.

RNA extraction and real-time quantitative PCR

Epidermal sheets were used for RNA extraction, and a DNase I treatment was performed following manufacturer's protocol (Invitrogen, Carlsbad, CA, USA). Reverse transcriptase reactions were performed with 1 µg RNA as described previously¹⁰. The reverse transcriptase reaction products were used for qPCR, which was performed with the MyiQ™ Single-Colour Real-Time Detection System for quantification with SYBR Green Supermix (Biorad, Richmond, CA, USA) and melting curve analysis, as described previously⁴⁸. DNA was PCR-amplified under the following conditions: 4.5 minutes at 95°C, followed by 40 cycles of 15 seconds at 95°C and 1 minute at 60°C, with data collection in the last 30 seconds. All primer concentrations were 300 nM in a total reaction volume of 25 µl. The amount of mRNA for a given gene in each sample was normalized to the amount of mRNA of the human ribosomal phosphoprotein P0 (RPLP0) reference gene in the same sample. The RPLP0 gene is, at least for skin biopsies, more suitable than commonly used genes such as actin or GAPDH, as RPLP0 correlates far better with 28S ribosomal RNA. Primers for qPCR were only accepted if their efficiency was $100 \pm 10 \%$, which means that the PCR product was doubled at each cycle and the threshold cycle (C_t) will be linear with the log of the initial concentration. Corrections were made for primer efficiency.

For graphic representation of relative mRNA expression levels we used the delta-delta C_t method⁴⁹. Primer sequences are shown in Table 4.1. All primers were obtained from Biolegio (Nijmegen, the Netherlands).

Immunohistochemistry

Skin biopsies were immediately fixed in a 10% formalin solution (Baker Mallinckrodt, Deventer, The Netherlands) for 4 hours and subsequently embedded in paraffin. Before staining with antibodies that recognize CD45 (Dako, Glostrup, Denmark), Ki67 (Immunotech, Fullerton, CA) and KRT16 (Monosan, Uden, The Netherlands), a citrate treatment was performed: sections were boiled for 10 minutes in a microwave in a solution containing 1.8 mM citric acid and 8.2 mM sodium citrate. 6 µm sections were blocked for 15 minutes with PBS with 20% normal rabbit serum (for hBD-2), normal goat serum (for elafin) or normal horse serum (for CD45, Ki67 and KRT16) and subsequently incubated with anti-hBD-2 (Abcam, Cambridge, UK) in a 1:100 dilution, anti-elafin in a 1:500 dilution, anti-CD45 in a 1:100 dilution, anti-Ki67 in a 1:50 dilution, and anti-KRT16 in a 1:50 dilution for 1 hour at room temperature. After washing in PBS, sections were incubated for 1 hour with a secondary antibody (biotinylated rabbit anti-goat, biotinylated goat anti-rabbit or biotinylated horse anti-mouse in PBS containing 1% BSA, Vector laboratories, Burlingame, CA). After 30 minutes incubation with Avidin-Biotin complex (Vector Laboratories), sections were treated with 3-amino-

9-ethyl carbazole (Calbiochem, San Diego, CA) for 10 minutes. Nuclei were stained with Mayer (Sigma-Aldrich), and subsequently sections were mounted in glycerol gelatin (Sigma-Aldrich).

Flow cytometry

Ethanol fixed cells were washed with PBS/1% fetal bovine serum and subsequently labeled with anti-CAII (Abcam) in a 1:500 dilution. After 30 minutes incubation at 4°C, cells were washed and incubated with Alexa fluor 488 goat anti-rabbit secondary antibody (Invitrogen). After 30 minutes incubation cells were washed, resuspended in propidium iodide and 0.1% RNase (Sigma-Aldrich). The labeled cell suspensions were analyzed on an EPICS Elite flow cytometer (Coulter, Luton, UK). A bandpass filter of 515–535 nm (green, FITC) was used to measure emitted light, while a gate in the right angle scatter (a measure of regularity) *versus* the forward scatter (a measure of size) was used to exclude debris. To test for CAII specificity, the CAII antibody was pre-incubated with excess CAII protein and added to epidermal cells instead of the primary antibody alone. Only a very few CAII positive cells could now be detected by flow cytometry (not shown), indicating a high specificity of the CAII antibody.

Cluster analysis and statistics

All data were analyzed with the Statistica software package version 7.0 (StatSoft Inc) or SPSS v16.0 (SPSS Inc). For the qPCR experiments, statistical analysis by ANOVA was performed on Δ Ct values corrected for primer efficiency. Δ Ct is the difference between the Ct of the target gene and the reference gene. These values are normally distributed. A Bonferroni post-hoc test was used to test the significance of the difference between each of the groups. Note that for graphical representation of the data (Figure 4.1) we used the relative expression levels as described by Livak and Schmittgen²⁴. Cluster analysis was performed on corrected Δ Ct-values of 7 selected genes (CAII, NELL2, hBD-2, IL-1F9, CXCL8, CXCL10 and CCL17). The values were subjected to a Z-transformation, where $Z = (x-\mu)/\sigma$. This will yield a matrix with a row mean of 0 and a SD of 1. After this transformation, the Euclidean distance is used as the dissimilarity measure. Samples were clustered by Ward's amalgamation rule. Polytomous logistic regression analysis, including forward selection procedure, was used to predict the diagnostic group based on the expression levels of the above mentioned 7 selected genes. Leave-one-out cross-validation was applied to obtain an estimate of the error rate that is not biased by overfitting.

Acknowledgements

This study was supported by grant 920-03-355 from the Netherlands Organization for Health Research and Development (ZONMW).

Supplementary information

Gene selection

A number of microarray studies on gene expression in psoriasis, atopic dermatitis and normal skin have been performed^{9,10,50-52}. These analyses have identified a large number of genes that were differentially expressed between lesional psoriatic epidermis and normal skin. Two of these studies^{9,10} have focused on a comparison of lesional psoriasis and atopic dermatitis skin in order to identify disease-specific expression patterns. These data have been deposited at the NCBI (Gene Expression Omnibus). A limited number of these genes have been verified by qPCR or immunohistochemistry. Our own study¹⁰ focused on host defense proteins, and we could indeed confirm most of the array data by qPCR. In this study we identified 180 genes that were differentially expressed between atopic dermatitis and psoriasis. These genes showed a significant difference after correcting for false discovery. Table S4.1 provides a list of all these genes. From this list we tested a number of genes with qPCR to verify the differential expression, including CA2, IL1F9, PI3 and VNN3. As the observed expression could be confirmed, they were included in the analyses of the current manuscript. Other genes that we examined were selected on the basis of available literature such as NELL2, CCL17 and VNN1^{9,10}. The remaining genes were selected for reasons that they have been associated with psoriasis or atopic dermatitis in other studies (e.g. KRT6 and CXCL10). IL1B and IL18 were selected because of the reported gene expression signature of psoriasis resembling that of IL-1 stimulated keratinocytes. Finally PTPRC (CD45) was not selected on the basis of known differential expression, but as a convenient marker to assess the presence of hematopoietic cells in our isolated epidermal sheets. We could indeed demonstrate, using qPCR and histology, that CD45+ cells are largely absent from normal skin, but clearly present in psoriasis, allergic contact dermatitis and atopic dermatitis.

Table S4.1

All genes that were found to be differentially expressed in a microarray analysis performed on isolated epidermal cells taken from lesional epidermis of 6 psoriasis and 6 atopic dermatitis patients. The experimental details of the microarray analysis has been published before^{10,11}, and the data on gene expression levels have been deposited, compliant with MIAME criteria, at <http://www.ncbi.nlm.nih.gov/geo/> and are accessible through GEO Series accession number GSE6601. For convenience of the reader we here present all 180 genes that passed the criterion for false discovery rate. Several genes from this list were used in the current study to define a limited gene set that could differentiate between inflammatory skin diseases.

Gene ID: the reference sequence from which the oligonucleotide sequence on the chip was derived. Mean and Standard deviation: 2log of the normalized

expression ratio of psoriasis/atopic dermatitis. N: the number of chips that gave a reliable signal and were used for analysis. Unigene ID: the Unigene entry identification code for each gene (see <http://www.ncbi.nlm.nih.gov/sites/entrez?db=unigene>). Description: the given gene name and HUGO gene name. Gene_Ontology: the putative function of the gene in a biological process.

The list is sorted from the highest mean (4.2 for the VNN3 gene) to the lowest mean (-2.9 for CA2). As the mean is the $2\log$ of the ratio psoriasis/atopic dermatitis, all genes with a mean >0 are overexpressed in psoriasis, whereas all genes with a mean <0 are overexpressed in atopic dermatitis. The selection criterion was set at a mean > 1 and < -1 , combined with false discovery rate correction. This gave a list of 180 genes whose expression was significantly different between psoriasis and atopic dermatitis.

Table S4.1

Gene ID	Mean	Stdev	N	UniGene ID	Description	Gene ontology
NM_018399	4.2	0.6	6	Hs.183656	Homo sapiens vanin 3 (VNN3), transcript variant 1, mRNA	cell motility [0006928]
NM_004942	3.0	0.8	4	Hs.105924	Homo sapiens DEFB4, mRNA	response to pest/pathogen/parasite
NM_005621	2.8	0.9	6	Hs.19413	Homo sapiens S100 calcium binding protein A12 (calgranulin C) (S100A12), mRNA	signal transduction [0007165]
NM_007231	2.8	0.9	6	Hs.162211	Homo sapiens solute carrier family 6 (neurotransmitter transporter), member 14 (SLC6A14), mRNA	neurotransmitter transport [0006636]
NM_002462	2.6	1.0	6	Hs.76391	Homo sapiens myxovirus (influenza virus) resistance 1, interferon-inducible protein p78 (mouse) (MX1), mRNA	signal transduction [0007165]
NM_014438	2.5	0.9	6	Hs.278909	Homo sapiens interleukin 1 family, member 8 (eta) (IL1F8), mRNA	response to pest/pathogen/parasite [0009613]
NM_006417	2.4	1.0	6	Hs.82316	Homo sapiens interferon-induced protein 44 (IFI44), mRNA	response to viruses [0009615]
NM_012337	2.4	0.8	6	Hs.158450	Homo sapiens nasopharyngeal epithelium specific protein 1 (NESG1), mRNA	developmental processes [0007275]
NM_017654	2.3	1.0	6	Hs.65641	Homo sapiens hypothetical protein FLJ20073 (FLJ20073), mRNA	biological_process unknown [0000004]
AF289028	2.2	0.8	6	Hs.14155	Homo sapiens transmembrane protein B7-H2 ICOS ligand mRNA, complete cds.	positive regulation of activated T-cell proliferation [0042104]
AF068236	2.2	0.5	5	Hs.193788	Homo sapiens inducible nitric oxide synthase (NOS) mRNA, complete cds.	electron transport [0006118]
AY009090	2.1	0.9	6	Hs.161786	Homo sapiens putative transmembrane protein declin-1 mRNA, complete cds.	cell surface receptor linked signal transduction [0007166]
NM_004559	2.1	0.8	6	Hs.74497	Homo sapiens nuclease sensitive element binding protein 1 (NSEP1), mRNA	regulation of transcription, DNA-dependent [0006355]
NM_019618	2.1	0.8	6	Hs.211238	Homo sapiens interleukin 1 family, member 9 (IL1F9), mRNA	response to pest/pathogen/parasite [0009613]
NM_001901	2.1	0.7	6	Hs.75511	Homo sapiens connective tissue growth factor (CTGF), mRNA	regulation of cell growth [0001558]
X56692	2.0	0.7	6	Hs.76452	H.sapiens mRNA for C-reactive protein.	acute-phase response [0006953]
NM_016590	2.0	0.8	6	Hs.96744	Homo sapiens prostate androgen-regulated transcript 1 (PART1), mRNA	cytoskeleton organization and biogenesis [0007010]
NM_000673	1.9	0.6	6	Hs.389	Homo sapiens alcohol dehydrogenase 7 (class IV), mu or sigma polypeptide (ADH7), mRNA	ethanol oxidation [0006069]
NM_005156	1.9	0.7	5	Hs.374634	Homo sapiens ROD1 regulator of differentiation 1 (S. pombe) (ROD1), mRNA	embryogenesis and morphogenesis [0007345]
NM_000045	1.9	0.8	6	Hs.332405	Homo sapiens arginase, liver (ARG1), mRNA	arginine catabolism [0006527]
AL117423	1.9	0.8	6	Hs.61628	Homo sapiens mRNA: cDNA DKFZp564C246 (from clone DKFZp564C246); complete cds.	defense response [0006952]
AL137489	1.9	0.5	4	Hs.7517	Homo sapiens mRNA: cDNA DKFZp434O1230 (from clone DKFZp434O1230); partial cds.	biological_process unknown [0000004]
NM_002963	1.8	0.6	6	Hs.112408	S100A7 S100 calcium binding protein A7 (psoriasin 1)	S100A7 S100 calcium binding protein A7 (psoriasin 1)
NM_017973	1.8	0.5	4	#N/B	#N/B	#N/B
NM_004673	1.8	0.3	6	Hs.241519	Homo sapiens angiotensin-like 1 (ANGPTL1), mRNA	development [0007275]
NM_003465	1.8	0.5	6	Hs.91093	Homo sapiens chitinase 1 (chitotriosidase) (CHIT1), mRNA	response to pest/pathogen/parasite [0009613]
NM_006440	1.7	0.6	6	Hs.12971	Homo sapiens thioredoxin reductase 2 (TXNRD2) transcript variant 1, nuclear gene, mRNA	response to pest/pathogen/parasite [0009613]

AB007978	1,7	0,5	6	s.158278	Homo sapiens mRNA, chromosome 1 specific transcript KIAA0509.	ribosomal protein-nucleus import [0006610]
NM_014683	1,7	0,5	6	Hs.151406	Homo sapiens unc-51-like kinase 2 (C. elegans) (ULK2), mRNA.	signal transduction [0007165]
NM_002377	1,7	0,5	4	Hs.99500	Homo sapiens MAS1 oncogene (MAS1), mRNA.	cell proliferation [0008283]
NM_005503	1,6	0,5	6	Hs.26468	Homo sapiens amyloid beta (A4) precursor protein-binding, family A, member 2 (X11-like) (APBA2), mRNA.	neurogenesis [0007399]
NM_018456	1,6	0,3	6	Hs.26892	Homo sapiens uncharacterized bone marrow protein BM040 (BM040), mRNA	biological_process unknown [0000004]
AK022035	1,5	0,6	6	Hs.151504	Homo sapiens cDNA FLJ11973 fis, clone HEIMBB1001221	biological_process unknown [0000004]
AK022213	1,5	0,2	4	Hs.287493	Homo sapiens cDNA FLJ12151 fis, clone MAMMA1000431.	development [0007275]
NM_019599	1,5	0,4	6	Hs.168278	Homo sapiens taste receptor, type 2, member 1 (TAS2R1), mRNA.	chemosensory behavior [0007635]
AL157455	1,5	0,4	6	Hs.22543	#N/B	#N/B
NM_018974	1,5	0,6	6	Hs.267749	Homo sapiens unc93 (C.elegans)Homolog A (UNC93A), mRNA.	protein secretion [0009306]
AB033044	1,5	0,6	6	Hs.114012	Homo sapiens mRNA for KIAA1218 protein, partial cds.	nuclear organization and biogenesis [0006997]
NM_016606	1,5	0,6	6	Hs.28088	Homo sapiens SGC32445 protein (LOC51308), mRNA.	hypersensitive response [0009626]
NM_018473	1,5	0,5	6	Hs.9676	Homo sapiens uncharacterized hypothalamus protein HT012 (HT012), mRNA.	translational initiation [0006413]
AJ293294	1,5	0,6	6	Hs.24678	Homo sapiens mRNA for sphingosine-1-phosphatase (ORF1).	signal transduction [0007165]
AL050035	1,5	0,4	6	Hs.133130	Homo sapiens mRNA; cDNA DKFZp566H0124 (from clone DKFZp566H0124).	metabolism [0008152]
AL110259	1,5	0,5	6	Hs.383803	Homo sapiens mRNA; cDNA DKFZp586B1221 (from clone DKFZp586B1221).	biological_process unknown [0000004]
AJ227863	1,5	0,2	6	Hs.310286	Homo sapiens partial mRNA; ID YG39-2B.	biological_process unknown [0000004]
NM_003137	1,4	0,5	6	Hs.75761	Homo sapiens SFRS protein kinase 1 (SRPK1), mRNA.	RNA splicing [0008380]
AF105067	1,4	0,5	6	Hs.154078	Homo sapiens lipopolysaccharide-binding protein (LBP) mRNA, complete cds.	response to pathogenic bacteria [0009618]
AF169158	1,4	0,6	6	Hs.117694	Homo sapiens CaBP3 (CABP3) mRNA, complete cds.	signal transduction [0007165]
AK024534	1,4	0,4	6	Hs.406845	Homo sapiens cDNA: FLJ20881 fis, clone ADKA03177.	regulation of transcription, DNA-dependent [0006355]
X74613	1,4	0,3	6	-	H.sapiens HERV-K mRNA (252 bp).	biological_process unknown [0000004]
AK022464	1,4	0,6	6	Hs.143303	Homo sapiens cDNA FLJ12402 fis, clone MAMMA1002807.	biological_process unknown [0000004]
L48516	1,4	0,4	6	Hs.335322	Homo sapiens paraoxonase 3 (PON3) mRNA, 3' end of cds.	DNA transposition [0006313]
NM_000116	1,4	0,3	6	Hs.389108	Homo sapiens tafazzin (cardiomyopathy, dilated 3A (X-linked); Barth syndrome) (TAZ), mRNA.	metabolism [0008152]
NM_004580	1,4	0,6	6	Hs.50477	Homo sapiens RAB27A, member RAS oncogene family (RAB27A), mRNA.	intracellular protein transport [0006886]
NM_007199	1,4	0,3	6	Hs.268552	Homo sapiens interleukin-1 receptor-associated kinase 3 (IRAK3), mRNA.	protein amino acid phosphorylation [0006468]
AF085981	1,3	0,2	4	0	Homo sapiens full length insert cDNA clone Y194C01	biological_process unknown [0000004]
NM_005420	1,3	0,5	6	Hs.54576	Homo sapiens sulfotransferase, estrogen-prefering (STE), mRNA.	steroid metabolism [0008202]
AK000792	1,3	0,5	5	Hs.306405	Homo sapiens cDNA FLJ20785 fis, clone COL02504.	biological_process unknown [0000004]

Table S4.1 continued

Gene ID	Mean	Stdev	N	UniGene ID	Description	Gene ontology
NM_016564	1,3	0,5	4	Hs.22140	Homo sapiens BM88 antigen. The protein encoded by this gene is a neuron-specific protein.	transmembrane receptor protein tyrosine phosphatase signaling pathway
NM_000718	1,3	0,5	6	Hs.69949	Homo sapiens calcium channel, voltage-dependent, L type, alpha 1B subunit (CACNA1B), mRNA.	synaptic transmission [0007268]
NM_001225	1,3	0,5	4	Hs.74122	Homo sapiens caspase 4, apoptosis-related cysteine protease (CASP4), transcript variant alpha, mRNA.	induction of apoptosis [0006917]
NM_005322	1,3	0,4	4	Hs.131956	Homo sapiens H1 histone family, member 5 (H1F5), mRNA.	nucleosome assembly [0006334]
AL137507	1,3	0,4	6	Hs.255348	Homo sapiens mRNA; cDNA DKFZp761P211 (from clone DKFZp761P211)	biological_process unknown [0000004]
NM_005564	1,3	0,3	6	Hs.204238	Homo sapiens lipocain 2 (oncogene 24p3) (LCN2), mRNA.	prostaglandin metabolism [0006693]
NM_014228	1,2	0,4	5	Hs.241597	Homo sapiens solute carrier family 6 (neurotransmitter transporter, L-proline), member 7 (SLC6A7), mRNA.	proline transport [0015624]
NM_016303	1,2	0,3	6	Hs.15984	Homo sapiens pp21Homolog (LOC51186), mRNA.	negative regulation of transcription from Pol II promoter [0000122]
AF263541	1,2	0,2	6	Hs.17154	Homo sapiens protein kinase DYRK4 (DYRK4) mRNA, partial cds.	cell cycle [0007049]
NM_005218	1,2	0,5	6	Hs.32949	Homo sapiens defensin, beta 1 (DEFB1), mRNA.	xenobiotic metabolism [0006805]
AK024799	1,2	0,3	5	Hs.17433	Homo sapiens cDNA: FLJ21146 fis, clone CAS09305.	signal transduction [0007166]
NM_017835	1,2	0,5	6	Hs.5811	Homo sapiens chromosome 21 open reading frame 59 (C21orf59), mRNA.	metabolism [0008152]
L77571	1,2	0,2	6	Hs.106311	Homo sapiens DGS-A mRNA, 3' end	biological_process unknown [0000004]
NM_002055	1,2	0,4	5	Hs.406397	Homo sapiens glial fibrillary acidic protein (GFAP), mRNA.	cytoskeleton organization and biogenesis [0007010]
AK026656	1,1	0,4	6	Hs.381566	Homo sapiens cDNA: FLJ23003 fis, clone LNG00331.	cholesterol catabolism [0006707]
NM_005694	1,1	0,5	6	Hs.16297	Homo sapiens COX17Homolog, cytochrome c oxidase assembly protein (yeast) (COX17)	copper ion transport [0006825]
AK025203	1,1	0,4	6	Hs.141269	Homo sapiens cDNA: FLJ21550 fis, clone COL06258.	biological_process unknown [0000004]
AF061566	1,1	0,4	4	Hs.147174	Homo sapiens ubiquitin-protein ligase E3-alpha (UBR1) mRNA, partial cds.	protein polyubiquitination [0000209]
AK023335	1,1	0,3	6	Hs.126119	Homo sapiens cDNA FLJ13273 fis, clone OVARC10010.	cell cycle [0007049]
NM_001163	1,1	0,3	6	Hs.4880	Homo sapiens amyloid beta (A4) precursor protein-binding, family A, member 1 (X11) (APBA1), mRNA.	neurogenesis [0007399]
AL049434	1,1	0,2	6	Hs.302062	Homo sapiens mRNA; cDNA DKFZp586M151 (from clone DKFZp586M151).	DNA replication dependent nucleosome assembly [0006335]
AL110185	1,1	0,5	6	Hs.171625	Homo sapiens mRNA; cDNA DKFZp586D211 (from clone DKFZp586D211).	protein biosynthesis [0006412]
AB002446	1,1	0,2	6	Hs.407689	Homo sapiens mRNA from chromosome 5q21-22, clone:sf2.	biological_process unknown [0000004]
NM_004083	1,1	0,3	6	Hs.400353	Homo sapiens DNA-damage-inducible transcript 3 (DDIT3), mRNA.	cell cycle arrest [0007050]
NM_003143	1,1	0,4	6	Hs.923	Homo sapiens single-stranded DNA binding protein (SSBP1), mRNA.	cell growth and/or maintenance [0008151]
AL133573	1,1	0,4	6	Hs.272312	Homo sapiens mRNA; cDNA DKFZp434J2235 (from clone DKFZp434J2235).	ribosomal protein-nucleus import [0006610]
NM_007238	1,1	0,3	6	Hs.241205	Homo sapiens 24 kDa intrinsic membrane protein (PMP24), mRNA	peroxisome organization and biogenesis [0007031]

AL117415	1,1	0,3	6	Hs.173716	Homo sapiens mRNA; cDNA DKFZp434K0521 (from clone DKFZp434K0521)	biological_process unknown [0000004]
M14200	1,1	0,3	6	Hs.78888	Human diazepam binding inhibitor (DBI) mRNA, complete cds.	lipid metabolism [0006629]
NM_006731	1,1	0,2	6	Hs.55777	Homo sapiens Fukuyama type congenital muscular dystrophy (fukutin) (FCMD), mRNA.	muscle development [0007517]
AL110240	1,0	0,4	6	Hs.32990	Homo sapiens mRNA; cDNA DKFZp566F084 (from clone DKFZp566F084); partial cds	biological_process unknown [0000004]
NM_000160	1,0	0,4	6	Hs.208	Homo sapiens glucagon receptor (GCGR), mRNA.	G-protein signaling, coupled to cAMP nucleotide second messenger [0007188]
AF217525	1,0	0,3	6	Hs.49002	Homo sapiens clone cDSC1 Down syndrome cell adhesion molecule (DSCAM) mRNA, complete cds.	neurogenesis [0007399]
NM_017876	1,0	0,3	6	Hs.69554	Homo sapiens hypothetical protein FLJ20552 (FLJ20552), mRNA.	cell cycle [0007049]
NM_004617	1,0	0,4	5	Hs.11881	Homo sapiens transmembrane 4 superfamily member 4 (TM4SF4), mRNA.	negative regulation of cell proliferation [0008285]
D31763	1,0	0,3	5	Hs.70617	Human mRNA for KIAA0065 gene, partial cds.	regulation of transcription, DNA-dependent [0006355]
NM_004397	1,0	0,2	6	Hs.316	Homo sapiens DEAD/H (Asp-Glu-Ala-Asp/His) box polypeptide 6 (RNA helicase, 54kDa) (DDX6), mRNA.	cell growth and/or maintenance [0008151]
NM_004477	1,0	0,2	6	Hs.203772	Homo sapiens FSHD region gene 1 (FRG1), mRNA.	pathogenesis [0009405]
U55185	1,0	0,3	6	Hs.385190	Human oral cancer candidate gene mRNA, clone T9, 3' end.	protein biosynthesis [0006412]
NM_004688	1,0	0,3	6	Hs.54483	Homo sapiens N-myc (and STAT) interactor (NMI), mRNA.	inflammatory response [0006954]
NM_005764	1,0	0,4	6	Hs.271473	Homo sapiens epithelial protein up-regulated in carcinoma, membrane associated protein 17 (DDP6), mRNA.	transmembrane receptor protein tyrosine phosphatase signaling pathway [0007185]
NM_018474	1,0	0,4	6	Hs.173515	Homo sapiens chromosome 20 open reading frame 19 (C20orf19), mRNA.	regulation of transcription, DNA-dependent [0006355]
NM_015715	-1,0	0,4	6	Hs.149623	Homo sapiens phospholipase A2, group III (PLA2G3), mRNA.	lipid catabolism [0016042]
AF217986	-1,0	0,4	6	Hs.7159	Homo sapiens clone PP1628 unknown mRNA	biological_process unknown [0000004]
AL359401	-1,0	0,3	6	Hs.7436	Isolform 1 of a novel human mRNA from chromosome 22.	metabolism [0008152]
NM_015946	-1,0	0,2	6	Hs.5798	Homo sapiens peltaHomolog (Drosophila) (PELO), mRNA.	translational termination [0006415]
NM_003032	-1,0	0,3	6	Hs.2554	Homo sapiens sialyltransferase 1 (beta-galactoside alpha-2,6-sialyltransferase) (SIAT1), mRNA.	protein modification [0006464]
NM_003651	-1,0	0,3	6	Hs.198726	Homo sapiens cold shock domain protein A (CSDA), mRNA.	negative regulation of transcription from Pol II promoter [0000122]
NM_002189	-1,0	0,4	4	Hs.12503	Homo sapiens interleukin 15 receptor, alpha (IL15RA), mRNA.	cell proliferation [0008283]
AK022649	-1,0	0,3	6	Hs.301338	Homo sapiens cDNA FLJ12587 fis, clone NT2RM4001217, mRNA.	development [0007275]
AK000554	-1,0	0,3	6	Hs.406646	Homo sapiens cDNA FLJ20547 fis, clone KAT11527.	cell growth and/or maintenance [0008151]
AL079314	-1,1	0,2	6	Hs.16537	Homo sapiens mRNA full length insert cDNA clone EUROIMAGE 469780.	cell cycle [0007049]
NM_012116	-1,1	0,2	6	Hs.156637	Homo sapiens Cas-Br-M (murine) ecotropic retroviral transforming sequence c (CBLC), mRNA.	cell surface receptor linked signal transduction [0007166]
NM_005804	-1,1	0,3	6	Hs.311609	DDX39 DEAD box proteins, characterized by the conserved motif Asp-Glu-Ala-Asp (DEAD), are putative RNA helicases.	ATP-dependent helicase activity

Table S4.1 continued

Gene ID	Mean	Stdev	N	UniGene ID	Description	Gene ontology
NM_014344	-1,1	0,3	6	Hs.39384	Homo sapiens four jointed box 1 (Drosophila) (FJX1), mRNA.	cell communication [0007154]
NM_004308	-1,1	0,3	6	Hs.138860	Homo sapiens Rho GTPase activating protein 1 (ARHGAP1), mRNA.	cytoskeleton organization and biogenesis [0007010]
NM_006848	-1,1	0,4	6	Hs.66713	Homo sapiens hepatitis delta antigen-interacting protein A (DIPA), mRNA.	virulence [0009406]
NM_001941	-1,1	0,4	6	Hs.41690	Homo sapiens desmocollin 3 (DSC3),transcript variant Dsc3a, mRNA.	Homophilic cell adhesion [0007156]
NM_004430	-1,1	0,3	4	Hs.74088	Homo sapiens early growth response 3 (EGR3), mRNA.	regulator of transcription, DNA-dependent [0006355]
NM_012414	-1,1	0,3	4	Hs.197289	RAB3-GAP150 rab3 GTPase-activating protein, non-catalytic subunit	GTPase activator activity
AK023496	-1,1	0,3	6	Hs.268843	Homo sapiens cDNA FLJ13434 fis, clone PLACE1002578.	protein amino acid phosphorylation [0006468]
NM_001300	-1,1	0,5	6	Hs.285313	Homo sapiens core promoter element binding protein (COPEB), mRNA.	regulation of transcription, DNA-dependent [0006355]
AK021858	-1,1	0,4	6	Hs.298020	Homo sapiens cDNA FLJ11796 fis, clone HEMBA1006158,	biological_process unknown [0000004]
AK002173	-1,1	0,3	6	Hs.5518	Homo sapiens cDNA FLJ11311 fis, clone PLACE1010102.	biological_process unknown [0000004]
M95929	-1,2	0,5	6	Hs.443452	PRRX1 The protein functions as a transcription co-activator.	regulation of transcription, DNA-dependent
AK000745	-1,2	0,4	6	Hs.243901	Homo sapiens cDNA FLJ20738 fis, clone HEP08257.	development [0007275]
NM_002414	-1,2	0,4	6	Hs.433387	Homo sapiens antigen identified by monoclonal antibodies 12E7, F21 and O13 (MIC2), mRNA.	ATP/ADP exchange [0006854]
NM_002101	-1,2	0,2	4	Hs.81994	Homo sapiens glycophorin C (Gerbich blood group) (GYPC) transcript variant 1, mRNA.	virulence [0009406]
NM_003472	-1,2	0,5	6	Hs.110713	Homo sapiens DEK oncogene (DNA binding) (DEK), mRNA.	regulation of transcription from Pol II promoter [0006357]
NM_018226	-1,2	0,4	6	Hs.5345	Homo sapiens arginyl aminopeptidase (aminopeptidase B)-like 1 (RNPEPL1), mRNA.	leukotriene metabolism [0006691]
NM_003897	-1,2	0,4	5	Hs.76095	Homo sapiens immediate early response 3 (IER3), transcript variant short, mRNA.	cell growth and/or maintenance [0008151]
X91195	-1,2	0,3	6	Hs.406326	Homo sapiens SOM172 mRNA.	protein amino acid phosphorylation [0006468]
AB040883	-1,2	0,5	6	Hs.83243	Homo sapiens mRNA for KIAA1450 protein, partial cds.	signal transduction [0007165]
NM_015874	-1,2	0,5	6	Hs.347340	Homo sapiens H-2K binding factor-2 (LOC51580), mRNA.	DNA transposition [0006313]
AK026985	-1,2	0,5	6	Hs.28794	Homo sapiens cDNA: FLJ23332 fis, clone HEP12754	biological_process unknown [0000004]
NM_002823	-1,2	0,3	6	Hs.250655	Homo sapiens prothymosin, alpha (gene sequence 28) (PTMA), mRNA.	immune response [0006955]
AL110280	-1,2	0,3	4	Hs.301152	Homo sapiens mRNA; cDNA DKFZp434F053 (from clone DKFZp434F053), partial cds.	proteolysis and peptidolysis [0006508]
AL050214	-1,2	0,4	5	Hs.55044	Homo sapiens mRNA; cDNA DKFZp586H2123 (from clone DKFZp586H2123); partial cds.	proteolysis and peptidolysis [0006508]
NM_006697	-1,2	0,5	6	Hs.166066	Homo sapiens cisplatin resistance associated (CRA), mRNA.	protein amino acid dephosphorylation [0006470]
NM_006664	-1,2	0,4	6	Hs.225948	Homo sapiens chemokine (C-C motif) ligand 27 (CCL27), mRNA.	chemotaxis [0006935]
AF039944	-1,2	0,5	6	Hs.318567	This gene is a member of the N-myc downregulated gene family	biological_process unknown [0000004]
AK024270	-1,3	0,4	4	Hs.4094	Homo sapiens cDNA FLJ14208 fis, clone NT2RP3003284	biological_process unknown [0000004]

NM_005842	-1,3	0,6	6	Hs.18676	Homo sapiens sprouty (Drosophila)Homolog 2 (SPRY2), mRNA	histogenesis and organogenesis [0007397]
AF036364	-1,3	0,3	6	Hs.110708	Homo sapiens epsilon-sarcoglycan (ESG), mRNA, complete cds.	muscle development [0007517]
NM_006180	-1,3	0,5	6	Hs.47860	Homo sapiens neurotrophic tyrosine kinase, receptor, type 2 (NTRK2), mRNA.	neurogenesis [0007399]
NM_007229	-1,3	0,4	5	Hs.18842	Homo sapiens protein kinase C and casein kinase substrate in neurons 2 (PACSLIN2), mRNA.	signal transduction [0007165]
NM_003016	-1,4	0,4	6	Hs.73965	Homo sapiens splicing factor, arginine/serine-rich 2 (SFRS2), mRNA.	RNA processing [0006396]
NM_018165	-1,4	0,4	5	Hs.44143	Homo sapiens polybromo 1 (PB1), mRNA.	DNA packaging [0006323]
NM_001311	-1,4	0,4	6	Hs.423190	Homo sapiens cysteine-rich protein 1 (intesimal) (CRIP1), mRNA.	cell proliferation [0008283]
NM_012282	-1,4	0,6	6	Hs.146372	Homo sapiens potassium voltage-gated channel, Isk-related family, member 1-like (KCNE1L), mRNA.	regulation of heart [0008016]
NM_020400	-1,4	0,4	6	Hs.155538	Homo sapiens G protein-coupled receptor 92 (GPR92), mRNA.	chemotaxis [0006935]
NM_003174	-1,5	0,6	6	Hs.154567	Homo sapiens supervillin (SVIL), transcript variant 1, mRNA.	cellular morphogenesis [0000902]
NM_019897	-1,5	0,5	6	Hs.283806	Homo sapiens olfactory receptor, family 2, subfamily S, member 2 (OR2S2), mRNA.	G-protein coupled receptor protein signaling pathway [0007186]
NM_007326	-1,5	0,3	6	Hs.274464	Homo sapiens diaphorase (NADH) (cytochrome b-5 reductase) (DIA1), nuclear gene encoding mitochondrial protein,	circulation [0008015]
AF205437	-1,5	0,6	6	Hs.7837	Homo sapiens G-protein-coupled receptor induced protein GIG2 (GIG2) mRNA, complete cds.	cell proliferation [0008283]
NM_003875	-1,6	0,3	5	Hs.5398	Homo sapiens guanine monophosphate synthetase (GMPs), mRNA.	GMP biosynthesis [0006177]
NM_000304	-1,6	0,3	6	Hs.103724	Homo sapiens peripheral myelin protein 22 (PMP22), mRNA.	synaptic transmission [0007268]
NM_017694	-1,6	0,5	4	Hs.390013	Homo sapiens hypothetical protein FLJ20160 (FLJ20160), mRNA.	transport [0006810]
NM_001614	-1,6	0,3	6	Hs.14376	Homo sapiens actin, gamma 1 (ACTG1), mRNA.	cytoskeleton organization and biogenesis [0007010]
NM_006022	-1,6	0,4	6	Hs.114360	Homo sapiens transforming growth factor beta-stimulated protein TSC-22 (TSC22), mRNA.	regulation of transcription, DNA-dependent [0006355]
AK022798	-1,6	0,6	6	Hs.147434	T3JAM TRAF3-interacting Jun N-terminal kinase (JNK)-activating modulator	muscle contraction [0006936]
NM_018043	-1,6	0,5	6	Hs.26176	Homo sapiens hypothetical protein FLJ10261 (FLJ10261), mRNA.	mitochondrial processing [0006627]
NM_016205	-1,6	0,5	6	Hs.43080	Homo sapiens platelet derived growth factor C (PDGFC), mRNA.	cell growth and/or maintenance [0008151]
NM_003627	-1,7	0,7	6	Hs.18910	Homo sapiens prostate cancer overexpressed gene 1 (POV1), mRNA.	oncogenesis [0007048]
AL133585	-1,7	0,7	5	Hs.279806	Homo sapiens mRNA; cDNA DKFZp434E109 (from clone DKFZp434E109)	biological_process unknown [0000004]
AK032388	-1,7	0,6	5	Hs.29397	Homo sapiens cDNA FLJ13226 fis, clone OVARC100068	biological_process unknown [0000004]
AB037725	-1,7	0,7	6	Hs.18995	Homo sapiens mRNA for KIAA1304 protein, partial cds.	Rho protein signal transduction [0007266]
NM_003311	-1,8	0,6	6	Hs.154036	Homo sapiens tumor suppressing subtransferable candidate 3 (TSSC3), mRNA.	embryogenesis and morphogenesis [0007345]
NM_002192	-1,8	0,7	6	Hs.727	Homo sapiens inhibin, beta A (activin A, activin AB alpha polypeptide) (INHBA), mRNA.	cell growth and/or maintenance [0008151]
AK000776	-1,8	0,5	4	Hs.128753	Homo sapiens cDNA FLJ20769 fis, clone COL06674	biological_process unknown [0000004]

Table S4.1 continued

Gene ID	Mean	Stdev	N	UniGene ID	Description	Gene ontology
AF218008	-1.8	0.5	6	Hs.347803	Homo sapiens clone PP3501 unknown mRNA.	biological_process unknown [0000004]
NM_000043	-1.9	0.7	5	Hs.82359	Homo sapiens tumor necrosis factor receptor superfamily, member 6 (TNFRSF6), transcript variant 1, mRNA.	anti-apoptosis [0006916]
NM_001657	-2.0	0.8	6	Hs.270833	Homo sapiens amphiregulin (schwannoma-derived growth factor) (AREG), mRNA.	cell-cell signaling [0007267]
NM_001692	-2.0	0.7	4	Hs.64173	Homo sapiens ATPase, H+ transporting, lysosomal 56/58kDa, V1 subunit B, isoform 1	excretion [0007588]
NM_001748	-2.1	0.5	5	Hs.76288	Homo sapiens calpain 2, (m/l) large subunit (CAPN2), mRNA.	proteolysis and peptidolysis [0006508]
AK024805	-2.1	0.6	4	Hs.375709	Homo sapiens cDNA: FLJ21152 fis, clone CAS09594.	electron transport [0006118]
NM_001109	-2.3	0.9	6	Hs.86947	Homo sapiens a disintegrin and metalloproteinase domain 8 (ADAM8), mRNA.	proteolysis and peptidolysis [0006508]
NM_012132	-2.4	0.9	5	Hs.162209	Homo sapiens claudin 8 (CLDN8), mRNA.	biological_process unknown [0000004]
AK001903	-2.5	0.9	6	Hs.28792	Homo sapiens cDNA FLJ11041 fis, clone PLACE1004405	biological_process unknown [0000004]
NM_001663	-2.6	0.6	4	Hs.89474	Homo sapiens ADP-ribosylation factor 6 (ARF6), mRNA.	intracellular protein transport [0006886]
NM_000067	-2.9	0.3	6	Hs.155097	Homo sapiens carbonic anhydrase II (CA2), mRNA.	protein targeting [0006605]

References

1. Leung DY, Bieber T. Atopic dermatitis. *Lancet* 361, 151-60 (2003)
2. Hollox EJ, Huffmeier U, Zeeuwen PL *et al.* Psoriasis is associated with increased beta-defensin genomic copy number. *Nat Genet* 40, 23-5 (2008)
3. de Cid R, Riveira-Munoz E, Zeeuwen PL *et al.* Deletion of the late cornified envelope LCE3B and LCE3C genes as a susceptibility factor for psoriasis. *Nat Genet* 41, 211-5 (2009)
4. Nair RP, Duffin KC, Helms C *et al.* Genome-wide scan reveals association of psoriasis with IL-23 and NF-kappaB pathways. *Nat Genet* 41, 199-204 (2009)
5. Palmer CN, Irvine AD, Terron-Kwiatkowski A *et al.* Common loss-of-function variants of the epidermal barrier protein filaggrin are a major predisposing factor for atopic dermatitis. *Nat Genet* 38, 441-6 (2006)
6. Lowes MA, Kikuchi T, Fuentes-Duculan J *et al.* Psoriasis vulgaris lesions contain discrete populations of Th1 and Th17 T cells. *J Invest Dermatol* 128, 1207-11 (2008)
7. Zaba LC, Fuentes-Duculan J, Eungdamrong NJ *et al.* Psoriasis is characterized by accumulation of immunostimulatory and Th1/Th17 cell-polarizing myeloid dendritic cells. *J Invest Dermatol* 129, 79-88 (2009)
8. Hamid Q, Boguniewicz M, Leung DY. Differential in situ cytokine gene expression in acute versus chronic atopic dermatitis. *J Clin Invest* 94, 870-6 (1994)
9. Nomura I, Gao B, Boguniewicz M *et al.* Distinct patterns of gene expression in the skin lesions of atopic dermatitis and psoriasis: a gene microarray analysis. *J Allergy Clin Immunol* 112, 1195-202 (2003)
10. de Jongh GJ, Zeeuwen PL, Kucharekova M *et al.* High expression levels of keratinocyte antimicrobial proteins in psoriasis compared with atopic dermatitis. *J Invest Dermatol* 125, 1163-73 (2005)
11. Zeeuwen PL, de Jongh GJ, Rodijk-Olthuis D *et al.* Genetically programmed differences in epidermal host defense between psoriasis and atopic dermatitis patients. *PLoS ONE* 3, e2301 (2008)
12. Mee JB, Johnson CM, Morar N *et al.* The psoriatic transcriptome closely resembles that induced by interleukin-1 in cultured keratinocytes: dominance of innate immune responses in psoriasis. *Am J Pathol* 171, 32-42 (2007)
13. Ong PY, Ohtake T, Brandt C *et al.* Endogenous antimicrobial peptides and skin infections in atopic dermatitis. *N Engl J Med* 347, 1151-60 (2002)
14. Kamsteeg M, Zeeuwen PL, de Jongh GJ *et al.* Increased expression of carbonic anhydrase II (CA II) in lesional skin of atopic dermatitis: regulation by Th2 cytokines. *J Invest Dermatol* 127, 1786-9 (2007)
15. Aihara K, Kuroda S, Kanayama N *et al.* A neuron-specific EGF family protein, NELL2, promotes survival of neurons through mitogen-activated protein kinases. *Brain Res Mol Brain Res* 116, 86-93 (2003)
16. Jansen PA, Kamsteeg M, Rodijk-Olthuis D *et al.* Expression of the vanin gene family in normal and inflamed human skin: induction by proinflammatory cytokines. *J Invest Dermatol* 129, 2167-74 (2009)
17. Howell MD, Boguniewicz M, Pastore S *et al.* Mechanism of HBD-3 deficiency in atopic dermatitis. *Clin Immunol* 121, 332-8 (2006)
18. Howell MD, Novak N, Bieber T *et al.* Interleukin-10 downregulates anti-microbial peptide expression in atopic dermatitis. *J Invest Dermatol* 125, 738-45 (2005)

19. Cavani A, De PO, Girolomoni G. New aspects of the molecular basis of contact allergy. *Curr Opin Allergy Clin Immunol* 7, 404-8 (2007)
20. Slodownik D, Lee A, Nixon R. Irritant contact dermatitis: a review. *Australas J Dermatol* 49, 1-9 (2008)
21. Minang JT, Troye-Blomberg M, Lundeberg L *et al.* Nickel elicits concomitant and correlated in vitro production of Th1-, Th2-type and regulatory cytokines in subjects with contact allergy to nickel. *Scand J Immunol* 62, 289-96 (2005)
22. Ulfgren AK, Klareskog L, Lindberg M. An immunohistochemical analysis of cytokine expression in allergic and irritant contact dermatitis. *Acta Derm Venereol* 80, 167-70 (2000)
23. de Jongh CM, Lutter R, Verberk MM *et al.* Differential cytokine expression in skin after single and repeated irritation by sodium lauryl sulphate. *Exp Dermatol* 16, 1032-40 (2007)
24. Spiewak R, Moed H, von Blomberg BM *et al.* Allergic contact dermatitis to nickel: modified in vitro test protocols for better detection of allergen-specific response. *Contact Dermatitis* 56, 63-9 (2007)
25. Kitagaki H, Ono N, Hayakawa K *et al.* Repeated elicitation of contact hypersensitivity induces a shift in cutaneous cytokine milieu from a T helper cell type 1 to a T helper cell type 2 profile. *J Immunol* 159, 2484-91 (1997)
26. Boron WF. Regulation of intracellular pH. *Adv Physiol Educ* 28, 160-79 (2004)
27. Kuroda S, Oyasu M, Kawakami M *et al.* Biochemical characterization and expression analysis of neural thrombospondin-1-like proteins NELL1 and NELL2. *Biochem Biophys Res Commun* 265, 79-86 (1999)
28. Watanabe TK, Katagiri T, Suzuki M *et al.* Cloning and characterization of two novel human cDNAs (NELL1 and NELL2) encoding proteins with six EGF-like repeats. *Genomics* 38, 273-6 (1996)
29. Nelson BR, Claes K, Todd V *et al.* NELL2 promotes motor and sensory neuron differentiation and stimulates mitogenesis in DRG in vivo. *Dev Biol* 270, 322-35.
30. Urashima R, Mihara M. Cutaneous nerves in atopic dermatitis. A histological, immunohistochemical and electron microscopic study. *Virchows Arch* 432, 363-70 (1998)
31. Flier J, Boorsma DM, Bruynzeel DP *et al.* The CXCR3 activating chemokines IP-10, Mig, and IP-9 are expressed in allergic but not in irritant patch test reactions. *J Invest Dermatol* 113, 574-8 (1999)
32. Gottlieb AB, Luster AD, Posnett DN *et al.* Detection of a gamma interferon-induced protein IP-10 in psoriatic plaques. *J Exp Med* 168, 941-8 (1988)
33. Giustizieri ML, Mascia F, Frezzolini A *et al.* Keratinocytes from patients with atopic dermatitis and psoriasis show a distinct chemokine production profile in response to T cell-derived cytokines. *J Allergy Clin Immunol* 107, 871-7 (2001)
34. Bernardini G, Hedrick J, Sozzani S *et al.* Identification of the CC chemokines TARC and macrophage inflammatory protein-1 beta as novel functional ligands for the CCR8 receptor. *Eur J Immunol* 28, 582-8 (1998)
35. Imai T, Baba M, Nishimura M *et al.* The T cell-directed CC chemokine TARC is a highly specific biological ligand for CC chemokine receptor 4. *J Biol Chem* 272, 15036-42 (1997)
36. Imai T, Nagira M, Takagi S *et al.* Selective recruitment of CCR4-bearing Th2 cells toward antigen-presenting cells by the CC chemokines thymus and activation-regulated chemokine and macrophage-derived chemokine. *Int Immunol* 11, 81-8 (1999)

37. Vestergaard C, Deleuran M, Gesser B *et al.* Thymus- and activation-regulated chemokine (TARC/CCL17) induces a Th2-dominated inflammatory reaction on intradermal injection in mice. *Exp Dermatol* 13, 265-71 (2004)
38. Kakinuma T, Nakamura K, Wakugawa M *et al.* Thymus and activation-regulated chemokine in atopic dermatitis: Serum thymus and activation-regulated chemokine level is closely related with disease activity. *J Allergy Clin Immunol* 107, 535-41 (2001)
39. Nakazato J, Kishida M, Kuroiwa R *et al.* Serum levels of Th2 chemokines, CCL17, CCL22, and CCL27, were the important markers of severity in infantile atopic dermatitis. *Pediatr Allergy Immunol* 19, 605-13 (2008)
40. Corsini E, Terzoli A, Bruccoleri A *et al.* Induction of tumor necrosis factor-alpha in vivo by a skin irritant, tributyltin, through activation of transcription factors: its pharmacological modulation by anti-inflammatory drugs. *J Invest Dermatol* 108, 892-6 (1997)
41. Enk AH, Katz SI. Early molecular events in the induction phase of contact sensitivity. *Proc Natl Acad Sci USA* 89, 1398-402 (1992)
42. Holliday MR, Corsini E, Smith S *et al.* Differential induction of cutaneous TNF-alpha and IL-6 by topically applied chemicals. *Am J Contact Dermat* 8, 158-64 (1997)
43. Meller S, Lauerma AI, Kopp FM *et al.* Chemokine responses distinguish chemical-induced allergic from irritant skin inflammation, memory T cells make the difference. *J Allergy Clin Immunol* 119, 1470-80 (2007)
44. Chew AL, Maibach HI. Occupational issues of irritant contact dermatitis. *Int Arch Occup Environ Health* 76, 339-46.
45. Aydin O, Engin B, Oguz O *et al.* Non-pustular palmoplantar psoriasis: is histologic differentiation from eczematous dermatitis possible? *J Cutan Pathol* 35, 169-73.
46. Hanifin JM, Rajka G. Diagnostic features of atopic dermatitis. *Acta Derm Venereol (Stockh)* 92 (Suppl.),44-7 (1980)
47. van Ruissen F, Jansen BJ, de Jongh GJ *et al.* A partial transcriptome of human epidermis. *Genomics* 79, 671-8 (2002)
48. Franssen ME, Zeeuwen PL, Vierwinden G *et al.* Phenotypical and functional differences in germinative subpopulations derived from normal and psoriatic epidermis. *J Invest Dermatol* 124, 373-83 (2005)
49. Livak KJ, Schmittgen TD. Analysis of relative gene expression data using real-time quantitative PCR and the 2(-Delta Delta C(T)) Method. *Methods* 25, 402-8 (2001)
50. Oestreicher JL, Walters IB, Kikuchi T *et al.* Molecular classification of psoriasis disease-associated genes through pharmacogenomic expression profiling. *Pharmacogenomics J* 1, 272-87 (2001)
51. Zhou X, Krueger JG, Kao MC *et al.* Novel mechanisms of T-cell and dendritic cell activation revealed by profiling of psoriasis on the 63,100-element oligonucleotide array. *Physiol Genomics* 13, 69-78 (2003)
52. Nomura I, Goleva E, Howell MD *et al.* Cytokine milieu of atopic dermatitis, as compared to psoriasis, skin prevents induction of innate immune response genes. *J Immunol* 171, 3262-9 (2003)

Rho kinase inhibitor Y-27632 prolongs the life span of adult human keratinocytes, enhances skin equivalent development and facilitates lentiviral transduction

5
CHAPTER

Ellen H van den Bogaard¹⁻²
Diana Rodijk-Olthuis¹
Patrick AM Jansen¹
Ivonne MJJ van Vlijmen-Willems¹
Piet E van Erp¹
Irma Joosten²
Patrick LJM Zeeuwen¹
Joost Schalkwijk^{1*}

¹ Department of Dermatology, Nijmegen Institute for Infection Inflammation and Immunity, Nijmegen Centre for Molecular Life Sciences, Radboud University Nijmegen Medical Centre, The Netherlands

² Department of Laboratory Medical Immunology, Nijmegen Institute for Infection Inflammation and Immunity, Radboud University Nijmegen Medical Centre, The Netherlands

Published in: *Tissue Eng Part A* 18, 1827-36 (2012)

Abstract

The use of tissue engineered human skin equivalents (HSE) for fundamental research and industrial application requires expansion of keratinocytes from a limited number of skin biopsies donated by adult healthy volunteers or patients. A pharmacological inhibitor of Rho-associated protein kinases, Y-27632, was recently reported to immortalize neonatal human foreskin keratinocytes. Here, we investigated the potential use of Y-27632 to expand human adult keratinocytes and evaluated its effects on HSE development and *in vitro* gene delivery assays. Y-27632 was found to significantly increase the life span of human adult keratinocytes (up to 5-8 passages). Epidermal morphology of HSEs generated from high passage, Y-27632-treated keratinocytes resembled native epidermis and was improved by supplementing Y-27632 during the submerged phase of HSE development. In addition, Y-27632-treated keratinocytes responded normally to inflammatory stimuli, and could be used to generate HSEs with a psoriatic phenotype, upon stimulation with relevant cytokines. Furthermore, Y-27632 significantly enhanced both lentiviral transduction efficiency of primary adult keratinocytes and epidermal morphology of HSEs generated thereof. Our study indicates that Y-27632 is a potentially powerful tool for a variety of applications of adult human keratinocytes.

Introduction

There is a growing demand for tissue engineered *in vitro* skin models for industrial applications and in fundamental research. *In vitro* pharmacotoxicological testing and industrial screening of drugs are nowadays accepted as an alternative to experimental animal testing and *in vitro* skin models are increasingly used to study skin biology and pathophysiology of skin diseases. Although the development of organotypic cultures, further designated as human skin equivalents (HSEs), for reconstructive purposes has been disappointing over the last decades, there are several indications that they may find their way to the clinic. Their potential use ranges from application in chronic ulcers¹, to treatment of patients with keratinization disorders or blistering diseases using epidermal grafts of keratinocytes derived from genetically corrected induced pluripotent stem cells².

Submerged keratinocyte cultures have been extensively used as *in vitro* skin models, however, over the last decade, or HSEs have emerged as a more biologically and physiologically relevant model as they more closely mimic native epidermis. To meet the increasing need for HSEs, large quantities of primary human keratinocytes are required. Recently, increased cloning efficiency of neonatal human foreskin keratinocytes³ and even efficient immortalization due to increased telomerase expression and stabilization of the telomere lengths⁴ has been described. Both studies used a selective inhibitor of the Rho-associated coiled-coil forming protein serine/threonine kinase (ROCK), Y-27632.

The Rho/ROCK pathway is essential in a variety of cellular functions in keratinocytes including, actin cytoskeletal organization⁵, keratinocyte adhesion⁶ and motility^{7,8}. Related to skin morphogenesis, it was recently described that RhoE, a member of the Rho GTPase family, is required for epidermal morphogenesis by regulating epidermal stratification⁹. RhoA, however, was found to be dispensable for skin development, as knockout mice lack a skin phenotype⁸. In contrast, downstream effectors of RhoA, ROCK I and II, have been reported to regulate keratinocyte differentiation^{10,11}.

Hitherto, studies describing ROCK inhibition by Y-27632 use HaCaT cell lines or neonatal foreskin keratinocytes. However, in HSE development, primary human adult keratinocytes are preferably used since they generate HSEs that more closely resemble native epidermis in structure and function¹². For application of HSEs in reconstructive surgery or gene therapy, expansion of primary keratinocytes isolated from a few biopsies is required to generate sufficient amounts of cells. However, the life span of primary adult keratinocytes is relatively short and senescence is usually observed after a few passages. In the light of the emerging applications of HSEs, we anticipate a strong need for human adult keratinocytes and have therefore evaluated the potential of Y-27632 to prolong the life span of these cells. In addition, we thoroughly investigated the effects of Y-27632 on HSE development. Finally, we studied the potential of Y-27632 to facilitate gene delivery studies using lentiviral-transduced adult keratinocytes to generate HSEs.

Results

Y-27632 increases the life span of primary adult keratinocytes

As described previously for freshly isolated neonatal foreskin keratinocytes⁴, we cultured liquid nitrogen-stored primary adult keratinocytes obtained from 3mm skin biopsies and neonatal foreskin keratinocytes with or without Y-27632. The population doubling rate was calculated at each passage. Based on previous work and dose optimization studies, a 10 μ M concentration of Y-27632 was used. As shown in Figure 5.1a, senescence was observed between days 30 and 60 of culture in all five adult keratinocyte donors cultured without Y-27632, this in contrast to neonatal foreskin keratinocytes which remained proliferative throughout the culture period, which indicates the profound differences between foreskin and adult keratinocytes. All adult keratinocytes cultured in presence of Y-27632 showed a markedly increased life span and three out of five keratinocyte donors remained proliferative for 80 days or longer. Morphologically, high passage keratinocytes cultured with Y-27632 resembled primary keratinocytes as they were small and homogenous in size and formed a honeycomb pattern of cohesive polygonal cells. Adult keratinocytes cultured in absence of Y-27632 became large and heterogeneous in size with bloated cytoplasm, which are signs of senescence (Figure 5.1b). Since immortalization of foreskin keratinocytes by Y-27632 due to induced telomerase expression was previously reported⁴,

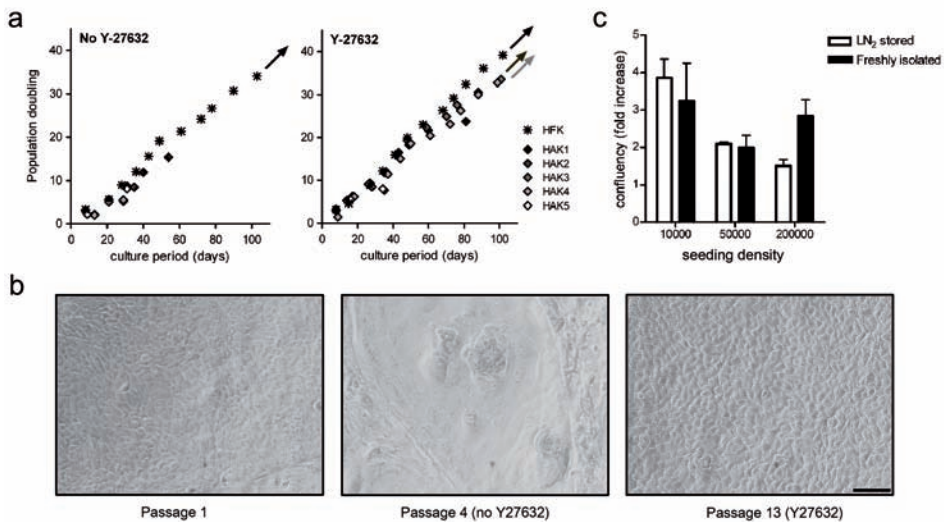


Figure 5.1 Effect of Y-27632 on life span and cloning efficiency of primary human adult keratinocytes. Growth rate of human keratinocytes from one neonatal foreskin (HFK) donor or five adult (HAK1-5) donors (abdominal wall skin) cultured in the presence or absence of 10 μ M Y-27632. The arrows indicate cells lines that continued to divide after 100 days in culture. The growth rate is measured as population doubling per day (a). Images of primary adult keratinocytes (left), passage 4 adult keratinocytes cultured without Y-27632 (middle) and passage 13 adult keratinocytes cultured with Y-27632 (right). Scale bar, 100 μ m (b). Fold increase in cloning efficiency of freshly isolated keratinocytes and liquid nitrogen-stored primary keratinocytes cultured with Y-27632 as compared to culture without Y-27632 (c). Error bars represent SD (n=3).

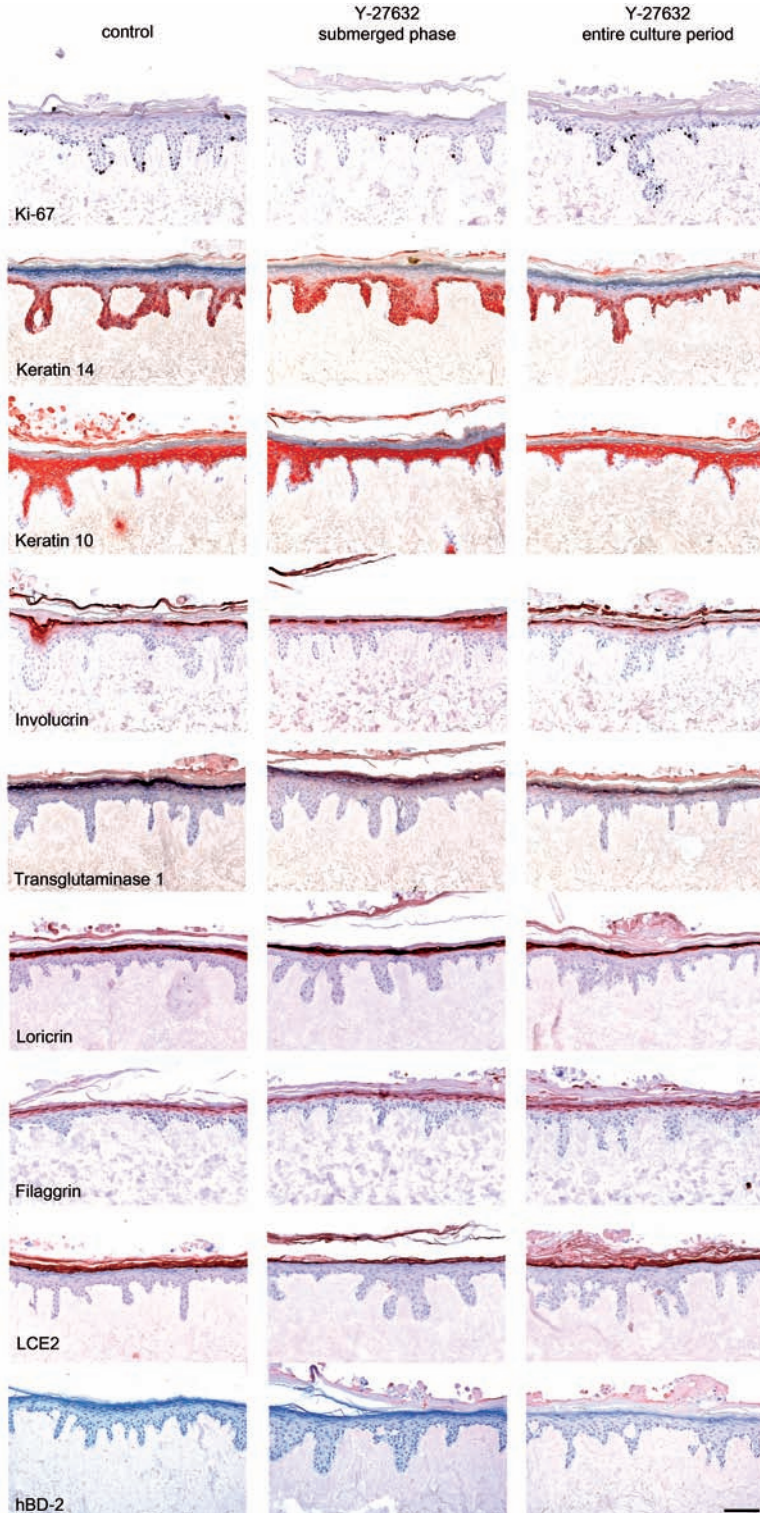


Figure 5.2 Epidermal differentiation patterns in human skin equivalents (HSEs) generated from passage 6, Y-27632-treated keratinocytes. HSEs were cultured without Y-27632 (left panel), with 10 μ M Y-27632 supplemented during the submerged phase (middle panel) or during the entire culture period (right panel). HSEs show normal expression patterns for all analyzed epidermal markers: Ki-67 (proliferative cells), keratin 14 (basal keratinocytes), keratin 10 (suprabasal keratinocytes) and involucrin and transglutaminase 1 (terminal differentiation). HSEs are negative for the stress/psoriatic marker, human beta defensin-2 (hBD-2). Scale bar, 100 μ m.

we analyzed telomerase mRNA expression in high passage, Y-27632-treated adult and foreskin keratinocytes, however, we were unable to detect telomerase expression in all samples (data not shown). We also studied the effect of Y-27632 on the proliferation rate of freshly isolated adult keratinocytes as compared to liquid nitrogen-stored, primary adult keratinocytes and found no differences between both keratinocyte batches (Figure 5.1c and Supplemental figure 5.1), suggesting that keratinocyte culture of previously isolated and liquid nitrogen stored adult keratinocytes can benefit from Y-27632 treatment.

Normal human skin equivalent can be generated from Y-27632-treated keratinocytes

To evaluate the effect of Y-27632 on HSE development, we used our 3D skin model consisting of de-epidermised dermis as a matrix, and supplemented the culture medium with 10 μ M Y-27632. Y-27632-treated keratinocytes (passage 6) were used to generate skin equivalents and we compared them to liquid nitrogen-stored, primary adult keratinocytes (passage 1), with Y-27632 supplemented during different phases of the skin equivalent development. Passage 6 adult keratinocytes generated high quality HSEs, with a multilayered epidermis, presence of *stratum granulosum* and a basket weave *stratum corneum* (Supplemental figure 5.2). Normal expression patterns of major epidermal differentiation proteins were observed and HSEs were negative for the stress/psoriatic marker human beta defensin-2 (hBD-2) (Figure 5.2). (See Supplemental Figure 5.3a for epidermal differentiation analysis in control HSEs). Even at passage 12, Y-27632-treated adult keratinocytes still generated high quality HSEs comparable to native epidermis (Supplemental Figure 3b). Furthermore, epidermal morphology appeared more regular when Y-27632 was supplemented during the submerged phase of the culture period (Supplemental figure 5.2c and d), this in contrast to HSEs cultured with Y-27632 during the entire culture period in which epidermal morphology was negatively affected and deep epidermal ridges were observed (Supplemental figure 5.2e and f). Therefore, it was decided to use Y-27632 only during the submerged phase of the HSE development for further experiments.

As we observed that timing of Y-27632 exposure clearly affected HSE morphology, we also addressed possible adverse effects of high concentrations of the ROCK inhibitor on epidermal morphology. At 30 and 100 μ M of Y-27632, deep epidermal ridges were observed and at 100 μ M epidermal protrusions were seen in the *stratum corneum* (Figure 5.3a). These morphological changes were, however, not associated with significant alterations in epidermal differentiation gene expression (Figure 5.3b) or protein expression (Supplemental Figure 5.4), or caused by induction of a keratinocyte inflammatory response as all HSEs lacked hBD-2 expression (Supplemental Figure 5.4). Protein expression of involucrin, however, was slightly extended towards the *stratum spinosum* in HSEs cultured with 30 and 100 μ M of Y-27632, which may be indicative of an activated epithelium.

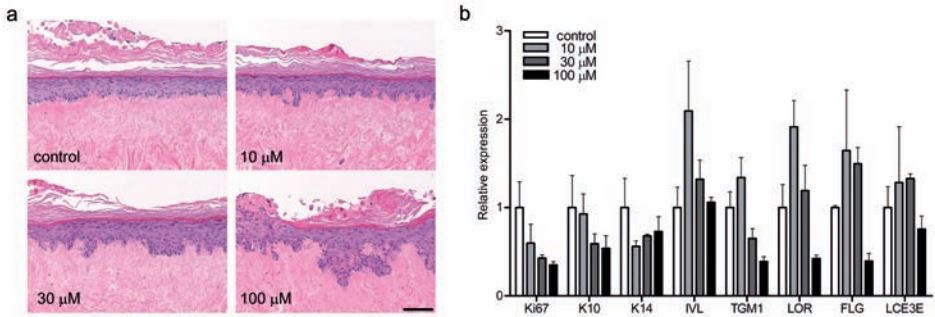


Figure 5.3 Y-27632 concentration dependent changes in epidermal morphology. (a) Deep rete ridges are observed in human skin equivalents (HSEs) generated in the presence of 30 or 100 μM Y-27632 and epidermal protrusions are observed at 100 μM. Scale bar, 100 μm. (b) Relative mRNA expression levels of various epidermal differentiation genes in HSEs generated with 10, 30 or 100 μM Y-27632. The relative amount of mRNA in Y-27632 stimulated HSEs is normalized to the mean of unstimulated HSEs. Error bars represent SD (n=2).

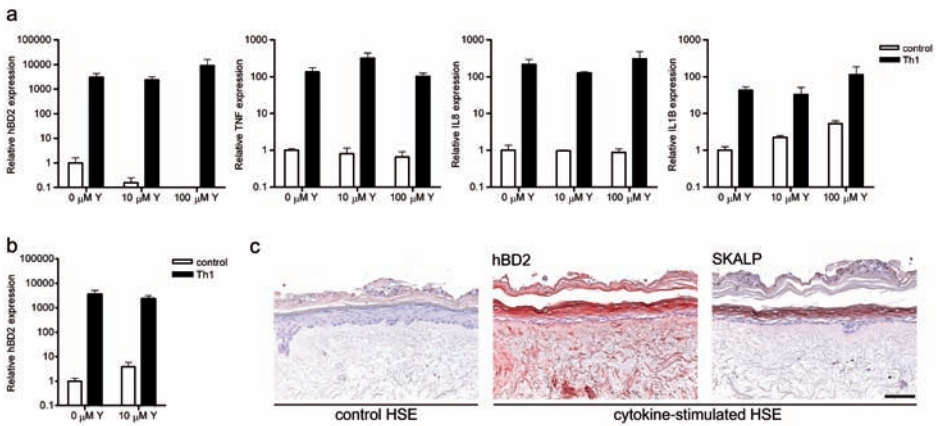


Figure 5.4 Normal keratinocyte response to inflammatory stimuli after exposure to Y-27632. Primary adult keratinocytes (a) and passage 6 Y-27632-treated keratinocytes (b) were cultured submerged with 10 or 100 μM Y27632 and stimulated with pro-inflammatory (Th1) cytokines IL-1α (10 ng/ml), TNF-α (50 ng/ml) and IFN-γ (500 U/ml). Relative mRNA expression levels of human beta defensin-2 (hBD-2), TNF-α, IL-8 and IL1-β were compared to unstimulated (control) keratinocytes. Significant induction ($P < 0.01$) of all analyzed genes was observed after cytokine stimulation. The already low basal hBD-2 levels further decreased by 10 ($P < 0.05$) and 100 μM ($P < 0.01$) of Y-27632, while basal IL-1β levels significantly increased ($P < 0.05$) at 10 and 100 μM of Y-27632. Error bars represent SD (n=3-5). (c) Immunohistochemical staining of psoriatic markers, hBD-2 and SKALP/elafin shows strong induction of both markers in HSEs generated from Y-27632-treated keratinocytes with 10 μM Y27632 supplemented during the submerged phase of HSE development, upon stimulation with psoriasis-associated cytokines IL-6 (5 ng/ml), TNF-α (5 ng/ml) and IL-1α (10 ng/ml). Scale bar, 100 μm.

In vitro psoriasis skin models can be generated from Y-27632-treated keratinocytes
 As human primary keratinocytes are extensively used *in vitro* to study their function in the innate immune system, we cultured adult keratinocytes (passage 1) submerged with various concentrations of Y-27632 and used pro-inflammatory cytokines IL-1α, TNF-α and IFN-γ to mimic an inflammatory milieu *in vitro*. As

depicted in Figure 5.4a, unstimulated (control) keratinocytes showed lower expression levels of hBD-2, while IL-1 β mRNA expression levels were slightly elevated at 10 and 100 μ M Y-27632. More importantly, keratinocyte activation was unaffected by Y-27632 as hBD-2, TNF- α , IL-8 and IL-1 β mRNA expression levels were still significantly induced after cytokine stimuli. High passage Y-27632-treated keratinocytes also showed significant induction of hBD-2 when cultured with 10 μ M Y-27632 (Figure 5.4b). To verify this in our 3D skin model, we generated HSEs from Y-27632-treated keratinocytes and added 10 μ M Y-27632 during the submerged phase of HSE development. Thereafter, HSEs were stimulated with psoriasis-associated cytokines, IL-6, IL-1 α and TNF- α during the last three days of air-exposed culture. Protein expression of the psoriatic markers hBD-2 and SKALP/elafin was strongly induced in cytokine-stimulated HSEs (Figure 5.4c), indicating that psoriatic skin equivalents can be generated from Y-27632 treated keratinocytes.

In the experiments described above we used keratinocytes from healthy donors to generate a psoriasis-like phenotype *in vitro*. We also successively used Y-27632 to prolong the life span of keratinocytes derived from patients with skin diseases such as psoriasis or atopic dermatitis (data not shown), which could be subsequently used for HSE development.

Y-27632 facilitates gene delivery studies in human adult keratinocytes

Application of gene knock-down or overexpression techniques in HSEs is an elegant way to functionally analyze individual genes in an organ-like environment. We have observed that the proliferative capacity of high passage adult keratinocytes after lentiviral transduction is insufficient to generate HSEs thereafter (data not shown). Therefore, we assessed whether adult keratinocyte culture and subsequent HSE development can benefit from Y-27632 treatment in gene delivery assays. We used eGFP lentivirus as a model system for gene transduction and generated HSEs of eGFP-transduced keratinocytes which were cultured in the presence or absence of Y-27632, and compared gene transduction efficiency and HSE morphology. eGFP-transduced HSEs generated in the absence of Y-27632, showed a poorly formed epidermis consisting of only few cell layers, no *stratum granulosum* and parakeratosis present in the *stratum corneum*. HSEs generated from Y-27632-treated keratinocytes with Y-27632 present during the submerged phase of the HSE development, generated significantly improved skin equivalents with a multilayered epidermis, presence of *stratum granulosum* and no parakeratosis in the *stratum corneum* (Figure 5.5a). Expression of epidermal differentiation markers in Y-27632 treated, eGFP-transduced HSEs appeared similar to native skin as shown by the normal expression pattern of major epidermal differentiation proteins: keratin 10, involucrin, loricrin and LCE2 (Figure 5.5b). Importantly, Y-27632-treated keratinocytes showed a significantly higher percentage of eGFP-transduced cells after recovery (Figure 5.5c), and this was also prominent in the Y-27632-treated HSEs with the majority of keratinocytes expressing eGFP (Figure 5.5d).

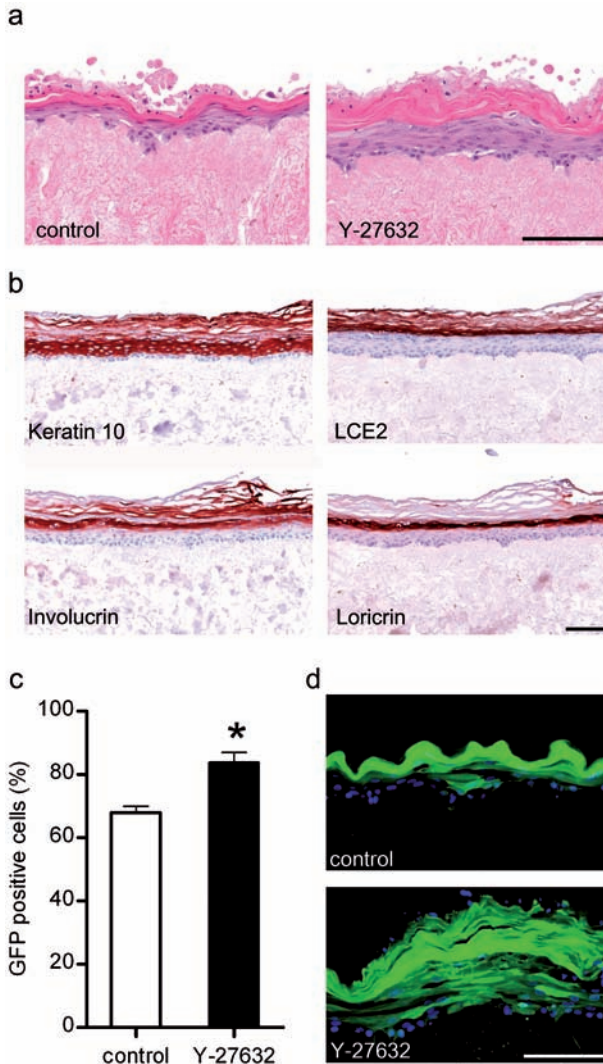


Figure 5.5 Lentiviral transduction of human adult keratinocytes. (a) HSEs generated from transduced keratinocytes that express eGFP driven by a GSK promoter cultured in presence of Y-27632 show superior epidermal morphology to transduced HSEs generated in absence of Y-27632 (control). (b) Epidermal differentiation markers keratin 10, LCE2, involucrin, and loricrin are normally expressed in Y-27632 treated, eGFP transduced HSEs. (c) Flow cytometric analysis shows a significantly higher percentage of eGFP-positive cells in Y-27632-treated keratinocytes. Error bars represent SD (n=3). * $P < 0.05$. (d) HSEs generated from Y-27632-treated keratinocytes show eGFP expression in the majority keratinocytes while in untreated lentiviral-transduced HSEs only few eGFP positive cells are detected (d). Scale bar, 100 μm .

Discussion

HSE development has been extensively optimized over the last decade to generate HSEs highly comparable to native skin. HSEs can nowadays be generated using a variety of dermal matrices such as animal-derived collagen matrices populated or not with human fibroblasts¹³, human de-epidermised dermis¹² or human fibroblast-derived dermal equivalents¹⁴. Large scale HSE development is therefore only restricted by the limited availability of human adult keratinocytes. Here, we demonstrate an adequate solution for this problem, as Y-27632 prolongs the life span of human adult keratinocytes and improves HSE

quality.

Increased cloning efficiency by Y-27632 has been described for several freshly isolated epithelial cells¹⁵, including, human neonatal foreskin keratinocytes^{3,4}, human and murine prostate epithelial cells^{3,16}, human vaginal and cervical epithelial cells⁴ and also for human embryonic stem cells¹⁷. Here, we describe increased cloning efficiency and a prolonged life span of human adult keratinocytes which have been stored in liquid nitrogen prior to Y-27632 treatment. Our findings may therefore have wide spread applications for other institutes to expand their established cell banks.

Immortalization of human foreskin and cervical keratinocytes due to increased telomerase expression and stabilized telomere lengths was described by Chapman *et al.* We, however, were not able to detect such phenomena in our adult keratinocytes. This is probably due to the very high passage number (from passage 34 onwards) in which they reported these characteristics while we were only able to culture our human adult keratinocytes till passage 15. The differences in life span between the Y-27632-treated keratinocytes used in our study and those used by Chapman *et al.* may result from differences in cell source (neonatal foreskin vs. adult keratinocytes). Moreover, liquid nitrogen stored keratinocytes might have a shorter life span than freshly isolated keratinocytes, although during the first passages we observed no differences in proliferation rate between freshly isolated or liquid nitrogen stored keratinocytes.

It has been reported that high passage Y-27632-treated epithelial cells display normal cell cycle progression, karyotype and DNA damage response^{4,15}. Also Y-27632-treated epithelial cells are not capable of inducing tumors after subcutaneous injection in mice¹⁵. These data suggest that Y-27632 treatment of epithelial cells does not result in permanent DNA damage or induction of tumor-like characteristics. Our study shows that, at least for the biomarkers used here, the Y-27632-treated adult keratinocytes do not behave differently from control cells.

Chapman *et al.* generated organotypic cultures from Y-27632-treated foreskin keratinocytes without the addition of Y-27632 during the entire culture period. The morphology of these organotypic cultures, however, did not completely resemble native epidermis, as a recognizable *stratum granulosum* was absent and involucrin expression extended into the *stratum spinosum*. The latter is abnormal and only observed in activated epidermis (e.g. psoriasis or skin injury). Also, from our previous studies we know that foreskin-derived HSEs show an activated phenotype as witnessed by parakeratosis and expression of the psoriasis marker SKALP/elafin¹². Here, we demonstrate that HSEs generated from high passage, Y-27632-treated, adult keratinocytes faithfully mimic native epidermis, both in epidermal morphology and protein expression. We performed elaborate protein expression analysis and all investigated major epidermal differentiation proteins showed similar expression patterns to that of native skin. We can, however, not exclude that other genes or biological processes may be affected by Y-27632 treatment. The beneficial effect of Y-27632 on HSE morphology when used during

the first three days (submerged phase) of HSE culture might be due increased keratinocyte survival and/or proliferation by Y-27632, resulting in a well formed multilayered epidermis later on. Even when Y-27632 was added during the terminal differentiation phase, we were able to generate HSEs with multilayered epidermis and *stratum granulosum* which corresponds to the finding that RhoA is dispensable for epidermal morphogenesis⁸. The previously reported effects of ROCK I and II depletion on keratinocyte differentiation were obtained from submerged keratinocyte cultures⁶ and/or HaCaT cell lines¹⁰. Such models are, however, considered less biologically relevant than *in vitro* generated HSEs. Also, the normal terminal differentiation observed in our Y-27632-treated HSEs may be indicative of compensatory mechanisms only present in an organ-like environment to overcome ROCK depletion as a necessity in epidermal morphogenesis. The observed changes in HSE epidermal morphology when using Y-27632 throughout the HSE culture period or at high concentrations of Y-27632, might be due to the roles of the Rho/ROCK pathway in actin-cytoskeletal architecture⁵ or cell migration^{7,8}. In addition, Y-27632 has also been described to inhibit other kinases such as citron kinase, protein kinase C and myosin light chain kinase¹⁸. Although the potency of Y-27632 for ROCK is >100 times higher than for these kinases, additional effects on other kinases when using Y-27632 at high concentrations cannot be completely excluded.

Primary keratinocytes are widely used to model skin inflammation *in vitro* as they play pivotal roles in inflammatory skin diseases as psoriasis and atopic dermatitis (reviewed by Guttman-Yassky *et al.*¹⁹). We have previously described induction of a psoriatic^{12,20} and atopic dermatitis²¹ phenotype in submerged keratinocytes cultures and HSE models. For these models, large quantities of human adult keratinocytes are required and here we demonstrated that Y-27632-treated keratinocytes can be used for such purposes as keratinocyte activation remains unaffected by Y-27632.

In vitro skin irritation and corrosion testing of new chemical compounds or drugs using HSEs is now recognized as a validated method to substitute experimental animal use^{22,23}. For this purpose, also, large quantities of human primary keratinocytes are needed. Companies developing HSEs at a large scale for commercial use, may therefore benefit from the effects of Y-27632 on adult keratinocytes herein reported.

Over the last decade, small interfering RNA (siRNA) and transgenic techniques have made it possible to investigate gene function and signaling pathways *in vitro*. Only few studies have described *in vitro* gene therapy in HSEs using various methods for gene delivery²⁴⁻²⁶. Low transduction efficiency and poor epidermal morphology of transduced HSEs appears to be a common hurdle for which Y-27632 might provide a solution. Here, we have demonstrated increased lentiviral transduction efficiency in Y-27632-treated keratinocytes and, importantly, epidermal morphology of transduced HSEs was markedly improved by Y-27632. As Y-27632 has been described to suppress dissociation-induced apoptosis in murine prostate cells¹⁶ and to increase thaw-survival rates of stem

cells after cryopreservation¹⁷, keratinocytes might overcome transduction-induced stress when cultured with Y-27632, and Y-27632 might prevent cell death after dissociation of transduced keratinocytes to generate HSEs.

We have demonstrated that Y-27632 is a powerful tool for large scale human adult keratinocyte culture and HSE development, as high passage adult keratinocytes generated HSEs comparable to native epidermis. Furthermore, Y-27632 enhances lentiviral transduction efficiency and improves epidermal morphology of transduced HSEs, thereby facilitating gene delivery studies in primary keratinocytes and providing biologically relevant applications.

Methods

Cell culture

Cells from the mouse fibroblast cell line 3T3 were cultured in Dulbecco's modified Eagle's medium (Life Technologies, Inc., Grand Island, NY) supplemented with penicillin/streptomycin (50 IU/ml; ICN Biomedicals, Zoetermeer, The Netherlands) and 10% calf serum with iron (Hyclone, Logan, UT). Keratinocytes were isolated from human abdominal skin derived from donors who underwent surgery for abdominal wall correction as previously described¹². The study was conducted according to the Declaration of Helsinki principles. Keratinocytes were stored in liquid nitrogen or were used directly. Keratinocytes were cultured in Greens medium (2:1 [v/v] DMEM:Ham's F12 (both from Life Technologies, Inc.) supplemented with 10% fetal bovine serum (Hyclone Laboratories, Inc., Logan, UT), l-glutamine (4 mmol/l; Life Technologies, Inc.), penicillin/streptomycin (50 IU/ml; Life Technologies, Inc.), adenine (24.3 µg/ml; Calbiochem, San Diego, CA), insulin (5 µg/ml; Sigma, St. Louis, MO), hydrocortisone (0.4 µg/ml; Merck, Darmstadt, Germany), triiodothyronine (1.36 ng/ml, Sigma) and cholera toxin (10^{-10} mol/l, Sigma) in the presence of irradiated 3T3-J2 feeder cells. After three days, medium was replaced by Greens medium containing epidermal growth factor (EGF, 10 ng/ml; Sigma). Cells were grown in the presence or absence of 10 µM Y-27632 (Sigma) as indicated and were refreshed every two to three days. Upon 90-100% confluency, cells were subcultured by removal of feeder cells by EDTA (Sigma) and subsequent trypsinization with trypsin-EDTA (0.05%; Sigma) after which they were passaged 1:10 on irradiated 3T3-J2 feeder cells.

Estimation of population doubling rate

At each passage the number of cells harvested was determined and population doubling was calculated as: $PD = 3.32(\log[\text{number of cells harvested}/\text{number of cells seeded}])^4$.

Analysis of cloning efficiency

To assess the effect of Y-27632 on cloning efficiency of freshly isolated adult keratinocytes versus liquid nitrogen stored adult keratinocytes, cells were seeded at different seeding densities on 3T3-J2 feeders cells and cultured as described

above. Cells were grown in presence or absence of 10 μM Y-27632 and after three days, 3T3-J2 feeder cells were removed by EDTA treatment and keratinocyte colonies were fixed using 3.7% paraformaldehyde for 20 minutes at room temperature. Cells were washed two times with PBS (Braun) and stained with freshly prepared 1% Rhodanile Blue (Sigma) in PBS for 15 minutes. Afterwards the cells were washed extensively with tap water and photographs were taken. Quantification analysis was performed using Image J software.

Generation of Human Skin Equivalent

De-epidermized dermis was generated as reported previously¹² and 8-mm tissue samples were obtained using a biopsy punch. De-epidermized dermis was placed in a 24-wells transwell system and seeded with 10^5 keratinocytes. Liquid nitrogen stored primary adult keratinocytes (passage 1) or Y-27632-treated keratinocytes (passage 6 or 13) were used for experiments as indicated. After culturing the HSEs submerged for three days in medium containing 5% serum, consisting of two parts Dulbecco's modified Eagle's medium and one part Ham's F12 medium (both from Life Technologies, Inc.) supplemented with 5% calf serum (Hyclone), 4 mmol/l L-glutamine and 50 IU/ml penicillin or streptomycin (both from Life Technologies, Inc.), 24.3 $\mu\text{g/ml}$ adenine (Calbiochem), 1 $\mu\text{mol/l}$ hydrocortisone (Merck KGaA), and 50 $\mu\text{g/ml}$ ascorbic acid, 0.2 $\mu\text{mol/l}$ insulin, 1.36 ng/ml triiodothyronine, and 10^{-10} mmol/l cholera toxin (all from Sigma), the HSEs were cultured at the air-liquid interface for ten days in medium without serum, consisting of two parts Dulbecco's modified Eagle's medium and one part Ham's F12 medium (both from Life Technologies, Inc.) supplemented with 4 mmol/l L-glutamine and 50 IU/ml penicillin or streptomycin (both from Life Technologies, Inc.), 24.3 $\mu\text{g/ml}$ adenine (Calbiochem), 1 mg/ml L-serine and 2 $\mu\text{g/ml}$ L-carnitine (both from Sigma), bovine serum albumin lipid mix (25 $\mu\text{mol/l}$ palmitic acid, 7 $\mu\text{mol/l}$ arachidonic acid, 15 $\mu\text{mol/l}$ linoleic acid, and 0.4 $\mu\text{g/ml}$ vitamin E; all from Sigma), 1 $\mu\text{mol/l}$ hydrocortisone (Merck KGaA), and 50 $\mu\text{g/ml}$ ascorbic acid, 0.1 $\mu\text{mol/l}$ insulin, 1.36 ng/ml triiodothyronine, 10^{-10} mmol/l cholera toxin, 5 ng/ml keratinocyte growth factor, and 2 ng/ml epidermal growth factor (all from Sigma). Y-27632 was supplemented in the culture medium at indicated culture periods and concentrations.

Cytokine stimulation

Liquid nitrogen-stored primary adult keratinocytes or Y-27632-treated adult keratinocytes (passage 6) were cultured to confluency in keratinocyte growth medium (KGM), consisting of KBM (0.15 mM Ca^{2+} BioWhittaker, Verviers, Belgium) supplemented with ethanolamine (0.1 mM; Sigma), phosphoethanolamine (0.1 mM, Sigma), bovine pituitary extract (0.4% vol/vol; BioWhittaker) epidermal growth factor (10 ng/ml; Sigma), insulin (5 $\mu\text{g/ml}$; Sigma), hydrocortisone (0.5 $\mu\text{g/ml}$; Collaborative Research, Lexington, MA), penicillin (100 U/ml; Life Technologies, Inc), and streptomycin (100 $\mu\text{g/ml}$; Life Technologies, Inc.), with different concentrations of Y-27632. Cells were switched to KGM depleted of

growth factors (bovine pituitary extract, epidermal growth factor, hydrocortisone, and insulin) for 48 hours. Differentiating cell cultures were stimulated with pro-inflammatory cytokines IL-1 α (30 ng/ml), TNF- α (30 ng/ml) and interferon- γ (500 U/ml) (all from Preprotech, London, UK), or left untreated. After 48 hours the cells were harvested for mRNA isolation using Trizol reagent (Life Technologies, Inc.).

Psoriatic skin equivalents were generated by stimulating HSEs during the last three days of the air-liquid interface culture with a mixture of IL-1 α (10 ng/ml) and TNF- α (5 ng/ml) and IL-6 (5 ng/ml) (all from Preprotech), as described previously¹².

Lentiviral vector production

For generation of recombinant lentiviral particles, we used the third-generation self-inactivating transfer vector pRLL-cPPT-PGK-GFP-PRE-SIN (kind gift from Dr F. van de Loo, Department of Rheumatology, Radboud University Medical Centre Nijmegen. See Geurts *et al.*²⁷ for details on plasmids and cells used for virus production). Packaging of VSV-G pseudotyped viruses was performed by transient transfection of 293T cells. 293T cells were seeded in a T225 flask at 1×10^5 cells/cm² in DMEM (Life Technologies, Inc.) supplemented with 10% bovine calcs serum (BCS, Hyclone), 100 μ g/ml penicillin (Life Technologies, Inc.), 100 μ g/ml streptomycin (Life Technologies, Inc.), 1 mM sodium pyruvate (Sigma) and 0.01 mM water-soluble cholesterol (Sigma). At least one hour prior transfection, the medium was replaced with 24 ml DMEM supplemented with 10% BCS, 1 mM sodium pyruvate and 0.01 mM water-soluble cholesterol. For each flask the following DNA mixture was prepared containing 56.7 μ g transfer vector, 42.3 μ g packaging vector pMDL-g/p-RRE, 20.0 μ g expression vector pHIT-G and 14.2 μ g expression vector pRSV-REV in a final volume of 100 μ l water. Subsequently 1.5 ml 0.5 M CaCl₂ (Sigma) was added and 1.5 ml 2xHBSS (Hepes-buffered saline solution, Sigma) was added gently under constant mixing. The formed precipitates were immediately added to the cells. 16 hours after transfection the medium was refreshed with DMEM supplemented with 100 μ g/ml penicillin, 100 μ g streptomycin and 1 mM sodium pyruvate. 48 hours post transfection the virus-containing supernatant was filtered through a 0.45 μ m Stericup (Millipore) to remove cell debris. Recombinant lentiviral particles were concentrated to 1.5 ml and dialyzed against sterile PBS using an Amicon filter (MWCO 100 kDa, Millipore). Viral stocks are aliquoted and stored at -80 °C. Viral titers were determined using an enzyme-linked immunosorbent assay (ELISA) kit (Abbott) targeting the viral envelope protein p24^{gag} and expressed as ng p24/ μ l.

Lentiviral transduction of adult keratinocytes

Primary adult keratinocytes from three different donors were grown to 40% confluency in a 6-wells plate using KGM medium (Lonza) supplemented or not with 10 μ M Y-27632. Subsequently, each well was incubated with 2 μ g of eGFP-lentivirus for 4 hours after which the cells were washed twice with sterile PBS. After 24 hours of recovery in KGM supplemented or not with 10 μ M Y-27632, cells

were harvested with trypsin-EDTA and washed twice using PBS. The percentage of eGFP positive keratinocyte was analyzed by flow cytometry (EPICS Elite flow cytometer, Coulter, Luton, UK).

To generate eGFP-transduced HSEs, 1.5×10^5 harvested keratinocytes were seeded onto DED in 24-wells inserts and HSEs were generated as described above with 10 μ M Y-27632 supplemented during the submerged phase of the HSE culture as indicated.

Quantitative real-time PCR

For the skin equivalents, epidermis was separated by dispase (Roche Diagnostics, Mannheim, Germany) treatment for 2 hours at 4°C, and total RNA was isolated from the epidermis using Trizol reagent (Life Technologies, Inc.) and subsequent RNeasy mini kit (Qiagen Benelux B.V.) according to manufacturers specifications. cDNA was generated and used for quantitative real-time PCR (qPCR), which was performed with the MyiQ Single-Colour Real-Time Detection System for quantification with Sybr Green and melting curve analysis (Bio-Rad Laboratories, Inc) as previously described²⁸. Primers for KRT10, KRT14, INV, LOR, Ki-67, FLG, TGM1, LCE3E, hBD-2, TNF- α , IL-8, IL-1 β , and the housekeeping gene human acidic ribosomal phosphoprotein P0 (RPLP0) were obtained from Bioglegio (Malden, The Netherlands). Relative mRNA expression levels of all examined genes were measured using the method described by Livak *et al.*²⁹. See Table 5.1 for primer sequences.

Morphological and immunohistochemical analysis

HSEs were fixed in buffered 4% formalin for 4 hours, processed for routine histology and embedded in paraffin. 6- μ m sections were stained with heamatoxylin and eosin (H&E) (Sigma) or processed for immunohistochemical staining using an indirect immunoperoxidase technique with avidin-biotin complex enhancement (Vectastain Laboratories, Burlingame, CA, USA). To study epidermal proliferation, an antibody directed against Ki-67 (1:50; MIB-1; Dako, Denmark) was used whereas epidermal differentiation was studied using antibodies directed against cytokeratin 10 (1:100; Sanbio, Uden, The Netherlands), cytokeratin 14 (1:50, Novocastra, UK), involucrin (1:50; Mon150; Sanbio), loricrin (1:500; BAbCO, Richmond, CA, USA), filaggrin (1:200; Novocastra), transglutaminase 1 (1:200, Santa Cruz) and late cornified envelope 2 (LCE2; 1:1000, See Bergboer *et al.*³⁰). The stress or psoriatic marker, hBD-2, was stained using goat anti-hBD-2 polyclonal serum (1:100; Abcam, Cambridge, UK) and SKALP/elafin was stained using polyclonal antibodies as described previously³¹. Detection by 3-amino-9-ethylcarbazole (Calbiochem) was followed by nuclei counterstaining with Mayer's hematoxylin solution (Sigma), and sections were mounted using glycerol gelatin (Sigma).

Statistics

Statistical significance was determined using paired two-tailed Student's *t* test.

Table 5.1 Primer sequences of all genes examined by qPCR

HUGO gene symbol	Description of gene/protein. In parentheses: name used in text	Forward primer (5'→3')	Reverse primer (5'→3')	E*
<i>KRT10</i>	Keratin 10, KRT10, (K10)	tggtcaatgaaaagagcaagga	gggattgtttcaaggccagt	1.93
<i>KRT14</i>	Keratin 14, KRT14, (K14)	ggcctgctgagatcaagaactac	cactgtggctgtgagaacttgtt	1.93
<i>MKI67</i>	Ki-67, (Ki-67)	aaaccaacaagaggaaacacaaait	gtctggagcgcagggatattc	2.21
<i>IVL</i>	Involucrin, (IVL)	actatttcgggtccgctaggt	gagacatgtagaggagacagagtcaag	1.93
<i>TGM1</i>	Transglutaminase 1, (TGM1)	ccccgcgaatgagatctaca	atcctcatggttccacgfacaca	1.99
<i>LOR</i>	Loricrin, (LOR)	aggftaagacatgaaggattgcaa	ggcaccgatgggcttagag	2.08
<i>FLG</i>	Filaggrin, (FLG)	actcaactgagtcttctctgatggtatt	toccagactgagggtcttttctcg	1.89
<i>LCE3E</i>	Late cornified envelope 3E, (LCE3E)	ctgatgctgagacaa-gcgatctt	gatccccacag gaaaaacct	2.20
<i>DEFB4</i>	Human β -defensin-2, (hBD-2)	gatgcctctccagggtgtttt	ggatgacatattggctccacttt	1.99
<i>IL8</i>	Interleukin 8, (IL-8), CXCL8	ctggcagcctctctgatt	ttcttagcactctctggcaaaa	2.11
<i>TNF</i>	Tumor necrosis factor alpha, (TNF)	ttctctgaacccccgagtga	cctctgatggcaccaccag	2.00
<i>IL1B</i>	Interleukin 1 beta, (IL1B)	aatctgtacctgtctcctcggtgt	tgggtaatttttgggatctacactct	2.19
<i>RPLP0</i>	Ribosomal phosphoprotein P0 (RPLP0)	caccattgaaatctctgagtgt	tgaccgcccaaaaggagaag	2.02

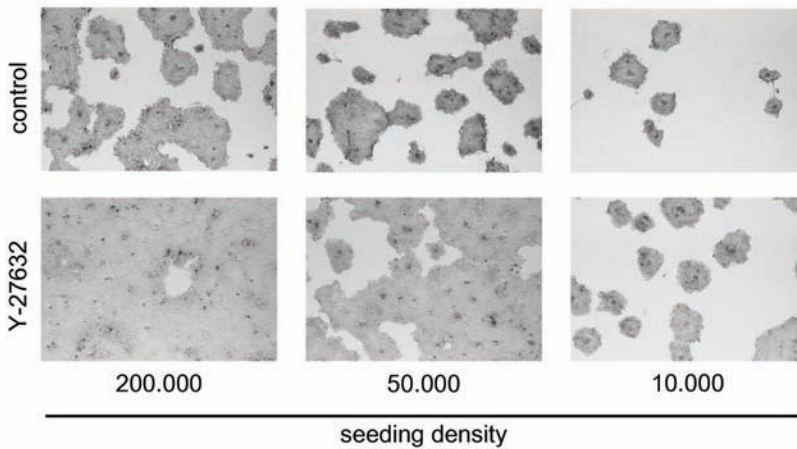
* E is efficiency as fold increase in fluorescence per PCR cycle

Acknowledgments

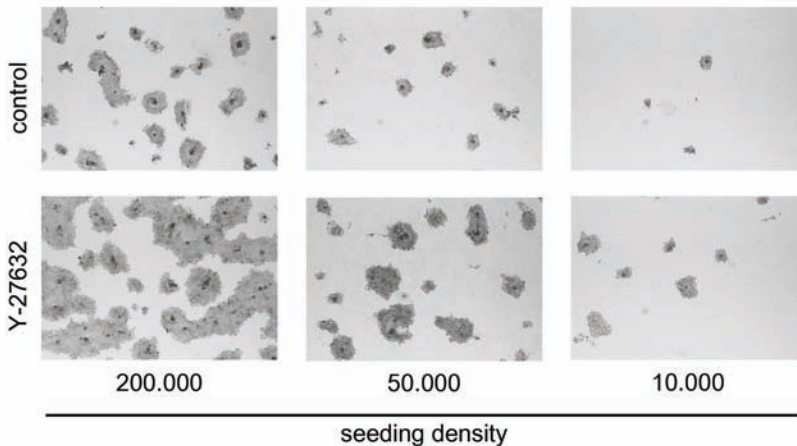
This work was supported by a grant from the Nijmegen Institute for Infection, Inflammation, and Immunity (N4i), Radboud University Nijmegen Medical Centre, The Netherlands. JS and PLJMZ are supported by The Alternatives to Animal Experiments programme of ZonMW grant (number 114000084) and PLJMZ by a Horizon Breakthrough grant from the Netherlands Genomics Initiative (number 93519004).

Supplementary information

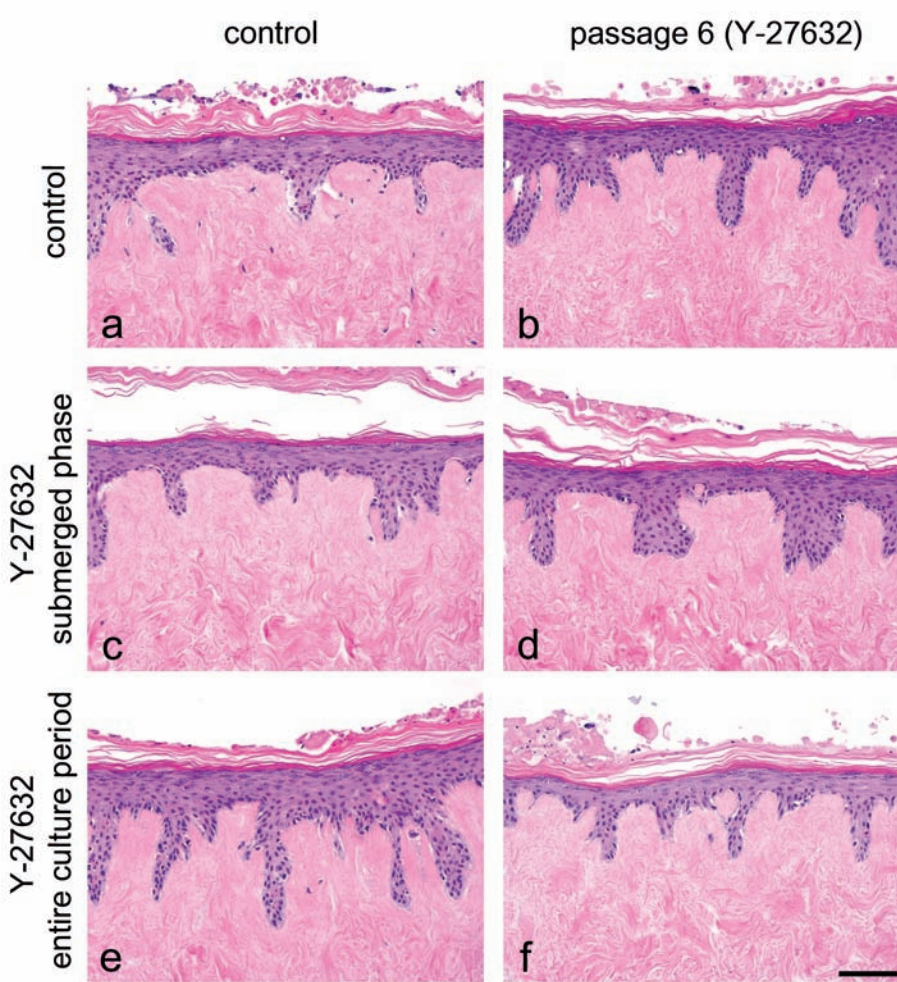
a



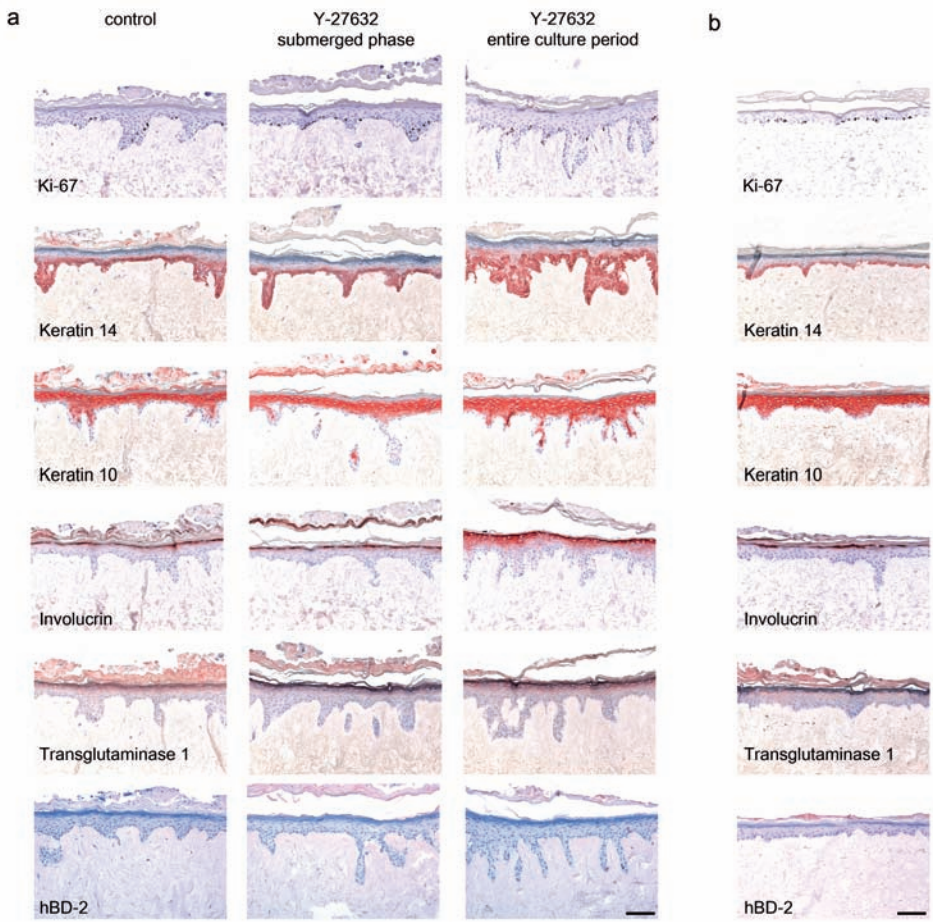
b



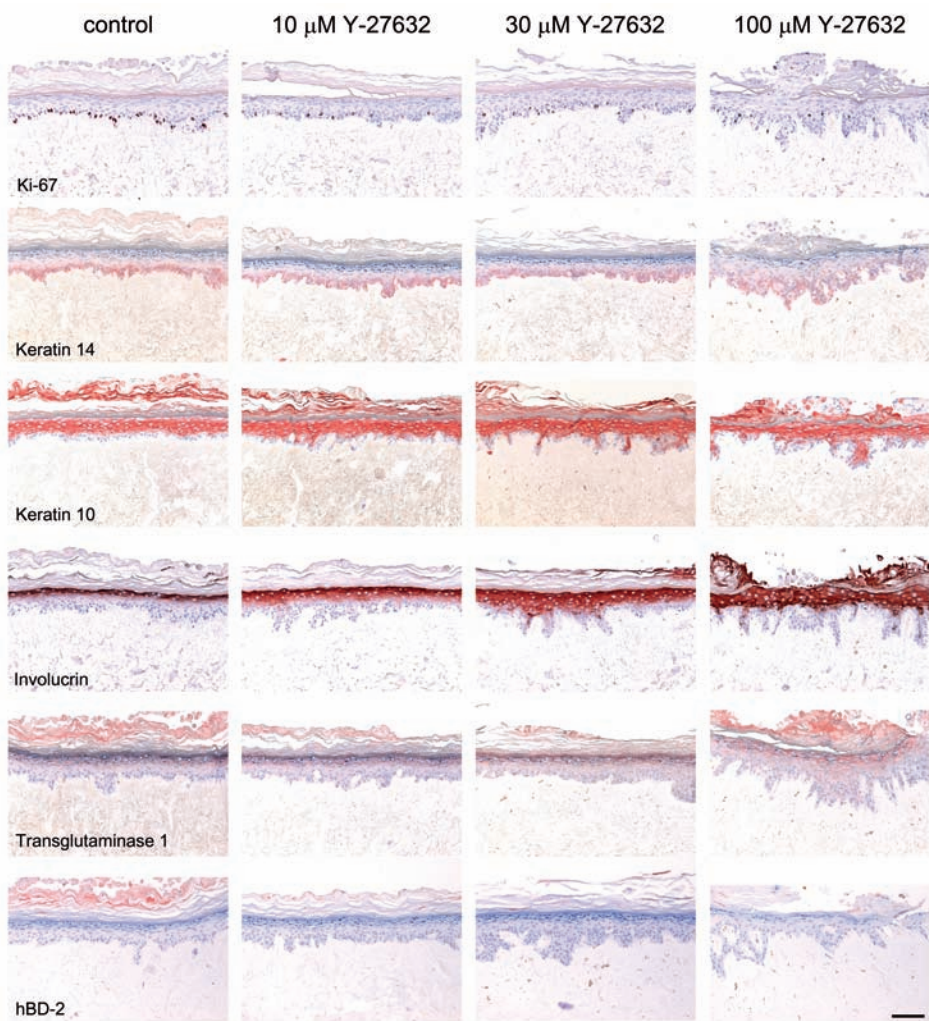
Supplemental figure 5.1 Effects of Y-27632 on cloning efficiency. Effects of Y-27632 on cloning efficiency of (a) liquid nitrogen-stored keratinocytes compared to (b) freshly isolated keratinocytes. Keratinocytes were cultured in the presence or absence of 10 μ M Y-27632 and images were taken after Rhodanile blue staining.



Supplemental figure 5.2 Epidermal morphology of human skin equivalents (HSEs) generated from Y-27632-treated keratinocytes. Primary adult keratinocytes (control) and passage 6, Y-27632-treated keratinocytes cultured on de-epidermised dermis without Y-27632 (a and b), with 10 μ M Y-27632 supplemented during the submerged phase (c and d) or during the entire culture period (e and f) of HSE development show a fully differentiated epidermis with a *stratum granulosum* and cornified layer with superior morphology in HSEs generated with Y-27632 supplemented during the submerged phase. Scale bar, 100 μ m.



Supplemental figure 5.3 Epidermal differentiation patterns in human skin equivalents (HSEs)
 Epidermal differentiation patterns in HSEs generated from (a) primary adult keratinocytes with 10 μM Y-27632 supplemented during HSE development and (b) HSEs generated from high passage, Y-27632-treated adult keratinocytes with 10 μM Y-27632 supplement only during the submerged phase of HSE development. HSEs show normal expression patterns for all analyzed epidermal markers: Ki-67 (proliferative cells), keratin 14 (basal keratinocytes), keratin 10 (suprabasal keratinocytes) and involucrin and transglutaminase 1 (terminal differentiation). HSEs are negative for the stress/psoriatic marker, human beta defensin-2 (hBD-2). Scale bar, 100 μm.



Supplemental figure 5.4 Epidermal differentiation patterns in human skin equivalents (HSEs) generated in the presence of 10, 30 or 100 μM Y-27632. HSEs show normal expression patterns for epidermal markers: Ki-67 (proliferative cells), keratin 14 (basal keratinocytes), keratin 10 (supra-basal keratinocytes) and transglutaminase 1 (terminal differentiation). Involucrin expression (terminal differentiation) is slightly extended towards the *stratum spinosum* at 30 and 100 μM Y-27632. HSEs are negative for the stress/psoriatic marker, human beta defensin-2 (hBD-2). Scale bar, 100 μm.

References

1. Gibbs S, van den Hoogenband HM, Kirtschig G, Richters CD, Spiekstra SW, Breetveld M *et al.* Autologous full-thickness skin substitute for healing chronic wounds. *Br J Dermatol* 155, 267-274 (2006)
2. Bilousova G, Chen J, Roop DR. Differentiation of mouse induced pluripotent stem cells into a multipotent keratinocyte lineage. *J Invest Dermatol* 131, 857-864 (2011)
3. Terunuma A, Limgala RP, Park CJ, Choudhary I, Vogel JC. Efficient procurement of epithelial stem cells from human tissue specimens using a Rho-associated protein kinase inhibitor Y-27632. *Tissue Eng Part A* 16, 1363-1368 (2010)
4. Chapman S, Liu X, Meyers C, Schlegel R, McBride AA. Human keratinocytes are efficiently immortalized by a Rho kinase inhibitor. *J Clin Invest* 120, 2619-2626 (2010)
5. Vaezi A, Bauer C, Vasioukhin V, Fuchs E. Actin cable dynamics and Rho/Rock orchestrate a polarized cytoskeletal architecture in the early steps of assembling a stratified epithelium. *Dev Cell* 3, 367-381 (2002)
6. Tu CL, Chang W, Bikle DD. The calcium-sensing receptor-dependent regulation of cell-cell adhesion and keratinocyte differentiation requires Rho and filamin A. *J Invest Dermatol* 131, 1119-1128 (2011)
7. Sarkar S, Egelhoff T, Baskaran H. Insights into the roles of non-muscle myosin IIA in human keratinocyte migration. *Cell Mol Bioeng* 2, 486-494 (2009)
8. Jackson B, Peyrollier K, Pedersen E, Basse A, Karlsson R, Wang Z *et al.* RhoA is dispensable for skin development, but crucial for contraction and directed migration of keratinocytes. *Mol Biol Cell* 22, 593-605 (2011)
9. Liebig T, Erasmus J, Kalaji R, Davies D, Loirand G, Ridley A *et al.* RhoE Is required for keratinocyte differentiation and stratification. *Mol Biol Cell* 20, 452-463 (2009)
10. McMullan R, Lax S, Robertson VH, Radford DJ, Broad S, Watt FM *et al.* Keratinocyte differentiation is regulated by the Rho and ROCK signaling pathway. *Curr Biol* 13, 2185-2189 (2003)
11. Lock FE, Hotchin NA. Distinct roles for ROCK1 and ROCK2 in the regulation of keratinocyte differentiation. *PLoS One* 4, e8190 (2009)
12. Tjabringa G, Bergers M, van Rens D, de Boer R, Lamme E, Schalkwijk J. Development and validation of human psoriatic skin equivalents. *Am J Pathol* 173, 815-823 (2008)
13. El-Ghalbzouri A, Gibbs S, Lamme E, Van Blitterswijk CA, Ponc M. Effect of fibroblasts on epidermal regeneration. *Br J Dermatol* 147, 230-243 (2002)
14. El-Ghalbzouri A, Commandeur S, Rietveld MH, Mulder AA, Willemze R. Replacement of animal-derived collagen matrix by human fibroblast-derived dermal matrix for human skin equivalent products. *Biomaterials* 30, 71-78 (2009)
15. Liu X, Ory V, Chapman S, Yuan H, Albanese C, Kallakury B *et al.* ROCK Inhibitor and Feeder Cells Induce the Conditional Reprogramming of Epithelial Cells. *Am J Pathol* (2011)
16. Zhang L, Valdez JM, Zhang B, Wei L, Chang J, Xin L. ROCK inhibitor Y-27632 suppresses dissociation-induced apoptosis of murine prostate stem/progenitor cells and increases their cloning efficiency. *PLoS One* 6, e18271 (2011)
17. Gauthaman K, Fong CY, Bongso A. Effect of ROCK inhibitor Y-27632 on normal and variant human embryonic stem cells (hESCs) in vitro: its benefits in hESC expansion. *Stem Cell Rev* 6, 86-95 (2010)

18. Ishizaki T, Uehata M, Tamechika I, Keel J, Nonomura K, Maekawa M *et al.* Pharmacological properties of Y-27632, a specific inhibitor of rho-associated kinases. *Mol Pharmacol* 57, 976-983 (2000)
19. Guttman-Yassky E, Nograles KE, Krueger JG. Contrasting pathogenesis of atopic dermatitis and psoriasis-part I: clinical and pathologic concepts. *J Allergy Clin Immunol* 127, 1110-1118 (2011)
20. van Ruissen F, de Jongh GJ, Zeeuwen PL, van Erp PE, Madsen P, Schalkwijk J. Induction of normal and psoriatic phenotypes in submerged keratinocyte cultures. *J Cell Physiol* 168, 442-452 (1996)
21. Kamsteeg M, Bergers M, de BR, Zeeuwen PL, Hato SV, Schalkwijk J *et al.* Type 2 helper T-cell cytokines induce morphologic and molecular characteristics of atopic dermatitis in human skin equivalent. *Am J Pathol* 178, 2091-2099 (2011)
22. OECD. In Vitro skin Irritation: Reconstructed Human Epidermis test Method, OECD Guideline for testing of chemicals No. 439 available at: www.oecdbookshop.org (2004)
23. OECD. In Vitro skin Corrosion: Human Skin Model Test, OECD Guideline for testing of chemicals No. 431 Available at: www.oecdbookshop.org (2010)
24. Hanakawa Y, Shirakata Y, Nagai H, Yahata Y, Tokumaru S, Yamasaki K *et al.* Cre-loxP adenovirus-mediated foreign gene expression in skin-equivalent keratinocytes. *Br J Dermatol* 152, 1391-1392 (2005)
25. Mildner M, Jin J, Eckhart L, Kezic S, Gruber F, Barresi C *et al.* Knockdown of filaggrin impairs diffusion barrier function and increases UV sensitivity in a human skin model. *J Invest Dermatol* 130, 2286-2294 (2010)
26. van Gele M, Geusens B, Speeckaert R, Dynoodt P, Vanhoecke B, Van Den BK *et al.* Development of a 3D pigmented skin model to evaluate RNAi-induced depigmentation. *Exp Dermatol* 20, 773-775 (2011)
27. Geurts J, Joosten LA, Takahashi N, Arntz OJ, Gluck A, Bennink MB *et al.* Computational design and application of endogenous promoters for transcriptionally targeted gene therapy for rheumatoid arthritis. *Mol Ther* 17, 1877-1887 (2009)
28. de Jongh GJ, Zeeuwen PL, Kucharekova M, Pfundt R, van der Valk PG, Blokx W *et al.* High expression levels of keratinocyte antimicrobial proteins in psoriasis compared with atopic dermatitis. *J Invest Dermatol* 125, 1163-1173 (2005)
29. Livak KJ, Schmittgen TD. Analysis of relative gene expression data using real-time quantitative PCR and the 2(-Delta Delta C(T)) Method. *Methods* 25, 402-408 (2001)
30. Bergboer JG, Tjabringa GS, Kamsteeg M, van Vlijmen-Willems IM, Rodijk-Olthuis D, Jansen PA *et al.* Psoriasis risk genes of the late cornified envelope-3 group are distinctly expressed compared with genes of other LCE groups. *Am J Pathol* 178, 1470-1477 (2011)
31. Wingens M, van Bergen BH, Hiemstra PS, Meis JF, van Vlijmen-Willems IM, Zeeuwen PL *et al.* Induction of SLPI (ALP/HUSI-I) in epidermal keratinocytes. *J Invest Dermatol* 111, 996-1002 (1998)

Cystatin M/E knockdown by lentiviral delivery of shRNA impairs epidermal morphogenesis in a human skin equivalent

6
CHAPTER

Patrick AM Jansen^{1,2*}

Ellen H van de Bogaard^{1-3*}

Ferry FJ Kersten^{1,2}

Corien Oostendorp¹

Ivonne MJJ van Vlijmen-Willems¹

Vinzenz Oji⁴

Heiko Traupe⁴

Hans C Hennies^{5,6}

Joost Schalkwijk¹⁻³

Patrick LJM Zeeuwen¹⁻³

¹ Department of Dermatology, Radboud University Nijmegen Medical Centre, The Netherlands

² Nijmegen Centre for Molecular Life Sciences (NCMLS), Nijmegen, The Netherlands

³ Nijmegen Institute for Infection, Inflammation and Immunity (N4i), Nijmegen, The Netherlands

⁴ Department of Dermatology, University Hospital, Münster, Germany

⁵ Cologne Center for Genomics and Cologne Cluster of Excellence on Cellular Stress Responses in Aging-associated Diseases, University of Cologne, Cologne, Germany

⁶ Division of Human Genetics and Department of Dermatology, Medical University of Innsbruck, Innsbruck, Austria.

* Contributed equally to this manuscript

Abstract

The protease inhibitor cystatin M/E regulates a biochemical pathway involved in *stratum corneum* homeostasis, and its deficiency in mice causes ichthyosis and neonatal lethality. Cystatin M/E deficiency has not been described in humans so far, and we did not detect disease-causing mutations in the cystatin M/E (*CST6*) gene in a large number of patients with autosomal recessive congenital ichthyosis (ARCI), who were negative for mutations in known ichthyosis-associated genes. To investigate the phenotype of cystatin M/E deficiency in human epidermis, we used lentiviral delivery of short hairpin RNAs that target cystatin M/E in a 3D reconstructed skin model. Knockdown of cystatin M/E expression did not lead to the expected ichthyosis-like phenotype, but prevented the development of a multilayered epidermis. The phenotypic discrepancy between mouse and human may be explained by the differences in specificity of cystatin M/E towards one of the target proteases (legumain), differences between the mouse and human cathepsin L orthologues or the presence of cathepsin V, a paralogous gene of cathepsin L that is absent in mice.

Introduction

Cystatin M/E (*CST6*) is a cysteine protease inhibitor that exerts regulatory and protective functions against uncontrolled proteolysis by the cysteine proteases cathepsins L and V (*CTSL*, *CTSV*) and the asparaginyl endopeptidase legumain (*LGMM*)^{1,2}. Cystatin M/E deficient mice display a hyperplastic, hyperkeratotic epidermis^{3,4} and die shortly after birth of dehydration, due to a disturbed skin barrier function⁵. Based on this phenotype we considered *CST6* as a candidate gene for human disorders of cornification with unknown etiology. We have performed mutation analysis for 106 autosomal recessive congenital ichthyosis (ARCI) patients, who were negative for mutations in known ichthyosis-associated genes. (Table 6.1), however no disease-causing mutations in the *CST6* gene were found⁶.

By generating several double knockout mouse models, we recently showed that a tightly regulated balance between cathepsin L and cystatin M/E is essential for tissue integrity of the epidermis, but also for maintenance of healthy hair follicles and corneal epithelium⁷. Considering this, we have screened three patients with ichthyosis follicularis with atrichia and photophobia (IFAP syndrome, MIM 308205) and one patient with keratosis pilaris (KP, MIM 604093) for mutations in the *CST6* gene (Table 6.1). However, no mutations were found in the *CST6* exons or exon/intron boundaries. Besides, the cystatin M/E protein expression in the skin of these patients were normal. We also performed mutation analysis in one patient with ichthyosis follicularis with photophobia (IFAP) syndrome, who presented with whorled follicular keratosis and focal scarring alopecia and in addition showed punctate corneal lesions of the eyes⁸, that resembled the phenotype of our *Cst6*^{-/-}*Ctsl*^{+/-} mice⁷. Again, we found no mutations in the *CST6* gene and also Multiplex Ligation-dependent Probe Amplification (MLPA) on the patient's DNA and its parents revealed no genomic deletions or insertions.

Even though no human patients with *CST6* mutations were found so far, we hypothesized that cystatin M/E deficiency in humans, like our mouse models, would lead to an ichthyosis-like phenotype. In the current study, we attempted to uncover the human skin phenotype of cystatin M/E deficiency by knockdown of the *CST6* gene in primary human keratinocytes by RNA interference using lentiviral vectors. These lentiviral-infected keratinocytes were subsequently

Table 6.1 Patients screened for *CST6* mutations

Diagnosis	Nijmegen	Munster	Cologne	Total
Ichthyosis (ARCI)	5*	13*	88**	106
Keratosis Pilaris	1	-	-	1
IFAP syndrome	2	1	-	3
IFAP syndrome with corneal lesions	1	-	-	1

* Negative for mutations in TGM1

** Negative for mutations in TGM1, ALOX12B, ALOXE3, NIPAL4 and CYP4F22

used to generate human skin equivalents, to study the pathway of epidermal differentiation and *stratum corneum* formation in which cystatin M/E is thought to play a crucial role (Figure 6.1). Surprisingly, cystatin M/E deficiency did not cause an ichthyosis-like phenotype but interfered with epidermal morphogenesis.

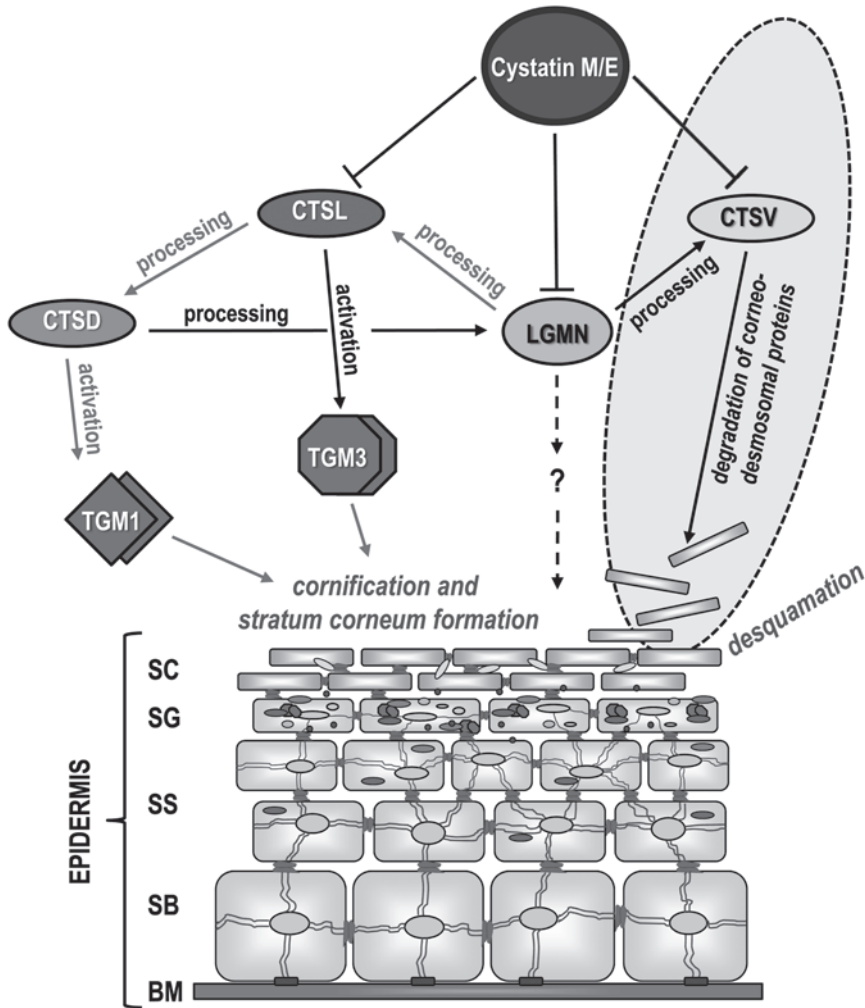


Figure 6.1 Regulation of epidermal protease activity by cystatin M/E. Regulation of epidermal protease activity by cystatin M/E in processes that control epidermal cornification and desquamation based on *in vivo* (mouse) and *in vitro* (human) studies^{2,7}. Inhibition of legumain (LGMN) regulates the processing of (pro)-cathepsins. Inhibition of cathepsin V (CTSV) regulates desquamation, as CTSV is able to degrade (corneo)-desmosomal proteins like desmoglein-1, desmocollin-1, and corneodesmosin. Inhibition of human cathepsin L (CTSL) activity by cystatin M/E is important in the cornification process, as CTSL is the elusive processing and activating enzyme for transglutaminase-3 (TGM3). CTSL is also able to process cathepsin D (CTSD), which in turn can activate transglutaminase-1 (TGM1). As CTSV is only expressed in humans (shaded oval), murine CTSL probably controls the specific functional enzymatic activities of both human CTSL and CTSV. Solid lines represent biochemical functions that are known from literature (grey) or deduced from our studies (black). Dashed lines represent unknown functions. BM, basal membrane; SB, *stratum basale*; SS, *stratum spinosum*; SG, *stratum granulosum*; SC, *stratum corneum*.

Results

Mutation analysis

An overview of all sequenced patients that were considered as candidates for *CST6* mutations are listed in Table 6.1.

Validation of lentiviral shRNA constructs for cystatin M/E knockdown

Primary human keratinocytes were infected with lentiviruses that were engineered to produce shRNAs that suppress the expression cystatin M/E. shRNA-CST6 (nos. 1-4) and controls (no virus and scrambled sequence) were first examined in submerged keratinocyte cultures. qPCR analysis revealed a strong reduction (80-90%) at the mRNA level for all designed shRNAs (2 μ g of virus/well), when compared to the scrambled “mock” control (Figure 6.2a).

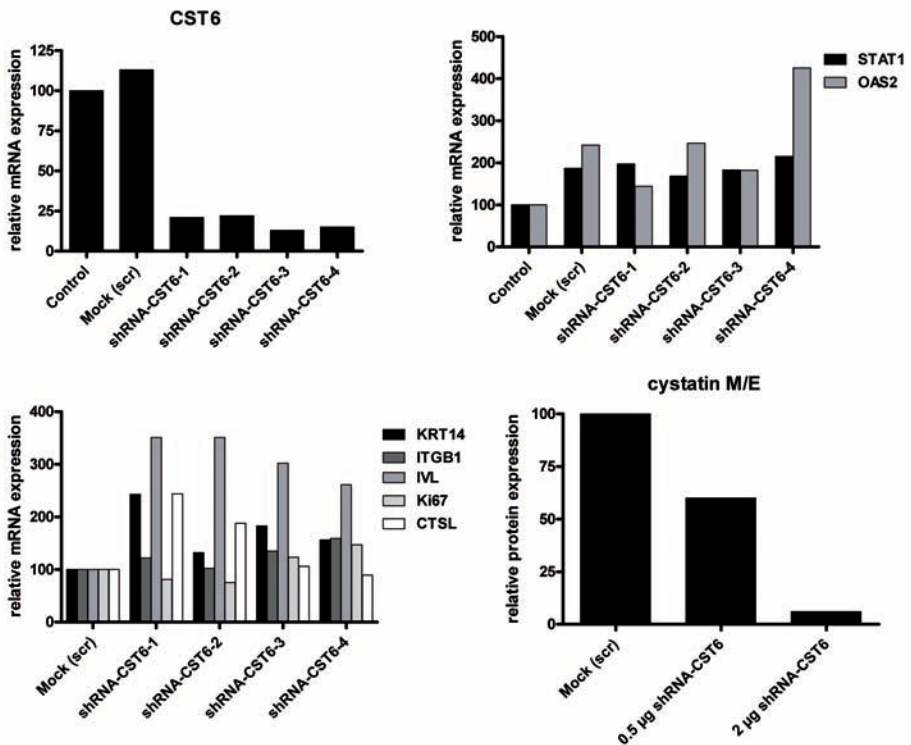


Figure 6.2 Validation of lentiviral expressed shRNAs to knockdown cystatin M/E. (a) Lentiviral (2 μ g/well) infection of monolayers with cultured primary human keratinocytes revealed that all four designed shRNAs significantly reduce the *CST6* mRNA expression. (b) *STAT1* and *OAS2* both showed slightly increased mRNA levels (not significant), as the control (no virus) was compared to the lentiviral infected keratinocytes. The mock control and shRNA-CST6 nos. 1-3 showed comparable levels of these interferon response genes. (c) Genes that are normally expressed in the basal layer (*ITGB1*, *KRT14*), all epidermal layers (*CTSL*) or are known as proliferation specific (*MKI67*), were not drastically affected by knockdown of the *CST6* gene. Only the expression of the *IVL* gene (supra-basal layer) was slightly increased. (d) Cystatin M/E protein knockdown was confirmed by ELISA on cell extracts of lentiviral infected keratinocytes.

Potential off-target effects including interferon activation due to gene knockdown by siRNA delivery must be checked^{9,10}, especially since keratinocytes are sensitive to interferon stimulation¹¹. Therefore, two genes that indicate an interferon response (*STAT1* and *OAS2*) were analyzed by qPCR (Figure 6.2b). The scrambled control showed a small increase (2-fold) for *STAT1* and *OAS2* expression levels. Three shRNA-*CST6* constructs (nos. 1-3) showed no differences in mRNA expression levels when compared to the mock control. shRNA-*CST6*-4, however, showed a 2-fold increase in *OAS2* mRNA expression when compared to the mock control, and a 4-fold increase when compared to the cultured cells that were not infected with virus.

In addition, we checked if infection with lentiviral shRNA-*CST6* constructs and subsequent knockdown of cystatin M/E showed off-target effects or exert influence on the expression level of other genes that are known to be expressed in human epidermis (Figure 6.2c). All shRNA-*CST6* constructs showed comparable levels (~2-fold induction) of gene expression for cathepsin L (physiologic target protease for cystatin M/E), the antigen identified by monoclonal antibody Ki-67 (proliferation marker), and β 1-integrin and keratin 14 (both expressed in the basal layer of the epidermis). Only involucrin (expressed in the suprabasal layers) showed a slight increased expression (approximately 3-fold) for all used shRNA-*CST6* lentiviral constructs, and was hence not considered to be an off-target effect but a genuine result of *CST6* knockdown. After we validated cystatin M/E knockdown at the protein level (Figure 6.2d), we used the shRNA-*CST6*-1 and shRNA-*CST6*-3 lentiviral constructs for knockdown studies of cystatin M/E in a 3D reconstructed skin model.

Cystatin M/E knockdown impairs epidermis formation in a human skin equivalent

The effect of cystatin M/E knockdown on the development and morphology of human skin equivalents was evaluated by histological analysis. A fully differentiated epidermis with a *stratum granulosum* and cornified layer is formed in the control and mock constructs (Figure 6.3a and b), whereas cystatin M/E knockdown with shRNA-*CST6*-1 and shRNA-*CST6*-3 completely disturbed the development of a multilayered epidermis (Figure 6.3c and d). From these skin equivalents no mRNA and protein could be extracted for respectively qPCR analyses and protease activity assays. Using lower concentrations of both viral constructs led to insufficient knockdown of cystatin M/E protein levels resulting in a normal epidermal development (shRNA-*CST6*-1) or a moderately disturbed (shRNA-*CST6*-3) morphology of the human skin equivalents (Figure 6.3e and f).

Discussion

In vitro biochemical approaches as well as the use of *in vivo* mouse models have revealed that cystatin M/E is a key molecule in a biochemical pathway that controls skin barrier formation by regulation of both crosslinking and desquamation of the *stratum corneum* (Figure 6.1). As cystatin M/E deficiency in mice causes

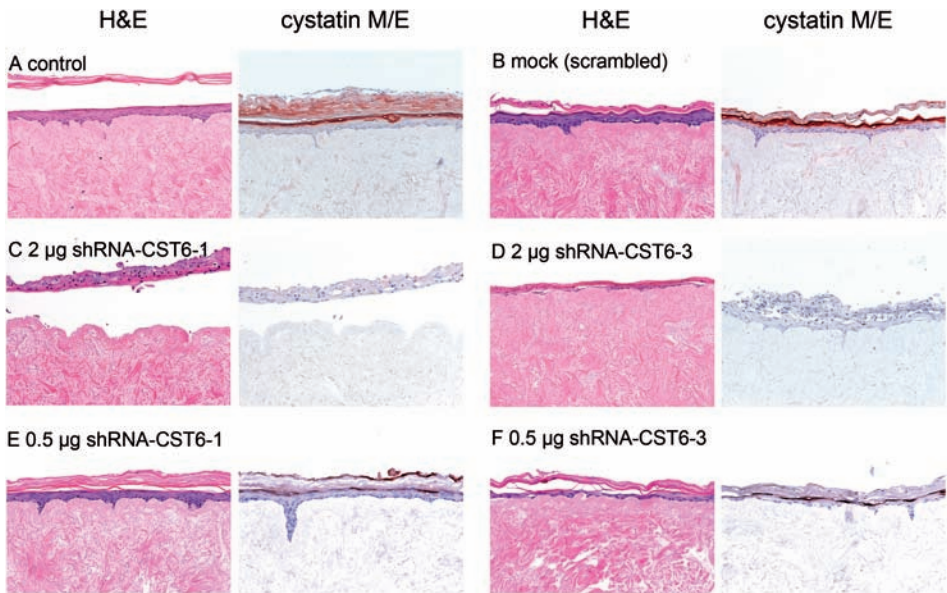


Figure 6.3 Cystatin M/E knockdown by lentiviral delivery of shRNA impairs epidermis formation in a human skin equivalent. Hematoxylin & Eosin staining showed the morphology of the human skin equivalents (left column). The control and mock (scrambled shRNA) showed a normal developed skin equivalent (a and b), whereas the formation of a multilayered epidermis is prevented by cystatin M/E knockdown (c and d). The use of lower shRNA-CST6 virus concentrations showed incomplete cystatin M/E knockdown (e and f). Scale bar: 100 μ m

ichthyosis, follicular hyperkeratosis and corneal abnormalities we first assumed that if *CST6* deficiency in humans exist the clinical symptoms might resemble the phenotype of the cystatin M/E deficient mice. We were, however, unable to find *CST6* mutations in a large number of patients with unexplained ichthyoses. Even in a patient with a phenotype that included ichthyosis and corneal abnormalities we did not find *CST6* mutations. In order to predict the epidermal phenotype of *CST6* deficiency in humans, we here examined the phenotype of cystatin M/E deficiency in human epidermis using *in vitro* 3D reconstructed skin equivalents. Surprisingly, we did not observe an expected ichthyosis-like phenotype, but rather an atrophic epidermis, which, we speculate, might lead to embryonic lethality in humans.

Recently, the use of synthetic siRNA or lentiviral-delivered transgenes has been described in reconstructed skin models^{12,13}. In pilot experiments with synthetic siRNAs directed against the *CST6* gene we have previously succeeded in gene-specific (>90%) knockdown of cystatin M/E at the protein level in a submerged culture system (unpublished data). Although delivery of synthetic siRNA has been used successfully in a 3D reconstructed skin model for several target genes^{13,14}, we found that this approach was not suitable for the *CST6* gene (data not shown). Therefore we decided to use lentiviral vectors for gene knockdown (by delivery of shRNA). We succeeded to design four shRNA-*CST6* constructs that resulted in a satisfying knockdown of cystatin M/E expression at the mRNA level as well as at

the protein level in submerged keratinocyte cultures. These lentiviral constructs did not induce significant changes in expression levels of genes that are known to be expressed in human epidermis. However, we detected a modest induction of *IVL* expression as a result of cystatin M/E deficiency. It is known that interferon- γ can stimulate human involucrin gene expression¹⁵, though we found no dramatic interferon responses compared to the mock control as measured by *STAT1* and *OAS2* mRNA expression levels. From this we conclude that the induction of *IVL* expression is a specific consequence of *CST6* knockdown, rather than an off-target effect^{16,17}.

Deficiency of cystatin M/E in 3D skin constructs resulted in an unexpected disturbance of epidermal development, which made it impossible to study the involvement of cystatin M/E in the pathway of epidermal differentiation and *stratum corneum* formation and maintenance. We were unable to extract epidermal proteins to study protease- and transglutaminase activity, nor could we measure consequences of cystatin M/E deficiency on the expression levels of genes involved in epidermal differentiation and cornification.

The phenotypic discrepancy between mouse and human may be explained by several factors. First, human legumain is strongly inhibited by human cystatin M/E, whereas mouse cystatin M/E is unable to inhibit legumain due to an aspartate residue (D64) in the proposed legumain inhibitory site instead of the important asparagine (N64)^{1,7}. Therefore we do not exclude that legumain has a function in human skin (e.g. processing of cathepsins) that is controlled directly by cystatin M/E, which might be essential for normal epidermal development. Furthermore, no orthologue of cathepsin V in mice has been discovered yet and differences exist between the mouse and human cathepsin L orthologues. In fact, human cathepsin V is phylogenetically more closely related to murine cathepsin L than to human cathepsin L¹⁸. Phenotypical differences between man and mice exist. For example, it was shown that cystatin A, a cysteine protease inhibitor like cystatin M/E found in the upper layers of the skin, has a role in cell-cell adhesion and loss-of-function mutations in *CSTA* underlie exfoliative ichthyosis¹⁹. However, no specific phenotype was observed in mice that lack the *Csta* gene²⁰.

The results of cystatin M/E knockdown in our reconstructed skin model showed an impaired epidermal morphogenesis rather than ichthyosis-like features. The lack of a well-formed suprabasal compartment precluded further analysis of the cystatin M/E regulated processes as we did before using our mouse models, e.g. *in situ* activities of transglutaminases and proteases⁷. From this study we conclude that cystatin M/E is indispensable for human skin development, and deficiency of this molecule may be incompatible with normal foetal development.

Materials and Methods

DNA samples

The study was conducted according to Declaration of Helsinki principles and approved by the medical ethical committee (Commissie Mensgebonden

Onderzoek Arnhem-Nijmegen), the ethical committee of the Medical Faculty of the University of Cologne, and the institutional review board of the University Hospital of Münster. In advance, approval and individual written informed consent were obtained.

Mutation analysis

Mutation analysis of all three *CST6* exons including exon/intron boundaries was performed in genomic DNA by direct sequencing of amplified DNA. Primers sequences and sequencing reactions are performed as described previously^{6,21}.

Keratinocyte isolation

Cells from the mouse fibroblast cell line 3T3 were cultured in Dulbecco's modified Eagle's medium (Life Technologies, Grand Island, NY) supplemented with 50 IU/ml penicillin/streptomycin (ICN Biomedicals, Zoetermeer, The Netherlands) and 10% calf serum with iron (Hyclone, Logan, UT). Keratinocytes were obtained from human abdominal skin derived from donors who underwent surgery for abdominal wall correction. After isolation by trypsin treatment for 16 to 20 hours at 4°C, keratinocytes were cultured in the presence of irradiated (3295 cGy for 4.10 minutes) cells from the 3T3 cell line. 3T3 cells were seeded at a concentration of 3×10^4 cells per cm^2 in Greens medium, which consisted of two parts Dulbecco's modified Eagle's medium (Life Technologies) and one part of Ham's F12 medium (Life Technologies) supplemented with 10% fetal bovine serum (Hyclone), 4 mmol/L L-glutamine (Life Technologies), 50 IU/ml penicillin/streptomycin (Life Technologies), 24.3 $\mu\text{g/ml}$ adenine (Calbiochem, San Diego, CA), 5 $\mu\text{g/ml}$ insulin (Sigma, St. Louis, MO), 0.4 $\mu\text{g/ml}$ hydrocortisone (Merck, Darmstadt, Germany), 1.36 ng/ml triiodothyronine (Sigma) and 10^{-10} mol/L cholera toxin (Sigma). The next day keratinocytes were added at a concentration of 5×10^4 cells per cm^2 . After three days, medium was replaced by Greens medium containing 10 ng/ml epidermal growth factor (EGF, Sigma). The cells were then refreshed every two to three days, and upon confluency, cells were trypsinized and stored in liquid nitrogen.

Lentiviral constructs

The generation of recombinant lentiviral particles were based on the third-generation self-inactivating transfer vector pRLL-cPPT-PGK-mcs-PRE-SIN in which the PGK promoter was replaced by the RNA polymerase III U6 promoter (referred as pSIN-U6) to allow expression of short hairpin RNAs (shRNAs) (a kind gift from Dr. Fons van de Loo, Department of Rheumatology, Radboud University Nijmegen Medical Centre, The Netherlands). A total of four different hairpins directed against the *CST6* gene were selected based on experiments with synthetic siRNAs that were transfected in keratinocytes (data not shown) and using the Block-It RNAi designer from Invitrogen (<https://rnaidesigner.invitrogen.com/rnaiexpress/>). Sequences for scrambled control hairpins were obtained from literature²². Table 6.2 shows location and sequence of the shRNA targets. Primers were designed containing the complete shRNA sequence followed by a polymerase III termination sequence. 40 μM of both primers were incubated in

Table 6.2 Primers used for construction of hairpins

shRNA	Position*	Orientation	Sequence**
CST6 shRNA1	nt 242	Forward	<u>TGGCAACAGCATCTACTACT</u> TCCTCCGAAGGAAGTAGTAGATGCTGTTGCTTTTTTATGCA
		Reverse	TAAAAAAGCAACAGCATCTACTACTTCCTTCGGGAAGTAGTAGATGCTGTTGCCA
CST6 shRNA2	nt 460	Forward	<u>TGCAGAACCTCCTCAGCTCCTA</u> CGAATAGGAGCTGAGAGGAGTTCTGTTTTTATGCA
		Reverse	TAAAAACAGAACTCCTCTCAGCTCCTATTTCGTAGGAGCTGAGAGGAGTTCTGCA
CST6 shRNA3	nt 263	Forward	<u>TGGAGACACGCATCATC</u> AGGCGAACCTTGATGATGTGCGTGTCTCTTTTTTATGCA
		Reverse	TAAAAAAGAGACACGCACATCATCAAGGTTCCGCCCTTGATGATGTGCGTGTCTCCA
CST6 shRNA4	nt 147	Forward	<u>TGGGAGCGCATGGT</u> CGGAGAACCTCGAAAGTTCTCCGACCATGCGCTCCTTTTTTATGCA
		Reverse	TAAAAAAGGAGCGCATGGTCCGAGAACCTTCGAGTTCTCCGACCATGCGCTCCCA
Scrambled (control)		Forward	TGCCTAAGGTTAAGTCCGCCCTCGCTCTAGCGAGGGCGACTTAACCTTAGGTTTTTATGCA
		Reverse	TAAAAAACCTAAGGTTAAGTCCGCCCTCGCTAGAGCGAGGGCGACTTAACCTTAGGCA

* Corresponds to the 5'-end of the shRNA

** CST6 target sequence is in bold and underlined

annealing buffer (10 mM Tris pH 8.0, 20 mM NaCl) at 95°C for 10 minutes and cooled down to room temperature overnight. The annealed primers, containing HpaI and NsiI compatible ends, were ligated into the HpaI/NsiI digested pSin-U6 vector with T4 DNA ligase (Invitrogen, Carlsbad, CA) and transformed into TOP10 cells (Invitrogen). Recombinant clones were selected on LB plates containing ampicillin (Invitrogen). Insertion of hairpins into pSin-U6 was confirmed by sequencing. Sequencing reactions were performed by the sequence facility of the Radboud University Nijmegen Medical Centre, based on the Sanger method using the BigDye Terminator version 3 chemicals (Applied Biosystems, Foster City, CA).

Lentiviral vector production

VSV-G pseudotyped lentiviruses were produced after transient transfection of 293T cells. Cells were seeded in a T225 flask at 1×10^5 cells/cm² in DMEM (Invitrogen) supplemented with 10% bovine calf serum (Hyclone), 100 µg/ml penicillin (Invitrogen), 100 µg/ml streptomycin (Invitrogen), 1 mM sodium pyruvate (Sigma) and 0.01 mM water-soluble cholesterol (Sigma). Prior to transfection, the media was replaced with 24 ml DMEM supplemented with 10% BCS, 1 mM sodium pyruvate and 0.01 mM water-soluble cholesterol. Per flask the following DNA mixture was prepared containing 56.7 µg transfer vector, 42.3 µg packaging vector pMDL-g/p-RRE, 20 µg expression vector pHIT-G and 14.2 µg expression vector pRSV-REV in a final volume of 100 µl water. The DNA was added to 1.5 ml 0.5 M CaCl₂ (Sigma) and subsequently 1.5 ml 2xHBSS (Hepes-buffered saline solution, Sigma) was added drop wise under constant stirring. The formed precipitates were added to the cells immediately afterwards. Sixteen hours post transfection the media was refreshed with DMEM supplemented with 100 µg/ml penicillin, 100 µg streptomycin and 1 mM sodium pyruvate. 48 hours post transfection the virus-containing supernatant was collected and cell debris was removed by filtration through a 0.45 µm Stericup (Millipore, Billerica, MA). Lentiviral particles were dialysed against PBS and concentrated to 1.5 ml using an Amicon filter (MWCO 100 kDa, Millipore). Viral stocks are aliquoted and stored at -80°C. Viral titres were determined using an enzyme-linked immunosorbent assay (ELISA) kit (Abbott, Chicago, IL) targeting the viral envelope protein p24^{gag} and expressed as ng p24/µl.

Lentiviral transduction of adult keratinocytes

Keratinocytes from two different donors were grown to 40% confluency in a 6-wells plate using KGM medium (Lonza, Verviers, Belgium) supplemented with 10 µM Y-27632 (Sigma), as described previously²³. Subsequently, each well was incubated with 0.5 or 2 µg of scrambled, shRNA-CST6-1 and shRNA-CST6-3 lentivirus for 4 hours after which the cells were washed twice with sterile PBS. After 24 hours of recovery in KGM supplemented with 10 µM Y-27632, cells were harvested for skin equivalent generation or grown to confluency after which they were let to differentiate for 48 hours in growth factor depleted KGM, supplemented

with 5% serum.

Generation of human skin equivalents

Lentiviral transduced human skin equivalents were generated as described previously²³. Briefly, 8-mm tissue samples of de-epidermized dermis were placed in a 24-wells transwell system and seeded with 1.5×10^5 lentiviral transduced keratinocytes. The human skin equivalents were cultured submerged for three days in medium containing 5% serum, consisting of two parts Dulbecco's modified Eagle's medium and one part Ham's F12 medium (both from Life Technologies) supplemented with 5% calf serum (Hyclone), 4 mmol/l L-glutamine and 50 IU/ml penicillin or streptomycin (both from Life Technologies), 24.3 µg/ml adenine (Calbiochem), 1 µmol/l hydrocortisone (Merck), and 50 µg/ml ascorbic acid, 0.2 µmol/l insulin, 1.36 ng/ml triiodothyronine, 10^{-10} mmol/l cholera toxin and 10 µM Y-27632 (all from Sigma). Thereafter, the human skin equivalents were cultured at the air-liquid interface for ten days in medium without serum, consisting of two parts Dulbecco's modified Eagle's medium and one part Ham's F12 medium (both from Life Technologies) supplemented with 4 mmol/l L-glutamine and 50 IU/ml penicillin or streptomycin (both from Life Technologies), 24.3 µg/ml adenine (Calbiochem), 1 mg/ml L-serine and 2 µg/ml L-carnitine (both from Sigma), bovine serum albumin lipid mix (25 µmol/l palmitic acid, 7 µmol/l arachidonic acid, 15 µmol/l linoleic acid, and 0.4 µg/ml vitamin E; all from Sigma), 1 µmol/l hydrocortisone (Merck), and 50 µg/ml ascorbic acid, 0.1 µmol/l insulin, 1.36 ng/ml triiodothyronine, 10^{-10} mmol/l cholera toxin, 5 ng/ml keratinocyte growth factor and 2 ng/ml epidermal growth factor (all from Sigma).

Morphological and immunohistochemical analysis

Human skin equivalents were fixed in buffered 4% formalin for 4 hours, and processed for routine histology. Skin equivalents were embedded in paraffin, and 6-µm sections were stained with haematoxylin and eosin (H&E) (Sigma) or processed for immunohistochemical staining using an indirect immunoperoxidase technique with avidin-biotin complex enhancement (Vectastain Laboratories, Burlingame, CA). To study cystatin M/E knockdown, a polyclonal goat anti-cystatin M/E antibody (AF1286, R&D) was used. Detection by 3-amino-9-ethylcarbazole (Calbiochem) was followed by nuclei counterstaining with Mayer's haematoxylin solution (Sigma), and sections were mounted using glycerol gelatin (Sigma).

mRNA isolation and real-time qPCR

Lentiviral transduced keratinocytes were harvested after 48 hours and total RNA was purified from these cells as previously described²⁴. A DNase I treatment was performed according to the manufacturer's protocol (Invitrogen, Carlsbad, CA). First strand cDNA was synthesized using an input of 1 µg of DNase I treated RNA with the iScript cDNA synthesis kit (Bio-Rad, Hercules, CA) according to the manufacturer's recommendation. Real-time quantitative PCR was performed with the MyiQ Single-Colour Real-Time Detection System for quantification with SYBR

Green and melting curve analysis (Bio-Rad) as previously described²⁵. Primer validation, qPCR reactions, and determination of relative mRNA expression were performed as previously described²⁴. Expression of the target genes (*CST6*, *ITGB1*, *IVL*, *Ki-67*, *KRT14*, *STAT1* and *OAS2*) was normalized to that of human ribosomal phosphoprotein P0 (*RPLP0*). Relative quantity of gene expression was measured with the delta-delta Cycle threshold ($\Delta\Delta Ct$) method²⁶. Primers for qPCR (Biolegio, Nijmegen, the Netherlands) were only accepted if their efficiency was $100\pm 10\%$. Corrections were made for primer efficiency. Primer sequences and efficiency are shown in Table 6.3.

Cystatin M/E ELISA

Lentiviral transduced keratinocytes were harvested after 48 hours and protein was extracted by repeated freeze/thawing of the cells in extraction buffer (50 mM Tris-HCl pH 7.5, 150 mM NaCl, 0.5% Triton-X-100, and a protease inhibitor cocktail) followed by centrifugation for 10 min at 15000 x g. The supernatants that harbor the soluble proteins were measured for the presence of cystatin M/E by ELISA as described previously²⁷.

Acknowledgements

We are grateful to all ARCI patients and their families for providing samples. We thank dr Khumalo (University of Cape Town, South Africa), and dr Stefano Cambiaghi (University of Milan, Italy) for providing DNA samples of individual IFAP syndrome patients and their parents. Eric-Jan Kamsteeg (Radboud University Nijmegen Medical Centre, The Netherlands) is acknowledged for performing MLPA analysis. We wish to thank Marc Nâtebus (Cologne) for excellent technical assistance. This study was funded by The Alternatives to Animal Experiments programme of ZonMW (project number 114.000.084), by the Dutch Organization for Scientific research (NWO-ALW, project number 821.02.013), in part by the German Federal Ministry for Education and Research with a grant to the Network for Ichthyoses and Related Keratinization Disorders (NIRK, GFGM01143901), and by the German Research Foundation (DFG).

Table 6.3 Primers used for quantitative real-time PCR

Gene Symbol	Ensemble Transcript no.	Description Gene/Protein	Forward primer	Reverse primer	E*
<i>CST6</i>	ENST00000312134	cystatin M/E (skin-specific protease inhibitor)	tccgagacacgcacatcatc	ccatctccatcgtcaggaagtac	1.96
<i>CTSL</i>	ENST00000257498	cathepsin L (target protease for cystatin M/E)	gtfgctattgatgcaggctcaga	actgctacagtctggctcaaaaataaa	1.90
<i>ITGB1</i>	ENST00000302278	b1-integrin (basal cell layer epidermis)	agttgcagtttggatcactgat	aaagtgaaccccgcatctg	2.20
<i>IVL</i>	ENST00000295365	involucrin (suprabasal layers epidermis)	acttattcgggtccgctaggt	gagacatgtagaggggacagagtgcaag	1.93
<i>MKI67</i>	ENST00000277994	antigen identified by monoclonal antibody Ki-67 (proliferation marker)	aaaccaacaagagggaacacaaaatt	gtctggagcgcaggggatattc	2.20
<i>KRT14</i>	ENST00000167586	keratin 14 (basal cell layer epidermis)	ggcctgctgagatcaaaagactac	cactgtggctgtgagaatctgtt	1.93
<i>OAS2</i>	ENST00000342315	2'-5'-oligoadenylate synthetase 2 (control IFN response)	caacctggataatgagttacct	gctctaggaagcattgtttg	2.03
<i>RPLP0</i>	ENST00000228306	ribosomal protein P0, hARP (household gene)	caccattgaaatccttgagtgatgt	tgaccagcccaaggagaag	2.00
<i>STAT1</i>	ENST00000361099	signal transducer and activator of transcription 1 (control IFN response)	ccatgctttggaaaatt	cacagaaatcaactcagtccttg	2.08

* E is efficiency as fold increase in fluorescence per PCR cycle

References

1. Cheng T, Hitomi K, van Vlijmen-Willems IM, de Jongh GJ, Yamamoto K, Nishi K *et al*. Cystatin M/E is a high affinity inhibitor of cathepsin V and cathepsin L by a reactive site that is distinct from the legumain-binding site. A novel clue for the role of cystatin M/E in epidermal cornification. *J Biol Chem* 281, 15893-15899 (2006)
2. Zeeuwen PL, Cheng T, Schalkwijk J. The biology of cystatin M/E and its cognate target proteases. *J Invest Dermatol* 129, 1327-1338 (2009)
3. Sundberg JP, Boggess D, Hogan ME, Sundberg BA, Rourk MH, Harris B *et al*. Harlequin ichthyosis (ichq): a juvenile lethal mouse mutation with ichthyosiform dermatitis. *Am J Pathol* 151, 293-310 (1997)
4. Zeeuwen PL, Vlijmen-Willems IM, Hendriks W, Merckx GF, Schalkwijk J. A null mutation in the cystatin M/E gene of ichq mice causes juvenile lethality and defects in epidermal cornification. *Hum Mol Genet* 11, 2867-2875 (2002)
5. Zeeuwen PL, Vlijmen-Willems IM, Olthuis D, Johansen HT, Hitomi K, Hara-Nishimura I *et al*. Evidence that unrestricted legumain activity is involved in disturbed epidermal cornification in cystatin M/E deficient mice. *Hum Mol Genet* 13, 1069-1079 (2004)
6. Oji V, Zeeuwen P, Schalkwijk J, Traupe H. Evaluation of cystatin M/E: a candidate for cornification disorders. *Arch Dermatol Res* 296, 408 (2005)
7. Zeeuwen PL, van Vlijmen-Willems IM, Cheng T, Rodijk-Olthuis D, Hitomi K, Hara-Nishimura I *et al*. The cystatin M/E-cathepsin L balance is essential for tissue homeostasis in epidermis, hair follicles, and cornea. *FASEB J* 24, 3744-3755 (2010)
8. Eisman S, Ngwanya RM, Pillay K, Khumalo NP. Whorled follicular keratosis, scarring alopecia in ichthyosis follicularis atrichia with photophobia syndrome. *J Eur Acad Dermatol Venereol* 23, 842-3 (2009)
9. Sledz CA, Holko M, de Veer MJ, Silverman RH, Williams BR. Activation of the interferon system by short-interfering RNAs. *Nat Cell Biol* 5, 834-9 (2003)
10. Bridge AJ, Pebernard S, Ducraux A, Nicoulaz AL, Iggo R. Induction of an interferon response by RNAi vectors in mammalian cells. *Nat Genet* 34, 263-4 (2003)
11. de Koning HD, Rodijk-Olthuis D, van Vlijmen-Willems IM, Joosten LA, Netea MG, Schalkwijk J *et al*. A comprehensive analysis of pattern recognition receptors in normal and inflamed human epidermis: upregulation of dectin-1 in psoriasis. *J Invest Dermatol* 130, 2611-2620 (2010)
12. Chen M, Li W, Fan J, Kasahara N, Woodley D. An efficient gene transduction system for studying gene function in primary human dermal fibroblasts and epidermal keratinocytes. *Clin Exp Dermatol* 28, 193-199 (2003)
13. Mildner M, Ballaun C, Stichenwirth M, Bauer R, Gmeiner R, Buchberger M *et al*. Gene silencing in a human organotypic skin model. *Biochem Biophys Res Commun* 348, 76-82 (2006)
14. Mildner M, Jin J, Eckhart L, Kezic S, Gruber F, Barresi C *et al*. Knockdown of filaggrin impairs diffusion barrier function and increases UV sensitivity in a human skin model. *J Invest Dermatol* 130, 2286-94 (2010)
15. Takahashi H, Asano K, Nakamura S, Ishida-Yamamoto A, Iizuka H. Interferon-gamma-dependent stimulation of human involucrin gene expression: STAT1 (signal transduction and activators of transcription 1) protein activates involucrin promoter activity. *Biochem J* 344 Pt 3, 797-802 (1999)

16. Jackson AL, Bartz SR, Schelter J, Kobayashi SV, Burchard J, Mao M *et al.* Expression profiling reveals off-target gene regulation by RNAi. *Nat Biotechnol* 21, 635-7 (2003)
17. Semizarov D, Frost L, Sarthy A, Kroeger P, Halbert DN, Fesik SW. Specificity of short interfering RNA determined through gene expression signatures. *Proc Natl Acad Sci U S A* 100, 6347-52 (2003)
18. Reinheckel T, Hagemann S, Dollwet-Mack S, Martinez E, Lohmuller T, Zlatkovic G *et al.* The lysosomal cysteine protease cathepsin L regulates keratinocyte proliferation by control of growth factor recycling. *J Cell Sci* 118, 3387-3395 (2005)
19. Blydson DC, Nitoiu D, Eckl KM, Cabral RM, Bland P, Hausser I *et al.* Mutations in CSTA, encoding Cystatin A, underlie exfoliative ichthyosis and reveal a role for this protease inhibitor in cell-cell adhesion. *Am J Hum Genet* 89, 564-71 (2011)
20. Bilodeau M, MacRae T, Gaboury L, Laverdure JP, Hardy MP, Mayotte N *et al.* Analysis of blood stem cell activity and cystatin gene expression in a mouse model presenting a chromosomal deletion encompassing Csta and Stfa2l1. *PLoS One* 4, e7500 (2009)
21. Zeeuwen PL, Dale BA, de Jongh GJ, Vlijmen-Willems IM, Fleckman P, Kimball JR *et al.* The human cystatin M/E gene (CST6): exclusion as a candidate gene for harlequin ichthyosis. *J Invest Dermatol* 121, 65-68 (2003)
22. Sarbassov DD, Guertin DA, Ali SM, Sabatini DM. Phosphorylation and regulation of Akt/PKB by the rictor-mTOR complex. *Science* 307, 1098-101 (2005)
23. van den Bogaard E, Rodijk-Olthuis D, Jansen PA, van Vlijmen-Willems IM, van Erp PE, Joosten I *et al.* Rho kinase inhibitor Y-27632 prolongs the life span of adult human keratinocytes, enhances skin equivalent development and facilitates lentiviral transduction. *Tissue Eng Part A* (2012)
24. de Jongh GJ, Zeeuwen PL, Kucharekova M, Pfundt R, van der Valk PG, Blokx W *et al.* High expression levels of keratinocyte antimicrobial proteins in psoriasis compared with atopic dermatitis. *J Invest Dermatol* 125, 1163-1173 (2005)
25. Franssen ME, Zeeuwen PL, Vierwinden G, van de Kerkhof PC, Schalkwijk J, van Erp PE. Phenotypical and functional differences in germinative subpopulations derived from normal and psoriatic epidermis. *J Invest Dermatol* 124, 373-383 (2005)
26. Livak KJ, Schmittgen TD. Analysis of relative gene expression data using real-time quantitative PCR and the 2(-Delta Delta C(T)) Method. *Methods* 25, 402-408 (2001)
27. Jansen BJ, van Ruissen F, de Jongh G, Zeeuwen PL, Schalkwijk J. Serial Analysis of Gene Expression in Differentiated Cultures of Human Epidermal Keratinocytes. *J Invest Dermatol* 116, 12-22 (2001)

Discovery of small molecule vanin inhibitors: new tools to study metabolism and disease

7 CHAPTER

Patrick AM Jansen¹

Janna A van Diepen²

Bas Ritzen³

Patrick LJM Zeeuwen¹

Ivana Cacciatore⁴

Catia Cornacchia⁴

Ivonne MJJ van Vlijmen-Willems¹

Erik de Heuvel⁵

Peter NM Botman⁵

Richard H Blaauw⁵

Pedro HH Hermkens³

Floris PJT Rutjes³

Joost Schalkwijk¹

¹ Nijmegen Centre for Molecular Life Sciences, Radboud University Nijmegen Medical Centre, The Netherlands

² Department of General Internal Medicine, Radboud University Nijmegen Medical Centre, The Netherlands

³ Department of Synthetic Organic Chemistry, Institute for Molecules and Materials, Radboud University Nijmegen, The Netherlands

⁴ Department of Pharmacy, "G. d'Annunzio" University, Chieti-Pescara, Italy

⁵ Chiralix B.V., Nijmegen, The Netherlands

Abstract

Vanins are enzymes with pantetheinase activity and are presumed to play a role in recycling of pantothenic acid (vitamin B5) from pantetheine. Pantothenic acid is an essential nutrient required to synthesize coenzyme A, a cofactor involved in many biological processes such as fatty acid synthesis and oxidation of pyruvate to fuel the citric acid cycle. Hydrolysis of pantetheine also liberates cysteamine, a known antioxidant. Vanin-1 is highly expressed in liver and is under transcriptional control of PPAR-alpha and nutritional status, suggesting a role in energy metabolism. The lack of potent and specific inhibitors of vanins has hampered detailed investigation of their function. We hereby report the design, synthesis and characterization of a novel pantetheine analog, RR6, that acts as a selective, reversible and competitive vanin inhibitor at nanomolar concentration. Oral administration of RR6 in rats completely inhibited plasma vanin activity and caused alterations of plasma lipid concentrations upon fasting, thereby illustrating its potential use in chemical biology research.

Members of the vanin (VNN) gene family encode proteins with pantetheinase activity^{1,2}. In humans, three vanins have been described, two of which have confirmed enzymatic activity (vanin-1 and vanin-2)^{3,4}. The natural substrate of vanins is pantetheine, which is hydrolyzed to pantothenic acid and cysteamine. On the basis of sequence similarities, vanins were classified as members of the biotinidase branch of the nitrilase superfamily⁵. Nitrilases are thiol enzymes that perform their hydrolytic reactions through a catalytic triad consisting of Glu, Lys and Cys, where the cysteine nucleophile produces a covalent intermediate. Although vanins are poorly characterized at the functional level, their primary function is assumed to be in pantothenate recycling, which is a necessary factor in the synthesis of Coenzyme A (CoA)⁶. Recent investigations, however, have shown that at least murine vanin-1 has additional functions⁷. *Vnn1* knockout mice did not have an obvious spontaneous phenotype, but were resistant to intestinal inflammation, oxidative stress and experimental colitis⁷⁻⁹. Other conditions with a putative role of vanins include malaria susceptibility¹⁰, psoriasis¹¹, carcinogenesis¹² and cardiovascular disease¹³. Vanins are the only known source of pantetheinase activity in mammalian tissues. Interestingly, the *Vnn1* gene was shown to be one of the major targets of PPAR- α in mouse liver¹⁴, suggesting a role for vanin-1 in metabolism¹⁵.

The lack of selective high-affinity vanin inhibitors has so far hampered investigation of vanin biology *in vitro* and *in vivo*. Recently, an inhibitor screen of Sigma's Library of Pharmacologically Active Compounds (LOPAC library), identified six compounds with anti-pantetheinase activity. These comprised widely different chemotypes with IC₅₀ values towards recombinant human vanin-1 in a range of 4-20 μ M¹⁶. All these compounds had known other pharmacological activities or cytotoxic properties that would preclude their use as specific vanin inhibitors. These observations emphasize the need for selective and potent vanin inhibitors as tools in chemical biology, to study the role of vanins in human biology and to evaluate these enzymes as potentially druggable targets. Herein, we report the design of pantetheine analogs as reversible, competitive inhibitors of mammalian vanins. It is shown that RR6, our most potent vanin inhibitor, is selective and displays excellent bioavailability and potency *in vivo*.

We reasoned that pantetheine analogues lacking the amide bond, but containing a warhead that would form a reversible covalent bond with the cysteine residue of the catalytic triad, could potentially interfere with vanin activity. We synthesized compounds substituting the amide bond by a keto group, a known warhead for proteases¹⁷, by applying the Weinreb ketone synthesis strategy (figure 7.1). Conversion of partially protected pantothenic acid 1 into Weinreb amide 2 allowed the addition of a variety of Grignard reagents. After acid mediated deprotection of the pantoic acid moiety a series of potential vanine inhibitors was obtained. (Table 7.1 and Supplemental Materials and Methods for details of chemical structures and synthetic procedures). Compounds were tested for vanin inhibition using pantothenate-7-amino-4-methylcoumarin (AMC-Pan) as a highly sensitive fluorogenic substrate¹⁶. As sources of vanin activity

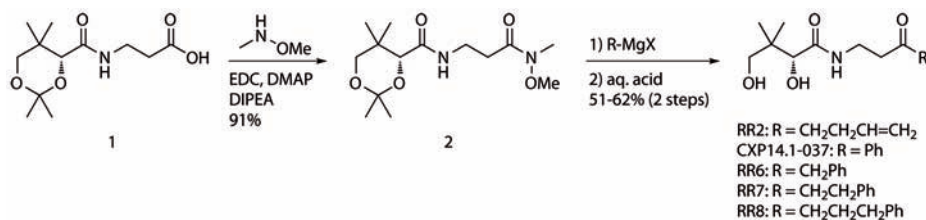


Figure 7.1 Weinreb ketone synthesis strategy including yields.

we used recombinant human vanin-1 as well as serum. Vanin-1, which is highly expressed in epithelia as a membrane-bound GPI-anchored ectoenzyme, was cloned without the C-terminal GPI-anchoring site, and expressed in a eukaryotic system as a 6-His tagged, secreted protein (Supplementary Figure 7.1). Affinity-purified vanin-1 was used for subsequent inhibitor assays. Attempts to express enzymatically active human vanin-2 were unsuccessful. We used serum (human, rat and bovine) as a natural, physiological source of pantetheinase activity. Serum pantetheinase activity likely represents vanin-2 (originally called GPI-80)¹⁸, which is known to be present in a secreted form¹⁹. From our first series of compounds, RR2 was identified as a hit compound, showing IC₅₀ values in the low micromolar range. Limited optimization of RR2 (Table 7.1), replacing the alkenyl moiety by an aromatic residue (RR6 compound), yielded a 30-fold improvement of the IC₅₀ value towards recombinant vanin-1 down to the nanomolar range. When serum was used, an even lower IC₅₀ (40 nM for human serum) was observed (Figure 7.2a). Reduction of the keto group to a hydroxyl (CXP14.1-034) caused a strong decrease of the potency, supporting the idea that the keto group has a warhead. The chain length between the keto group and the phenyl moiety clearly affected the potency, as indicated by the reduced potency of CXP14.1-037, RR7 and RR8. One carbon atom turned out to be optimal, as increasing the chain length showed a decrease in potency, while leaving out the linker led to a similar result (Table 7.1).

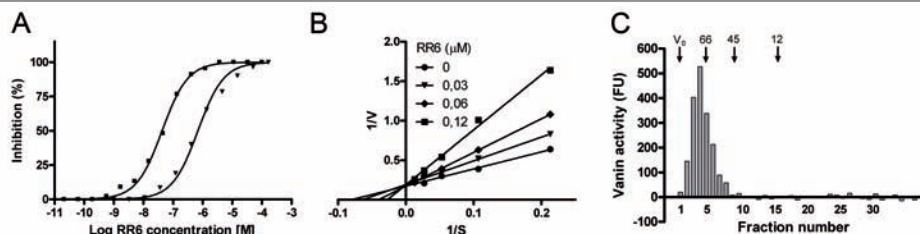


Figure 7.2 Characterization of the pantetheinase/vanin inhibitor RR6. (A) Inhibition of pantetheinase activity of recombinant human vanin-1 (▼) and bovine serum vanin (■) by RR6, using the synthetic substrate AMC-Pan. (B) A Lineweaver-Burk plot of reaction velocities at different substrate concentrations and inhibitor concentrations indicates that RR6 is a competitive inhibitor. The kinetic constants Km (12 μM) and the Vmax (6 pmol/min) were read from this graph. Bovine serum was used as source of vanin activity. (C) Superdex-75 chromatography of fetal bovine serum in the presence of excess RR6. Complete recovery of vanin activity in the high molecular weight fraction was obtained, indicating a reversible binding of RR6. V0: void volume of the column. Molecular mass markers: bovine serum albumin (66 kDa), ovalbumin (45 kDa) and cytochrome c (12 kDa). FU: fluorescence units.

In a next step we sought to characterize the mechanism of binding. As the inhibitor is an analogue of its natural substrate we assumed that inhibition would be competitive. Figure 7.2b shows that, using RR6 as an inhibitor, this is indeed the case. A Lineweaver-Burk plot of the data indicated that RR6 did not change V_{max} , but caused an increase of the apparent K_m . To investigate the reversibility of binding, we used serum diluted in PBS with excess RR6 (100 μ M) to achieve complete inhibition of vanin activity. Gel permeation chromatography of this sample showed complete recovery of serum vanin activity in the high molecular weight fractions, indicating a reversible binding of RR6 (Figure 7.2c).

To characterize the selectivity of RR6 we first tested biotinidase, an enzyme that has the highest structural similarity to vanins. Only RR2 has significant biotinidase inhibiting activity ($IC_{50} = 30 \mu$ M), whereas none of the other compounds showed activity up to the highest concentration tested (200 μ M) (Table 7.1). As the scissile bond between pantothenate and the AMC group resembles a peptide bond, and knowing that nitrilases use a cysteine in their active site, we considered the possibility that cysteine proteases could hydrolyze the AMC-Pan substrate. None of the ubiquitous human cysteine proteases cathepsin B and L, nor the plant cysteine protease papain hydrolyzed the AMC-pan substrate. RR6, up to the highest concentration tested (200 μ M) did not inhibit the activity of any of these cysteine proteases towards their own specific synthetic substrates. Similarly, we did not observe any inhibition of serum vanin activity by the generic cysteine protease inhibitor E-64 or the generic serine protease inhibitor PMSF.

To investigate the *in vivo* potency of our lead compound RR6 on vanin inhibition and subsequent downstream biological effects, we first investigated its pharmacodynamic properties. Oral administration in rats showed a strong dose-dependent inhibition of plasma vanin activity (Figure 7.3a). After a single oral dose of 50 mg/kg, a prolonged complete inhibition of plasma vanin activity was achieved which lasted up to 8 hours after the initial dose. No adverse effects on the animals were noted at any dose given. These data suggested that RR6 could be used as a tool to study *in vivo* biological processes that involved vanin activity. In order to facilitate animal-friendly and easy experimentation we investigated

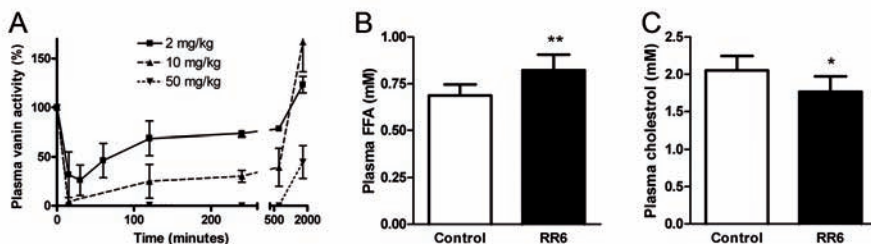


Figure 7.3 Pharmacodynamics of RR6 in rats. (A) Inhibition of plasma pantetheinase activity by RR6 following oral administration to rats at the indicated doses. Plasma vanin activity is dose-dependently inhibited, as determined by hydrolysis of the synthetic AMC-Pan substrate *ex vivo*. (B) RR6 in drinking water (3 mg/mL) increases plasma free fatty acid levels in rats after a 24h fast as compared with rats without RR6 in the drinking water (control). Values are means \pm SD (n=7). (C) RR6 in drinking water (3 mg/mL) reduced plasma cholesterol levels after a 24h fast in rats as compared with rats without RR6 in the drinking water (control). Values are means \pm SD (n=7). * $P < 0.05$ ** $P < 0.01$.

whether RR6 could be given in the drinking water of rats to achieve prolonged complete vanin inhibition without the need of multiple daily drug administrations. We found that dosing of RR6 at 3 mg/mL in rats caused a nearly complete inhibition of plasma vanin activity (Supplementary Figure 7.2).

Finally, we investigated if vanin inhibition by RR6 could affect a biological process. It is not known if vanins have non-redundant biological functions in normal physiology, as the *Vnn1* knockout mouse only displays a phenotype upon challenge (infection, inflammation, cancer). Previous studies have shown that pantetheine the dimer of pantetheine, the presumed natural substrate of vanins is involved in lipid metabolism^{20,21}. This suggested to us that pharmacological modulation of vanin activity could have an effect on lipid homeostasis. Similarly, a number of studies have shown that vanin-1 expression in liver is induced by peroxisome proliferator activated receptor (PPAR)- α agonists. PPARs are ligand activated transcription factors and play an important role in nutrient homeostasis. Oral administration of triglycerides or PPAR- α ligands such as WY14643 and fenofibrate caused a strong increase of vanin-1 expression in mouse liver¹⁴. Although the functional effect of vanin-1 upregulation in PPAR- α dependent metabolic changes is completely unknown and unexplored, these findings also suggested a possible role of vanin-1 in lipid homeostasis. Moreover, a recent study has shown that fasting induces a huge increase in liver vanin-1 expression in wild type mice¹⁵. We therefore investigated the effect of RR6 administration on lipid metabolism following fasting. Rats were given RR6 for 4 days in the drinking water (3 mg/mL) and were subjected to fasting for 24 hours at day 4. Analysis of a limited set of metabolites in plasma showed modest but statistically significant changes such as an increase in plasma free fatty acids (FFA) and a decrease of plasma cholesterol (Figure 7.3b and 7.3c) as compared with rats without RR6 in drinking water (control). Plasma glucose levels were not altered. Upon fasting, lipids are mobilized from tissue fat stores as a source of energy, thereby causing an increase of plasma FFA and liver steatosis. At the same time fasting will induce high levels of liver vanin-1 activity in a PPAR- α dependent manner. This suggests a role of vanin-1 in mobilization and/or conversion of triglycerides, fatty acids and cholesterol. Detailed investigation of these metabolic changes was beyond the scope of this report, but these findings clearly offer a starting point to study the physiological role of vanins in lipid metabolism.

Based on its potency, selectivity and bioavailability, RR6 represents a novel biological chemistry tool that will greatly facilitate the study of vanin function in health and disease. It is assumed that pantetheine is the major vanin substrate and hence a role in vitamin B5 recycling (pantothenate release) and antioxidant production (cysteamine release) has been proposed. The fact that vanin-1 is a PPAR- α target and appears to have a role in nutrient or lipid metabolism as witnessed by the current study, suggests that enzymatic activity of vanins may not be restricted to pantetheine alone. We propose that RR6 and optimized versions of this novel chemotype constitute a promising starting point for a platform of vanin inhibitors which may open up a new field of research.

Materials and methods

Synthesis of probes

The detailed description of the synthesis of the vanin inhibitors can be found in the supplementary information.

Pantothenate-7-amino-4-methylcoumarin (AMC-Pan)

AMC-Pan was synthesized according to the published method by Ruan *et al.*¹⁶

Assay of pantetheinase activity and pantetheinase inhibition

Pantetheinase activity was measured largely as described by Ruan *et al.*¹⁶ Samples (10 μ L volume) with pantetheinase activity (recombinant human vanin-1 or diluted serum from different origin) were added to the substrate AMC-Pan (10 μ M final concentration) in a 100 μ L final volume, in PBS at pH 7.4. Five hundred ng of recombinant vanin-1 was used per reaction. Human serum was diluted 2.5 times, FBS was diluted 100 times and rat serum was diluted two times before addition to the reaction (all in PBS at pH 7.4). In the case that inhibition was measured, 10 μ L of inhibitor solution was added to 10 μ L of sample (recombinant vanin or diluted serum) and allowed to equilibrate for 10 min, whereafter substrate was added. From these reaction mixtures 10 μ L was taken after 10 minutes incubation, diluted 10-fold in PBS and measured in a 96-well plate fluorescence reader (Perkin Elmer LS55) at excitation 360 nm and emission 450 nm. IC₅₀ determinations were made in duplicate, by measuring the inhibition of inhibitors in a 10⁻¹⁰ to 10⁻³ M dilution range. IC₅₀ values were calculated from the fit of the % inhibition of the dose response curve (Graphpad Prism version 4.0). The mode of inhibition was investigated by assaying RR6 inhibition of plasma vanin activity in the presence of varying substrate concentrations, from 300 μ M to 1 μ M (Graphpad Prism version 4.0). When we wished to determine pantetheinase activity under near physiological conditions, like in undiluted rat plasma taken from animals that received oral RR6, we used the following procedure. A buffered substrate solution (20 μ L) was put in 96-well plates and evaporated to dryness. The rat plasma samples were added and substrate hydrolysis was allowed to proceed. Substrate hydrolysis and inhibition by our experimental compounds was measured as described above.

Biotinidase and cysteine protease assays

Biotinidase activity was assayed by the hydrolysis of 6-amidoquinoline (Apollo Scientific) as a fluorimetric substrate²², and IC₅₀ for biotinidase was determined as described for vanin activity. Cathepsins B and L (R&D Systems) and papain (Sigma) were assayed as described previously, using the substrates Z-Leu-Arg-AMC (R&D Systems) for the cathepsins and Z-Phe-Arg-AMC (Bachem) for papain²³.

Cloning and expression of recombinant human vanin-1

Human vanin-1 cDNA was obtained from image clone 40006204 (Geneservice)²⁴. Using PCR the vanin-1 ORF (aa 1-483) was amplified without its GPI-anchor and cloned into the eukaryotic expression vector pHLsec²⁵. Transfection of pHLsec-VNN1 into 293T cells using PEI transfection reagent results in the production of His-tagged recombinant human vanin-1 protein. Media containing the secreted recombinant protein were collected 72 hours post transfection and recombinant protein was affinity purified using Ni-NTA agarose beads. After the protein was eluted from the column it was concentrated and dialysed to PBS using Microcon YM-10 filters (Millipore).

Gel permeation chromatography

Bovine serum diluted 1:3 with PBS was used and incubated with 100 μ M RR6 for 2 h. At this concentration a complete inhibition of serum vanin activity is achieved. A 50 μ L sample was injected on a Superdex-75 HR 10/30 SMART column (GE Health Sciences) in PBS at a flow rate of 40 μ L per min. The column was calibrated with bovine serum albumin (66 kDa), ovalbumin (45 kDa) and cytochrome c (12 kDa), all obtained from Sigma. Eluted proteins were monitored at 280 nm using a microflow cell. Fractions (40 μ L) were collected and measured for pantetheinase activity.

Pharmacodynamic studies

Female Wistar rats (Harlan), weighing 200-250 gram were housed in groups of two or three animals in the Central Animal Laboratory of the Radboud University and given water and chow ad libitum. Protocols were approved by our local committee for animal experiments (DEC). Rats (2-3 per group) were given RR6 by a single oral administration (dissolved in 10% DMSO in PBS at doses of 2, 10 and 50 mg/kg) or via their drinking water (dissolved at doses of 0.3, 1 and 3 mg/mL in water). Heparinized blood samples were drawn at several time points, and plasma was obtained by centrifugation of the blood samples for 20 minutes at 465 g at 4° C, for pantetheinase activity determination as indicated above.

Metabolic studies

Male Wistar rats (Harlan), weighing 150-200 gram were housed in groups of two or three animals in the Central Animal Laboratory of the Radboud University and given water and chow ad libitum. Protocols were approved by our local committee for animal experiments (DEC). Rats were given RR6 via drinking water (3 mg/mL) for 4 days. Blood was collected after a 24 h period of fasting and placed on ice, centrifuged and plasma was assayed for free fatty acids (FFA) using the NEFA-C kit (Wako Diagnostics). Glucose and cholesterol were determined using kits from Human Diagnostics.

Data analysis

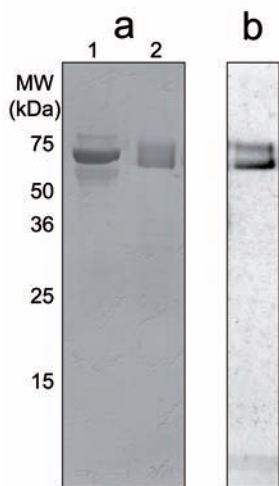
Data were analyzed using Graphpad Prism version 4. Kinetic constants were

determined with the non-linear regression analysis module. Statistical analysis of FFA and cholesterol measurements was performed using a Student's T-test (SPSS Inc). $P < 0.05$ was considered statistically significant.

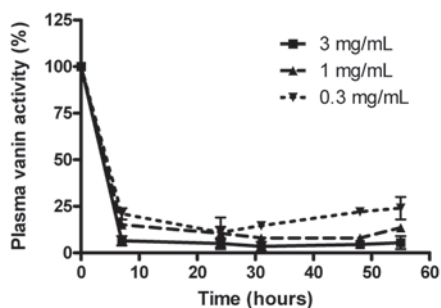
Acknowledgements

Jody Theunissen, Ezra Disco, Dieu-Linh Nguyen, René Aben and Daphne Reijnen are acknowledged for technical assistance.

Supplementary information



Supplementary figure 7.1 SDS-PAGE of purified recombinant human vanin-1. (a) Coomassie Brilliant Blue staining of an SDS-PAGE gel loaded with a sample of the culture medium 72 hours post transfection (lane 1) and affinity purified recombinant human vanin-1 (lane 2). (b) Western blot analysis of purified recombinant human vanin-1 detected with a Penta-His monoclonal antibody.



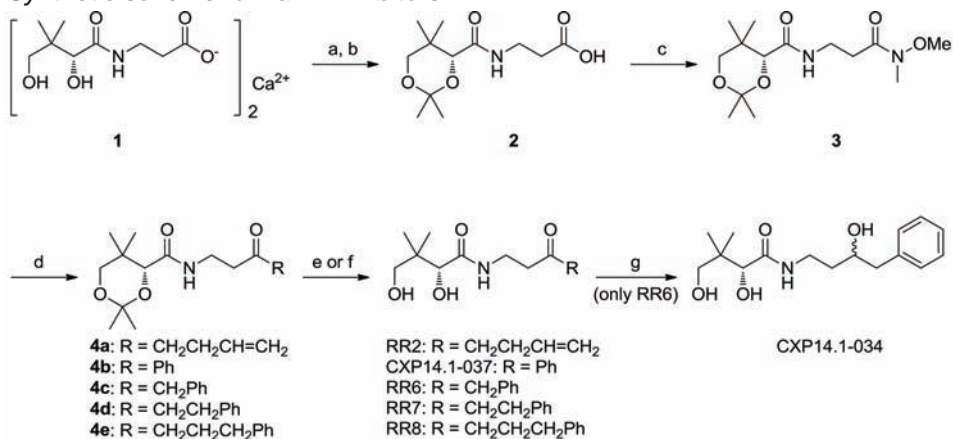
Supplementary figure 7.2 Vanin inhibition in rat plasma following administration of RR6 in the drinking water. Rats were given RR6 dissolved in the drinking water at concentrations of 0.3, 1 and 3 mg/mL for 3 days. Every morning and evening, blood samples were taken and the pantetheinase activity was measured. A dose-dependent pantetheinase inhibition was found with a stable (>95%) pantetheinase inhibition at 3 mg/mL.

Synthesis of probes: general remarks

All reactions were performed under a nitrogen atmosphere, unless stated otherwise. Solvents were distilled from appropriate drying agents prior to use. Standard syringe techniques were applied for the transfer of air sensitive reagents and dry solvents. All other chemicals were purchased from commercial suppliers and were used without further purification, unless stated otherwise. Reactions

were followed, and R_f values are obtained using thin layer chromatography (TLC) on silica gel-coated plates (Merck 60 F254) with the indicated eluent and compounds were detected with UV-light and/or by charring at ca. 150 °C after dipping into a solution of potassium permanganate, or ninhydrin. Column chromatography was carried out using ACROS silica gel (0.035-0.070 mm, pore diameter ca. 6 mm). IR spectra were recorded on an ATI Mattson Genesis Series FTIR spectrometer. High-resolution mass spectra were recorded on a JEOL AccuTOF (ESI) or a MAT900 (EI, CI, and ESI). NMR spectra were recorded at 298 K on a Bruker DMX 300 (300 MHz) and a Varian 400 (400 MHz) spectrometer in the solvent indicated. Chemical shifts are given in parts per million (ppm) with respect to tetramethylsilane (0.00 ppm), or CHD₂OD (3.31 ppm) as internal standard for ¹H NMR; and CDCl₃ (77.16 ppm), or CD₃OD (49.00 ppm) as internal standard for ¹³C NMR. Coupling constants are reported as J values in hertz (Hz). All compounds used for assays/metabolic studies were obtained with a chemical purity >97% based on ¹H NMR.

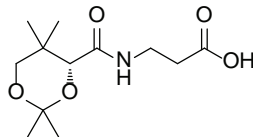
Synthetic scheme for vanin inhibitors



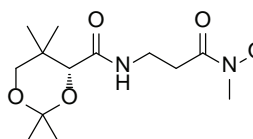
Reagents and conditions: (a) 1M aq. HCl, EtOAc; (b) 2-methoxyprop-1-ene, TsOH·H₂O (cat.), acetone, 0 °C to rt, 45 min; (c) *N,N*-dimethylhydroxylamine-HCl, EDC-HCl, DMAP, DIPEA, CH₂Cl₂, rt, 18 h; (d) RMgCl or RMgBr, Et₂O/THF, 0 °C to rt; (e) BiCl₃ (cat.), H₂O, MeCN, rt, 4 h; (f) AcOH, H₂O, rt, 5 h; (g) NaBH₄, MeOH, rt, 2 h.

(*R*)-3-(2,4-dihydroxy-3,3-dimethylbutanamido)propanoic acid [(*R*)-pantothenic acid]

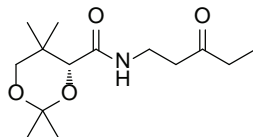
A suspension of calcium (*R*)-pantothenate (**1**) (25.0 g, 52.6 mmol) in 1M aqueous HCl (125 mL) was stirred vigorously until the starting material was completely dissolved. The solution was saturated by the addition of NaCl and the resulting suspension was extracted with EtOAc (3 × 250 mL). The combined organic layers were dried over Na₂SO₄ and concentrated *in vacuo* to yield (*R*)-pantothenic acid as a colorless oil (20.8 g, 90%). Spectral data were in correspondence with reported data in literature²⁶.

(R)-3-(2,2,5,5-tetramethyl-1,3-dioxane-4-carboxamido)propanoic acid (**2**)

To a cooled solution (0 °C) of *(R)*-pantothenic acid (20.8 g, 94.0 mmol) in acetone (500 mL) were added subsequently 2-methoxyprop-1-ene (27.1 mL, 283 mmol) and *p*TsOH·H₂O (0.89 g, 4.72 mmol). After 15 min the temperature was raised to room temperature and the mixture was stirred for another 30 min. The mixture was diluted with saturated aqueous NaHCO₃ (10 mL) and concentrated *in vacuo* to yield **2** as a yellow solid, which was used without purification. TLC (CH₂Cl₂:MeOH, 9:1 v/v): R_f = 0.67. Spectral data were in correspondence with reported data in literature²⁶.

(R)-*N*-{3-[methoxy(methyl)amino]-3-oxopropyl}-2,2,5,5-tetramethyl-1,3-dioxane-4-carboxamide (**3**)

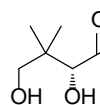
To a solution of **2** (1.80 g, 6.92 mmol) in dry CH₂Cl₂ (65 mL) at room temperature were added EDC·HCl (2.09 g, 10.9 mmol), *N,N*-dimethylhydroxylamine·HCl (1.04 g, 10.7 mmol) and DIPEA (3.43 mL, 19.6 mmol), followed by DMAP (483 mg, 3.95 mmol). The reaction mixture was stirred overnight at room temperature, quenched with saturated aqueous NH₄Cl (40 mL), extracted with CH₂Cl₂ (3 × 50 mL), dried over Na₂SO₄ and concentrated *in vacuo*. The product was purified by flash column chromatography (MeOH:CH₂Cl₂, 0:1→1:4 v/v) to afford **3** (1.90 g, 91%) as a colorless oil. TLC (MeOH:CH₂Cl₂, 1:9 v/v): R_f = 0.56; [α]_D = +44.5 (c 1.32, CH₂Cl₂); IR (ATR): 3417, 3334, 2980, 2940, 2871, 1661, 1520, 1378, 1196, 1095, 873 cm⁻¹; ¹H NMR (400 MHz, CDCl₃): δ 7.13 (t, *J* = 5.7 Hz, 1H), 4.07 (s, 1H), 3.68 (d, *J* = 11.7 Hz, 1H), 3.67 (s, 3H), 3.64–3.48 (m, 2H), 3.27 (d, *J* = 11.7 Hz, 1H), 3.18 (s, 3H), 2.76–2.59 (m, 2H), 1.46 (s, 3H), 1.42 (s, 3H), 1.03 (s, 3H), 0.96 (s, 3H); ¹³C NMR (75 MHz, CDCl₃): δ 172.9, 169.9, 99.0, 77.1, 71.5, 61.2, 34.0, 33.0, 32.1, 31.8, 29.4, 22.1, 18.8, 18.7; HRMS (ESI) *m/z*: [M+Na]⁺ calcd. for C₁₄H₂₆N₂O₅Na, 325.1739; found, 325.1746.

(R)-2,2,5,5-tetramethyl-*N*-(3-oxohept-6-en-1-yl)-1,3-dioxane-4-carboxamide (**4a**)

To a solution of **3** (2.10 g, 6.95 mmol) in a mixture of dry Et₂O/THF (70 mL, 1:1 v/v) at 0 °C, was added dropwise 3-butenylmagnesium bromide (28.0 mL of a 0.5 M solution in THF, 13.9 mmol). After 15 min the reaction mixture was allowed to warm to rt and stirred for 4 h. Next, saturated aqueous NH₄Cl was added to quench the reaction, followed by extraction with CH₂Cl₂ (3 × 70 mL). The organic layers were combined, dried (Na₂SO₄), and concentrated *in vacuo*. The product was purified by flash column chromatography (EtOAc/heptane, 0:1→1:2) to afford **4a** (1.23 g, 59%) as a colorless oil. TLC (MeOH:CH₂Cl₂, 1:9 v/v): R_f = 0.86; [α]_D = +44.1 (c 1.38, CH₂Cl₂); IR (ATR) 3421, 2915, 2849, 1709, 1666, 1519, 1377, 1092, 871, 701 cm⁻¹; ¹H NMR (400 MHz, CDCl₃): δ 6.96–6.87 (m, 1H), 5.79 (ddt, *J* = 16.7, 10.2, 6.5 Hz, 1H), 5.05–4.96 (m, 2H), 4.05 (s, 1H), 3.68 (d, *J* = 11.7 Hz, 1H), 3.58–3.42 (m, 2H), 3.27 (d, *J* = 11.7 Hz, 1H), 2.68 (t, *J* = 6.0 Hz, 2H), 2.53–2.49 (m, 2H), 2.36–2.30 (m, 2H), 1.46 (s, 3H), 1.41 (s, 3H), 1.04 (s, 3H), 0.95 (s, 3H); ¹³C NMR (75 MHz, CDCl₃): δ 209.2, 169.9, 136.9, 115.6, 99.1, 77.3, 71.6, 42.3, 42.1, 33.4, 33.1, 29.6, 27.8, 22.3, 19.0, 18.8; HRMS

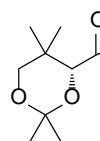
(ESI) m/z : $[M+Na]^+$ calcd. for $C_{16}H_{27}NO_4Na$, 320.1838; found, 320.1837.

(R)-2,4-dihydroxy-3,3-dimethyl-*N*-(3-oxohept-6-en-1-yl)butanamide (**RR2**)

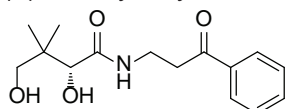


To a solution of **4a** (30 mg, 0.10 mmol) in MeCN (1.0 mL) was added, $BiCl_3$ (6.5 mg, 20 mol%), followed by demineralized H_2O (36 μ L, 20 equiv). The reaction was stirred at room temperature for 4 h, then filtered and concentrated *in vacuo*. After dilution with EtOAc (10 mL), the reaction mixture was washed with saturated aqueous $NaHCO_3$ (2×8 mL) and the aqueous layer was extracted with EtOAc (3×8 mL). The organic layers were combined, dried over Na_2SO_4 and concentrated *in vacuo*. The product was purified by flash column chromatography (EtOAc/heptane, 1:1 \rightarrow 1:0) to afford **RR2** (24 mg, 92%) as a colorless oil. TLC (MeOH: CH_2Cl_2 , 1:9 v/v): R_f = 0.52; $[\alpha]_D = +32.6$ (c 1.18, CH_2Cl_2); IR (ATR) 3347, 2955, 2872, 1706, 1646, 1532, 1079, 1041, 919 cm^{-1} ; 1H NMR (400 MHz, $CDCl_3$): δ 7.25 (t, J = 6.0 Hz, 1H), 5.78 (ddt, J = 16.7, 10.2, 6.5 Hz, 1H), 5.03 (ddd, J = 16.7, 3.4, 1.3 Hz, 1H), 4.99 (ddd, J = 10.2, 3.4, 1.3 Hz, 1H), 4.16 (d, J = 4.5 Hz, 1H), 3.98 (d, J = 4.3 Hz, 1H), 3.66 (bs, 1H), 3.59-3.45 (m, 4H), 2.70 (t, J = 5.9 Hz, 2H), 2.53 (t, J = 7.4 Hz, 2H), 2.35-2.30 (m, 2H), 0.98 (s, 3H) 0.89 (s, 3H); ^{13}C NMR (75 MHz, $CDCl_3$): δ 209.6, 173.4, 136.8, 115.6, 77.6, 71.2, 42.2, 42.0, 39.4, 33.8, 27.7, 21.4, 20.4; HRMS (ESI) m/z : $[M+H]^+$ calcd. for $C_{13}H_{24}NO_4$, 258.1705; found, 258.1699.

(R)-2,2,5,5-tetramethyl-*N*-(3-oxo-3-phenylpropyl)-1,3-dioxane-4-carboxamide (**4b**)

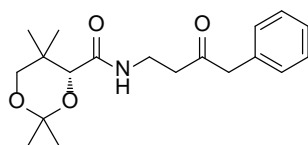


To a cooled (0 $^{\circ}C$) solution of **3** (266 mg, 0.88 mmol) in dry THF (5.0 mL) was added phenylmagnesium bromide (0.88 mL, 2.6 mmol, 3M solution in Et_2O) over a period of 5 min. The mixture was allowed to warm to room temperature and after 2 h more phenylmagnesium bromide (1 equiv.) was added. The reaction mixture was stirred for an additional hour and then quenched with a mixture of saturated aqueous NH_4Cl (25 mL) and water (5 mL) and extracted twice with EtOAc (30 and 10 mL). The combined organic phases were washed with saturated aqueous NH_4Cl (20 mL) and brine (20 mL), dried over Na_2SO_4 and concentrated *in vacuo*. The crude product was purified by flash column chromatography (EtOAc/heptane = 1:2 \rightarrow 1:1 \rightarrow 2:1) yielding **4b** as a colorless oil (209 mg, 74%). TLC (EtOAc:heptane, 3:1 v/v): R_f = 0.61; $[\alpha]_D = +53.4$ (c 0.98, CH_2Cl_2); IR (ATR) 3429, 2993, 2945, 2872, 1674, 1521, 1377, 1218, 1197, 1159, 1096, 873, 755, 690, 615 cm^{-1} ; 1H NMR (400 MHz, $CDCl_3$): δ 7.95 (m, 2H), 7.58 (m, 1H), 7.47 (m, 2H), 7.05 (br s, 1H), 4.07 (s, 1H), 3.76-3.62 (m, 3H), 3.27-3.22 (m, 3H), 1.47 (s, 3H); 1.41 (s, 3H), 1.04 (s, 3H), 0.92 (s, 3H); ^{13}C NMR (75 MHz, $CDCl_3$): δ 198.8, 169.8, 136.5, 133.3, 128.6, 127.9, 98.9, 77.1, 71.4, 38.1, 33.6, 32.9, 29.4, 22.1, 18.8, 18.6; HRMS (ESI) m/z : $[M+Na]^+$ calcd. for $C_{18}H_{25}NO_4Na$, 342.1681; found, 342.1689.

(R)-2,4-dihydroxy-3,3-dimethyl-N-(3-oxo-3-phenylpropyl)butanamide (CXP14.1-037)

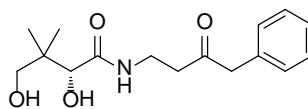
A solution of **4b** (236 mg, 0.739 mmol) in AcOH (3 mL) and H₂O (1.5 mL) was stirred for 5 h at room temperature. The solution was poured carefully into a stirring mixture of saturated aqueous NaHCO₃ (60 mL) and EtOAc (100 mL). The organic layer was

washed with saturated aqueous NaHCO₃ (30 mL) and brine (30 mL), dried over Na₂SO₄ and concentrated *in vacuo*. Purification was performed by flash column chromatography (EtOAc), yielding **CXP14.1-037** as a colorless oil (159 mg, 77%). TLC (EtOAc:heptane, 3:1 v/v): R_f = 0.21; [α]_D = +34.5 (c 0.32, CH₂Cl₂)²⁷ [α]_D = +37.1 (c 1.00, EtOH); IR (ATR) 3356, 2962, 2876, 1674, 1644, 1527, 1441, 1359, 1212, 1069, 1043, 750, 685 cm⁻¹; ¹H NMR (400 MHz, CDCl₃): δ 7.96 (m, 2H), 7.59 (m, 1H), 7.48 (m, 2H), 7.22 (br s, 1H), 4.00 (d, *J* = 5.2 Hz, 1H), 3.73 (AB d, *J* = 6.0 Hz, 2H), 3.49 (AB dd, *J* = 11.2, 5.8 Hz, 2H), 3.30 (d, *J* = 5.2 Hz, 1H), 3.26 (dd, *J* = 6.0, 5.2 Hz, 2H), 2.87 (t, *J* = 5.8 Hz, 1H), 1.00 (s, 3H), 0.88 (s, 3H); ¹³C NMR (75 MHz, CDCl₃): δ 199.1, 173.4, 136.2, 133.5, 128.6, 127.9, 77.4, 71.0, 39.2, 38.0, 34.0, 21.1, 20.1; HRMS (ESI) *m/z*: [M+Na]⁺ calcd. for C₁₅H₂₁NO₄Na, 302.1368; found, 302.1366.

(R)-2,2,5,5-tetramethyl-N-(3-oxo-5-phenylbutyl)-1,3-dioxane-4-carboxamide (**4c**)

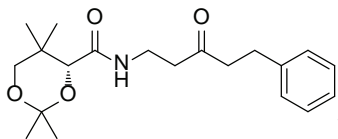
Prepared as described for **4a**, starting from **3** (412 mg, 1.36 mmol) and benzylmagnesium chloride (3.41 mL of a 2.0 M solution in THF, 6.81 mmol). Purification by flash column chromatography (EtOAc/heptane, 1:2→2:1) afforded **4c** (384 mg, 85%) as a colorless oil. TLC (EtOAc): R_f = 0.69; [α]

_D = +41.1 (c 1.15, CH₂Cl₂); IR (ATR) 3430, 2993, 2950, 2868, 2358, 1713, 1670, 1522, 1377, 1196, 1095 cm⁻¹; ¹H NMR (300 MHz, CDCl₃): δ 7.35–7.17 (m, 5H), 6.88 (m, 1H), 4.02 (s, 1H), 3.68 (s, 2H), 3.65 (d, *J* = 11.7 Hz, 1H), 3.55–3.38 (m, 2H), 3.25 (d, *J* = 11.7 Hz, 1H), 2.73–2.64 (m, 2H), 1.45 (s, 3H), 1.40 (s, 3H), 1.01 (s, 3H), 0.88 (s, 3H); ¹³C NMR (75 MHz, CDCl₃): δ 207.4, 169.8, 133.8, 129.4, 128.9, 127.3, 99.1, 77.1, 71.5, 50.3, 41.5, 33.3, 33.0, 29.5, 22.2, 18.9, 18.8; HRMS (ESI) *m/z*: [M+H]⁺ calcd. for C₁₉H₂₈NO₄, 334.2018; found, 334.2017.

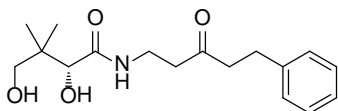
(R)-2,4-dihydroxy-3,3-dimethyl-N-(3-oxo-5-phenylbutyl)butanamide (**RR6**)

Prepared as described for **RR2**, starting from **4c** (367 mg, 1.10 mmol). Flash column chromatography (EtOAc/heptane, 0:1→1:0) afforded **RR6** (197 mg, 61%) as a colorless oil.

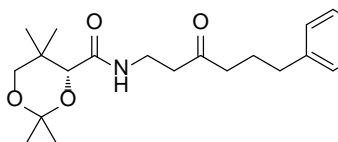
TLC (EtOAc): R_f = 0.30; [α]_D = +28.7 (c 1.17, CH₂Cl₂); IR (ATR) 3372, 3058, 3036, 2960, 2868, 1710, 1643, 1530, 1496, 1453, 1366, 1287, 1076, 1041 cm⁻¹; ¹H NMR (300 MHz, CDCl₃): δ 7.36–7.18 (m, 5H), 7.04 (m, 1H), 3.93 (d, *J* = 4.5 Hz, 1H), 3.69 (s, 2H), 3.52–3.45 (m, 2H), 3.47–3.30 (m, 3H), 2.90 (br s, 1H), 2.73 (t, *J* = 5.8 Hz, 2H), 0.96 (s, 3H), 0.83 (s, 3H); ¹³C NMR (75 MHz, CDCl₃): δ 207.9, 173.2, 133.7, 129.5, 129.0, 127.4, 77.6, 71.3, 50.3, 41.4, 39.4, 33.8, 21.5, 20.3. HRMS (ESI) *m/z*: [M+H]⁺ calcd. for C₁₆H₂₄NO₄, 294.1705; found, 294.1694.

(R)-2,2,5,5-tetramethyl-*N*-(3-oxo-5-phenylpentyl)-1,3-dioxane-4-carboxamide (**4d**)

Prepared as described for **4a**, starting from compound **3** (1.03 g, 3.40 mmol) and phenethylmagnesium chloride (1.0 M solution in THF) (6.96 mL, 6.96 mmol). The reaction was completed in 2 h. Purification by flash column chromatography yielded **4d** (754 mg, 64%) as colorless oil. TLC (EtOAc): $R_f = 0.71$; $[\alpha]_D^{25} = +37.7$ (c 1.07, CH_2Cl_2); IR (ATR): 3426, 3334, 2989, 2952, 2870, 2362, 2332, 1712, 1671, 1521, 1377, 1197, 1095 cm^{-1} ; ^1H NMR (300 MHz, CDCl_3): δ 7.30-6.94 (m, 5H), 6.94-6.90 (m, 1H), 4.05 (s, 1H), 3.67 (d, $J = 11.7$ Hz, 1H), 3.58-3.39 (m, 2H), 3.27 (d, $J = 11.7$ Hz, 1H), 2.90 (m, 2H), 2.76-2.70 (m, 2H), 2.65 (t, $J = 6.0$ Hz, 2H), 1.47 (s, 3H), 1.41 (s, 3H), 1.03 (s, 3H), 0.93 (s, 3H); ^{13}C NMR (75 MHz, CDCl_3): δ 209.0, 169.9, 140.9, 128.7, 128.4, 126.3, 99.2, 77.3, 71.6, 44.5, 42.4, 33.4, 33.1, 29.8, 29.6, 22.3, 19.0, 18.8; HRMS (ESI) m/z : $[\text{M}+\text{H}]^+$ calcd. for $\text{C}_{20}\text{H}_{30}\text{NO}_4$, 348.2175; found, 348.2175.

(R)-2,4-dihydroxy-3,3-dimethyl-*N*-(3-oxo-5-phenylpentyl)butanamide (**RR7**)

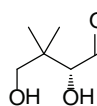
Prepared as described for **RR2**, starting from compound **4d** (366 mg, 1.05 mmol), yielding **RR7** (260 mg, 80%) as colorless oil. TLC (EtOAc): $R_f = 0.33$; $[\alpha]_D^{25} = +28.6$ (c 1.61, CH_2Cl_2); IR (ATR): 3354, 2933, 2859, 1708, 1644, 1529, 1452, 1369, 1287, 1075, 1041 cm^{-1} ; ^1H NMR (300 MHz, CDCl_3): δ 7.31-7.15 (m, 5H), 7.09 (m, 1H), 3.96 (s, 1H), 3.58 (br s, 1H), 3.54-3.42 (m, 4H), 3.12 (br s, 1H), 2.92-2.87 (m, 2H), 2.78-2.72 (m, 2H), 2.66 (t, $J = 5.8$ Hz, 2H), 0.99 (s, 3H), 0.87 (s, 3H). ^{13}C NMR (75 MHz, CDCl_3): δ 209.4, 173.1, 140.8, 128.7, 128.4, 126.4, 77.7, 71.3, 44.4, 42.3, 39.5, 33.9, 29.7, 21.6, 20.3. HRMS (ESI) m/z : $[\text{M}+\text{H}]^+$ calcd. for $\text{C}_{17}\text{H}_{26}\text{NO}_4$, 308.1861; found 308.1851.

(R)-2,2,5,5-tetramethyl-*N*-(3-oxo-6-phenylhexyl)-1,3-dioxane-4-carboxamide (**4e**)

Magnesium (1.00 g, 41.2 mmol, 12.0 equiv) was stirred in Et_2O (20 mL) with three drops 1,2-dibromoethane and heated briefly. (3-bromopropyl)benzene (3.08 mL, 20.2 mmol, 6.0 equiv) was dissolved in Et_2O (20 mL) and added dropwise to the magnesium over a period of 15 min. The hazy solution was stirred at room temperature for 2 h. The Grignard reagent was added dropwise to a cooled (0°C) solution of compound **3** (1.02 g, 3.37 mmol) in THF (20 mL) and stirred at 0°C for 3.5 h. The reaction mixture was quenched with saturated aqueous NH_4Cl (100 mL) and extracted with CH_2Cl_2 (3×70 mL). The combined organic layers were dried over Na_2SO_4 and concentrated *in vacuo*. The crude product was purified by flash column chromatography (heptane/EtOAc, 1:0 \rightarrow 1:1), yielding compound **4e** (950 mg, 78%) as a colorless oil. TLC (EtOAc): $R_f = 0.70$; $[\alpha]_D^{25} = +34.4$ (c 1.23, CH_2Cl_2); IR (ATR): 3421, 2997, 2947, 2872, 1710, 1672, 1522, 1454, 1377, 1260, 1222, 1197, 1159, 1096 cm^{-1} ; ^1H NMR (300 MHz, CDCl_3): δ 7.31-7.14 (m, 5H), 6.92 (m, 1H), 4.05 (s, 1H), 3.67 (d, $J = 11.7$ Hz, 1H), 3.56-3.41 (m, 2H), 3.27 (d, $J = 11.7$ Hz, 1H), 2.64 (t, $J = 6.1$ Hz, 2H), 2.61 (t, $J = 6.0$ Hz, 2H), 2.41 (t, $J = 7.3$ Hz, 2H), 1.91 (app. quintet, $J = 7.7$ Hz, 2H), 1.45 (s, 3H), 1.40 (s, 3H), 1.03 (s, 3H), 0.94 (s, 3H); ^{13}C NMR (75 MHz, CDCl_3): δ 209.8,

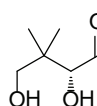
169.9, 141.5, 128.6, 128.5, 126.2, 99.2, 77.3, 71.6, 42.2, 42.1, 35.1, 33.5, 33.1 29.6, 25.3, 22.3, 19.0, 18.8. HRMS (ESI) m/z : $[M+H]^+$ calcd. for $C_{21}H_{32}NO_4$, 362.2331; found, 362.2352.

(R)-2,4-dihydroxy-3,3-dimethyl-N-(3-oxo-6-phenylhexyl)butanamide (RR8)



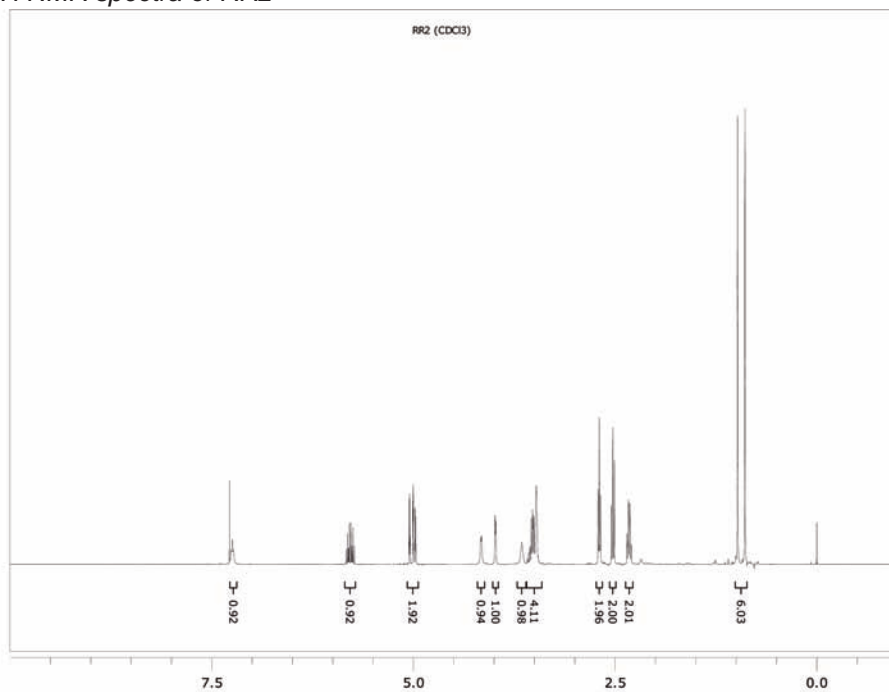
Prepared as described for **RR2**, starting from compound **4e** (380 mg, 1.05 mmol), yielding **RR8** (268 mg, 79%) as colorless oil. TLC (EtOAc): $R_f = 0.36$; $[\alpha]_D^{25} = +26.6$ (c 1.16, CH_2Cl_2); IR (ATR): 3358, 3028, 2946, 2868, 1708, 1643, 1530, 1453, 1368, 1269 cm^{-1} ; 1H NMR (300 MHz, $CDCl_3$): δ 7.31–7.05 (m, 6H), 3.98 (s, 1H), 3.54–3.43 (m, 5H), 3.04 (br s, 1H), 2.66–2.59 (m, 4H), 2.42 (t, $J = 7.4$ Hz, 2H), 1.91 (app. quintet, $J = 7.5$ Hz, 2H), 1.00 (s, 3H), 0.88 (s, 3H); ^{13}C NMR (75 MHz, $CDCl_3$): δ 210.2, 173.1, 141.5, 128.6, 126.2, 77.7, 71.3, 42.2, 42.1, 39.5, 35.1, 33.9, 25.2, 21.5, 20.3; HRMS (ESI) m/z : $[M+H]^+$ calcd. for $C_{18}H_{28}NO_4$, 322.2018; found, 322.2009.

(2R/S)-2,4-dihydroxy-N-(3-hydroxy-4-phenylbutyl)-3,3-dimethylbutanamide (CXP14.1-034)

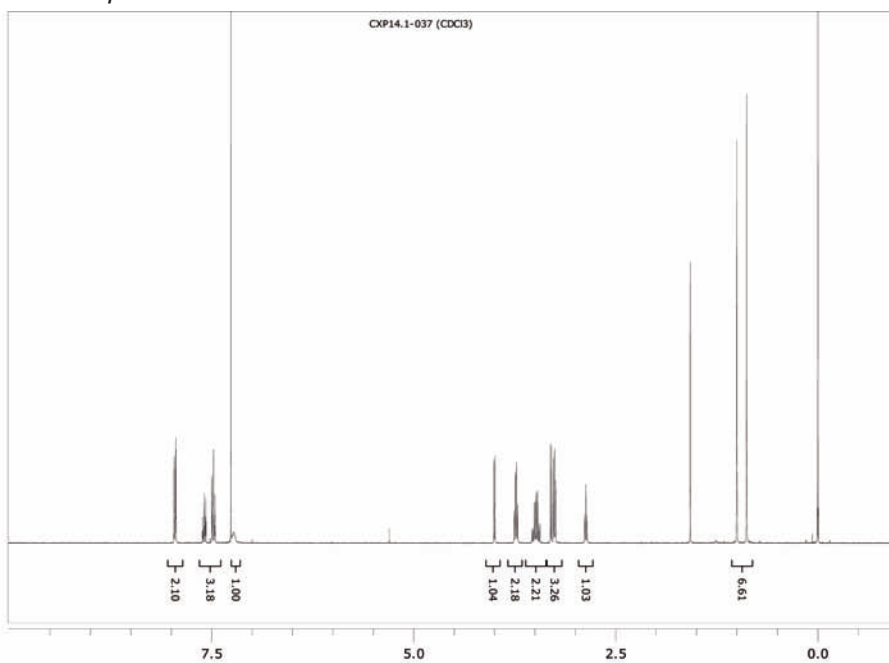


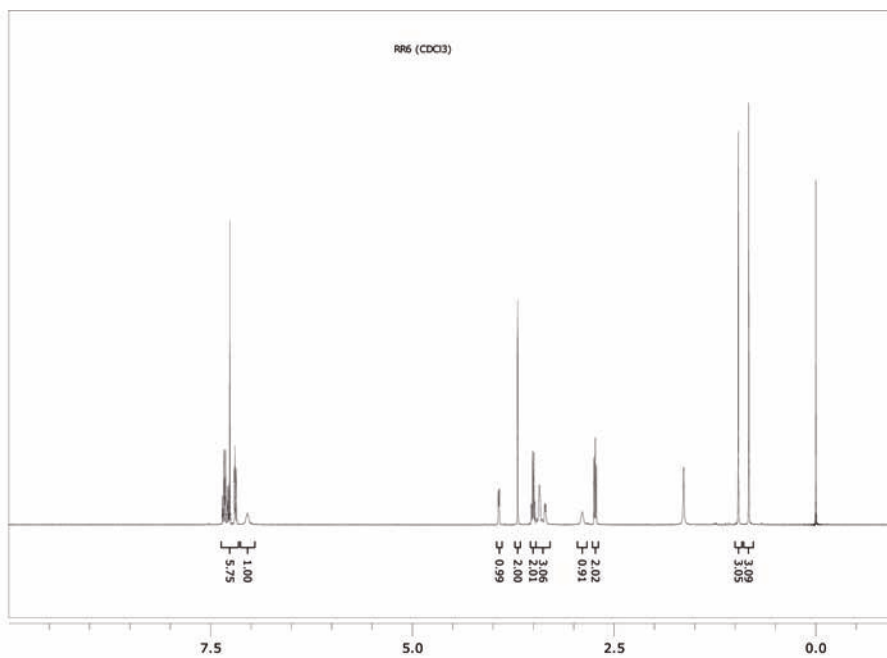
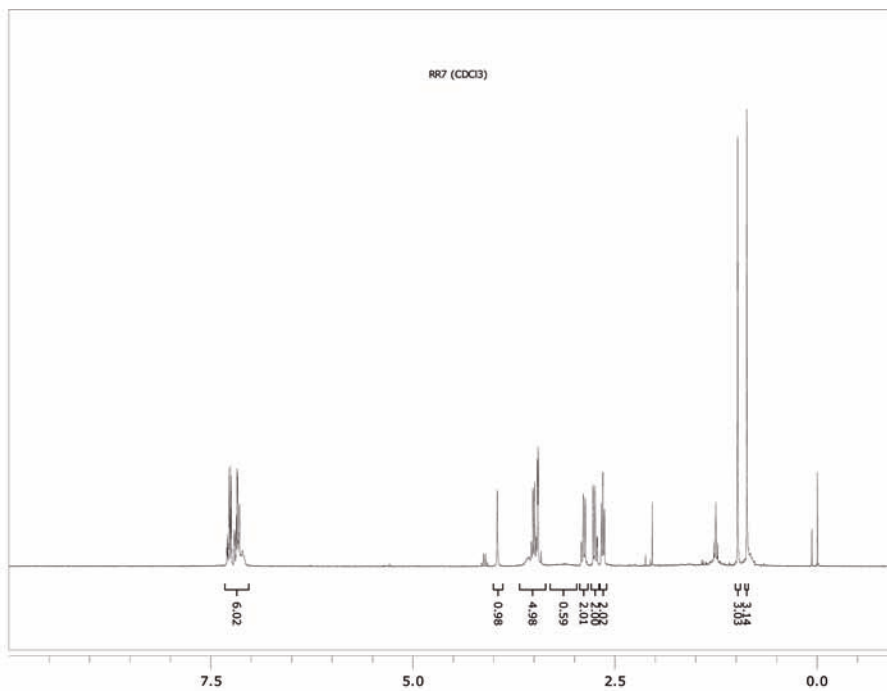
To a cooled solution (0 °C) of **RR6** (108 mg, 0.37 mmol) in MeOH (3 mL) was carefully added $NaBH_4$ (27.9 mg, 0.74 mmol) over a period of 10 min. The mixture was stirred for 15 min at 0 °C, followed by 15 min at room temperature, before it was diluted with EtOAc (15 mL) and washed with a mixture of saturated aqueous NH_4Cl (15 mL) and H_2O (2 mL). The aqueous phase was extracted with EtOAc (2 × 10 mL). The combined organic layers were washed with brine (10 mL), dried over Na_2SO_4 and concentrated *in vacuo*. Purification by flash column chromatography (EtOAc/MeOH, 40:1→20:1→9:1→5:1 v/v) yielded **CXP14.1-034** as a 1:1 mixture of diastereomers as a colorless oil (89 mg, 75%). TLC (EtOAc): $R_f = 0.11$; IR (ATR) 3308, 2928, 2872, 1636, 1532, 1454, 1272, 1216, 1078, 1039, 737, 702 cm^{-1} ; 1H NMR (400 MHz, $CDCl_3$) δ 7.33–7.18 (m, 2 × 5H), 7.10 (br s, 2 × 1H), 4.02 (s, 2 × 1H), 3.87 (s, 2 × 1H), 3.71 (m, 2 × 1H), 3.49 (m, 2 × 3H), 3.25 (m, 2 × 1H), 2.96–2.84 (m, 2 × 2H), 2.78 (m, 2 × 2H), 1.75 (m, 2 × 1H), 1.61 (m, 2 × 1H), 1.04 (s, 3H), 1.02 (s, 3H), 0.94 (s, 3H), 0.92 (s, 3H); ^{13}C NMR (75 MHz, $CDCl_3$): δ 173.9, 173.8, 138.2 (2C), 129.4 (2C), 129.3 (2C), 128.5 (4C), 126.4 (2C), 77.4 (2C), 71.0 (2C), 70.6 (2C), 43.9, 43.8, 39.3, 39.2, 36.4, 36.3, 36.0 (2C), 21.2, 21.2, 20.4, 20.3; HRMS (ESI) m/z : $[M+Na]^+$ calcd. for $C_{16}H_{25}NO_4Na$, 318.1681; found, 318.1681.

¹H NMR spectra of RR2

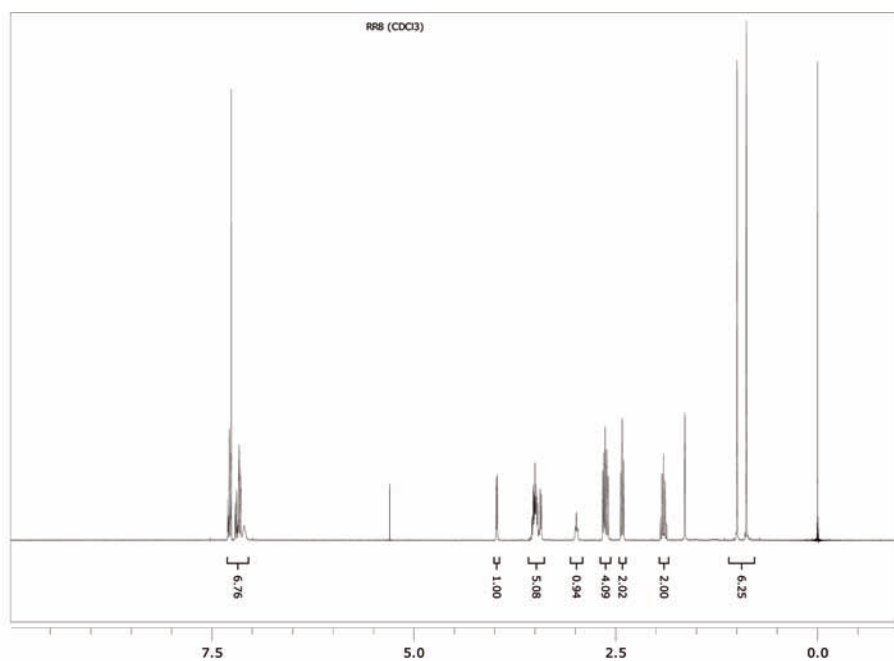


¹H NMR spectra of CXP14.1-037

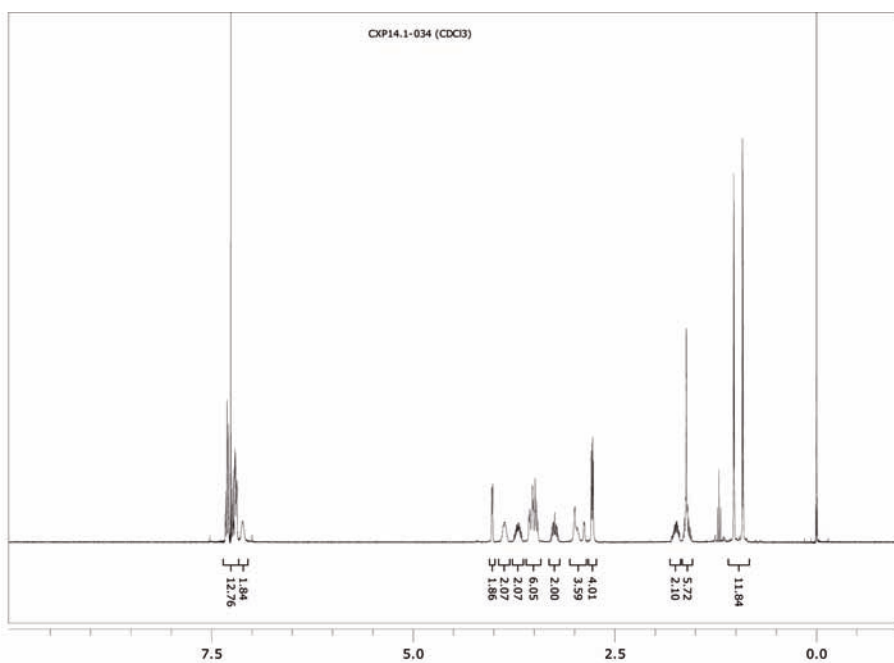


^1H NMR spectra of RR6 ^1H NMR spectra of RR7

¹H NMR spectra of RR8



¹H NMR spectra of CXP14.1-034



References

1. Maras B, Barra D, Dupre S, Pitari G. Is pantetheinase the actual identity of mouse and human vanin-1 proteins? *FEBS Lett* 461, 149-52 (1999)
2. Kaskow BJ, Proffitt JM, Blangero J, Moses EK, Abraham LJ. Diverse biological activities of the vascular non-inflammatory molecules - the Vanin pantetheinases. *Biochem Biophys Res Commun* 417, 653-8 (2012)
3. Martin F, Malergue F, Pitari G, Philippe JM, Philips S, Chabret C *et al.* Vanin genes are clustered (human 6q22-24 and mouse 10A2B1) and encode isoforms of pantetheinase ectoenzymes. *Immunogenetics* 53, 296-306 (2001)
4. Pitari G, Malergue F, Martin F, Philippe JM, Massucci MT, Chabret C *et al.* Pantetheinase activity of membrane-bound Vanin-1: lack of free cysteamine in tissues of Vanin-1 deficient mice. *FEBS Lett* 483, 149-54 (2000)
5. Brenner C. Catalysis in the nitrilase superfamily. *Curr Opin Struct Biol* 12, 775-82 (2002)
6. Leonardi R, Zhang YM, Rock CO, Jackowski S. Coenzyme A: back in action. *Prog Lipid Res.* 44, 125-53 (2005)
7. Martin F, Penet MF, Malergue F, Lepidi H, Dessein A, Galland F *et al.* Vanin-1(-/-) mice show decreased N. *J Clin Invest* 113, 591-97 (2004)
8. Berruyer C, Martin FM, Castellano R, Maccone A, Malergue F, Garrido-Urbani S *et al.* Vanin-1-/- mice exhibit a glutathione-mediated tissue resistance to oxidative stress. *Mol Cell Biol.* 24, 7214-24 (2004)
9. Berruyer C, Pouyet L, Millet V, Martin FM, LeGoffic A, Canonici A *et al.* Vanin-1 licenses inflammatory mediator production by gut epithelial cells and controls colitis by antagonizing peroxisome proliferator-activated receptor gamma activity. *J Exp Med* 203, 2817-27 (2006)
10. Min-Oo G, Fortin A, Pitari G, Tam M, Stevenson MM, Gros P. Complex genetic control of susceptibility to malaria: positional cloning of the Char9 locus. *J Exp Med* 204, 511-24 (2007)
11. Jansen PA, kamsteeg M, Rodijk-Olthuis D, van Vlijmen-Willems IM, de Jongh GJ, Bergers M *et al.* Expression of the vanin gene family in normal and inflamed human skin: induction by proinflammatory cytokines. *J Invest Dermatol.* 129, 2167-74 (2009)
12. Pouyet L, Roisin-Bouffay C, Clement A, Millet V, Garcia S, Chasson L *et al.* Epithelial vanin-1 controls inflammation-driven carcinogenesis in the colitis-associated colon cancer model. *Inflamm Bowel Dis.* 16, 96-104 (2010)
13. Dammanahalli KJ, Stevens S, Terkeltaub R. Vanin-1 pantetheinase drives smooth muscle cell activation in post-arterial injury neointimal hyperplasia. *PLoS One* 7, e39106 (2012)
14. Yamazaki K, Kuromitsu J, Tanaka I. Microarray analysis of gene expression changes in mouse liver induced by peroxisome proliferator- activated receptor alpha agonists. *Biochem Biophys Res Commun* 290, 1114-22 (2002)
15. Rakhshandehroo M, Knoch B, Muller M, Kersten S. Peroxisome proliferator-activated receptor alpha target genes. *PPAR Res*, 612089 (2010)
16. Ruan BH, Cole DC, Wu P, Quazi A, Page K, Wright JF *et al.* A fluorescent assay suitable for inhibitor screening and vanin tissue quantification. *Anal Biochem.* 399, 284-92 (2010)

17. Lee JT, Chen DY, Yang Z, Ramos AD, Hsieh JJ, Bogyo M. Design, syntheses, and evaluation of Taspase1 inhibitors. *Bioorg Med Chem Lett* 19, 5086-90 (2009)
18. Suzuki K, Watanabe T, Sakurai S, Ohtake K, Kinoshita T, Araki A *et al.* A novel glycosylphosphatidyl inositol-anchored protein on human leukocytes: a possible role for regulation of neutrophil adherence and migration. *J Immunol* 162, 4277-84 (1999)
19. Huang J, Takeda Y, Watanabe T, Sendo F. A sandwich ELISA for detection of soluble GPI-80, a glycosylphosphatidyl-inositol (GPI)-anchored protein on human leukocytes involved in regulation of neutrophil adherence and migration--its release from activated neutrophils and presence in synovial fluid of rheumatoid arthritis patients. *Microbiol Immunol* 45, 467-71 (2001)
20. Bocos C, Herrera E. Pantethine stimulates lipolysis in adipose tissue and inhibits cholesterol and fatty acid synthesis in liver and intestinal mucosa in the normolipidemic rat. *Environ Toxicol Pharmacol* 6, 59-66 (1998)
21. Rumberger JA, Napolitano J, Azumano I, Kamiya T, Evans M. Pantethine, a derivative of vitamin B(5) used as a nutritional supplement, favorably alters low-density lipoprotein cholesterol metabolism in low- to moderate-cardiovascular risk North American subjects: a triple-blinded placebo and diet-controlled investigation. *Nutr Res* 31, 608-15 (2011)
22. Broda E, Baumgartner ER, Scholl S, Stopsack M, Horn A, Rhode H. Biotinidase determination in serum and dried blood spots--high sensitivity fluorimetric ultramicro-assay. *Clin Chim Acta* 314, 175-85 (2001)
23. Cheng T, Hitomi K, van Vlijmen-Willems IM, de Jongh GJ, Yamamoto K, Nishi K *et al.* Cystatin M/E is a high affinity inhibitor of cathepsin V and cathepsin L by a reactive site that is distinct from the legumain-binding site. A novel clue for the role of cystatin M/E in epidermal cornification. *J Biol Chem* 281, 15893-99 (2006)
24. Lennon G, Auffray C, Polymeropoulos M, Soares MB. The I.M.A.G.E. Consortium: an integrated molecular analysis of genomes and their expression. *Genomics* 33, 151-2 (1996)
25. Aricescu AR, Lu W, Jones EY. A time- and cost-efficient system for high-level protein production in mammalian cells. *Acta crystallogr D Biol Crystallogr* 62, 1243-50 (2006)
26. Sewell AL, Villa MV, Matheson M, Whittingham WG, Marquez R. Fast and flexible synthesis of pantothenic acid and CJ-15,801. *Org Lett* 13, 800-3 (2011)
27. Lutz RE, Wilson JW 3th, Deinet AJ, Harnest GH, Martin GH, Freek JA. Antimalarials; amides related to phenylpantothenone. *J Org Chem* 12, 96-107. (1947)

Combination of pantothenamides with vanin inhibitors: a novel antibiotic strategy against gram-positive bacteria

8
CHAPTER



Patrick AM Jansen¹
Pedro HH Hermkens²
Patrick LJM Zeeuwen¹
Peter NM Botman³
Richard H Blaauw³
Peter Burghout⁴
Peter M van Galen²
Johan W Mouton⁵
Floris PJT Rutjes²
Joost Schalkwijk¹

¹ Department of Dermatology and Nijmegen Centre for Molecular Life Sciences, Radboud University Nijmegen Medical Centre, The Netherlands

² Department of Synthetic Organic Chemistry, Institute for Molecules and Materials, Radboud University Nijmegen, The Netherlands

³ Chiralix B.V., Nijmegen, The Netherlands

⁴ Laboratory of Pediatric Infectious Diseases, Radboud University Nijmegen Medical Centre, The Netherlands

⁵ Department of Medical Microbiology, Radboud University Nijmegen Medical Centre, The Netherlands

Abstract

The emergence of resistance against current antibiotics calls for the development of new compounds to treat infectious diseases. Synthetic pantothenamides are pantothenate analogs that possess broad spectrum antibacterial activity *in vitro* in minimal media. Pantothenamides were shown to be substrates of the bacterial coenzyme A (CoA) biosynthetic pathway, causing cellular CoA depletion and interference with fatty acid synthesis. In spite of their potential use and selectivity for bacterial metabolic routes, these compounds have never made it to the clinic. In the present study we show that pantothenamides are not active as antibiotics in the presence of serum, and we found that they were hydrolyzed by ubiquitous pantetheinases of the *vanin* family. To address this further, we synthesized a series of pantetheinase inhibitors based on a pantothenate scaffold that inhibited serum pantetheinase activity in the nanomolar range. Mass spectrometric analysis showed that addition of these pantetheinase inhibitors prevented hydrolysis of pantothenamides by serum. We found that combination of these novel pantetheinase inhibitors and prototypic pantothenamides like N5-Pan and N7-Pan exerted antimicrobial activity *in vitro* particularly against gram-positive bacteria (*Staphylococcus aureus*, *Streptococcus pneumoniae*) even in the presence of serum. These results indicate that pantothenamides, when protected against degradation by host pantetheinases, are potentially useful antimicrobial agents.

Introduction

There is a continuous battle between humans and microorganisms, and the development of resistance against current antibiotics creates a need to develop new drug scaffolds and targets¹. There are several classes of antibiotic-resistant pathogens that emerge as major threats. Methicillin-resistant and vancomycin-resistant *Staphylococcus aureus* strains (MRSA and VRSA), and multidrug-resistant *Streptococcus pneumoniae* are a serious health problem in both hospital settings and the community. Multidrug-resistant gram-negative bacteria (e.g. *Escherichia coli*, *Klebsiella pneumoniae* and *Pseudomonas aeruginosa*) are a second group of organisms that pose a threat of untreatable infections. Finally, poverty-related conditions such as tuberculosis and parasitic diseases, particularly important in developing countries are a cause of great concern, as the already limited number of treatment modalities is decreasing because of resistance. The development of new antibiotics has been slow, and most compounds to date have been derived from a limited number of molecular scaffolds targeting a few microbial molecular pathways. Discovery of new scaffolds and new targets should clearly be a priority, although the commercial prospects of antibiotics development are unfavorable¹.

In 1970, amides derived from pantothenic acid (vitamin B5), were reported to possess antibiotic activity *in vitro*². During the last decades many of these pantothenamides have been synthesized and the putative modes of action have been studied in detail³⁻¹⁰. Pantothenamides, of which N-pentylpantothenamide (N5-Pan) and N-heptylpantothenamide (N7-Pan) are the prototypes, are active against gram-negative² and gram-positive¹¹ bacteria, but they have also been shown to possess activity against fungi and malaria parasites^{2,8}. Pantothenamides were found to be substrates of the key rate-controlling enzyme pantothenate kinase (CoaA), and the rate of conversion of N5-Pan was found to be more rapid than that of pantothenate itself. This led to the conclusion that the mechanism for toxicity towards *E. coli* is due to the formation of CoA analogs that lead to the transfer of an inactive 4'-phosphopantothenamide moiety to acyl carrier protein (ACP) which is the first step in the bacterial type II route (FASII) of fatty acid synthesis^{10,12}. A recent study showed that N5-Pan causes a 10-fold reduction of cellular CoA levels in *E. coli*⁷. The same study also showed that ethyldethia-ACP, is readily hydrolyzed by ACP-phosphodiesterase (AcpH). Neither overexpression of CoA biosynthetic enzymes or pantothenate supplementation could relieve growth inhibition by N5-Pan. These findings indicate that the mechanisms by which pantothenamides inhibit bacterial viability are not yet completely resolved.

Mammalian pantetheinases have only recently been discovered. The first one that was cloned was the mouse vanin-1 (*Vnn1*) gene, which encoded a GPI-anchored leukocyte cell surface protein of unknown function¹³. Analysis of human vanins revealed three family members named VNN1, 2 and 3, clustered on chromosome 6¹⁴. The encoded proteins were shown to possess pantetheinase activity by the hydrolysis of pantetheine into pantothenic acid (vitamin B5) and

the low molecular weight thiol cysteamine¹⁵. We found vanin family members to be broadly expressed in nearly all human tissues¹⁶. On the basis of sequence similarities, vanins were classified as members of the biotinidase branch of the nitrilase superfamily¹⁷. The most obvious function of biotinidases and pantetheinases is that of amidases involved in vitamin recycling.

In the present paper we address the possible application of pantothenamides as antibiotics, considering the current knowledge on human pantetheinases. Based on the fact that vanins are active on the carbon-nitrogen bond of pantetheine, we hypothesized that antibiotic pantothenamides could also be hydrolyzed by pantetheinase activity, which was indeed found to be the case. We further show that inhibition of pantetheinase activity by novel chemotypes that we recently developed¹⁸, protects pantothenamides against hydrolysis thereby preserving their antibiotic activity. We thereby provide proof of concept that combination of pantetheinase inhibitors with pantothenamides might be a novel antimicrobial strategy.

Results

Pantothenamides are inactive as antibiotics in serum-containing medium

To test whether pantothenamides have antibiotic activity under physiological conditions, *E. coli* was cultured in minimal medium in the presence of complement-inactivated serum (in this case fetal bovine serum, but human serum gives similar results). Addition of the prototypic pantothenamide N5-Pan to log phase cultures of *E. coli* in the absence of serum shows the expected growth inhibiting properties as described before² (Figure 8.1). Addition of 1% and 10% serum dose-dependently abolishes the inhibitory effect of N5-Pan.

We next investigated if the effect of serum on pantothenamides was due to a heat-labile factor. Figure 8.2A shows that heat-inactivated serum (5 minutes at 100° C) is unable to interfere with N5-Pan mediated growth inhibition of *E. coli*. This made is very likely that the effect was due to one or more proteins present in serum.

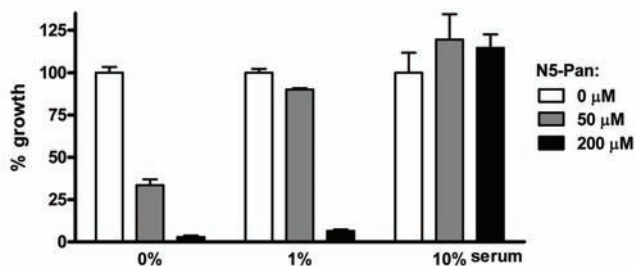


Figure 8.1 The effect of serum on pantothenamides. Growth inhibiting effect of N5-Pan on *E. coli* in media containing increasing amounts of serum. In serum-free medium a low concentration of N5-Pan is sufficient to inhibit bacterial growth, while in a 1% serum medium, a high concentration N5-Pan is needed for bacterial growth inhibition. In 10% serum a high concentration of N5-Pan is insufficient to be antibiotic. All samples N=4.

Pantothenamides are hydrolyzed in serum

Based on structural homology of pantothenamides with pantetheine and the knowledge that pantetheine is hydrolyzed by pantetheinases of the vanin family into pantothenic acid and cysteamine, we hypothesized that this class of enzymes could also hydrolyze pantothenamides. In a previous study we have shown that vanins are ubiquitously expressed¹⁶. Using an aminomethylcoumarine derivative of pantothenic acid, which is a pantothenamide with a fluorescent leaving group as a substrate¹⁹ pantetheinase activity in serum is readily detected. We found that this hydrolytic activity was completely abolished by heat-inactivation of the serum (Figure 8.2B).

Subsequently, we analyzed if known antibiotic pantothenamides are also hydrolyzed in the presence of serum. Mass spectrometric analysis of N7-Pan incubated in 1% serum for 24 h revealed a complete disappearance of the N7-Pan peak, whereas a clear peak of heptylamide, the expected hydrolysis product, appears (Figure 8.3A). This indicates that pantothenamides are indeed hydrolyzed in the presence of serum.

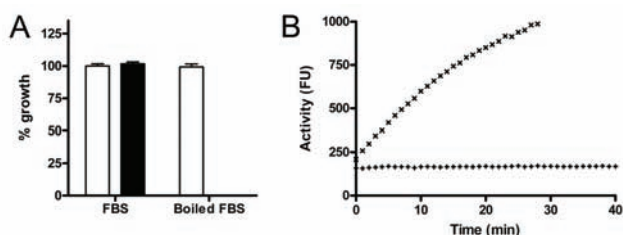


Figure 8.2 Inactivation of N5-Pan by serum is heat-labile (A) N5-Pan (64 $\mu\text{g/ml}$) (filled bars) does not inhibit growth of *E. coli* in the presence of FBS. Upon heat-inactivation of serum (5 min at 100°C) N5-Pan effectively inhibit bacterial growth. Open bars: bacterial growth without N5-Pan. All samples N=4. (B) Pantetheinase activity assay shows pantetheinase activity in serum (x), but none in inactivated serum (+), confirming that pantetheinases might be involved in pantothenamide inactivation.

Pantetheinase inhibitors prevent degradation of antibiotic pantothenamides in serum

We reasoned that inhibitors of serum pantetheinases could prevent degradation of pantothenamides in biological fluids thereby preserving their antibiotic activity. As there were no selective high-affinity (sub-nanomolar) pantetheinase inhibitors available, we designed and synthesized a number of new inhibitors starting from pantetheine, the natural substrate of pantetheinases, as a scaffold. Synthesis and characterization of these new chemotypes, pantetheine analogs lacking the hydrolysable amide bond, has recently been published elsewhere¹⁸. The most potent and selective inhibitor (RR6) showed an IC_{50} of 40 nM against pantetheinase activity present in human or bovine serum. See Table S8.1 for the structures and IC_{50} values of all compounds used here.

We next investigated if these pantetheinase inhibitors could protect pantothenamide antibiotics from hydrolysis by serum pantetheinase activity. Figure 8.3B shows mass spectrometric analysis of N7-Pan incubated in 1% serum

for 24 h in the presence of 256 $\mu\text{g/ml}$ RR6. Whereas in Figure 8.3A a complete disappearance of the N7-Pan peaks is observed and only the hydrolysis product heptylamine can be identified, Figure 8.3B shows that in the presence of RR6 the N7-Pan peaks are still present. Although we found a minor peak corresponding to heptylamide, we conclude that N7-Pan is clearly protected against hydrolysis by the addition of a pantetheinase inhibitor.

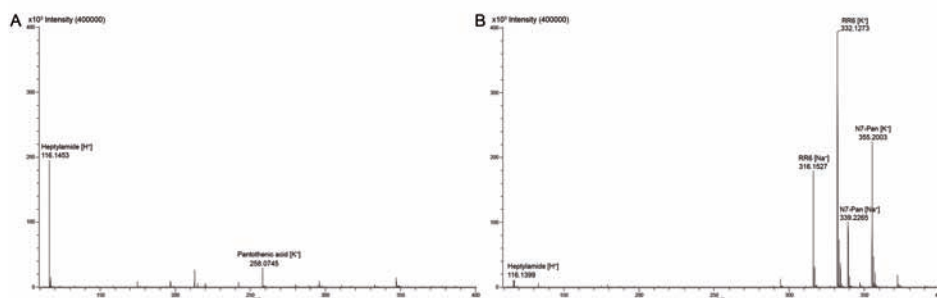


Figure 8.3 Hydrolysis of N7-Pan is inhibited RR6 (A) Mass spectrometric analysis of a sample containing 1% serum and N7-Pan after 24 hours incubation showed a heptylamine peak, but no N7-Pan-peak. Note that the produced pantothenic acid will only be partially visualized under the used settings. (B) Pantetheinase inhibitor RR6 is able to protect N7-Pan against hydrolysis as clear peaks corresponding to the N7-Pan adducts are shown on the mass spectrum. Also the RR6 adducts and a very small peak corresponding to heptylamine are detected. The reaction was performed in the same way as in (A).

In vitro antibiotic effects of combinations of pantothenamides and pantetheinase inhibitors

We next examined if inhibition of serum pantetheinase could preserve the antibiotic effect of the pantothenamides N5-Pan and N7-Pan which were previously reported to be active against bacterial strains of *E. coli* and *S. aureus* respectively. Figure 8.4 shows the effects of pantothenamides or a pantetheinase inhibitor (RR6) alone, and combinations of these. Addition of pantothenamides had no antibacterial effect in media with 10% FBS as shown before for N5-Pan (see Figure 8.1). Similarly, the pantetheinase inhibitor RR6 on its own did not affect bacterial growth of *E. coli* or *S. aureus*. Combination of RR6 with pantothenamides, however, showed a clear antimicrobial effect for N5-Pan on *E. coli* (Figure 8.4A) and for N7-Pan on *S. aureus* (Figure 8.4B). We performed checkerboard titration of pantothenamides and the pantetheinase inhibitor RR6 to obtain a range of MIC (minimum inhibitory concentration) values for the combined compounds as shown in Figure 8.4C. The protective effect of RR6 towards pantothenamides is clearly visible for both *E. coli* and *S. aureus*. The amount of pantothenamides decreased to MIC values in cultures without serum and RR6 (Figure 8.4D).

Specificity and toxicity of pantothenamide antibiotics and vanin inhibitors

The efficacy of pantothenamides has so far only been studied *in vitro* on a limited

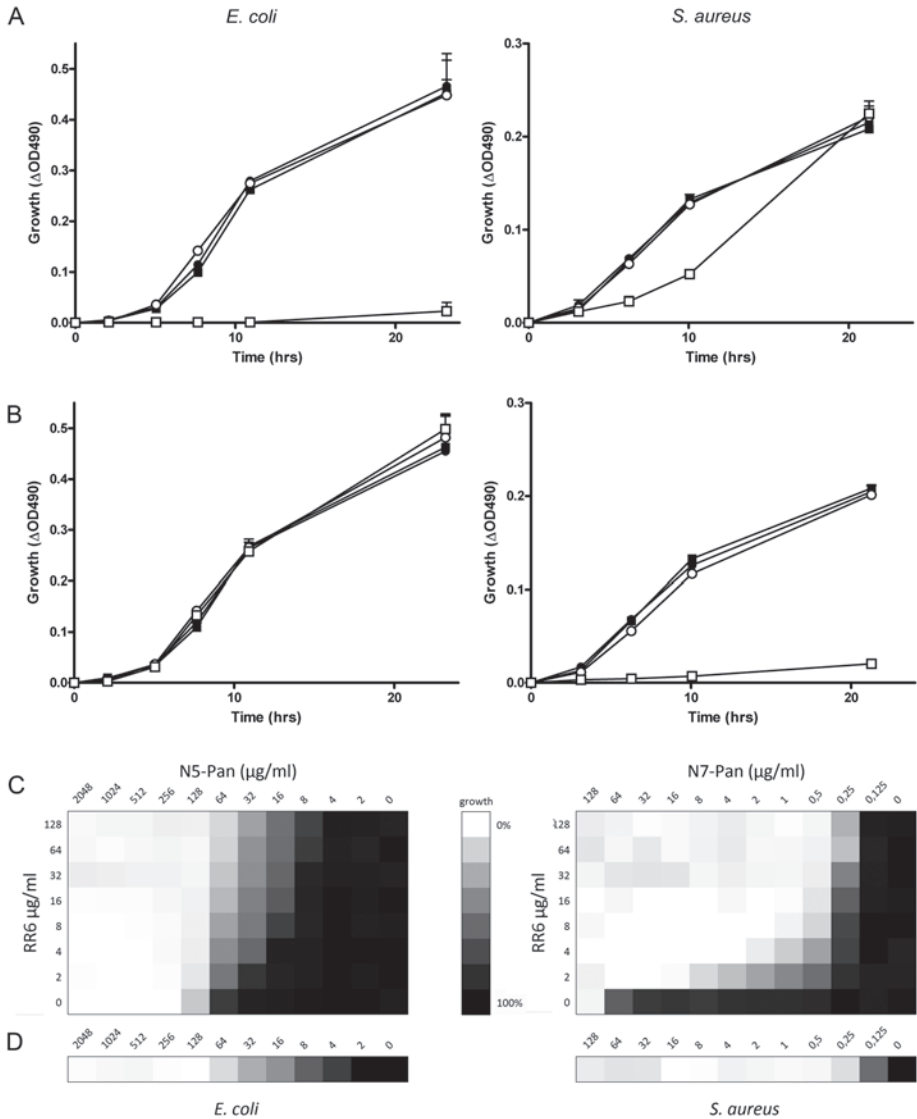


Figure 8.4 Pantetheinase inhibition preserves the antibiotic effect of pantothenamides (A) Growth curves of respectively *E. coli* and *S. aureus* in 1% tryptone with 10% FBS alone (■), or supplemented with 64 $\mu\text{g/ml}$ N5-Pan (●), 256 $\mu\text{g/ml}$ RR6 (○) or a combination of N5-Pan and RR6 (□). Only the combination of RR6 and N5-Pan showed long-term bacterial growth inhibition of *E. coli*. All samples N=3. (B) Same conditions as in (A), but N7-Pan instead of N5-Pan was added. Only the combination of RR6 and N7-Pan results in *S. aureus* growth inhibition. All samples N=3. (C) Bacterial growth of *E. coli* and *S. aureus* in 1% tryptone with 10% decomplexed human serum in the presence of different concentrations of RR6 and N5-Pan (*E. coli*) and N7-Pan (*S. aureus*). The checkerboard titration shows that addition of RR6 increased the potency of pantothenamides in serum-containing media to concentrations comparable to cultures without serum as shown in (D). N=2. (D) Bacterial growth of *E. coli* and *S. aureus* in 1% tryptone without serum in the presence of different concentrations of N5-Pan and N7-Pan respectively. N=2.

number of bacterial species^{2,11}. To delineate the taxa that are potential targets for antibiotic therapy we determined the MIC values for a number of clinically relevant species. Table 8.1 shows that only gram-positive bacteria are sensitive to pantothenamides in pharmaceutically realistic concentrations (8 µg/ml). Sensitive species include *S. aureus*, *S. pneumoniae* and *S. epidermidis*. Within one genus (*Streptococcus*), there is differential sensitivity, as *S. agalactiae* and *S. pyogenes* were resistant as opposed to *pneumococci*. We tested 18 strains of *S. pneumoniae* and these were all found to be sensitive to N5-Pan (Table S8.2).

As the putative mode of action of pantothenamides is at the level of CoA-dependent biochemical pathways, this raised the question of selectivity for microbial versus host targets. We therefore investigated if pantothenamides and pantetheinase inhibitors were tolerated by mammalian cells. Using concentrations of N5-Pan, N7-Pan and RR6 up to 200 µM, no effects on cell growth or viability were observed in a human cell line (293T kidney cells) (Figure 8.5).

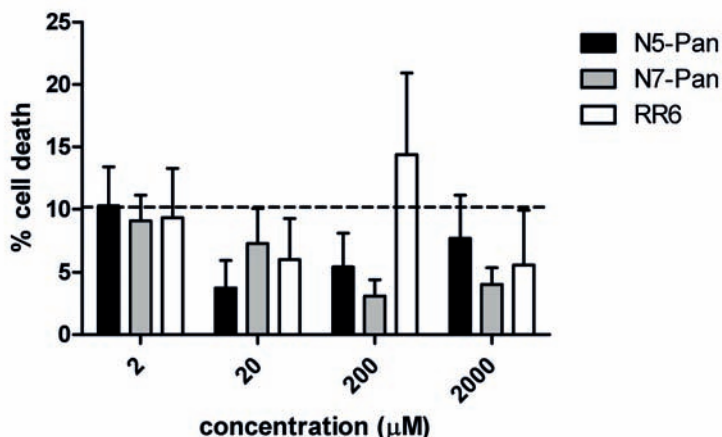


Figure 8.5 *In vitro* toxicity of compounds Cytotoxicity was measured on human embryonic kidney 293T cells treated with or without N5-Pan, N7-Pan or RR6. None of the tested compounds resulted in increased cell death up to 2000 µM. The dotted line represents the percentage cell death in untreated cells (N=3).

Discussion

We here provide detailed experimental evidence for the concept that pantetheinase inhibitors can prevent the enzymatic degradation of pantothenamide antibiotics. Combination of a pantetheinase inhibitor with pantothenamides could be a successful strategy to preserve the antibiotic properties of pantothenamides in the presence of host pantetheinases. We propose that our data provide proof of concept for a novel antibiotic strategy that could be used against clinically relevant gram-positive bacteria.

Since pantothenic acid was first described as a nutritional requirement for almost, if not, all organisms, its potential for antibiotic drug design has

Table 8.1 MIC values of most potent pantothenamide against various bacterial strains

Organism	Gram staining	Strain	Most effective pantothenamide	MIC ($\mu\text{g/ml}$)
<i>S. aureus</i>	positive	ATCC6538	N7-Pan	0.5
<i>S. pneumoniae</i>	positive	R6	N5-Pan	0.25
<i>S. epidermidis</i>	positive	ATCC12228	N7-Pan	1
<i>S. agalactiae</i>	positive	RIVM861352	none	>256
<i>S. pyogenes</i>	positive	ATCC43202	N7-Pan	64
<i>E. coli</i>	negative	ATCC25922	N5-Pan	64
<i>K. pneumoniae</i>	negative	ATCC43816	N5-Pan	32
<i>M. catarrhalis</i>	negative	RH4	N7-Pan	128
<i>P. aeruginosa</i>	negative	Xen41	none	>256

been investigated. The different mechanisms by which organisms were able to obtain pantothenic acid for CoA biosynthesis and the relatively low homology between enzymes involved in pantothenic acid processing opened the field to design growth inhibiting molecules specific for pathogens. Based on pantothenic acid, different classes of molecules were described to possess anti-bacterial, anti-fungal and anti-parasitic activity *in vitro*, including N-pantoyl-substituted amines, pantoylhydrazides, pantothenones and pantothenamides²⁰. Most of these analogues were expected to be competing with endogenous pantothenic acid for the first enzyme of the CoA biosynthesis, CoaA. In contrast, the working mechanism of pantothenamides is expected to be different. Strauss and Begley¹⁰ showed that N-pentylpantothenamide is rather a substrate for CoA than an inhibitor. They showed that the pantothenamide is completely processed to a CoA analogue, called ethyldethia-CoA and that the conversion is over 10 times faster than pantothenic acid processing. Subsequently Zhang *et al.* showed that acyl carrier protein (ACP) is the cellular target, which results in an inactive ACP analogue, that lacks the sulfhydryl group for the attachment of acyl chains for fatty acid synthesis³. Mercer *et al.* have shown that pantothenamide azido-pantetheine could be processed to ACP via FAS type II in bacteria, while it cannot be processed via FAS type I in human SKBR3 cell-line²¹. Apparently, CoA analogues are only recognized by type II fatty acid synthase, which is found in most bacteria, while FAS type I system is present in mammals and fungi. Because the structural arrangement of fungal and mammalian synthases differs, selective pantothenamides could theoretically also target fungal FAS type I. Assuming that pantothenamides target the bacterial FASII pathway, administration of exogenous fatty acids could potentially overcome the antibiotic effects of pantothenamides. Work by Zhang *et al.* showed that this is not the case for *E. coli*. The MIC for *S. pneumoniae*, however, was increased 4-fold, suggesting that pantothenamides

target FASII but may also have other effects³. A recent paper by Parsons *et al.* elucidated the basis of differential susceptibility of gram-positive bacteria to fatty acid synthesis inhibitors like cerulinin and platensimycin²². From this work it was concluded that fatty acids cannot overcome FASII inhibition in *S. aureus* in contrast to *S. pneumoniae*. Whether this also holds for pantothenamides remains to be investigated, as they are likely to inhibit other pathways in addition to FASII. This is supported by recent findings describing that, at least in *E. coli*, both holo-ACP and ethyldethia-ACP can be hydrolysed to Apo-ACP by ACP phosphodiesterase (AcpH)⁷. Their data suggest that the antibacterial effect of N5-Pan is due to cellular depletion of CoA⁷.

The first step in CoA biosynthesis is the phosphorylation of pantothenic acid by pantothenate kinase (PanK), the key regulatory enzyme that is subject to selfregulation through feedback inhibition by CoA. Structures of PanK enzymes among different species have been investigated, which showed differences in binding capacity for pantothenic acid^{23,24}. This might explain why N5-Pan is more active against *E. coli* and N7-Pan has specificity for *S. aureus*. Binding features of human PanK family members with pantothenic acid have not been investigated. Although structures of human PanK1 α and PanK3 in complex with acetyl-CoA have been analyzed, the structure of human PanK isoforms in complex with pantothenic acid would further facilitate the knowledge of binding properties of PanK, and thus would provide more insight into possible modifications of pantothenic acid to aid medicinal chemistry efforts.

We have no data whether our pantetheinase inhibitors are PanK substrates. We have shown that pantetheinase inhibitors by themselves are not antibiotic, which suggests that they are not a substrate for the CoA biosynthetic machinery. This may be caused by the loss of the amide bond which is likely to be a necessary structural requirement for entering the first step of CoA synthesis leading to CoA antimetabolites, as recently suggested in a study by Mercer *et al.*⁵

A recent publication has identified pantetheinase inhibitors derived from various chemical scaffolds in the LOPAC library, via a high-throughput approach¹⁹. These compounds are all non-selective and have modest potency. As they are known to target various mammalian cellular pathways at concentrations that are lower than required for vanin inhibition, it is unlikely that these compounds are useful in pharmacology or biological chemistry approaches^{25,26}.

The antibiotic strategy described here includes a combination of an enzyme inhibitor and a molecule that interferes with bacterial growth. Although a dual compound formulation is not a preferred pharmaceutical approach, it is not unprecedented as witnessed by the use of beta lactamase inhibitors (combined with penicillin) and a dehydropeptidase inhibitor (combined with iminipem)²⁷. Here, we provide detailed experimental data of a concept that we previously put forward^{28,29}. Recently, indirect evidence for this concept was found in the case of *Plasmodium falciparum* growth inhibition by pantothenamides³⁰.

Obviously, a number of steps need to be taken before combination therapy of pantothenamide antibiotics and vanin inhibitors can enter drug development.

As witnessed by Figure 8.4C, the potency of our current vanin inhibitors needs to be improved to achieve complete protection of pantothenamides in serum and to maintain the required MIC values³¹ (e.g. around 1 µg/ml for *S. aureus*). We found a good bioavailability and pharmacodynamic profile of the vanin inhibitor RR6¹⁸, which is encouraging to explore this further. Clearly, an increase of the potency of current pantothenamides (N5-Pan and N7-Pan) is required. If this can be achieved, their application and may even extend the sensitivity beyond the gram-positive species that we have identified here.

Materials and methods

Bacterial growth assays

Bacterial strains of *Escherichia coli*, *Staphylococcus aureus*, *Staphylococcus epidermidis*, *Streptococcus agalactiae*, *Streptococcus pyogenes*, *Moraxella catarrhalis*, *Klebsiella pneumonia* and *Pseudomonas aeruginosa* were grown overnight in 1% Bacto Tryptone media (BD, Sparks, MD). Cultures were then diluted 1:1000 in fresh assay media supplemented with or without 20% FBS (HyClone, Celbio, Logan, UT) or 20% decomplexed human serum (Sanquin, Bloodbank, NL) and added to 96 well sterile ELISA plate (100 µl per well). The compounds to be tested were diluted in the media without serum and added to the bacteria (100 µl per well). Plates were incubated at 37 °C and bacterial growth was followed in time by reading the optical density at 490 nm using a microplate-reader (Model 450, Bio-Rad Laboratories Inc., Hercules, CA). Pantothenic acid was purchased from Sigma Aldrich (Dorset, UK). *Streptococcus pneumonia* were grown till mid-log phase ($OD_{620} = 0,3$) and stored in 15% glycerol at -80°C till further use. Bacteria were diluted 10-fold in Mueller Hinton media (BD, Sparks, MD) and added to 96 well sterile ELISA plate (150 µl per well). The compounds to be tested were diluted in the media without serum and added to the bacteria (150 µl per well). Plates were incubated overnight at 37 °C, 5% CO₂. MIC was defined as the lowest concentration of pantothenamide where no growth was visible.

Synthesis of pantothenamides and pantetheinase inhibitors

All reactions were performed under an argon atmosphere, unless stated otherwise. Solvents were distilled from appropriate drying agents prior to use. Et₃N was distilled and stored over KOH. Reactions were followed, and Rf values are obtained using thin layer chromatography (TLC) on silica gel-coated plates (Merck 60 F254) with the indicated eluent and compounds were detected with UV-light and/or by charring at ca. 150 °C after dipping into a solution of potassium permanganate, or ninhydrin. Column or flash chromatography was carried out using ACROS silica gel (0.035-0.070 mm, pore diameter ca. 6 mm). IR spectra were recorded on an ATI Mattson Genesis Series FTIR spectrometer. High-resolution mass spectra were recorded on a JEOL AccuTOF (ESI) or a MAT900 (EI, CI, and ESI). Melting points were analyzed with a Büchi melting point B-545 and are not corrected. NMR spectra were recorded at 298 K on a

Bruker DMX 300 (300 MHz) and a Varian 400 (400 MHz) spectrometer in the solvent indicated. Chemical shifts are given in parts per million (ppm) with respect to tetramethylsilane (0.00 ppm), or CHD₂OD (3.31 ppm) as internal standard for ¹H-NMR; and CDCl₃ (77.16 ppm), or CD₃OD (49.00 ppm) as internal standard for ¹³C-NMR. Coupling constants are reported as *J* values in hertz (Hz). See Supplementary Information for detailed synthesis of pantothenamides. Details on the synthesis of pantetheinase inhibitors are described previously by Jansen *et al*¹⁸.

Pantetheinase activity

Pantetheinase activity was measured by the amount of free 7-amino-4-methylcoumarin (AMC) released by the hydrolysis of the pantetheine-analogue pantothenate-AMC¹⁹. Pantothenate-AMC (final concentration 10 μM) was incubated in phosphate buffer (100 mM potassium phosphate buffer pH 8.0) in the presence of serum (1%) as pantetheinase source with or without a potential pantetheinase inhibitor. In time, samples were taken and the reaction was terminated by addition of 180 μl 100 mM CaCO₃ pH 10.5. Fluorescence was measured using a luminescence spectrometer (LS55, Perkin Elmer, EX 350 ± 2.5 nm, EM 450 ± 2.5 nm) against samples without serum as negative control.

For mass spectrometric analysis 64 μg/ml N7-Pan was incubated for 24 hours at room temperature with 1% fetal bovine serum diluted in phosphate buffer (500 μM potassium phosphate buffer pH 8.0) with and without the addition of 256 μg/ml RR6.

Mass spec analysis

Mass spectrometry was performed on a JEOL JMS-T100CS (AccuTOF CS) connected to a Agilent 1100 series HPLC system. Analysis was performed in infusion mode, 3 μl of sample 1% of sample in methanol (HPLC grade, Fisher Scientific) was injected into a stream of methanol (HPLC grade, Fisher Scientific) containing 0.1% formic acid (puriss. Pa for mass spectrometry, Fluka) and 50 nanomolar PPG425 (polypropylene glycol, average M.W. 425, Sigma-Aldrich Chemie GmbH) for use as an internal mass drift compensator. Total analysis time with a flow rate of 100 μl/min was 2.5 minutes per sample. Sample information elutes between 0.3 and 1.0 minutes. Data between 0 and 0.3 minutes was used to mass drift compensate the calibration against PPG425 peaks resulting in a mass precision better than 2 ppm.

In vitro toxicity

Human embryonic kidney 293T cells were grown in Dulbecco's Modified Eagle Medium (DMEM-Glutamax, Gibco Invitrogen) containing 10% FBS (HyClone, Celbio, Logan, UT), 100 μg/ml penicillin-streptomycin, 1% pyruvate (Gibco Invitrogen) at 37°C and 5% CO₂. Pantothenamide or pantetheinase inhibitors were added to these cultures for 48 hours and effect on growth and toxicity was determined microscopically. Cytotoxicity was detected using the LDH cytotoxicity

detection kit according to the manufacturer's protocol (Roche Applied Science, Indianapolis, IN).

Statistics

Data were analyzed using Graphpad Prism version 5. Data are expressed as mean \pm standard deviation.

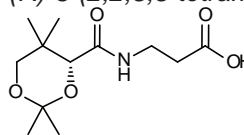
Acknowledgements

This work was supported by a preseed grant of The Netherlands Genomics Initiative, grant nr 93611013. We would like to thank Bas Ritzen and René Aben for technical assistance and Roberta Leonardi for critical reading of the manuscript. P.J., J.S., B.R., P.Z., P.H. and F.R. are inventors on the below mentioned patents filed by the Radboud University Nijmegen Medical Centre.

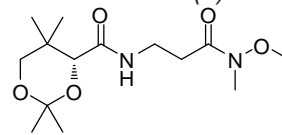
Supplementary information

Synthesis of N5-Pan and N7-Pan

(R)-3-(2,2,5,5-tetramethyl-1,3-dioxane-4-carboxamido)propanoic acid (**1**)

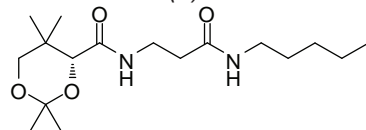
 To a cooled solution (0 °C) of (R)-pantothenic acid (20.8 g, 94.0 mmol) in acetone (500 mL) were added subsequently 2-methoxyprop-1-ene (27.1 mL, 283 mmol) and pTs-OH·H₂O (0.89 g, 4.72 mmol). After 15 min the temperature was raised to room temperature and the mixture was stirred for another 30 min. The mixture was diluted with saturated aqueous NaHCO₃ (10 mL) and concentrated *in vacuo* to yield **1** as a yellow solid, which was used without purification. TLC (CH₂Cl₂:MeOH, 9:1 v/v): R_f = 0.67. Spectral data were in correspondence with reported data in literature³².

(R)-N-{3-[methoxy(methyl)amino]-3-oxopropyl}-2,2,5,5-tetramethyl-1,3-dioxane-4-carboxamide (**2**)

 To a solution of **1** (1.80 g, 6.92 mmol) in dry CH₂Cl₂ (65 mL) at rt were added, EDC (2.09 g, 1.5 equiv), N,O-dimethylhydroxylamine hydrochloride (1.04 g, 1.5 equiv) and DIPEA (3.43 mL, 3.0 equiv), followed by DMAP (483 mg, 0.5 equiv). The reaction mixture was stirred over night at rt, quenched with saturated aqueous NH₄Cl (40 mL), extracted with CH₂Cl₂ (3 x 50 mL), dried (Na₂SO₄), and concentrated *in vacuo*. The product was purified by column chromatography (MeOH/CH₂Cl₂, 0:1→1:4) to afford **2** (1.90 g, 91% yield) as a colorless oil. R_f 0.56 (MeOH/CH₂Cl₂, 1:9). [α]_D²⁰+44.5 (c 1.32, CH₂Cl₂). IR (ATR) 3417, 3334, 2980, 2940, 2871, 1661, 1520, 1378, 1196, 1095, 873 cm⁻¹. ¹H NMR (CDCl₃, 400 MHz): δ 7.13 (t, J = 5.7 Hz, 1H), 4.07 (s, 1H), 3.68 (d, J = 11.7 Hz, 1H), 3.67 (s, 3H), 3.64-3.48 (m, 2H), 3.27 (d, J = 11.7 Hz, 1H), 3.18 (s,

3H), 2.76-2.59 (m, 2H), 1.46 (s, 3H), 1.42 (s, 3H), 1.03 (s, 3H), 0.96 (s, 3H). ^{13}C NMR (CDCl_3 , 75 MHz): δ 169.9, 99.1, 77.3, 71.6, 61.4, 34.2, 33.1, 32.3, 31.9, 29.6, 22.3, 19.0, 18.8. HRMS (ESI) m/z calcd for $\text{C}_{14}\text{H}_{26}\text{N}_2\text{O}_5$ ($\text{M}+\text{Na}$) $^+$: 325.1739, found: 325.1746.

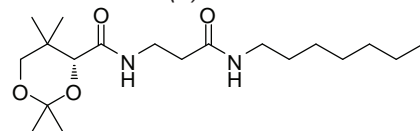
(R)-2,2,5,5-tetramethyl-*N*-[3-oxo-3-(pentylamino)propyl]-1,3-dioxane-4-carboxamide (**3**)



Prepared as described for **2**, starting from **1** (3.40 g, 13.1 mmol) and *n*-amylamine (2.30 mL, 1.5 equiv). Column chromatography (EtOAc/heptane, 0:1→4:1) afforded **3** (1.89 g, 44% yield) as a white

solid. R_f 0.56 (MeOH/ CH_2Cl_2 , 1:9). Mp 81.5 °C. $[\alpha]_{\text{D}}^{20} +41.6$ (c 1.01, CH_2Cl_2). IR (ATR) 3430, 3317, 3300, 2954, 2931, 2868, 1649, 1526, 1463, 1377, 1197, 1098, 873 cm^{-1} . ^1H NMR (CDCl_3 , 400 MHz): δ 7.02 (t, J = 5.2 Hz, 1H), 5.88-5.84 (m, 1H), 4.07 (s, 1H), 3.68 (d, J = 11.7 Hz, 1H), 3.64-3.46 (m, 2H), 3.28 (d, J = 11.7 Hz, 1H), 3.26-3.21 (m, 2H), 2.43 (t, J = 6.2 Hz, 2H), 1.49 (dt, J = 7.3, 14.6 Hz, 2H), 1.46 (s, 3H), 1.42 (s, 3H), 1.38-1.24 (m, 4H), 1.04 (s, 3H), 0.97 (s, 3H), 0.90 (t, J = 6.8 Hz, 3H). ^{13}C NMR (CDCl_3 , 75 MHz): δ 170.9, 170.3, 99.2, 77.3, 71.6, 39.7, 36.4, 35.1, 33.1, 29.6, 29.4, 29.2, 22.5, 22.3, 19.0, 18.8, 14.1. HRMS (ESI) m/z calcd for $\text{C}_{17}\text{H}_{33}\text{N}_2\text{O}_4$ ($\text{M}+\text{H}$) $^+$: 329.2440, found: 329.2426.

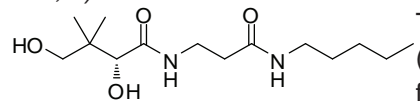
(R)-*N*-[3-(heptylamino)-3-oxopropyl]-2,2,5,5-tetramethyl-1,3-dioxane-4-carboxamide (**4**)



Prepared as described for **2**, starting from **1** (4.50 g, 17.4 mmol) and *n*-heptylamine (3.90 mL, 1.5 equiv). Column chromatography (EtOAc/heptane, 1:2→1:0) afforded **4** (3.15

g, 51% yield) as a colorless oil. R_f 0.56 (MeOH/ CH_2Cl_2 , 1:9). $[\alpha]_{\text{D}}^{20} +39.4$ (c 1.00, CH_2Cl_2). IR (ATR) 3425, 3321, 2927, 2863, 1650, 1526, 1459, 1377, 1196, 1098, 875 cm^{-1} . ^1H NMR (CDCl_3 , 400 MHz): δ 7.04 (t, J = 5.9 Hz, 1H), 6.03 (t, J = 4.9 Hz, 1H), 4.06 (s, 1H), 3.68 (d, J = 11.7 Hz, 1H), 3.63-3.46 (m, 2H), 3.28 (d, J = 11.7 Hz, 1H), 3.26-3.20 (m, 2H), 2.42 (t, J = 6.2 Hz, 2H), 1.53-1.47 (m, 2H), 1.46 (s, 3H), 1.41 (s, 3H), 1.32-1.24 (m, 8H), 1.03 (s, 3H), 0.97 (s, 3H), .88 (t, J = 6.9 Hz, 3H). ^{13}C NMR (CDCl_3 , 75 MHz): δ 170.8, 170.2, 99.1, 77.1, 71.5, 39.6, 36.2, 35.0, 33.0, 31.7, 29.6, 29.5, 29.0, 26.9, 22.6, 22.2, 18.9, 18.7, 14.1. HRMS (ESI) m/z calcd for $\text{C}_{19}\text{H}_{37}\text{N}_2\text{O}_4$ ($\text{M}+\text{H}$) $^+$: 357.2753, found: 357.2747.

(R)-2,4-dihydroxy-3,3-dimethyl-*N*-[3-oxo-3-(pentylamino)propyl]butanamide (*N*5-Pan, **5**)



To a solution of **3** (30 mg, 0.10 mmol) in MeCN (1.0 mL) was added, BiCl_3 (6.5 mg, 20 mol%), followed by distilled H_2O (36 μL , 20 equiv).

The reaction was stirred at rt for 4 h, then filtered and concentrated *in vacuo*. After dilution with EtOAc (10 mL), the reaction mixture was washed with saturated

aqueous NaHCO_3 (2×8 mL) and the aqueous layer was extracted with EtOAc (3×8 mL). The organic layers were combined, dried (Na_2SO_4), and concentrated *in vacuo*. The product was purified by column chromatography (EtOAc/heptane, 1:1→1:0) to afford **5** (1.22 g, 75% yield) as a white solid. R_f 0.46 (MeOH/ CH_2Cl_2 , 1:9). Mp 89.4 °C. $[\alpha]_D^{20} +29.7$ (c 1.00, MeOH). IR (ATR) 3330, 3280, 3088, 2937, 2872, 1642, 1546, 1089, 1033, 691 cm^{-1} . ^1H NMR (CD_3OD , 400 MHz): δ 3.88 (s, 1H), 3.54-3.37 (m, 4H), 3.17-3.13 (m, 2H), 2.41 (t, J = 6.7 Hz, 2H), 1.53-1.46 (m, 2H), 1.40-1.27 (m, 4H), 0.94-0.90 (m, 9H). ^{13}C NMR (CDCl_3 , 75 MHz): δ 174.1, 171.6, 77.5, 70.9, 39.8, 39.4, 35.9, 35.4, 29.2, 22.4, 21.4, 20.6, 14.1 HRMS (ESI) m/z calcd for $\text{C}_{14}\text{H}_{28}\text{N}_2\text{O}_4\text{Na}$ ($\text{M}+\text{Na}$) $^+$: 311.1947, found: 311.1933.

(*R*)-*N*-[3-(heptylamino)-3-oxopropyl]-2,4-dihydroxy-3,3-dimethylbutanamide (N7-Pan, **6**)

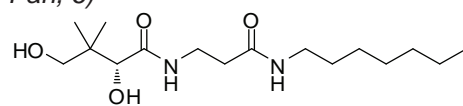
 Prepared as described for **5**, starting from **4** (2.90 g, 8.13 mmol). Column chromatography (MeOH/ CH_2Cl_2 , 0:1→1:9) afforded **6** (2.21 g, 86% yield) as a white solid. R_f 0.47 (MeOH/ CH_2Cl_2 , 1:9). Mp 78.2 °C. $[\alpha]_D^{20} +26.9$ (c 1.01, MeOH). IR (ATR) 3352, 2483, 2068, 1119, 973 cm^{-1} . ^1H NMR (CD_3OD , 400 MHz): δ 3.89 (s, 1H), 3.54-3.37 (m, 4H), 3.15 (dt, J = 1.2, 6.9 Hz, 2H), 2.41 (t, J = 6.7 Hz, 2H), 1.53-1.46 (m, 2H), 1.32-1.31 (m, 8H), 0.92-0.89 (m, 9H). ^{13}C NMR (CD_3OD , 75 MHz): δ 176.1, 173.6, 77.3, 70.4, 40.5, 40.4, 36.4, 32.9, 30.4, 30.1, 28.0, 23.7, 21.3, 20.9, 14.4. HRMS (ESI) m/z calcd for $\text{C}_{16}\text{H}_{33}\text{N}_2\text{O}_4$ ($\text{M}+\text{H}$) $^+$: 317.2440, found: 317.2429.

Table S8.1 Structure and anti-vanin properties of N5-Pan, N7-Pan and RR6

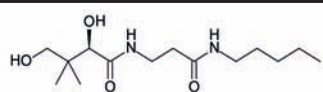
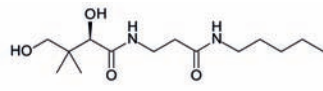
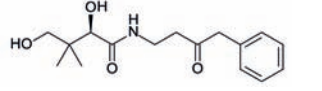
Name	Structure	IC_{50} (μM)		
		Rec. VNN1	Human serum	FBS
N5-Pan		-	-	-
N7-Pan		-	-	-
RR6		0.54	0.040	0.041

Table S8.2 Complete list of MIC values of N5-Pan and N7-Pan against various bacterial strains

Organism	Gram staining	Strain	N5-Pan (µg/ml)	N7-Pan (µg/ml)
<i>S. aureus</i>	positive	Xen8.1	8	0.5
		ATCC6538	8	0.5
		MRSA	8	0.5
<i>S. pneumoniae</i>	positive	R6	0.25	2
		D39	0.5	16
		TIGR4	0.5	8
		G54	1	32
		PMEN-1	4	16
		PMEN-3	2	32
		PMEN-4	0.5	8
		PMEN-9	2	16
		PMEN-13	2	32
		PMEN-14	1	16
		PMEN-15	0.5	8
		PMEN-18	1	16
		PMEN-19	0.5	16
		PMEN-20	1	32
		PMEN-21	1	16
		PMEN-23	0.5	16
		PMEN-24	0.5	16
PMEN-25	1	8		
<i>S. epidermidis</i>	positive	ATCC12228	32	1
<i>S. agalactiae</i>	positive	RIVM861352	>256	>256
		RIVM801284	>256	>256
		RIVM861167	>256	>256
		RIVM821256	>256	>256
		RIVM782651	>256	>256
<i>S. pyogenes</i>	positive	ATCC43202	>256	64
<i>E. coli</i>	negative	BL21	64	256
		ATCC25922	64	128
<i>K. pneumoniae</i>	negative	ATCC43816	32	>256
<i>M. catarrhalis</i>	negative	RH4	>256	128
<i>P. aeruginosa</i>	negative	Xen41	>256	>256

References

1. Fischbach MA, Walsh CT. Antibiotics for emerging pathogens. *Science* 325, 1089-93 (2009)
2. Clifton G, Bryant SR, Skinner CG. N'-(substituted) pantothenamides, antimetabolites of pantothenic acid. *Archives of biochemistry and biophysics* 137, 523-8 (1970)
3. Zhang YM, Frank MW, Virga KG, Lee RE, Rock CO, Jackowski S. Acyl carrier protein is a cellular target for the antibacterial action of the pantothenamide class of pantothenate antimetabolites. *J Biol Chem* 279, 50969-75 (2004)
4. Virga KG, Zhang YM, Leonardi R, Ivey RA, Hevener K, Park HW *et al.* Structure-activity relationships and enzyme inhibition of pantothenamide-type pantothenate kinase inhibitors. *Bioorg Med Chem* 14, 1007-20 (2006)
5. Mercer AC, Meier JL, Hur GH, Smith AR, Burkart MD. Antibiotic evaluation and in vivo analysis of alkynyl Coenzyme A antimetabolites in *Escherichia coli*. *Bioorg Med Chem Lett* 18, 5991-4 (2008)
6. Choudhry AE, Mandichak TL, Broskey JP, Egolf RW, Kinsland C, Begley TP *et al.* Inhibitors of pantothenate kinase: novel antibiotics for staphylococcal infections. *Antimicrob Agents Chemother* 47, 2051-5 (2003)
7. Thomas J, Cronan JE. Antibacterial activity of N-pentylpantothenamide is due to inhibition of coenzyme a synthesis. *Antimicrob Agents Chemother* 54, 1374-7 (2010)
8. Spry C, Chai CL, Kirk K, Saliba KJ. A class of pantothenic acid analogs inhibits *Plasmodium falciparum* pantothenate kinase and represses the proliferation of malaria parasites. *Antimicrob Agents Chemother* 49, 4649-57 (2005)
9. Akinnusi TO, Vong K, Auclair K. Geminal dialkyl derivatives of N-substituted pantothenamides: synthesis and antibacterial activity. *Bioorg Med Chem* 19, 2696-706 (2011)
10. Strauss E, Begley TP. The antibiotic activity of N-pentylpantothenamide results from its conversion to ethyldethia-coenzyme a, a coenzyme a antimetabolite. *J Biol Chem* 277, 48205-9 (2002)
11. Leonardi R, Chohnan S, Zhang YM, Virga KG, Lee RE, Rock CO *et al.* A pantothenate kinase from *Staphylococcus aureus* refractory to feedback regulation by coenzyme A. *J Biol Chem* 280, 3314-22 (2005)
12. Zhang YM, White SW, Rock CO. Inhibiting bacterial fatty acid synthesis. *J Biol Chem* 281, 17541-44 (2006)
13. Aurrand-Lions M, Galland F, Bazin H, Zakharyev VM, Imhof BA, Naquet P. Vanin-1, a novel GPI-linked perivascular molecule involved in thymus homing. *Immunity* 5, 391-405 (1996)
14. Martin F, Malergue F, Pitari G, Philippe JM, Philips S, Chabret C *et al.* Vanin genes are clustered (human 6q22-24 and mouse 10A2B1) and encode isoforms of pantetheinase ectoenzymes. *Immunogenetics* 53, 296-306 (2001)
15. Maras B, Barra D, Dupre S, Pitari G. Is pantetheinase the actual identity of mouse and human vanin-1 proteins? *FEBS Lett* 461, 149-52 (1999)
16. Jansen PA, Kamsteeg M, Rodijk-Olthuis D, van Vlijmen-Willems IM, de Jongh GJ, Bergers M *et al.* Expression of the vanin gene family in normal and inflamed human skin: induction by proinflammatory cytokines. *J Invest Dermatol* 129, 2167-74 (2009)
17. Brenner C. Catalysis in the nitrilase superfamily. *Curr Opin Struct Biol* 12, 775-82 (2002)

18. Jansen PA, van Diepen JA, Ritzen B, Zeeuwen PL, Cacciatore I, Cornacchia C *et al.* Discovery of Small Molecule Vanin Inhibitors: New Tools To Study Metabolism and Disease. *ACS Chem Biol* 8, 530-4 (2013)
19. Ruan BH, Cole DC, Wu P, Quazi A, Page K, Wright JF *et al.* A fluorescent assay suitable for inhibitor screening and vanin tissue quantification. *Anal Biochem* 399, 284-92 (2010)
20. Spry C, Kirk K, Saliba KJ. Coenzyme A biosynthesis: an antimicrobial drug target. *FEMS Microbiol Rev* 32, 56-106 (2008)
21. Mercer AC, Meier JL, Torpey JW, Burkart MD. In vivo modification of native carrier protein domains. *Chembiochem* 10, 1091-100 (2009)
22. Parsons JB, Rock CO. Is bacterial fatty acid synthesis a valid target for antibacterial drug discovery? *Curr Opin Microbiol* 14, 544-9 (2011)
23. Yang K, Eyobo Y, Brand LA, Martynowski D, Tomchick D, Strauss E *et al.* Crystal structure of a type III pantothenate kinase: insight into the mechanism of an essential coenzyme A biosynthetic enzyme universally distributed in bacteria. *J Bacteriol* 188, 5532-40 (2006)
24. Hong BS, Yun MK, Zhang YM, Chohnan S, Rock CO, White SW *et al.* Prokaryotic type II and type III pantothenate kinases: The same monomer fold creates dimers with distinct catalytic properties. *Structure* 14, 1251-61 (2006)
25. Delvaux M, Bastie MJ, Chentoufi J, Cragoe EJ, Jr., Vaysse N, Ribet A. Amiloride and analogues inhibit Na(+)-H+ exchange and cell proliferation in AR42J pancreatic cell line. *Am J Physiol* 259, G842-9 (1990)
26. Lazo JS, Nemoto K, Pestell KE, Cooley K, Southwick EC, Mitchell DA *et al.* Identification of a potent and selective pharmacophore for Cdc25 dual specificity phosphatase inhibitors. *Mol Pharmacol* 61, 720-8 (2002)
27. Drawz SM, Bonomo RA. Three decades of beta-lactamase inhibitors. *Clin Microbiol Rev* 23, 160-201 (2010)
28. Jansen PA, Schalkwijk J, Rutjes FP, Sauerwein R, Hermkens PH. Derivatives of pantothenic acid and their use for the treatment of malaria. Patent application Nr EP11725212, Publication Nr WO2011152721 (2011)
29. Jansen PA, Zeeuwen PL, Schalkwijk J, Rutjes FP, Ritzen B, Hermkens PH. Pantothenic acid derivatives and their use in the treatment of microbial infections. Patent Application Nr EP11725211, Publication Nr WO2011152720 (2011)
30. Spry C, Macuamule C, Lin Z, Virga KG, Lee RE, Strauss E *et al.* Pantothenamides Are Potent, On-Target Inhibitors of Plasmodium falciparum Growth When Serum Pantetheinase Is Inactivated. *PLoS One* 8, e54974 (2013)
31. Mouton JW, Dudley MN, Cars O, Derendorf H, Drusano GL. Standardization of pharmacokinetic/pharmacodynamic (PK/PD) terminology for anti-infective drugs: an update. *J Antimicrob Chemother* 55, 601-7 (2005)
32. Sewell AL, Villa MV, Matheson M, Whittingham WG, Marquez R. Fast and flexible synthesis of pantothenic acid and CJ-15,801. *Org Lett* 13, 800-3 (2011)

Summary and concluding remarks

9 CHAPTER

Patrick AM Jansen¹
Patrick LJM Zeeuwen¹
Joost Schalkwijk¹

¹Department of Dermatology and Nijmegen Centre for Molecular Life Sciences, Radboud University Nijmegen Medical Centre, The Netherlands

Historically, psoriasis and atopic dermatitis are considered to be immunological skin disorders in which immune cells are expected to play a causal role. Over the past 10 years this perspective has been changed, since keratinocytes appear to be involved as well. Nowadays, it is generally accepted that a complex interplay between immune cells and keratinocytes is responsible in the pathogenesis of psoriasis and atopic dermatitis.

The department of Dermatology at the Radboud university of Nijmegen has a history in epidermal skin biology with a focus on keratinocytes and its gene expression. In this context a microarray study was performed in which gene expression in involved skin of psoriasis patients was compared with involved skin of atopic dermatitis patients. These results has formed the basis for this thesis. The challenge was, after confirmation of results from this microarray, to investigate the relevance of disease-specific gene expression in aetiologic, diagnostic and therapeutic perspectives of these diseases.

The skin, its structure and its function are described in **chapter 1**. Also the current status on the two most common skin diseases, psoriasis and atopic dermatitis, is described. Furthermore different *in vitro* skin models and approaches for transgenic gene expression or specific gene knockdown in cultured keratinocytes are summarized.

Molecules & Markers

The most differentially expressed gene (VNN3) found in the microarray study performed by our department was further analyzed. In **chapter 2** we first confirmed that VNN3 was indeed overexpressed in psoriatic skin as compared with atopic dermatitis skin and uninvolved/healthy skin. Besides the expression of VNN3, also the expression of VNN1, but not of VNN2, appears to be higher in psoriatic skin. The vanin expression was found to be induced by T cell derived cytokines of the Th1 (interferon- γ and TNF- α) and Th17 (IL22 and IL17) types, which are present at high levels in psoriatic skin lesions. The functional significance of vanin expression in psoriatic skin remains unclear, although it has been proposed that cysteamine, the metabolite that is formed after hydrolysis of pantetheine, plays a role in the regulation of cutaneous inflammation and differentiation.

The discovery of the beta-defensin copy number variation and its correlation with psoriasis in combination with the knowledge that beta-defensin-2 is highly upregulated in psoriatic skin, led us investigate hBD-2 expression at the protein level. In **chapter 3** we describe a weak correlation between the beta-defensin copy number in healthy volunteers and the amount of hBD2 in their circulation. Subsequently, we examined the concentration of hBD-2 protein in the circulation of psoriasis patients and showed a much stronger correlation with disease activity (PASI) than with genomic beta-defensin copy number. We also confirmed the correlation between disease severity and hBD-2 expression in atopic dermatitis, although this correlation was less strong. In another disease which is characterized by inflammation (rheumatoid arthritis) we found no correlation between disease severity and hBD-2 levels in the circulation. These findings implicate that hBD-2

levels in the circulation of psoriasis patients could act as a surrogate marker for disease severity in psoriasis patients, but might also be used within individual patients to monitor disease severity in time.

The outcome of microarray studies on the epidermal transcriptome of psoriatic and atopic dermatitis skin gave insight in disease-specific gene expression. In **chapter 4** we show that using these disease-specific expression profiles, we were able to distinguish samples from healthy, psoriatic and eczematous skin. We further investigated whether we could select a set of genes, which expression was able to distinguish healthy, psoriatic, atopic dermatitis skin, irritant and allergic contact dermatitis. We found that a set of only seven genes could discriminate these various skin diseases based on the epidermal expression profiles, indicating that molecular diagnostics may be used for those patients where a distinction between psoriasis or eczema cannot be made clinically.

Methods

Over the past years our department has developed several models using human skin equivalents (HSE). These *in vitro* skin models can be used to study normal skin biology, but also diseased skin can be mimicked after addition of disease-specific cytokines to the culture medium. Primary human keratinocytes are a limited factor for these skin equivalents, as their normal life span is between 30 and 60 days of culturing before they stop dividing and reach senescence. For this reason only a very limited number of experiments can be performed using keratinocytes derived from patients as the keratinocytes first have to divide several times before enough cells are available for experiments. **Chapter 5** describes that addition of Rho kinase inhibitor Y-27632 to the culture media increases the life span to over 100 days, without showing any signs of senescence. This implies that from the same number of skin biopsies large quantities of keratinocytes can be cultured and more experiments can be performed. Addition of Y-27632 also improved the quality of HSEs when added to the cells during the submerged phase.

Since primary human keratinocytes are hard to transfect using the traditional methods, the development of third-generation self-inactivating lentiviral transfection systems seems promising for this purpose. Indeed, lentiviral particles appeared to be able to infect keratinocytes efficiently, resulting in prolonged transgenic expression. In **chapter 5** we showed that addition of Y-27632 to keratinocytes during transfection, the transfection efficiency is even higher. Another positive effect of Y-27632 on lentiviral transduced keratinocytes was that the increased quality of the subsequently formed HSE. In **chapter 6** we used the lentiviral transfection system as a tool for delivering short hairpin RNAs into keratinocytes and examined the effects of knockdown of the CST6-gene on the formation of HSEs. Lack of the development of a multilayered epidermis suggested that CST6 deficiency would be incompatible with normal human skin development in the fetus. So far, no cases of patients or stillborn fetuses harboring CST6 mutations have been reported.

Medicines

In chapter 2 we examined the expression of the vanin gene family in skin and other tissues. Because vanins are enzymes, we reasoned that it should be possible to inhibit the activity by specific inhibitors. We hypothesized that analogues of its natural substrate (pantetheine) that lack the amide-bond that is hydrolyzed by the enzyme, would act as competitive vanin inhibitors. **Chapter 7** described the design, synthesis and analysis of pantetheine analogues and we report that some of these compounds have anti-vanin activity. Among these, RR6 was the most potent one, with an IC_{50} of 40 nM in human serum. Unfortunately, we could not find any consistent and positive effects in our *in vitro* psoriatic skin models (data not shown).

We found that RR6 is able to achieve a prolonged complete inhibition of plasma vanin activity in rats given RR6 orally in doses of 50 mg/kg or via their drinking water at a concentration of 3 mg/l. Because the exact biological role of vanins remain unclear and some studies suggested a possible role for vanins in lipid homeostasis we investigated the effect of RR6 on fasting in rats. In RR6-treated rats we found increased levels of free fatty acids in their plasma, while cholesterol levels decrease. These results indeed show that vanins are involved in lipid metabolism.

In our search for possible applications for vanin inhibitors, we ran into literature from the forties of the last century describing pantothenic acid analogs as possible antibiotic or antimalarial agents^{1,2}. In 1970, Clifton *et al.*³ was the first who described a specific subset of pantothenic acid analogs (referred to as pantothenamides) that have antimicrobial activity against *E. coli* and *S. aureus*. Based on the structural similarities to pantetheine, the natural substrate for vanins, we reasoned that pantothenamides could be hydrolyzed by vanins as well, thereby preventing pantothenamides to be active in an *in vivo* situation. In **chapter 8** we first showed that the effect of pantothenamides on bacterial growth was diminished when serum is added to bacterial cultures. Subsequently, we proved that pantothenamides are indeed hydrolyzed in serum. Finally, the addition of vanin inhibitors to pantothenamides result in protection of them, thus preserving their antibiotic activity in the presence of serum. These data provide evidence that the combination of an antimicrobial pantothenamide with an inhibitor of host (mammalian) pantetheinase activity, could act as a novel antibiotic strategy.

Final Remarks and outlook on future directions

The research presented in this thesis has potential application (1) in molecular diagnostics of inflammatory skin diseases, (2) analysis of skin biology in 3D tissue engineered models and (3) drug development of vanin inhibitors. The findings of chapter 4 require further translational research on diagnostic problems in dermatology. It would be a challenge for clinical dermatologists to validate these findings in real clinical practice, and to see e.g. in hand eczema, if molecular diagnostics on epidermal expression profiles would have therapeutic

consequences. The application of 3D skin models combined with lentiviral delivery of transgenes or shRNA, is currently used and further optimized in our lab. We think that this holds great promise for studying keratinocyte biology, disease mechanisms and drug development. An example of the application of these models is a recent paper from our group that used gene knockdown in 3D models for atopic dermatitis to elucidate the mechanism of action of coal tar⁴. The third application, drug development of vanin inhibitors, is actively pursued by our lab and will be discussed here in more detail.

Vanin inhibitors may have application in various fields of medicine, including metabolism and cancer, but the most obvious application would be the one outlined in chapter 7, the combination with pantothenamides as a novel antibiotic strategy. A number of issues, not addressed in my thesis, are important in this respect. These include selectivity of the compounds, potential toxicity and side effects, bioavailability, pharmacodynamics and pharmacokinetics. As the putative mode of action of pantothenamides is at the level of CoA-dependent biochemical pathways, this raised the question of selectivity for microbial versus host targets. Using high concentrations of vanin inhibitors and pantothenamides, no toxicity or significant inhibition of cell growth in the human kidney cell line 293T nor in primary epidermal keratinocytes was observed up to 100 μ M (not shown).

For an effective protection of pantothenamides *in vivo* in experimental animals, complete inhibition of endogenous pantetheinase activity is crucial. *In vitro* experiments in chapter 7 suggest that in the presence of 10% human serum (not heat-inactivated) a concentration of N7-Pan of at least 2 μ g/ml is required with at least 4 μ g/ml of RR6, to establish complete growth inhibition of *S. aureus*. A number of experiments were performed to address the question if these levels can be achieved *in vivo* in rodents. Administration of RR2 and RR6 at 100 mg/kg to mice should theoretically result in concentrations of pantetheinase inhibitor near 2 mM in serum. This concentration should be high enough for complete pantetheinase inhibition. After administration of pantetheinase inhibitor RR2 (intraperitoneally or orally), sequential serum samples were collected and tested for pantetheinase activity. The administered compounds were well tolerated by the mice, but unfortunately no complete pantetheinase inhibition was achieved as shown in figure 9.1A. No differences were observed between the ways of administration. Oral administration of RR6, which is 100-fold more potent than RR2, resulted in a significantly stronger decrease in pantetheinase activity (figure 9.1B), but still no complete pantetheinase inhibition was obtained and the half-life time remained relatively short (~80 min).

Although mice are the preferred experimental animals because many well characterized mouse models are available, the poor pharmacodynamics led us to test our compounds in other species. As shown in figure 7.2A, RR6 was able to completely inhibit pantetheinase activity in rats up to 8 hours after a single dose of 50 mg/kg.

Information on the concentration of pantothenamides *in vivo* is obviously important, as it should be high enough to have a bacteriostatic effect. Using

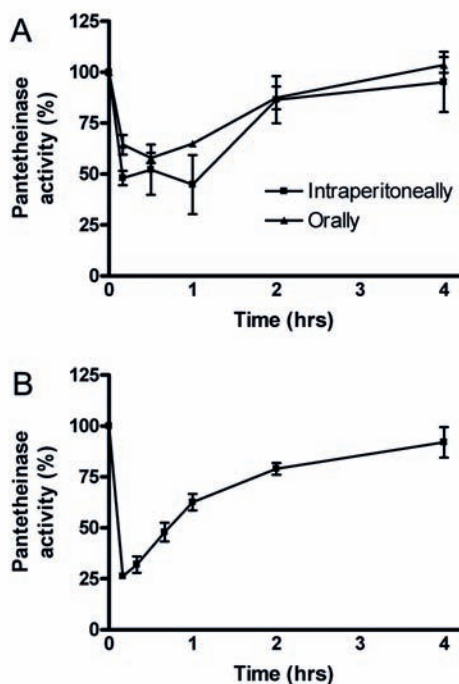


Figure 9.1 Pharmacodynamics of vanin inhibitors in mice. In (a) the type of administration was tested. RR2 was intraperitoneally and orally given at 100 mg/kg and blood samples were collected in time. Pantetheinase activity was measured and compared with pantetheinase activity in samples collected before administration. $n=3$. (b) Oral administration of 50 mg/kg of the more potent vanin inhibitor RR6, resulted in a stronger decrease of pantetheinase activity, but still no complete inhibition was achieved. $n=3$.

LC-MS we conducted pharmacokinetics of RR6 and N7-Pan in rats following a single dose of orally administered N7-Pan (250 mg/kg) alone, or in combination with 250 mg/kg RR6. When pantothenamides are not protected, their *in vivo* concentration decreases rapidly. Addition of RR6 increases the availability of N7-pan dramatically, as expected (figure 9.2). *In vitro* we found approximate MIC values of *S. aureus* for N7-Pan of 4 $\mu\text{g/ml}$ in 10% human serum (chapter 8). Extrapolating this to the *in vivo* situation, this implies that at the dosage of 250 mg/kg for both compounds, the N7-Pan concentration is above MIC for 3 hours. This is at a borderline value, considering that *in vivo* the plasma concentration is 100% (as opposed to 10% serum *in vitro*). This was investigated in a pilot experiment where we did not find a clear antimicrobial effect of N7-Pan at 250 mg/ml combined with 50 mg/ml RR6, using the rat thigh-muscle model with *S. aureus* (not shown here).

We are currently trying to improve our lead compound RR6, in a project funded by the Netherlands Genomics Initiative. This is done via a classical medicinal chemistry approach. In addition, we are building a homology model of human vanins based on published structures of the nitrilase family. Once such a model is established, this may allow a more rational lead optimization. So far,

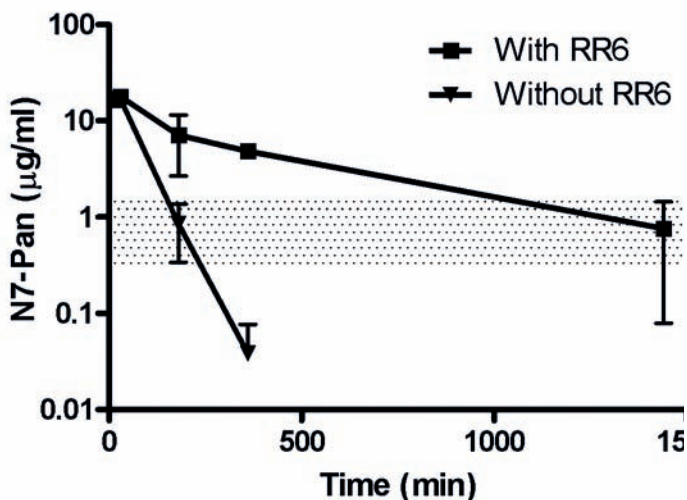


Figure 9.2 Pharmacokinetics of N7-Pan in rats. Pharmacokinetics of N7-Pan in rats after a single oral dose of 250 mg/kg N7Pan with and without 250 mg/kg RR6. RR6 is able to prolong the presence of N7-Pan. The dotted box represents the MIC for *S. aureus* based on *in vitro* determinations in 10% serum.

attempts to improve the potency of pantothenamides have failed. N5-Pan and N7-Pan, already known for more than 40 years are still the most potent compounds in their class. Although the targets of pantothenamides have been studied and were shown to affect CoA and lipid biosynthetic pathways⁵⁻⁷, there may be other targets. Identification of pantothenamide targets will further aid the optimization of these compounds to achieve antimicrobial potencies in the submicromolar range. Ideally, non-hydrolysable, vanin-resistant pantothenamides or analogues thereof would be an even better option as this will make the presence of vanin inhibitors superfluous.

In conclusion, we have proven that the principle of our strategy, protection of pantothenamide antibiotics against vanin hydrolysis, works. Current efforts are aimed at taking a next step to the development of vanin inhibitors for clinical use.

References

1. Mead JF, Koepfli JB. The synthesis of potential antimalarials; the preparation of methylated amides of taurine and their pantoyl derivatives. *J Org Chem* 12, 295-7 (1947)
2. Mead JF, Rapport MM, *et al.* The synthesis of potential antimalarials; derivatives of pantoyltaurine. *J Biol Chem* 163, 465-73 (1946)
3. Clifton G, Bryant SR, Skinner CG. N'-(substituted) pantothenamides, antimetabolites of pantothenic acid. *Arch Biochem Biophys* 137, 523-8 (1970)
4. van den Bogaard EH, Bergboer JG, Vonk-Bergers M, van Vlijmen-Willems IM, Hato SV, van der Valk PG *et al.* Coal tar induces AHR-dependent skin barrier repair in atopic dermatitis. *J Clin Invest* doi: 10.1172/JCI65642 (2013)
5. Zhang YM, Frank MW, Virga KG, Lee RE, Rock CO, Jackowski S. Acyl carrier protein is a cellular target for the antibacterial action of the pantothenamide class of pantothenate antimetabolites. *J Biol Chem* 279, 50969-75 (2004)
6. Thomas J, Cronan JE. Antibacterial activity of N-pentylpantothenamide is due to inhibition of coenzyme a synthesis. *Antimicrob Agents Chemother* 54, 1374-7 (2010)
7. Strauss E, Begley TP. The antibiotic activity of N-pentylpantothenamide results from its conversion to ethyldethia-coenzyme a, a coenzyme a antimetabolite. *J Biol Chem* 277, 48205-9 (2002)



Appendix

Nederlandse samenvatting

Dankwoord

List of publications

Curriculum vitae

Nederlandse samenvatting

Historisch gezien worden psoriasis en atopisch eczeem beschouwd als immunologische huidaandoeningen, waarbij immuuncellen een belangrijke rol spelen. De afgelopen 10 jaar is dit beeld bijgesteld, omdat keratinocyten (de grootste groep huidcellen) ook een grote rol blijken te spelen. Tegenwoordig wordt algemeen aangenomen dat een complexe interactie tussen immuuncellen en keratinocyten verantwoordelijk is voor de pathogenese van psoriasis en atopische dermatitis.

De afdeling Dermatologie aan de Radboud Universiteit van Nijmegen onderzoekt al geruime tijd de epidermale huid biologie, met een focus op keratinocyten en hun genexpressie. In dit verband is een microarray studie uitgevoerd waarin de genexpressie in die aangedane huid van psoriasispatiënten werd vergeleken met aangedane huid van atopisch eczeem patiënten. Deze resultaten vormen de basis voor dit proefschrift. De uitdaging was, nadat de resultaten uit de microarray studie bevestigd waren, om de relevantie van ziekte-specifieke genexpressie in etiologische, diagnostische en therapeutische perspectieven van deze ziekten te achterhalen.

De huid, de structuur en de functie worden beschreven in **hoofdstuk 1**. Tevens wordt de huidige status van de twee meest voorkomende huidziekten, psoriasis en atopisch eczeem, beschreven. Verder worden in dit hoofdstuk verschillende *in vitro* huid modellen en methodes voor transgene genexpressie of specifieke gen knockdown in gekweekte keratinocyten samengevat.

Moleculen & Markers

Het meest differentieel tot expressie komend gen uit de microarray studie (VNN3) is door ons verder onderzocht. In **hoofdstuk 2** hebben we eerst bevestigd dat VNN3 inderdaad tot overexpressie gebracht wordt in psoriatische huid in vergelijking met atopische eczeem huid en huid van gezonde vrijwilligers. Naast de expressie van VNN3 blijkt ook de expressie van VNN1, maar niet van VNN2, te zijn verhoogd in psoriatische huid. De Vanine expressie wordt geïnduceerd door T-cel afgeleide cytokinen van de Th1 (interferon- γ en TNF- α) en Th17 (IL22 en IL17) types, die in hoge mate aanwezig zijn in aangedane psoriatische plaques. Het klinische effect van een verhoogde vanine expressie blijft onduidelijk, maar cysteamine, de metabool die wordt gevormd na hydrolyse van pantetheine, zou een rol kunnen spelen in de regulatie van huidontsteking en differentiatie.

Het bestaan van beta-defensine kopienummer variatie en de correlatie daarvan met psoriasis, in combinatie met de wetenschap dat beta-defensine-2 (hBD-2) sterk opgereguleerd wordt in psoriatische huid, leidde ons ertoe de hBD-2 expressie op eiwitniveau te onderzoeken. In **hoofdstuk 3** beschrijven we een zwakke correlatie tussen het beta-defensine kopienummer bij gezonde vrijwilligers en de hoeveelheid hBD2 in hun circulatie. Vervolgens onderzochten we de concentratie van hBD-2-eiwit in de bloedsomloop van psoriasis patiënten. Hier vonden we een veel sterkere correlatie met ziekteactiviteit (PASI) dan met

genomisch beta-defensine kopienummer. We tonen ook aan dat er bij atopisch eczeem patiënten een correlatie is tussen de ernst van de ziekte en hBD-2 expressie, maar dat deze correlatie een stuk minder sterk is dan in psoriasis. In een andere ziekte die wordt gekenmerkt door ontsteking (reumatoïde artritis) werd geen correlatie tussen ernst van de ziekte en hBD-2 waardes in de circulatie gevonden. Deze bevindingen impliceren dat hBD-2 niveaus in de circulatie van patiënten met psoriasis zouden kunnen fungeren als een surrogaat marker voor de ernst van hun ziekte. Ook kan het gebruikt worden om in individuele patiënten de ernst van de ziekte in de tijd te volgen.

De resultaten van de microarray studies naar het epidermale transcriptoom van psoriasis en atopische eczeem huid verschaftte inzicht in ziekte-specifieke genexpressie. In **hoofdstuk 4** laten we zien dat door gebruik te maken van deze ziekte-specifieke expressie profielen, we in staat waren om onderscheid te maken tussen samples van gezonde, psoriatische en eczematuze huid. Verder hebben we onderzocht of we een set van genen konden selecteren die in staat is om gezonde, psoriatische, atopische eczeem huid, irriterende en allergische contact eczeem te onderscheiden. We vonden dat met een set van slechts zeven genen deze verschillende huidziekten op basis van de epidermale expressieprofielen onderscheiden kunnen worden. Dit toont aan dat moleculaire diagnostiek gebruikt kan worden bij patiënten bij wie een onderscheid tussen psoriasis of eczeem niet klinisch vastgesteld kan worden.

Methodes

In de afgelopen jaren heeft onze afdeling diverse modellen ontwikkeld op basis van menselijke huidequivalenten. Deze in vitro huid modellen kunnen worden gebruikt om de biologie van normale huid te bestuderen, maar ook zieke huid kan worden nagebootst na toevoeging van ziekte-specifieke cytokines aan het kweekmedium. De hoeveelheid primaire humane keratinocyten is de beperkte factor bij de productie van deze huidequivalenten. De normale levensduur van deze cellen in kweek ligt tussen de 30 en 60 dagen, waarna ze stoppen met delen en in een rusttoestand raken. Daarom kan slechts een zeer beperkt aantal experimenten uitgevoerd worden met keratinocyten afkomstig van patiënten als keratinocyten eerst meerdere keren moeten delen voordat genoeg cellen beschikbaar zijn om experimenten mee uit te kunnen voeren. **Hoofdstuk 5** beschrijft dat toevoeging van Rho kinase remmer Y-27632 aan het kweekmedium de levensduur verhoogt tot meer dan 100 dagen, zonder enige tekenen van veroudering. Dit betekent dat van hetzelfde aantal huidbiopten grotere hoeveelheden keratinocyten kunnen worden gekweekt, waarmee meer experimenten uitgevoerd kunnen worden. Toevoeging van Y-27632 verbetert ook de kwaliteit van huidequivalenten wanneer deze toegevoegd wordt aan de cellen tijdens de eerste fase van de kweek.

Aangezien primaire humane keratinocyten moeilijk te transfecteren zijn met de traditionele methoden is de ontwikkeling van de zogenoemde derde generatie zelf-inactiverende lentivirale transfectiesystemen veelbelovend voor dit doel.

Lentivirussen blijken keratinocyten efficiënt te kunnen infecteren wat resulteert in langdurige transgen-expressie. In **hoofdstuk 5** laten we zien dat door toevoeging van Y-27632 aan het medium tijdens de transfectie de transfectie-efficiëntie nog hoger wordt. Een ander positief effect van Y-27632 op lentiviraal getransduceerde keratinocyten was dat de kwaliteit van het later gevormde huidequivalent beter was.

In **hoofdstuk 6** gebruiken we het lentivirale transfectie systeem om short hairpin RNA's (shRNA) in keratinocyten tot expressie te laten komen. Hierdoor kunnen de effecten van het missen van het CST6-gen op de vorming van huidequivalanten onderzocht worden. De ontwikkeling van een meerlagige epidermis bleek zonder CST6 niet mogelijk, wat suggereert dat CST6 deficiëntie onverenigbaar is met de vorming van menselijke huid tijdens de ontwikkeling van de foetus. Tot nu toe zijn geen gevallen van patiënten of doodgeboren foetussen gemeld, waarbij mutaties in CST6 gevonden zijn.

Geneesmiddelen

In **hoofdstuk 2** hebben we gekeken naar de expressie van de vanine genfamilie in de huid en andere weefsels. Omdat vanines enzymen zijn, beredeneerden we dat het mogelijk zou moeten zijn om de activiteit hiervan te remmen door specifieke remmers te ontwikkelen. Competitieve remmers zouden verkregen kunnen worden door analogen van het natuurlijke substraat (pentetheine) zonder de amide-binding, welke gehydrolyseerd wordt door vanines, te maken. **Hoofdstuk 7** beschrijft het ontwerp, de synthese en de analyse van pantetheine analogen. Een aantal van deze verbindingen blijkt anti-vanine activiteit te hebben. Hiervan is RR6 de meest potente, met een IC_{50} van 40 nM in humaan serum. Helaas vonden we geen consistente en positieve effecten in onze *in vitro* psoriatische huid modellen (gegevens niet getoond).

Door de toediening van RR6 in ratten (oraal in doses van 50 mg/kg of via het drinkwater in een concentratie van 3 mg/l) bleek een langdurige volledige remming van plasma vanine activiteit haalbaar. Omdat de exacte biologische rol van vanines niet bekend is en sommige studies een mogelijke rol voor vanines in lipide homeostase suggereren, zijn we het effect van RR6 op vasten bij ratten gaan onderzoeken. In RR6-behandelde ratten vonden we verhoogde niveaus van vrije vetzuren in het plasma, terwijl de cholesterol waardes daalden. Deze resultaten tonen aan dat vanines inderdaad betrokken zijn bij het vetmetabolisme.

In onze zoektocht naar mogelijke toepassingen voor vanine remmers, vonden we in de literatuur uit de jaren veertig van de vorige eeuw de beschrijving van pantotheenzuur analogen die mogelijk als antibioticum of als anti-malariamiddel gebruikt konden worden^{1,2}. In 1970 beschrijft Clifton *et al.*³ als eerste een specifieke subset van pantotheenzuur analogen (hierna pantothenamides genoemd) die antimicrobiële activiteit tegen *E. coli* en *S. aureus* vertoonden. Gebaseerd op de structurele overeenkomsten met pantetheine, het natuurlijke substraat voor vanines, beredeneerden we dat pantothenamides ook wel eens gehydrolyseerd konden worden door vanines. Hierdoor zullen pantothenamides *in vivo* niet actief

zijn. In **hoofdstuk 8** laten we eerst zien dat het effect van pantothenamides op bacteriële groei vermindert, wanneer serum wordt toegevoegd aan bacteriekweken. Vervolgens tonen we aan dat pantothenamides inderdaad gehydrolyseerd worden in serum. Tenslotte laten we zien dat door toevoeging van vanine remmers, de pantothenamides niet afgebroken worden. Hierdoor blijft de antibiotische activiteit in de aanwezigheid van serum behouden. Deze gegevens tonen aan dat de combinatie van een antimicrobiële pantothenamide met een remmer van gastheer (zoogdieren) vanine activiteit, zou kunnen dienen als een nieuwe antibioticumstrategie.

Slotopmerkingen en toekomstplannen

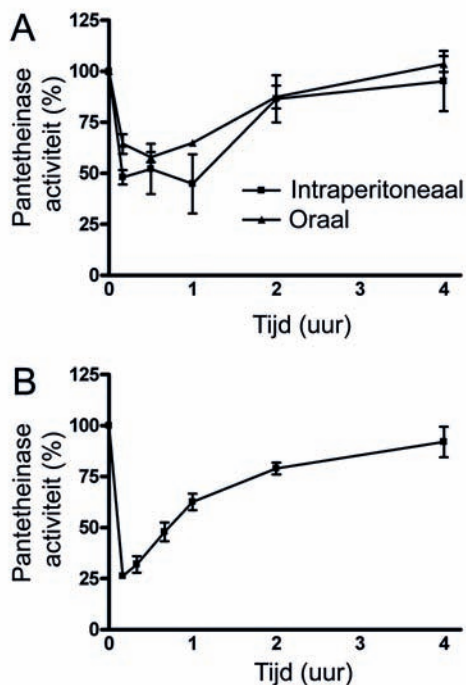
Het onderzoek beschreven in dit proefschrift heeft potentiële toepassingen (1) in de moleculaire diagnostiek van inflammatoire huidziekten, (2) in de analyse van de huid biologie in 3D weefselkweek modellen en (3) in de ontwikkeling van geneesmiddelen met vanine remmers. De bevindingen van hoofdstuk 4 vereisen meer translationeel onderzoek met betrekking tot diagnostische belemmeringen. Het zou een uitdaging voor de klinische dermatologen zijn om deze bevindingen te valideren in de echte klinische praktijk, en om bijvoorbeeld bij handeczeem te kijken of moleculaire diagnostiek op epidermale expressieprofielen therapeutische consequenties kan hebben. De toepassing van 3D-huid, gecombineerd met lentivirale toediening van transgenen of shRNA, wordt op dit moment gebruikt en verder geoptimaliseerd in ons lab. Wij verwachten dat dit een grote invloed kan hebben bij het bestuderen van keratinocyt biologie, ziekte mechanismen en de ontwikkeling van geneesmiddelen. Een voorbeeld van de toepassing van deze modellen is een recent artikel van onze groep waarbij gen knockdown in een 3D model voor atopische eczeem het werkingsmechanisme van koolteer⁴ opgehelderd heeft. De derde applicatie, de ontwikkeling van geneesmiddelen met vanine remmers, wordt actief nagestreefd door ons lab en worden hieronder in meer detail besproken.

Vanine remmers kunnen toepassingen hebben in verschillende vakgebieden, zoals metabolisme en kanker, maar de meest voor de hand liggende toepassing zou degene zijn die in hoofdstuk 7 besproken is: de combinatie met pantothenamides als een nieuwe antibioticumstrategie. Een aantal, niet in mijn proefschrift benoemde zaken, zijn in dit verband van belang, zoals selectiviteit van de verbindingen, potentiële toxiciteit en eventuele bijwerkingen, biobeschikbaarheid, farmacodynamische en farmacokinetische eigenschappen. De vermeende werking van pantothenamides is op het niveau van CoA-afhankelijke biochemische processen, die de vraag rijzen over selectiviteit voor microbiële versus gastheer targets. Hoge concentraties vanine remmers en pantothenamides tonen geen toxiciteit of significante remming van celgroei in een menselijke nier cellijn (293T) noch in primaire epidermale keratinocyten waargenomen tot 100 μ M (niet getoond).

Voor een doeltreffende bescherming van pantothenamides *in vivo* is in proefdieren een volledige remming van endogene vanine activiteit cruciaal. *In*

vitro experimenten in hoofdstuk 7 suggereren dat de aanwezigheid van 10% humaan serum (niet hitte-geïnactiveerd) een concentratie van N7-Pan van ten minste 2 µg/ml nodig is met ten minste 4 µg/ml RR6 om volledig groeiremming van *S. aureus* te realiseren. We hebben een aantal experimenten uitgevoerd om te kijken of deze waarden *in vivo* kunnen worden bereikt in knaagdieren. Toediening van RR2 en RR6 van 100 mg/kg in muizen zouden in theorie moeten leiden tot concentraties van de remmers in de buurt van de 2 mM in serum. Deze concentratie moet hoog genoeg zijn om de volledige pantetheinase activiteit te remmen. Na toediening van vanine remmer RR2 (intraperitoneaal of oraal), werden in de tijd serummonsters verzameld en getest op pantetheinase activiteit. De toegediende verbindingen werden goed verdragen door de muizen, maar er werd geen volledige pantetheinase remming bereikt (zie figuur 1A). Er werden geen verschillen waargenomen tussen de toedieningsvormen. Orale toediening van RR6, die 100 maal krachtiger dan RR2, resulteerde in een significant sterkere daling van de pantetheinase activiteit (figuur 1B), maar nog steeds werd geen volledige remming van pantetheinase activiteit verkregen. Tevens was de halfwaardetijd relatief kort (~ 80 min).

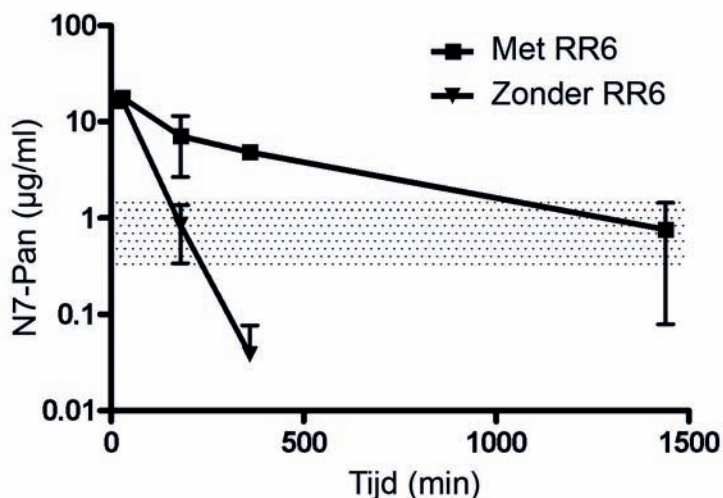
Doordat veel goed gekarakteriseerde muismodellen beschikbaar zijn, is dit het proefdiermodel bij voorkeur. Door de slechte farmacodynamiek van onze



Figuur 1 Farmakodynamiek van vanine remmers in muizen. In (a) is toedieningsmethode getest. RR2 (100 mg/kg) is intraperitoneaal en oraal toegediend, waarna bloedsamples in de tijd verzameld zijn. Pantetheinase activiteit in deze samples is gemeten en vergeleken met de pantetheinase activiteit in het bloed van voor de toediening. n=3. (b) Orale toediening (50 mg/kg) van de potentere vanine remmer RR6 resulteert in een sterkere daling van de pantetheinase activiteit. Een complete remming wordt echter niet bereikt. n=3.

stoffen in muizen zijn we onze verbindingen in andere diersoorten gaan testen. Zoals getoond in figuur 7.2A (hoofdstuk 7) kan RR6 de pantetheinase activiteit in ratten volledig remmen tot wel 8 uur na een enkele dosis van 50 mg/kg.

Informatie over de concentratie pantothenamides *in vivo* is uiteraard belangrijk, omdat deze hoog genoeg moet zijn om een bacteriostatisch effect te hebben. Met LC-MS hebben we de farmacokinetiek van RR6 en N7-Pan bepaald in ratten na een enkele dosis oraal toegediend N7-Pan (250 mg/kg) alleen of in combinatie met 250 mg/kg RR6. Wanneer pantothenamides niet beschermd worden, neemt de concentratie *in vivo* snel af. Toevoeging van RR6 verhoogt, zoals verwacht, de beschikbaarheid van N7-pan enorm (figuur 9.2). *In vitro* vonden we MIC waarde voor N7-Pan tegen *S. aureus* van 4 µg/ml in 10% humaan serum (hoofdstuk 8). Geëxtrapolleerd naar de *in vivo* situatie betekent dit dat bij een dosering van 250 mg/kg van beide verbindingen de N7-Pan concentratie ongeveer 3 uur boven deze MIC is. Dit is een borderline waarde, aangezien de *in vivo* plasma concentratie 100% is (tegenover 10% serum *in vitro*). Dit hebben we onderzocht in een pilot experiment met behulp van een rat dijbeen-spier infectie model met *S. aureus*, waarbij we geen duidelijk antimicrobiële werking van N7-Pan vonden bij 250 mg/ml N7-Pan in combinatie met 50 mg/ml RR6, (hier niet getoond).



Figuur 2 Farmacokinetiek van N7-Pan in ratten. Farmacokinetiek van N7-Pan in ratten na een enkele orale dosis N7-Pan (250 mg/kg) met en zonder RR6 (250 mg/kg). In aanwezigheid van RR6 is N7-Pan langer aanwezig. Het gestippelde blok geeft de MIC van *S. aureus* aan, gebaseerd op *in vitro* bepalingen in 10% serum.

Wij zijn momenteel bezig om onze lead compound RR6 te verbeteren via een klassieke medicinale chemie benadering. Dit project wordt gefinancierd door het Nederlands Genomisch Initiatief. Daarnaast bouwen we een homologiemodel van menselijke vanines gebaseerd op gepubliceerde structuren van de nitrilase familie. Zodra een dergelijk model klaar is, kan dit mogelijk zorgen voor een meer

rationele lead optimalisatie. Pogingen om de sterkte van de pantothenamides te verbeteren zijn tot dusver mislukt. N5-Pan en N7-Pan, die al meer dan 40 jaar bekend zijn, zijn nog steeds de meest potente verbindingen in hun klasse. Hoewel de moleculaire targets van pantothenamides reeds onderzocht zijn en betrokken blijken te zijn in het CoA metabolisme en lipide biosynthese⁵⁻⁷, kunnen er nog andere targets zijn. De identificatie van targets van pantothenamides kan de optimalisatie van deze verbindingen om antimicrobiële potentie in submicromolaire range te bereiken verder verbeteren. De meest ideale compound zou een niet-hydrolyseerbare, vanine-resistente pantothenamide of analoog daarvan zijn, zodat dit de aanwezigheid van vanine remmers overbodig zou maken.

Tot slot hebben we bewezen dat het basis idee van onze strategie, de bescherming van pantothenamides tegen vanine hydrolyse, werkt. De huidige inspanningen zijn gericht op het nemen van een volgende stap de ontwikkeling van vanine remmers voor klinisch gebruik.

Referenties

1. Mead JF, Koepfli JB. The synthesis of potential antimalarials; the preparation of methylated amides of taurine and their pantoyl derivatives. *J Org Chem* 12, 295-7 (1947)
2. Mead JF, Rapport MM, *et al.* The synthesis of potential antimalarials; derivatives of pantoyltaurine. *J Biol Chem* 163, 465-73 (1946)
3. Clifton G, Bryant SR, Skinner CG. N'-(substituted) pantothenamides, antimetabolites of pantothenic acid. *Arch Biochem Biophys* 137, 523-8 (1970)
4. van den Bogaard EH, Bergboer JG, Vonk-Bergers M, van Vlijmen-Willems IM, Hato SV, van der Valk PG *et al.* Coal tar induces AHR-dependent skin barrier repair in atopic dermatitis. *J Clin Invest* doi: 10.1172/JCI65642 (2013)
5. Zhang YM, Frank MW, Virga KG, Lee RE, Rock CO, Jackowski S. Acyl carrier protein is a cellular target for the antibacterial action of the pantothenamide class of pantothenate antimetabolites. *J Biol Chem* 279, 50969-75 (2004)
6. Thomas J, Cronan JE. Antibacterial activity of N-pentylpantothenamide is due to inhibition of coenzyme a synthesis. *Antimicrob Agents Chemother* 54, 1374-7 (2010)
7. Strauss E, Begley TP. The antibiotic activity of N-pentylpantothenamide results from its conversion to ethyldethia-coenzyme a, a coenzyme a antimetabolite. *J Biol Chem* 277, 48205-9 (2002)

Dankwoord

Ruim 7 jaar nadat ik begon aan mijn promotieavontuur ga ik dan eindelijk beginnen aan het laatste stuk, het dankwoord. Dit is niet alleen het meest gelezen stukje proefschrift, maar waarschijnlijk ook het meest gewaardeerde. Ik heb het geluk gehad met enorm veel mensen samen te mogen werken, wat er helaas voor kan zorgen dat ik onverhoopt iemand vergeet te bedanken hieronder. Vandaar dat ik begin met iedereen die, in de breedst mogelijke zin, een bijdrage heeft geleverd aan dit proefschrift te bedanken. Zonder jullie bijdrage is het resultaat er nooit in deze vorm gekomen: Bedankt!

Allereerst wil ik mijn beide promotoren bedanken. Joost, met Patrick sr. als rechterhand. Als ik nu terug kijk op de weg die we bewandeld hebben, kunnen we denk ik rustig concluderen dat het nooit de makkelijkste, kortste weg geweest is. Vergelijkbaar met een navigatie-systeem, waarbij naast de kortste en de energiezuinigste route ook de mooiste, zeg maar toeristische, route ingesteld kan worden. We hebben het aangedurfd om de grenzen van dermatologisch onderzoek te overschrijden. Dit heeft mij enorm geïnspireerd en gemotiveerd. Hopelijk gaan er nog leuke resultaten uit het vanine-werk komen. Mocht het onverhoopt toch tegenvallen uiteindelijk, dan hebben we in elk geval een leuke, leerzame weg bewandeld. Bedankt dat jullie mij deze mogelijkheden gegeven hebben. Hierbij wil ik ook Peter van de Kerkhof graag bedanken dat ik op zijn afdeling onderzoek heb mogen doen.

Uiteraard wil ik ook graag een aantal directe collega's bedanken. Judith, je kwam, zag, overwon en vloog naar Boston. Je enthousiasme heeft het een genot gemaakt om met je te mogen werken. En na een week hard werken in de stad even stoom uitblazen met een Bessen, of zelfs Goldstrike, was ook altijd een avontuur. Jeroen, we hadden eenzelfde gevoel voor zowel slechte muziek als slechte grappen. We hebben dus veel gelachen samen, maar ook praktisch hebben we prima samen kunnen werken. Je was voor mij dan ook een logische keuze om je te vragen me bij te staan als paranimf. Diana, Ivonne en Mieke, jullie waren als 'analytische ondersteuning' onmisbaar voor het lab in het algemeen, maar zeker ook voor mijn promotie onderzoek. Waar mogelijk hebben jullie me geholpen met kweken (Diana), histologie (Ivonne) en allerlei overige (rot)klusjes (Mieke). Het was altijd prettig met jullie samenwerken! Sandra en Ellen, dankzij jullie 3D kweekkwaliteiten heeft mijn boekje meer diepgang gekregen. Sandra, bedankt voor de samenwerking en gezelligheid op onze kamer. Ellen, we hebben elkaar goed kunnen helpen met onze gezamenlijk projectjes. Succes met het afronden van je boekje. Het wordt vast een meesterwerk. Marijke, de basis van ons onderzoek was hetzelfde. Jij meer gericht op eczeem en ik meer op psoriasis. We vulden elkaar denk ik goed aan. Bedankt voor je inzet en succes als dermatologe. Ook Piet wil ik graag even persoonlijk bedanken. Zijn FACS kwaliteiten en technische inzicht zijn ook voor dit proefschrift waardevol gebleken.

Als laatste wil ik Tsing graag even apart bedanken voor zijn gezelligheid. Je zit inmiddels alweer ruim 3 jaar in The Big Apple, maar de jaren dat we samen hebben gewerkt hebben we veel lol gehad in o.a. de Refter, de kroeg en op congressen.

Verder wil ik 'mijn' studenten graag bedanken. Mirjam, Paul, Corien en Linh. Ik heb jullie met veel plezier zowel wetenschappelijk als praktisch het een en ander bij proberen te spijkeren en ik hoop dat ik hier in geslaagd ben. Jullie inspanningen voor mij zijn door dit proefschrift heen terug te vinden. Ik wens jullie veel succes en plezier met jullie (wetenschappelijke) loopbaan. Linh, thanks for your contribution to my thesis. I hope that you've learned a lot during your time at our department. I wish you all the best with your career.

Verder wil ik de mensen van het CDL die geholpen hebben bij mijn onderzoek graag bedanken. Met name Daphne, Linda en Debby hebben mij veel werk (letterlijk) uit handen genomen. Maar ook Alex, Sophie, Annet en Helma zijn een vermelding waard voor hun inspanningen. En het was nog gezellig ook!

Ook de "vanine-groep" wil ik graag apart bedanken. Vanaf de synthese van de eerste remmers, vernoemd naar de chemici Rutjes en Ritsen, is het enthousiasme van de synthese-kant groot, wat uiteraard erg prettig samenwerkte. Dus Jodie, Bas, Floris, Pedro, Peter (Botman), Richard, Erik, Geeske en Christien: bij deze bedankt voor de prettige samenwerking. Uiteraard ben ik ook de overige betrokkenen bij het vanine onderzoek dank verschuldigd. Peter (van Galen), jouw hulp bij de HPLC heeft ons het directe bewijs gegeven dat de pantothenamides beschermd werden door de vanine-remmers. Peter (Burghout) en Marco wil ik graag bedanken voor het testen van de pantothenamides op *pneumococcon* en het leggen van de basis om de moleculaire targets te identificeren. Marga, Wouter en Geert-Jan wil ik graag bedanken voor hun hulp bij het testen van de pantothenamides en vanine-remmers in malaria. Hopelijk gaat dit nog leuke resultaten opleveren.

Op de laatste kamer van de gang heb ik tussen het labwerk door enorm veel tijd doorgebracht. In deze kamer-voor-4 heb ik in de loop der jaren veel kamergenoten mogen verwelkomen en uitzwaaien. De (weten)schappelijke en (on)zin besprekingen hebben zeker een goede invloed op me gehad. Het is bijna een wonder dat hier nooit conflicten zijn ontstaan. In chronologische volgorde, hopelijk zonder iemand te vergeten, wil ik de volgende (ex)roomies bedanken voor de gezelligheid: David, Marijke, Desiree, Sandra, Judith, Corien, Jeroen, Helmi, Ferry en Jorine. Hiervoor jullie dank!

Verder wil ik graag de overige (ex)-collega's bedanken voor de gezelligheid op het lab, in de koffiekamer, met dagjes uit en de (kerst)borrels. Er heerst een prettige werksfeer, wat de resultaten alleen maar ten goede kan komen. Bedankt!

Buiten het werk was er genoeg afleiding om het hoofd te legen. De atletiekbaan was een prima lokatie om frustraties van tegenvallende experimenten te relativeren en om nieuwe ideeën op te doen. Daarom wil ik graag Theo en alle me(d)e-lopers bedanken voor het afpeigeren tijdens de trainingen. Uiteraard wil ik ook mijn vrienden bedanken voor de nodige ontspanning onder het genot van een (speciaal) biertje.

Klaas, aan jou de eer om een hele alinea te krijgen! We hebben elkaar leren kennen op de atletiekbaan, maar ook daarbuiten konden we het altijd goed vinden. Ik mocht je zelfs bijstaan bij jouw promotie en nu heb je dezelfde taak bij de mijne. Het was prettig met iemand inhoudelijk over werk te kunnen praten, zonder dat je er direct bij betrokken was. Hierdoor keek je er net wat anders tegenaan, wat soms verhelderend werkte. Bedankt voor de gezelligheid en bedankt dat je mijn paranimf wilt zijn.

Verder wil ik graag mijn (schoon)familie bedanken voor hun interesse in en betrokkenheid bij mijn onderzoek. Een speciale dank gaat uit naar mijn ouders en zus(je) Suzanne. Jullie hebben me altijd gesteund in mijn (studie)keuzes en hier is dan eindelijk een fysiek resultaat. Ik ben blij dat na een aantal roerige jaren de rust is wedergekeerd. Ik ben blij dat iedereen weer gelukkig is.

Lieve Marjon, aan jou de eer om als laatste aan bod te komen in dit dankwoord. Jouw geduld en aanmoedigen hebben indirect misschien wel het meest bijgedragen aan dit boekje. Vanaf de eerste dag heb je me gesteund en geprobeerd te begrijpen wat ik aan het doen was. Hoewel ik mijn werk erg leuk vind, is het nog steeds veel leuker om 's avonds weer thuis te komen en om samen leuke dingen te doen. Ik hoop dan ook dat we de komende decenia nog ontelbaar veel leuke tripjes zullen gaan maken en dat we samen heel gelukkig oud mogen worden!

List of publications

Noordman YE, **Jansen PA**, Hendriks WJ. Tyrosine-specific MAPK phosphatases and the control of ERK signaling in PC12 cells. *J Mol Signal* 1, 4 (2005)

Jansen PA, Rodijk-Olthuis D, Hollox EJ, Kamsteeg M, Tjabringa GS, de Jongh GJ, van Vlijmen-Willems IM, Bergboer JG, van Rossum MM, de Jong EM, den Heijer M, Evers AW, Bergers M, Armour JA, Zeeuwen PL, Schalkwijk J. Beta-defensin-2 protein is a serum biomarker for disease activity in psoriasis and reaches biologically relevant concentrations in lesional skin. *PLoS One* 4, e4725 (2009)

Jansen PA, Kamsteeg M, Rodijk-Olthuis D, van Vlijmen-Willems IM, de Jongh GJ, Bergers M, Tjabringa GS, Zeeuwen PL, Schalkwijk J. Expression of the vanin gene family in normal and inflamed human skin: induction by proinflammatory cytokines. *J Invest Dermatol* 129, 2167-74 (2009)

Kamsteeg M, **Jansen PA**, van Vlijmen-Willems IM, van Erp PE, Rodijk-Olthuis D, van der Valk PG, Feuth T, Zeeuwen PL, Schalkwijk J. Molecular diagnostics of psoriasis, atopic dermatitis, allergic contact dermatitis and irritant contact dermatitis. *Br J Dermatol* 162, 568-78 (2010)

Medendorp K, Vreede L, van Groningen JJ, Hetterschijt L, Brugmans L, **Jansen PA**, van den Hurk WH, de Bruijn DR, van Kessel AG. The mitotic arrest deficient protein MAD2B interacts with the clathrin light chain A during mitosis. *PLoS One* 5, e15128 (2010)

Bergboer JG, Tjabringa GS, Kamsteeg M, van Vlijmen-Willems IM, Rodijk-Olthuis D, **Jansen PA**, Thuret JY, Narita M, Ishida-Yamamoto A, Zeeuwen PL, Schalkwijk J. Psoriasis risk genes of the late cornified envelope-3 group are distinctly expressed compared with genes of other LCE groups. *Am J Pathol* 178, 1470-7 (2011)

Jansen PA, Zeeuwen PL, Schalkwijk J, Rutjes FP, Ritzen B, Hermkens PH. Pantothenic acid derivatives and their use in the treatment of microbial infections. Patent Application Nr EP11725211, Publication Nr WO2011152720 (2011)

Jansen PA, Schalkwijk J, Rutjes FP, Sauerwein R, Hermkens PH. Derivatives of pantothenic acid and their use for the treatment of malaria. Patent application Nr EP11725212, Publication Nr WO2011152721 (2011)

van den Bogaard EH, Rodijk-Olthuis D, **Jansen PA**, van Vlijmen-Willems IM, van Erp PE, Joosten I, Zeeuwen PL, Schalkwijk J. Rho kinase inhibitor Y-27632 prolongs the life span of adult human keratinocytes, enhances skin equivalent

development, and facilitates lentiviral transduction. *Tissue Eng Part A*. 18, 1827-36 (2012)

Jansen PA, van den Bogaard EH, Kersten FF, Oostendorp C, van Vlijmen-Willems IM, Oji V, Traupe H, Hennies HC, Schalkwijk J, Zeeuwen PL. Cystatin M/E knockdown by lentiviral delivery of shRNA impairs epidermal morphogenesis of human skin equivalents. *Exp Dermatol* 21, 889-91 (2012)

Baerveldt EM, Onderdijk AJ, Kurek D, Kant M, Florencia EF, Ijpma AS, van der Spek PJ, Bastiaans J, **Jansen PA**, van Kilsdonk JW, Laman JD, Prens EP. Ustekinumab improves psoriasis-related gene expression in non-involved psoriatic skin without inhibition of the antimicrobial response. *Br J Dermatol* doi: 10.1111/bjd.12175. [Epub ahead of print] (2012)

Jansen PA, van Diepen JA, Ritzen B, Zeeuwen PL, Cacciatore I, Cornacchia C, van Vlijmen-Willems IM, de Heuvel E, Botman PN, Blaauw RH, Hermkens PH, Rutjes FP, Schalkwijk J. Discovery of small molecule vanin inhibitors: new tools to study metabolism and disease. *ACS Chem Biol* 8, 530-4 (2013)

Jansen PA, Hermkens, HH, Zeeuwen PL, Botman PN, Blaauw RH, Burghout P, van Galen PM, Mouton JW, Rutjes FP, Schalkwijk J. Combination of pantothenamides with vanin inhibitors: a novel antibiotic strategy against gram-positive bacteria. *Submitted for publication* (2013)

Curriculum vitae

Patrick Jansen werd geboren op 28 augustus 1979 te Cuijk. Na het behalen van zijn VWO diploma in 1999, begon hij zijn studie op de Hogere Laboratorium Opleiding aan de Hogeschool van Arnhem en Nijmegen met biochemie en biotechnologie als afstudeerrichting. Tijdens het laatste jaar van deze studie heeft hij stage gelopen bij de Animal Science Group te Lelystad onder begeleiding van René van Gennip. Nadat hij in 2003 zijn bachelor diploma behaald had, is hij aan zijn master Moleculaire Levenswetenschappen aan de Radboud Universiteit Nijmegen begonnen. Tijdens deze master heeft hij eerst stage gelopen bij de afdeling Urologie van het Universitair Medisch Centrum St. Radboud te Nijmegen onder begeleiding van Mirjam de Weijert en dr. Gerald Verhaegh. De laatste stage heeft hij gelopen bij de afdeling Celbiologie van het Universitair Medisch Centrum St. Radboud te Nijmegen onder begeleiding van dr. Yvet Noordman en dr. Wiljan Hendriks. In 2005 heeft hij zijn masterdiploma in ontvangst genomen en is hij als junior onderzoeker begonnen bij de afdeling Experimentele Dermatologie van het Universitair Medisch Centrum St. Radboud te Nijmegen onder begeleiding van prof. dr. Joost Schalkwijk. De resultaten van dit onderzoek zijn deels in dit proefschrift te lezen. Gedurende zijn promotietraject heeft hij meerdere malen zijn resultaten mogen presenteren op (inter)nationale congressen. In 2006 ontving hij bij de jaarvergadering van de Nederlandse Vereniging voor Experimentele Dermatologie de prijs voor "beste poster". Tijdens de laatste jaren van zijn promotieonderzoek is hij betrokken geweest bij het opzetten van een vanine-platform. Hierbij werkte hij intensief samen met de afdeling Synthetisch-organische Chemie van de Radboud Universiteit Nijmegen, de afdeling Parasitologie van het Universitair Medisch Centrum St. Radboud en de bedrijven Chiralix en TropIQ Health Sciences, beide op de campus van het universiteitsterrein te Nijmegen gevestigd. Na zijn promotieonderzoek blijft hij als onderzoeker betrokken bij de ontwikkeling en optimalisatie van vanine remmers en bij het verder opzetten van het vanine-platform.

